UNIVERSIDAD AUTÓNOMA DE MADRID

PhD in Molecular Biosciences

CD69 CONTROLS INFLAMMATION IN TRANSPLANT REJECTION AND CARDIOVASCULAR DISEASES

Marta Relaño Orasio

Madrid - 2019

Departamento de Bioquímica

Facultad de Medicina

UNIVERSIDAD AUTÓNOMA DE MADRID

CD69 CONTROLS INFLAMMATION IN TRANSPLANT REJECTION AND CARDIOVASCULAR DISEASES

Marta Relaño Orasio

Bachelor in Biochemistry, from the Universidad Complutense de Madrid

The research presented in this memory was carried out at the Spanish National Center for Cardiovascular Research (CNIC), under the direction of **Dr. Pilar Martín Fernández**

Madrid, 8th July 2019

Doctor María Pilar Martín Fernández, Assistant Professor and Group Leader of "Regulatory Molecules of Inflammatory Processes" group from Vascular Pathophysiology Area at *Centro Nacional de Investigaciones Cardiovasculares* (CNIC), CERTIFY:

That Ph.D. Thesis titled: ***"Cd69 controls inflammation in transplant rejection and cardiovascular diseases",*** has been performed by Ms. Marta **Relaño Orasio**, Bachelor in Biochemistry from the Universidad Complutense de Madrid, under my assessment and I consider this memory satisfactory and authorize its presentation for being evaluated by the corresponding committee.

To whom it may concern, I sign this certificate in Madrid, on 8th July 2019.

Dr. M. Pilar Martín.

Assistant Professor
Group Leader Regulatory Molecules Lab.
Vascular Pathophysiology Area
Centro Nacional de Investigaciones cardiovasculares (CNIC)
28029 Madrid, Spain
Phone: +34 91 453 1200-ext 2009
pmartinf@cnic.es
web: http://www.cnic.es/es/inflamacion/moleculas/index.php

To my parents, Sagrario and Ernesto, who have made it possible for me to get here.

A mis padres, Sagrario y Ernesto, quienes han hecho posible que haya llegado hasta aquí.

"I learned that courage was not the absence of fear, but the triumph over it. The brave man is not he who does not feel afraid, but he who conquers that fear."

Nelson Mandela

“Aprendí que el coraje no es la ausencia de miedo, sino el triunfo sobre él. Una persona valiente no es aquella que no tiene miedo, sino aquella que conquista ese miedo”

Nelson Mandela

AGRADECIMIENTOS

AGRADECIMIENTOS

Lo primero de todo agradecer a mi directora de Tesis Pilar Martín por haberme dado la oportunidad y los medios necesarios para desarrollar esta tesis doctoral con ella. Entré en este laboratorio siendo una niña recién salida de la carrera para hacer el trabajo fin de máster y poco a poco he ido aprendiendo lo que es la ciencia, lo difícil que es la mayoría de las veces que todo salga como uno quiere y el cuidado que hay que poner en todo lo que haces. De Pilar he aprendido que en este mundo quien quiere algo tiene que luchar por ello e insistir las veces que haga falta hasta que te hagan caso.

Agradecer también a Katerina Tsilingiri, que ha estado conmigo desde el principio de este trabajo enseñándome todo lo que he aprendido. Muchas veces no era fácil aguantarme, sobre todo cuando cuestionaba algún procedimiento o echaba a perder experimentos enteros… pero al final yo creo que hasta me cogió cariño.

También tengo que mencionar a Rafael Blanco, Beatriz Linillos e Irene Fernández, compañeros de poyata casi desde el principio y casi hasta el final, con los que he pasado la mayor parte del tiempo durante los últimos 4 años. Las risas y las bromas hacían más ameno el tiempo que pasábamos en el laboratorio. Más tarde llegó Rosa Jiménez, quien ha heredado con mucha ilusión uno de los proyectos que también empecé. Todos ellos más de una vez me han ayudado con algún experimento interminable, pasando conmigo horas y horas en el animalario o en poyata para que pudiera terminar a una hora decente. Al igual que todos los estudiantes que han ido pasando por el laboratorio.

No me puedo olvidar de Raquel Sánchez, la guía definitiva del trabajo en el laboratorio. Gracias por aguantar mis eternas preguntas, mis fallos y mis despistes y por estar ahí cada vez que he necesitado ayuda.

Tengo que agradecer también a Juan José Lazcano y Elisabeth Palomares, quienes siempre han estado dispuestos a ayudarme en el animalario.

Quiero agradecer también a mis amigas Marta, Ana y Laura, las pipetillas, porque siempre me han animado en los momentos de mayores dudas, me han escuchado cuando necesitaba desahogarme y me han dado ánimos para seguir adelante.

Me gustaría agradecer esta tesis también a mi primo Juan López, quien me ayudó a dar mis primeros pasos en un laboratorio y siempre me ha animado a seguir adelante en este maravilloso pero difícil mundo de la ciencia.

Por último, dar las gracias a mi hermano Javi y a mis padres que, aunque no me entendieran, siempre estaban dispuestos a escuchar en qué estaba trabajando. Ellos han tenido que aguantar primero mis dudas e inseguridades antes de empezar el doctorado y más adelante los días malos, los nervios y el agobio, sobre todo en esta última etapa. Siempre me han apoyado y me han dado ánimos para seguir adelante y llegar a terminar esta tesis doctoral.

RESUMEN

RESUMEN

El antígeno CD69 es una proteína transmembrana que se expresa rápidamente en leucocitos tras su activación. Más recientemente ha sido descrita como una molécula que regula negativamente la inflamación mediante la inhibición de la respuesta T efectora. Los ratones deficientes en CD69 son proclives a desarrollar respuestas autoinmunes de tipo Th17 y además tienen defectos en la diferenciación y función de las células T reguladoras, lo que lleva al desarrollo exacerbado de distintas enfermedades inflamatorias crónicas como artritis, colitis, asma, dermatitis o miocarditis autoinmune. Estudios previos demuestran que los ratones *Cd69*$^{-/-}$ son resistentes al crecimiento de tumores e infección por el virus *Vaccinia*. Sin embargo, la contribución específica de las células "Natural Killer" (NK) y el mecanismo por el que CD69 podría estar regulando su función se desconocía. En este trabajo hemos realizado un estudio fenotípico exhaustivo de estas células mediante citometría de masas (CyTOF). Este análisis reveló que las células NK *Cd69*$^{-/-}$ presentan alteraciones de expresión de los receptores Ly49H y Ly49G2 entre otros, implicados en las respuestas frente a MCMV, frente a tumores o en el reconocimiento de células alogénicas. Mediante la interacción con NKG2D, CD69 participa activamente en la reorganización de los receptores de las NKs en la membrana, jugando un papel esencial en su función efectora.

Uno de los principales objetivos de este trabajo ha sido el análisis del papel del receptor CD69, expresado en linfocitos, en el desarrollo de aterosclerosis. Estudios previos demostraban que las LDL-oxidadas (LDLox) eran un ligando funcional de CD69 en linfocitos. En este trabajo hemos analizado el papel de esta molécula mediante el estudio de quimeras deficientes en el receptor de LDL (*ldlr*$^{-/-}$) en el compartimento linfoide, en régimen de dieta grasa como modelo de aterosclerosis. En este modelo, la deficiencia de CD69 en linfocitos incrementa el *ratio* Th17/Treg lo que conlleva a un aumento en el tamaño de la placa de ateroma y de la progresión de la enfermedad cardiovascular.

La microbiota intestinal modula la inflamación local y sistémica, siendo ciertas bacterias como SFB inductoras de respuestas Th17 que pueden migrar a la periferia afectando la inmunidad sistémica. Varias enfermedades autoinmunes como la escleroris múltiple, encefalomielitis autoinmune, artritis o diabetes tipo I han sido asociadas con la composición de la microbiota. En este estudio comprobamos que la microbiota es esencial en la generación de respuesta Th17 responsable de la inducción y progresión de miocarditis a cardiomiopatía dilatada. En condiciones libres de gérmenes, tanto ratones silvestres como deficientes en CD69 preservan la función cardiaca y no presentan infiltrado leucocitario en el corazón tras inducción de miocarditis autoinmune. Por último, CD69 regula las respuestas Th17 y la composición de la microbiota intestinal.

ABSTRACT

ABSTRACT

The early lymphocyte activation antigen CD69 is a transmembrane protein that is induced early after activation of all bone marrow-derived cells except erythrocytes. It has been described as an anti-inflammatory molecule that negatively regulates inflammation. CD69 deficient mice display enhanced Th17 differentiation and defective Treg cell function presenting an exacerbated form of chronic inflammatory diseases like arthritis, colitis, allergic asthma, contact dermatitis or autoimmune myocarditis due to their inability to resolve inflammation or to maintain immune tolerance. Previous works have shown that *Cd69*$^{-/-}$ mice are resistant to tumor growth and vaccinia virus infection in part due to NK cells activity. However, the specific contribution of these cells and the mechanism by which CD69 could be regulating their function has not been elucidated. The activation of NK cells depends on the balance between activating/inhibitory signals. Thus, in this work we take advantage of the new Mass Cytometry (CyTOF) technology to perform an unbiased multiparametric phenotyping of *Cd69*$^{-/-}$ NK cells. By using different animal models such as anti-viral and anti-tumor immunity and graft vs host disease, we have studied the *in vivo* consequences of *Cd69*$^{-/-}$ NK cells phenotype. Our study revealed that *Cd69*$^{-/-}$ NK cells repertoire of inhibitory/activating receptors is altered, exhibiting high levels of non-self and missing self recognition receptors, due to modulation of NKG2D activity. *Cd69*$^{-/-}$ NK cells are then more efficient in the killing of allogenic and tumor cells, being Cd69$^{-/-}$ mice resistant to aGvHD. All these effects can be reproduced by an anti-CD69 mAb treatment, suggesting that it may be employed in the clinics to reduce GvH effects while potentially maintaining GvL effects.

One of the main objectives of this work has been to analyze the role of CD69 expression in lymphocytes in atherosclerosis development. Using chimeric *ldlr*$^{-/-}$ mice subjected an HFD as atherosclerosis model, we show that the specific deletion of CD69 on the lymphoid compartment leads to an altered Th17/Treg equilibrium and a consequent increase in atheroma plaque size during HFD.

Finally, it is well known that gut microbiota shapes local and systemic inflammation. Certain bacteria like SFB induce the accumulation of Th17 cells that might migrate to the periphery affecting systemic immunity. Indeed, several autoimmune disorders, such as multiple sclerosis, EAE, arthritis, type I diabetes or pancreatitis, have been associated with the gut microbiota composition. In this study we have seen that myocarditis induction and progression depends on the microbiota, as in germ free conditions both CD69 proficient and deficient mice preserve heart function and do not present leukocyte infiltration in the heart after EAM induction. Last, CD69 regulates Th17 responses and microbiota composition.

INDEX

INDEX

I. INDEX……1

II. ABBREVIATIONS……7

III. INTRODUCTION……13

1. The Immune system…… 13
2. The Innate Immune Response…… 14
   - 2.1. Natural Killer cells…… 14
   - 2.2. Natural Killer receptors……16
     - 2.2.1.1. NKp46……16
     - 2.2.1.2. NKG2D……16
     - 2.2.1.3. CD94/NKG2A heterodimer……17
     - 2.2.1.4. Ly49 Receptors……17
3. The adaptive immune response…… 19
   - 3.1. T lymphocytes…… 19
     - 3.1.1. Th17 cells……20
     - 3.1.2. Regulatory T cells (Treg)……20
4. CD69: early leukocyte activation marker ……21
   - 4.1. Location and structure of CD69……21
   - 4.2. Regulation of CD69 expression……22
   - 4.3. CD69 ligands……22
   - 4.4. Immunomodulatory properties of CD69……23
5. Immune related pathologies…… 24
   - 5.1. Acute graft versus host disease (aGvHD)……24
   - 5.2. Atherosclerosis: adaptive immune response model……24
   - 5.3. Myocarditis: autoimmune response……27
6. Gut microbiota…… 29
   - 6.1. Role of gut microbiota in immunity and autoimmune disorders……30
   - 6.2. Gut microbiota and heart failure……31

IV. OBJECTIVES……35

V. MATERIALS AND METHODS……39

1. Mice…… 39
2. Animal models and procedures…… 40
2.1. Graft versus host disease induction…… 40
2.2. Tumor growth “in vivo”…… 41
2.3. “In vivo” model of atherosclerosis……41
2.4. Experimental Autoimmune Myocarditis (EAM) induction…… 42
3. NK cell isolation ……42
4. Cell culture……42
5. RNA isolation and assessment of mRNA transcripts……43
6. RNA-Seq……43
7. Cell staining for Flow cytometry…… 43
8. Mass cytometry……44
9. Bioinformatics analysis of Mass cytometry……45
10. Anti-CD69 mAb production……45
11. Co-immunoprecipitation and Western Blot……45
12. Immunofluorescence microscopy……46
13. Analysis of microbiota composition from mouse fecal samples……46
14. Echocardiography and Magnetic Resonance Imaging……46
15. Histopathology analysis……47
16. Statistical analysis……48

VI. RESULTS…… 51

1. Role of CD69 in the regulation of “Natural Killer” (NK) cells activity in the context of innate immunity……51
1.1. *Cd69*$^{-/-}$ NK cells present an altered inhibitory/activating receptor repertoire…… 51
1.2. C57BL/6 *Cd69*$^{-/-}$ mice and anti-CD69mAb-treated littermates are highly susceptible to MCMV infection……52
1.3. NK cell-targeted anti-CD69mAb treatment is efficient against a poorly immunogenic tumor……54
1.4. Cd69$^{-/-}$ mice are highly resistant to aGvHD after allogeneic HSCT……55

1.5. NK cells account for allogeneic killing in Cd69-/- hosts and anti-CD69mAb-treated littermates ……56
1.6. Ablation of CD69 renders NK cells resistant to apoptosis and enhances NK cell signaling during allogeneic cell elimination……58
1.7. CD69 controls NKG2D expression, membrane clustering and signaling……..59
1.8. CD69 can be targeted to prevent aGVHD without compromising engraftment……60
2. Role of CD69 in an "in vivo" model of atherosclerosis in the context of adaptive immunity……62
2.1. CD69 regulates adaptive immune responses in HFD conditions……62
2.2. Analysis of blood leukocyte subsets during high fat diet……64
2.3. CD69 deficiency in lymphoid cells aggravates atherosclerosis……66
2.4. CD69 deficiency in myeloid cells does not influence atherosclerosis development……67
2.5. Analysis of circulating lipids in mice subjected to HFD……69
3. Role of CD69 in the development of cardiomyopathy in the absence of microbiota..70
3.1. CD69 deficient mice exhibit different gut microbiota composition……70
3.2. Antibiotics treatment reduce heart failure after myocarditis induction……71
3.3. Systemic inflammation and autoimmune myocarditis are abrogated in the absence of microbiota……73
VII. DISCUSSION……79
VIII. CONCLUSIONS……95
IX. CONCLUSIONES……99
X. REFERENCES……103
XI. ANNEX……119
xii. Annex index: published articles related to this thesis……121

ABBREVIATIONS

ABBREVIATIONS

aGvHD: Acute Graft Versus Host Disease

α-MyHC: α -isoform of the myosin heavy chain

ANOVA: Anaysis of Variance

APCs: Antigen Presenting Cells

BM: Bone Marrow

cGvHD: Chronic Graft Versus Host Disease

CFA: Complete Freud Adyuvant

CoIP: Co-Immunoprecipitation

CTDL: C-Type Lectin like Domain

CyTOF: Cytometry by Time of Flight

DC: Dendritic Cell

DCM: Dilated Cardiomyopathy

DRep: Double reporter

EAE: Experimental Autoimmune Encephalomyelitis

EAM: Experimental Autoimmune Myocarditis

EF: Ejection Fraction

FACS: Fluorescent Activated Cells Sorting

FCS: Fetal Calf Serum

FMT: Fluorescence Molecular Tomography

Foxp3: Forkhead Box Protein 3

FS: Fractional Sortening

GALT: Gut Associated Lymphoid Tissue

GF: Germ Free

GFP: Green Fluorescent Protein

IL: Interleukin

IFNγ: Interferon gamma

HFD: High Fat Diet

HSCT: Hematopoietic Stem Cell Transplant

iTreg: Induced T regulatory cells

IP: Immunoprecipitation

I.P: Intraperitoneal

ITAM: immunoreceptor tyrosine-based activation motif

ITIM: immunoreceptor tyrosine-based inhibitory motif

I.V: Intravenously

KO: Knock-out

LC: Lymphoid Chimera

LDL: Low Density Lipoprotein

LVEF: Left Ventricule Ejection Fraction

mAb: Monoclonal Antibody

MC: Myeloid Chimera

MCMV: Murine Citomegalovirus

MFI: Mean Fluorescence Intensity

MHC: Major Histocompatibility Complex

MRI: Magnetic Resonance Imaging

mRNA: Messenger RNA

mLNs: Mesenteric Lymph Nodes

NCR: Natural Cytotoxic Receptors

NGS: Next Generation Sequencing

NKC: Natural Killer Gene Complex

NKG2D: NK group 2 member D

NKs: Natural Killer Cells

Ox-LDL: Oxidized Low Density Lipoprotein

PBLs: Peripheral Blood Lymphocytes

PBMCs: Peripheral Blood Mononuclear Cells

pLNs: Peripheric Lymph Nodes

PMA: Phorbol Myristate Acetate

pTreg: Peripheral T Regulatory cells

qPCR: Quantitative Polimerase Chain Reaction

RFP: Red Fluorescent Protein

RORγt: Retinoic Acid-Related Orphan Receptor gamma

SFB: Segmented Filamentous Bacteria

S1P1: Sphingosine 1-phosphate Receptor 1

SPF: Specific Pathogen Free

TCR: T Cell Receptor

Tfh: T Follicular Helper Cell

TGFb: Transforming Growth Factor beta

Th: T helper cell

TMAO: trimethylamine–*N*-oxide

TLR: Toll Like Receptor

Treg: Regulatory T cells

t-SNE: t-Distributed Stochastic Neighbor Embedding

T1D: Type-1 Diabetes

VSCM: Vascular Smooth Muscle Cells

WB: Western Blot

WT: Wild Type

INTRODUCTION

INTRODUCTION

1. The immune system

The immune system comprises a group of cells and molecules which main role is to defend the body against microorganisms, macromolecules or little chemical substances that can be harmful for the organism and are recognized as foreign agents. The coordinated response against these agents is known as the immune response.

Briefly, there are two types of immune response (Figure 1). The innate immune response is the first line of defense against microorganisms and adaptive or specific immune response that takes place after exposure to an infectious agent. This response is stronger upon sustained exposure to the same agent. Adaptive immune response can be further subdivided into humoral and cellular immunity. The first one protects from extracellular pathogens and is mediated by antibodies produced by B lymphocytes that specifically recognize microbial antigens, neutralizing them and facilitating its destruction by multiple effector mechanisms. Additionally, cellular immunity protects the host from intracellular pathogens that escape humoral immunity and it is mediated by T lymphocytes.

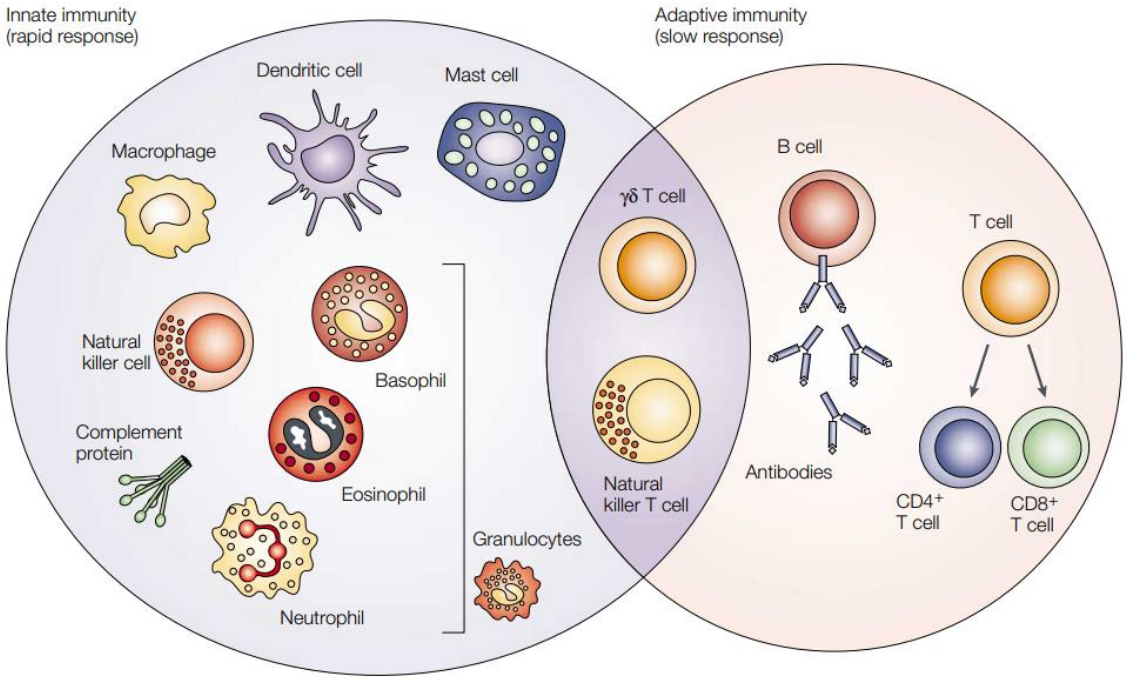

Figure 1. The innate and adaptive immune response. The innate immune system consists of soluble factors, such as complement proteins, and diverse cellular components including granulocytes (basophils, eosinophils and neutrophils), mast cells, macrophages, dendritic cells and natural killer cells. The adaptive immune response is slower to develop and it consists of antibodies, B cells, and CD4+ and CD8+ T lymphocytes. Natural killer T cells and γδ T cells are cytotoxic lymphocytes that straddle the interface of innate and adaptive immunity (Dranoff, 2004)

The innate and adaptive immune systems are often described as contrasting, separate arms of the host response; however, they usually act together, with the innate response representing the first line of host defence, and with the adaptive response becoming prominent after several days, as antigen-specific T and B cells have undergone clonal expansion. Components of the innate system contribute to activation of the antigen-specific cells. Additionally, the antigen-specific cells amplify their responses by recruiting innate effector mechanisms to bring about the complete control of invading microbes. Thus, while the innate and adaptive immune responses are fundamentally different in their mechanisms of action, synergy between them is essential for an intact, fully effective immune response.

2. The innate immune response

The first line of defence in innate immunity is provided by epithelial barriers and by specialized cells and natural antibiotics present in epithelia, all of which function to block the entry of microbes. If microbes do breach epithelia and enter the tissues or circulation, they are attacked by phagocytes, specialized lymphocytes called natural killer (NK) cells, and several plasma proteins, including the proteins of the complement system. All these mechanisms of innate immunity specifically recognize and react against microbes but do not react against non-infectious foreign substances. Different mechanisms of innate immunity may be specific for molecules produced by different classes of microbes. In addition to providing early defence against infections, innate immune responses enhance adaptive immune responses against the infectious agents.

2.1. Natural Killer cells

Natural killer (NK) cells are a subset of innate lympochytes that respond to intracellular pathogens or tumoral cells (hence their name). NK cells kill infected or transformed cells through the release of cytolytic granules containing perforin and granzymes or through the ligation of death-inducing receptors, but they also secrete pro-inflammatory cytokines, such as interferon-γ (IFN-γ) or tumour necrosis factor (TNF), that contribute to the shaping of the adaptive immune response (Vivier et al., 2011, Vivier et al., 2008) They recognize their targets by two different ways. Like many other cells, they possess Fc receptors that bind IgG (FcγR). These receptors link natural killer cells to IgG-coated target cells, which they kill by a process called antibody-dependent cellular cytotoxicity. The second way of recognition relies on a wide range of natural killer receptors that are classified in activating or inhibitory receptors depending on the signal they transmit. Depending on the balance between these two signals the NK cell is going to be activated or remain tolerant (Figure 2).

Activating receptors mainly recognize pathogen or cell stress-induced ligands, while inhibitory receptors bind to MHC class I molecules present on all nucleated cells, thus allowing self-tolerance (Moretta et al., 1997, Lanier, 1998). In the absence of self-molecules or "missing-self", signals from activating receptors lead to induction of NK cell cytotoxic function and cytokine release. When the activating signal is not strong enough to overcome the inhibitory signals the cell remains inhibited, allowing tolerance to healthy tissue. There is also an indirect pathway of NK cell activation that involves release of cytokines and upregulation of co-stimulatory receptors by DCs. This pathway is important in controlling viral infections (Steinberg et al., 2009, Amadei et al., 2010).

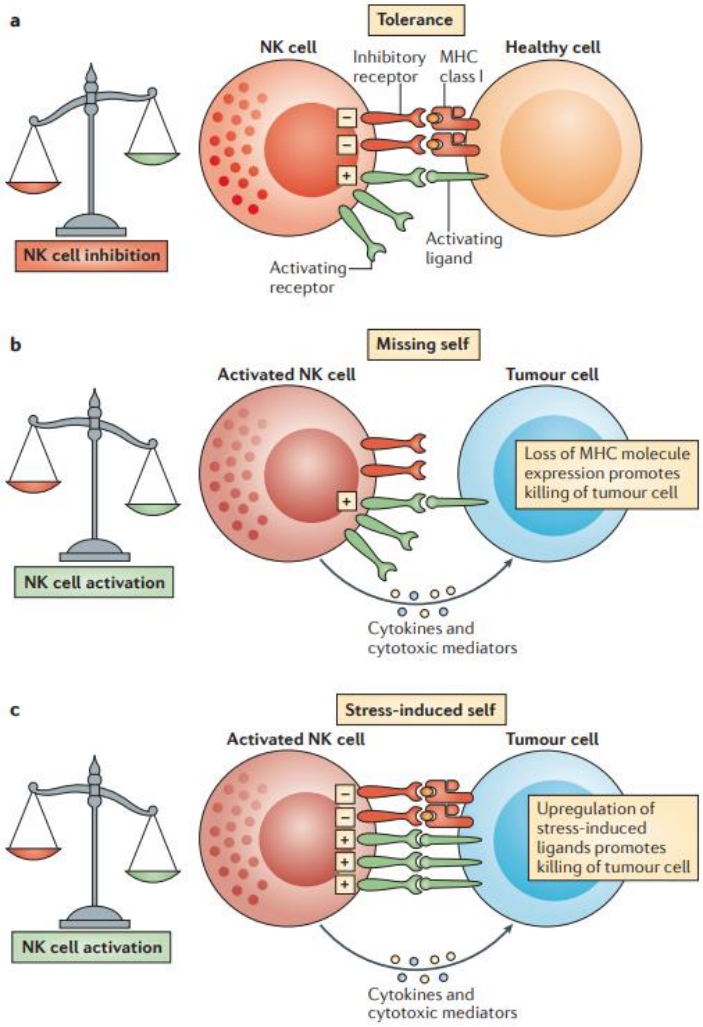

Figure 2. NK cell activation depends on a balance between activating and inhibitory signals. **a**. Healthy host cells express MHC-I molecules that engage inhibitory receptors (tolerance). **b**. Tumour cells may lose expression of MHC-I molecules. There is no inhibitory signal and NK cell get activated (missing self). **c.** Stressed cells can activate NK cells by upregulation of activating ligands that overcome the inhibitory signal induced by MHC-I molecules (Stress-induced self). In addition, NK cells are selectively activated by 'stressed' cells, which upregulate activating ligands for NK cells and thereby overcome the inhibitory signalling delivered by MHC class I molecules. NK cell activation leads to tumour elimination directly (through NK cell-mediated cytotoxicity) or indirectly (through the production of pro-inflammatory cytokines, such as interferon-γ) (Vivier et al., 2012).

2.2. Natural Killer receptors

2.2.1. NKp46

NKp46 is a potent stimulatory receptor that belongs to the immunoglobulin superfamily of natural cytotoxic receptors (NCR) together with NKp44 and NKp30 (Biassoni et al., 2001). These receptors are strictly confined to NK cells, and their engagement induces a strong activation of NK-mediated cytolysis. Like other NK-activating receptors, NKp46 is involved in the elimination of tumors and infected cells by recognition of viral hemagglutinin (Mandelboim et al., 2001)

2.2.2. NKG2D

NK group 2, member D (NKG2D) is a lectin-like type II transmembrane homodimer expressed on practically all mouse NK cells, activated CD8+T, γδT cells, and some NKT cells (Bauer et al., 1999, Wu et al., 1999). It specifically recognizes self-ligands related to MHC class I molecules including the MHC class-I-chain-related protein A (MICA) and MICB encoded in the human MHC (Bauer et al., 1999), and a diverse family of proteins present in both mice and humans — retinoic acid early transcript 1 (Rae1), H60 and mouse UL16-binding protein-like transcript 1 (Mult1) in mice, and the UL16-binding proteins (ULBPs) or RAET1 proteins in humans (Cerwenka et al., 2000, Diefenbach et al., 2000, Carayannopoulos et al., 2002). These ligands are generally poorly expressed by normal cells but are induced on damaged self-tissues undergoing transformation, infection, or autoimmune aggression. NKG2D plays an important role in the elimination of tumors (Le Bert and Gasser, 2014), virally infected cells (Jonjic et al., 2008), and organ transplants (Ogasawara et al., 2005). For this reason, NKG2D was originally thought to predominantly mediate direct cytotoxicity of stressed target cells (Raulet, 2003). However, recent studies suggest that this receptor may mediate NK cell education in the bone marrow and peripheral tolerance upon chronic ligand exposure mediating its own downregulation and subsequent hypo-responsiveness to stimulation. This way, rather than activating NK cells, high NKG2D ligand expression mediates downregulation of the receptor on tumor infiltrating lymphocytes (TILs) and reduced responsiveness to NKG2D engagement (Groh et al., 2002). In most cases, both NK and T cells require a secondary signal before NKG2D is able to mediate a measurable effect (Ho et al., 2002, Groh et al., 2001, Bryceson et al., 2006). The primary function of NKG2D therefore appears to be regulation of signaling through other receptors, being able to both inhibit and potentiate signaling of multiple receptors during different stages of the life cycle of immune cells, such as hematopoietic development, priming, and effector responses (Zafirova et al., 2011). NKG2D regulates receptor responsiveness differently following acute or chronic stimulation (Figure 3).

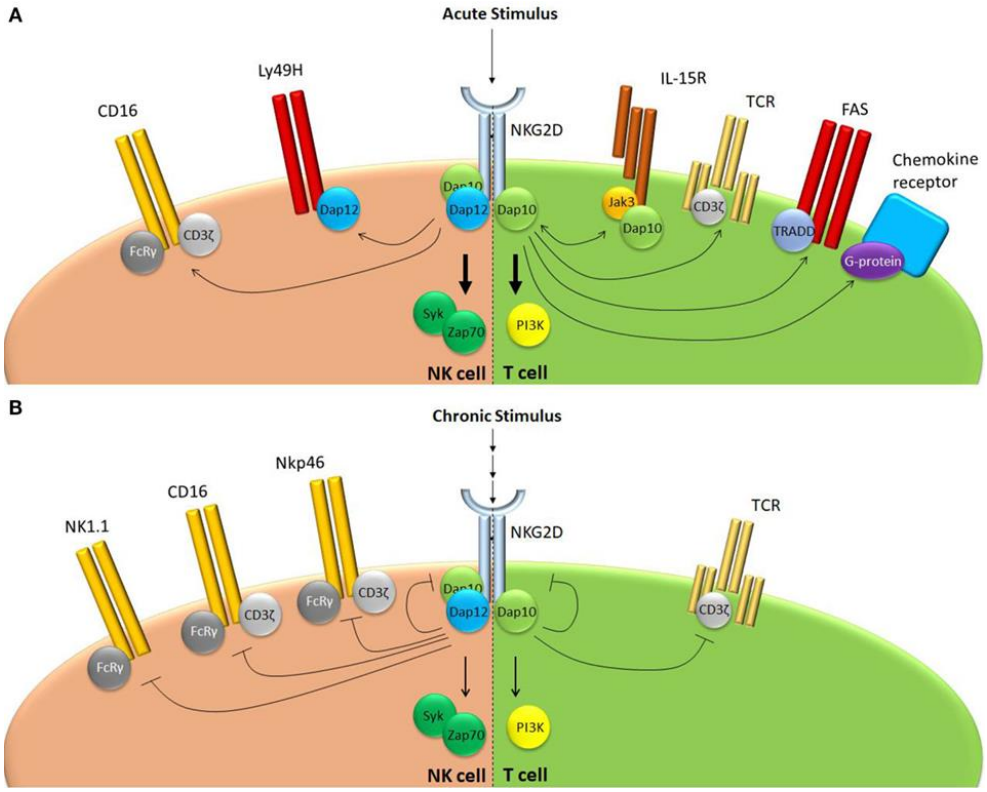

Figure 3. NKG2D regulates receptor responsiveness differently following acute or chronic stimulation. A. After acute stimulation, NKG2D promotes responsiveness of variety of receptors that use largely distinct intracellular signaling modalities. B. Chronic NKG2D engagement mediates its own downregulation and subsequent hypo-responsiveness to stimulation. In addition, chronic NKG2D stimulation impairs T cell receptor responsiveness in T cells. (Wensveen et al., 2018)

2.2.3. CD94/NKG2A heterodimer

CD94/NKG2A heterodimer is an inhibitory receptor belonging to C-type lectin superfamily. In human NK cells it recognizes the non-classical MHC class I molecule HLA-E which is expressed on normal cells (Borrego et al., 1998), while in mice it binds the MHC class I molecule Qa-1(b) (Vance et al., 1998)

2.2.4. Ly49 Receptors

The best characterized mouse NKC family is the Ly49 receptor family, which are functional homologues of the human killer Ig-related receptors (KIRs). These can be activating or inhibitory depending on their intracellular domain or the adaptor protein associated with them, and they are encoded by a family of highly polymorphic and variably polygenic genes that clustered together in the natural killer gene complex (NKC) on mouse chromosome 6 (Yokoyama and Plougastel, 2003) (Carlyle et al., 2008), generating a wide variety of Ly49 haplotypes that differ between mouse strains (Figure 4).

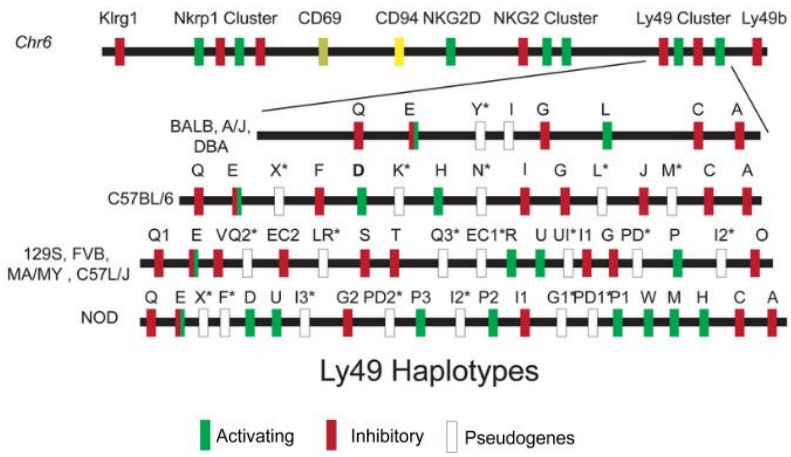

Figure 4. Ly49 haplotypes. The Ly49 gene cluster on mouse chr 6 within the Natural Killer gene Complex. Schematic organization of the Ly49 haplotype is described for the indicated mouse strains. Adapted from genetic dissection of NK cell responses (Moussa et al., 2012)

Inhibitory receptors contain an immunoreceptor tyrosine-based inhibitory motif (ITIM) domain in their cytoplasmic tail (Vivier and Daeron, 1997). Upon activation by engagement of their ligand on a target cell, the inhibitory receptors become tyrosine phosphorylated on their ITIMs and associate with intracellular phosphatases, such as SH2-domain-containing protein tyrosine phosphatase 1 (SHP1), resulting in an inhibitory signal that prevents killing of the target cell (Mason et al., 1997). This is the case of Ly49A, Ly49C or Ly49G among others. By contrast, activating receptors like Ly49D and Ly49H lack this ITIM motif but they transduce signals through associated adaptor proteins, such as DAP12, which contain an immunoreceptor tyrosine-based activation motif (ITAM) (Smith et al., 1998) that is phosphorylated in its tyrosine residue upon cross-linking of activating receptors, leading to the phosphorylation of other proteins like Syk and Zap70 that act as mediators of downstream activating signaling events (McVicar et al., 1998) (Tomasello et al., 2000).

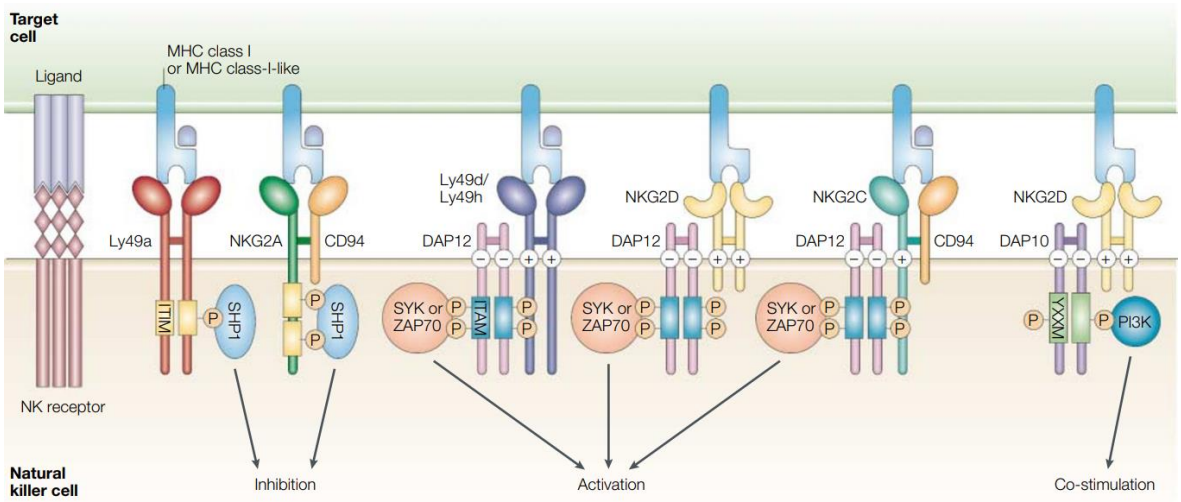

Figure 5. NK cell receptors. After interaction with their target-cell ligands, the inhibitory receptors become tyrosine phosphorylated on their immunoreceptor tyrosine-based inhibitory motifs (ITIMs) and associate with intracellular phosphatases, such as SH2-domain-containing protein tyrosine phosphatase 1 (SHP1), resulting in an inhibitory signal. The activating receptors are associated to adaptor molecules

such as DAP12, bearing immunoreceptor tyrosine-based activation motifs (ITAMs) that are phosphorylated upon ligand encounter, resulting in cytotoxicity and cytokine production. Natural-killer group 2D (NKG2D) molecules can associate with the DAP12 or DAP10 adaptor molecules. After ligand binding, NKG2D associated with a DAP10 molecule seems to deliver a co-stimulatory signal rather than an activating signal. NK, natural killer; PI3K, phosphatidylinositol 3-kinase; ZAP70, ζ-chain-associated protein 70 kDa. *(Yokoyama and Plougastel, 2003)*

3. The adaptive immune response

Unlike the innate immune response, the adaptive immune system presents specificity for its target antigens. Adaptive responses are based primarily on the antigen-specific receptors expressed on the surfaces of T- and B-lymphocytes. These antigen-specific receptors are encoded by genes that are assembled by somatic rearrangement of germ-line gene elements to form intact T cell receptor (TCR) and immunoglobulin (B cell antigen receptor; Ig) genes. The assembly of antigen receptors from a collection of a few hundred germ-line-encoded gene elements permits the formation of millions of different antigen receptors, each with potentially unique specificity for a different antigen.

3.1. T lymphocytes

T cells are predominantly produced in the thymus. They recognise foreign antigens by a surface expressed, highly variable, T cell receptor (TCR). There are two main types of T cells: cytotoxic or $CD8^+$ T cells and helper or $CD4^+$ T cells. $CD4^+$ cells differentiate into different subsets: Th (T helper)1, Th2, Th9, Th17, Th22, Treg (regulatory T cells), and Tfh (follicular helper T cells), which are characterized by different cytokine profiles (Raphael et al., 2015).

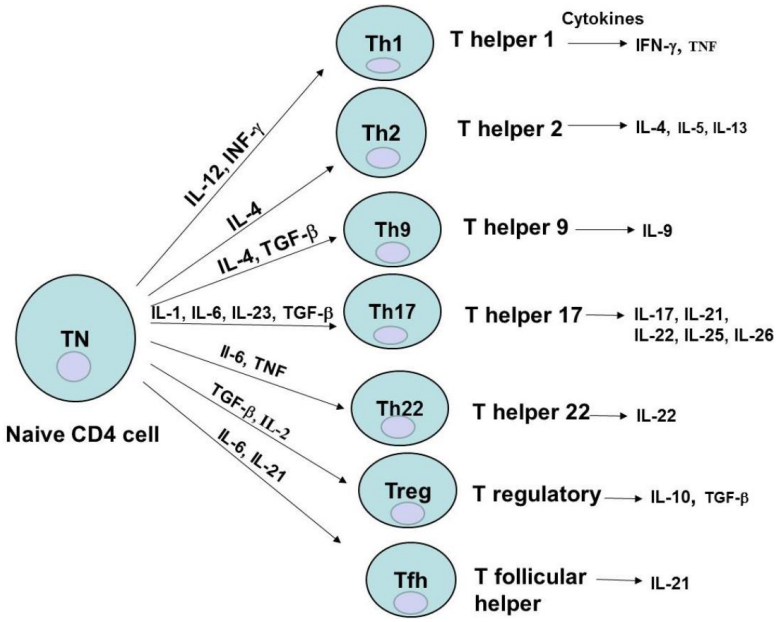

Figure 6. Different $CD4^+$ T cell subsets. The different $CD4^+$ subsets are generated from naïve T cells by specific cytokines. Each $CD4^+$ subset produces a different type of interleukins. (Golubovskaya and Wu, 2016)

3.1.1. Th17 cells

Th17 cells are the main producers of IL-17 (Park et al., 2005*)*, a cytokine that plays an important role in host defence against bacteria and fungi. These cells differentiate from $CD4^+$ naïve T cells after IL-23 production by stimulated dendritic cells and macrophages. They are involved in the disease progression of many autoimmune and inflammatory disorders like rheumatoid arthritis (Sanchez-Diaz et al., 2017), multiple sclerosis (Cua et al., 2003), intestinal bowel disease (Zhang et al., 2006) (Yen et al., 2006), atherosclerosis (Gong et al., 2015) (Taleb et al., 2015) or myocarditis (Rangachari et al., 2006) (Sonderegger et al., 2006). Their pathogenic effect is due to their secretion of the IL-17, as well as IL-22 and granulocyte-macrophage colony-stimulating factor (GM-CSF) (Bedoya et al., 2013). These cytokines induce neutrophil production and recruitment, activation of innate immune cells and enhancement of B cell functions. IL-17 also stimulates the production and expression of proinflammatory cytokines, IL1-β and TNF-α by macrophages (Jovanovic et al., 1998) (Chen et al., 2013). Additionally, IL-17 signalling induces the expression and/or release of chemokines and other inflammatory mediators, including intercellular adhesion molecule 1 (ICAM-1), prostaglandin E2 (PGE2), as well as promoting tissue damage through the induction of matrix metalloproteinases (MMPs) and antimicrobial-peptides (Zhu and Qian, 2012). Importantly, these events initiate several positive-feedback loops that further increase IL-17 production, sustain a proinflammatory environment, and can cause excessive tissue damage (Benedetti and Miossec, 2014). RORγT directs the transcription of genes encoding IL-17A and IL-17F among others; however, RORγT deficiency does not completely abrogate Th17 differentiation.

3.1.2. Regulatory T cells (Treg)

Treg cells are a subset of T cell that play a critical role in the regulation of immune response. During infection or inflammation, Treg cells migrate from the blood to draining lymph nodes and inflamed tissues to inhibit the activation and proliferation of antigen-specific T-cells, limiting the immune response and maintaining immune tolerance by secretion of immunosuppressive cytokines such as IL-10 and TGF-β1 (Sakaguchi et al., 1995). IL-10 inhibits both the proliferation and the cytokine synthesis of $CD4^+$ T-cells. Treg cells express the signature Foxp3 transcription factor, critical for their development, lineage commitment, and suppressive functions (Hori et al., 2003, Fontenot et al., 2003). Regulatory T cells can differentiate in the thymus and migrate to the periphery as natural Treg (nTreg) or can differentiate in secondary lymphoid organs or tissues as adaptive or induced Tregs (iTreg) by acquiring Foxp3 expression (Workman et al., 2009)

There is also another subset of Foxp3$^-$ CD4$^+$ T cells called type 1 regulatory (Tr1) cells that can suppress inflammation and produce IL-10, but unlike Treg cells they do not require constitutive expression of FoxP3 for their generation and immunosuppressive functions (Levings and Roncarolo, 2000) (Zeng et al., 2015). Th3 regulatory cells are a unique T-cell subset, which mainly secretes TGF-β, provides help for IgA secretion, and has suppressive features for both Th1 and Th2 cells (Fukaura et al., 1996) (Weiner, 2001). Numerous studies have identified Treg cells as important immunoregulators in many inflammatory and autoimmune disease conditions (Dominguez-Villar and Hafler, 2018) including asthma (Robinson, 2009), multiple sclerosis (Costantino et al., 2008) (Dominguez-Villar et al., 2011), and type-I diabetes (Jaeckel et al., 2008).

4. CD69: early leukocyte activation marker

The receptor CD69 is an early leukocyte activation molecule that belongs to the C-type lectin family and is transiently expressed in all activated bone marrow-derived cells except erythrocytes (Testi et al., 1994). C-type lectin proteins are characterized by the presence of a carbohydrate recognition receptor domain (CTDL, C-type lectin like domain) that has lost its capacity to bind Ca^{2+} (Ng et al., 1998) named NK (NKD, NK Domain) due to its presence in multiple NK cell specific receptors. CD69 does not bind monosaccharides nor polysaccharides and has a low affinity binding to fucoidans (sulfated polysaccharides) (Childs et al., 1999).

4.1. Location and structure of CD69

The CD69 gene is located within the natural killer (NK) gene complex on human chromosome 12 and mouse chromosome 6 (Ziegler et al., 1994, Lopez-Cabrera et al., 1993). This gene encodes a phosphorylated disulfide-linked transmembrane homodimeric glycoprotein with two differentially glycosylated subunits (28–32 kDa). Each subunit consists of an extracellular C-type lectin domain (CTLD) and a short cytoplasmic region linked by a single-spanning transmembrane region (Lanier et al., 1988, Testi et al., 1988, Sanchez-Mateos and Sanchez-Madrid, 1991) (Figure 7).

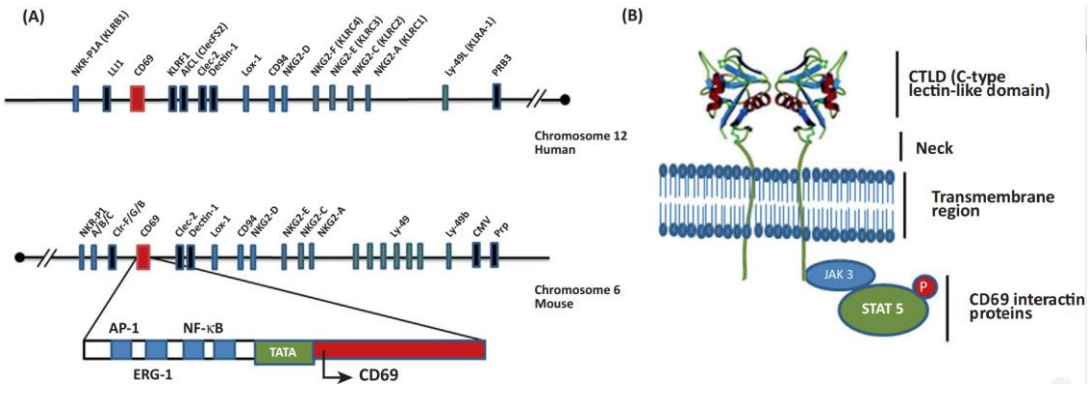

Figure 7. Main characteristics of CD69. Continues on next page

(A) Gene encoding for CD69 is localized in the natural killer (NK) gene complex at human chromosome 12 and mouse chromosome 6 (B) CD69 protein structure and interacting proteins. Abbreviations: NF-κB, nuclear factor-κB; Jak, Janus family kinase; Stat, signal transducer and activator of transcription; ROR, retinoic acid receptor-related orphan nuclear receptor; Th, T helper; ERG-1, erythroblast transformation-specific related gene-1; AP-1, activator protein-1.(Gonzalez-Amaro et al., 2013)

4.2. Regulation of CD69 expression

CD69 expression is readily upregulated upon activation in most leukocytes, which underlies its widespread use as a marker of activated lymphocytes and NK cells, mainly. Transcriptional expression of the CD69 gene is detected after TCR/CD3 engagement, PKC activating agents like phorbol esters or mitogenic stimulators like phytohaemagglutinin (Gonzalez-Amaro et al., 2013, Cebrian et al., 1988). Its expression can be also induced by cytokines like IL-2, TNFa, IL-6 (Unutmaz et al., 1994) and IL-15 that specifically induces CD69 expression on T lymphocytes and NK cells (Kanegane and Tosato, 1996) (Setoguchi, 2016) (Boieri et al., 2017). Regarding transcriptional regulation of CD69 expression, sequence analysis of the 5'-flanking region of the CD69 gene revealed the presence of a potential TATA element 30 base pairs upstream of the major transcription initiation site and several putative binding sequences for inducible transcription factors (NF-κB, Egr-1, AP-1), which might mediate the inducible expression of this gene (Lopez-Cabrera et al., 1995).

4.3. CD69 ligands

There are few known ligands for CD69. CD69 can interact with both carbohydrate moieties and protein residues. Galectin 1 (Gal-1) is a carbohydrate-binding protein expressed in dendritic cells and macrophages that has been identified as a specific ligand of CD69 (de la Fuente et al., 2014). The binding of CD69 to Gal-1 on DCs negatively modulates the in vitro differentiation of Th17 cells, which could control inflammatory responses in vivo. Gal-1 also enhances IL-10 secretion in T cells through the activation of the aryl hydrocarbon receptor (AHR) pathway (Cedeno-Laurent et al., 2012). Another putative ligand of CD69 is the S100A8/S100A9 complex, which binds to CD69 in a glycosylation-dependent manner, this interaction is needed for Treg cell differentiation induction by CD69 (Lin et al., 2015). In addition to these ligands, which bind CD69 in a trans manner, CD69 establishes lateral (cis) interactions with the sphingosine 1-phosphate receptor 1 (S1P1) negatively regulating its functions and promoting lymphocyte retention in lymphoid organs (Shiow et al., 2006). More recently it has been reported that CD69 associates with the amino acid transporter complex LAT1-CD98 (Cibrian et al., 2016) and regulates its surface expression and uptake of L-

tryptophan (L-Trp). Finally, a recent study from the group identifies CD69 as an oxidized low density lipoprotein receptor in T lymphocytes that contributes to the regulatory action of the adaptive immune system. Binding of ox-LDL particles to CD69 on T cells confers a regulatory phenotype to human and mouse T cells, dampening Th17 responses and ameliorating atherosclerosis. (Tsilingiri et al., 2019)

4.4. Immunomodulatory properties of CD69

The physiological role of CD69 has been studied in CD69-deficient mice in different models of chronic inflammation like arthritis (Sancho et al., 2003) allergic asthma and contact dermatitis (Martin et al., 2010b, Cortes et al., 2014), autoimmune myocarditis (Cruz-Adalia et al., 2010) or colitis (Radulovic et al., 2012). Overall, CD69 was shown as a negative regulator of inflammation through the inhibition of Th17 responses and the regulation of Treg cells differentiation and function. It has been established that CD69 inhibits Th17 cell differentiation both *in vitro* and *in vivo* via its interaction with Jak3 and subsequent phosphorylation of the transcription factor Stat5, which dimerizes and translocates to the nucleus activating the transcription factor FoxP3 and stimulating the differentiation of regulatory T cells (Figure 8). In parallel, CD69 dampens Th17 cell differentiation by inhibition of Stat3 phosphorylation and RORγt transcription factor activation (Martin et al., 2010a, Martin and Sanchez-Madrid, 2011).

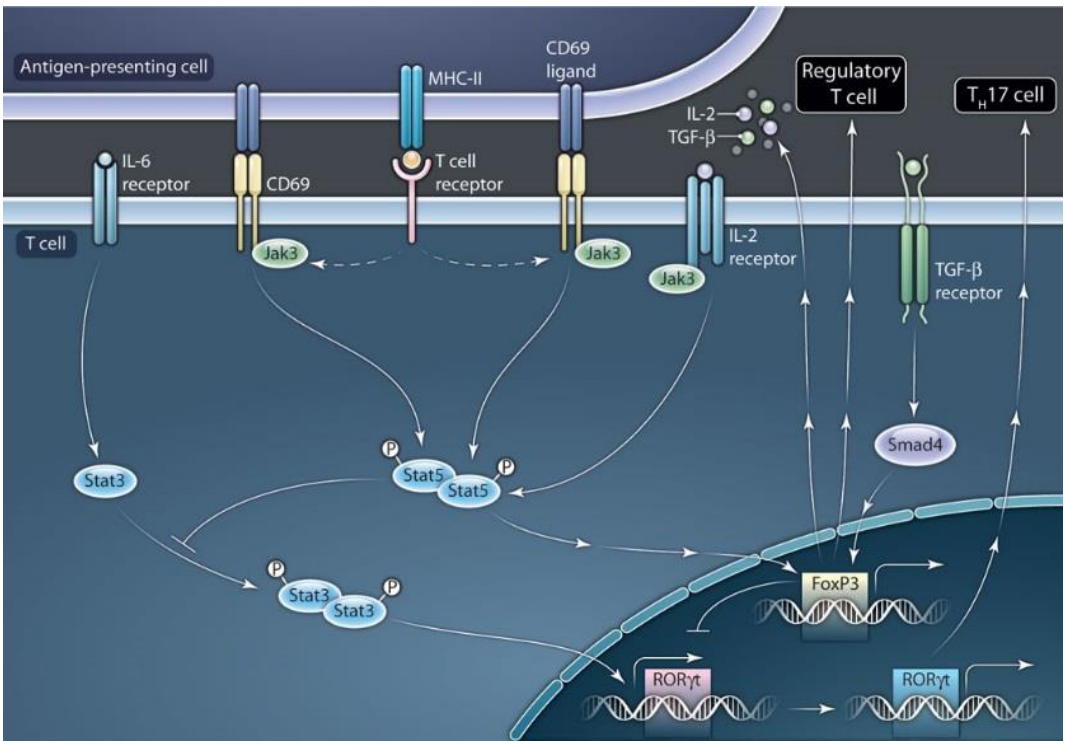

Figure 8. CD69 receptors are present on the membrane of T cells after activation. MHC II, major histocompatibility complex II; P, phosphorylation. Dashed lines indicate indirect effects or interactions, and multiple arrows indicate multistep processes.(Martin and Sanchez-Madrid, 2011)

5. Immune related pathologies

5.1. Acute Graft Versus Host Disease (aGVHD)

Hematopoietic stem cell transplantation (HSCT) has proven to be an effective treatment for a wide range of hematologic malignancies and some solid tumors (Copelan, 2006) (Ljungman et al., 2010). However, in most cases it is impossible to find a donor with identical major histocompatibility complex (MHC) proteins and up to 80% of patients in mismatch settings develop graft-versus host disease (GvHD) (Perez-Simon et al., 2006). In humans, GvHD can manifest as acute GvHD (aGvHD) or chronic GvHD (cGvHD). The former occurs within 100 days of transplant, while the latter typically appears later than 100 days after transplant and development of clinical symptoms can take 2-5 years (Mohty and Apperley, 2010). However, this temporal distinction may not translate to mouse models of the disease, which have been widely studied (Schroeder and DiPersio, 2011). The conditioning or preparative regimen to the recipient is essential for success of the transplant. In mouse models, total body irradiation is the most common method of myeloablating conditioning to eliminate or suppress host immunity (Schroeder and DiPersio, 2011), allowing donor stem cell engraftment and preventing graft rejection. However, this conditioning regimen also damages the healthy epithelial tissues, including the intestinal barrier, and this is the trigger of aGvHD. Antigen presenting cells (APCs) in damaged host tissues secrete pro-inflammatory cytokines (e.g., TNF-α, IL-1β), which contribute to an initial "cytokine storm", increasing the expression of adhesion molecules, major histocompatibility complex (MHC) antigens and costimulatory molecules by these cells. This danger signal, together with the translocation of microbe-associated molecular patterns (MAMPs) due to the loss of gastrointestinal tract integrity (Cooke et al., 2001), activates host and donor antigen presenting cells (APCs), which migrate into draining LNs, where they present antigens and activate donor $CD4^+$ and $CD8^+$ T cells. Thus, there is an alloreactive T-cell expansion, trafficking and tissue damage mediated mostly by effector $CD4^+$ T cells. This inflammatory cascade contributes to a systemic syndrome of weight loss, diarrhea, skin changes and high mortality. Data from this work suggest that CD69 deficient mice are resistant to aGvHD.

5.2. Atherosclerosis: adaptive immune response model

Atherosclerosis is one of the main causes of morbidity and mortality in developed countries. It is a chronic, generalized and progressive disease characterized by the accumulation of atheroma plaques in the medium and big vessels (Figure 9). Different pro-atherogenic factors (hyperlipidemia, hypertension, smoking, toxins…) can induce a damage in the endothelium of the arterial wall leading to endothelial cell activation, NO reduction and increased permeability of the endothelial barrier. This increased permeability facilitates the entry and accumulation of low density

lipoproteins (LDL) in the intima, where they are oxidized by reactive oxygen species (ROS). Ox-LDL particles induce the expression of tumoral necrosis factor α (TNF-α) and interleukin 1 (IL-1), favoring the expression of adhesion molecules like VCAM-1 or ICAM-1 and the secretion of chemotactic molecules like the monocyte chemotactic protein 1 (MCP-1) by endothelial cells. This allows the attraction, migration and adhesion of circulating monocytes to the intima (Galkina and Ley, 2007) (Sakakura et al., 2013), where they transform into macrophages that phagocyte and accumulate ox-LDL particles becoming foam cells and attracting more monocytes and smooth muscle cells that proliferate and fill in with lipids generating more foam cells that accumulate in the lesion site. All this process induces a local chronic inflammation and the growth of the atheroma plaque (Llodra et al., 2004). There is an interaction of macrophages with T lymphocytes and other leukocytes that contributes to the inflammation and atherogenic process through the liberation of reactive oxygen species (ROS), growth factors and cytokines. At the same time, the proliferative smooth muscle cells migrate from the media to the intima and secrete extracellular matrix proteins that are going to generate a fibrous cap (Dzau et al., 2002). Under this fibrous cap it is formed the necrotic core by apoptotic and necrotic vascular and inflammatory cells. As the inflammation persists, leucocytes start secreting metaloproteinases and collagen synthesis inhibitors that together with the hypoxia induced neovascularization lead to the plaque rupture and release of the content into the blood torrent, inducing platelets activation and aggregation and finally the formation of an occlusive thrombus (Newby, 2008).

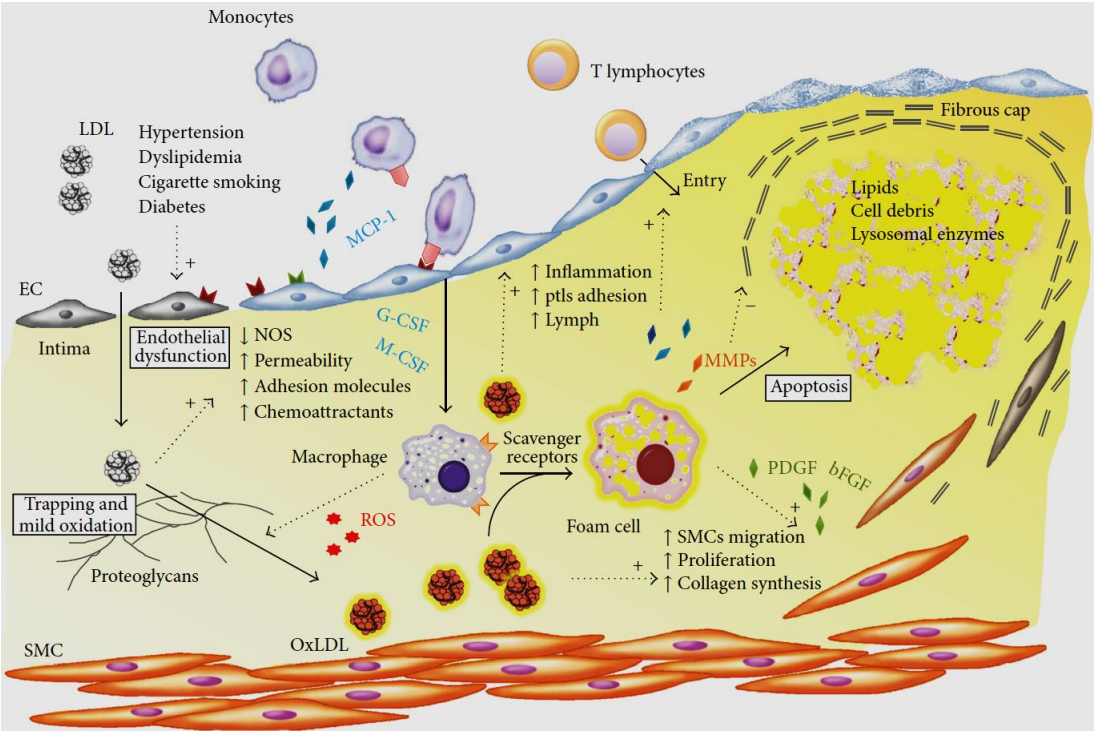

Figure 9. Schematic overview of key mechanisms of atherosclerosis in an evolving atherosclerotic plaque. (Maiolino et al., 2013)

For many years it has been thought that the main cause of atherosclerosis is the lipid accumulation in the arterial wall. However, during the last decades different animal models susceptible for atherosclerosis have revealed and important role of the adaptive immunity in the initiation, progression and persistence of the disease (Figure 10). It has been shown that Th1 cells promote atherogenesis (Buono et al., 2005). These cells secrete cytokines like IFNγ, IL-1 and TNFα, well known as promoters of inflammation through activation of macrophages and vascular cells.

Moreover, Treg cells have been associated with suppressive inflammatory responses and atherosclerosis mitigation, both in human and animal models. It has been shown a reduction in the proportion of Treg cells as well as Treg cell produced cytokines (IL-10, TGF-β) in patients with acute coronary syndrome (Cheng et al., 2008). Furthermore, Treg depletion in hypercholesterolemic mice results in increase atherosclerosis and vascular inflammation (van Es et al., 2010) (Wigren et al., 2011). Also, overexpression of IL-10 by activated T lymphocytes inhibits atherosclerosis in LDL receptor-deficient mice (Pinderski et al., 2002) while deficiency of this interleukin leads to higher atherosclerotic lesions in ApoE deficient mice (Caligiuri et al., 2003), showing that IL-10 may reduce atherogenesis and improve the stability of plaques.

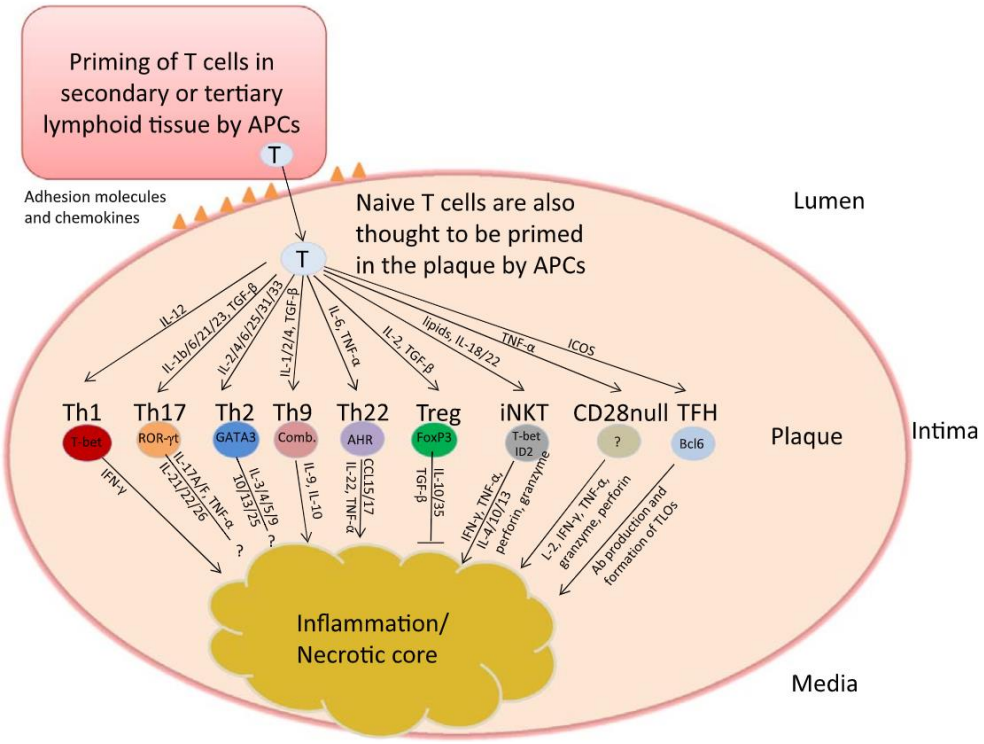

Figure 10. T helper cells and their role in atherosclerosis. The inflammatory activity in atherosclerotic plaques is determined by the balance between pro- and anti-inflammatory immune responses. T helper cells can be primed into several different cell types (Th1, 2, 9, 17, 22, regulatory and follicular) in lymphoid organs or in the atherosclerotic plaque. Regulatory T cells dampen the inflammation in the atherosclerotic plaque by reducing the availability of IL-2 to the other cells as well as by producing IL-10 and TGF-β. (Gronberg et al., 2017)

However, the role of Th17 cells in atherosclerosis remains controversial, existing studies both in favor and against its pro-atherogenic effects. Recent studies have shown increased levels or Th17 cells and their main effector cytokine, IL-17, in patients with coronary atherosclerosis. Moreover, it has been detected IL-17 expression in atherosclerotic plaques and infiltrating T lymphocytes both in humans and mice (Eid et al., 2009) (Cheng et al., 2008). ApoE deficient mice present higher levels of IL-17A in serum as well as higher mRNA levels of that cytokine and CD3+ IL17+ cells in aorta, lamina propria and peripheral lymph nodes compared to wild type animals (Lim et al., 2014) (Smith et al., 2010) (Erbel et al., 2009). Also, Apoe$^{-/-}$ IL-17$^{-/-}$ mice present reduced atherosclerosis after high fat diet feeding (Usui et al., 2012). However, the opposite role was claimed in a different study in which these mice developed more atherosclerosis than wild type animals and the progression of the disease was reduced after intraperitoneal injection of recombinant IL17A, thus giving evidence of a protective role for IL-17 (Danzaki et al., 2012). Other study supports the anti-atherogenic role of IL-17 in SOCS-3 deficient mice which develop less atherosclerosis than their wild type littermates. However, these mice present higher levels of both IFN-g and IL-17 together with IL-10, making difficult to elucidate whether the observed effect is mediated by IL-17 or IL-10 (Taleb et al., 2009).

5.3. Myocarditis: autoimmune response.

Myocarditis is defined as inflammation of the myocardium. This inflammation often resolves spontaneously but in some cases it progresses towards a dilated cardiomyopathy and subsequent heart failure, being the cause of 8.6–12% of sudden deaths in young adults (Fabre and Sheppard, 2006). Myocarditis is diagnosed by endomyocardial biopsy using established histological, immunological and immunohistochemical criteria (Aretz et al., 1987).

According to the widely used “Dallas” criteria published in 1987, a diagnosis of active myocarditis requires the presence of inflammatory infiltrates of non-ischemic origin in myocardial tissue associated with necrosis and/or degeneration of adjacent cardiomyocytes (Aretz et al., 1987). More recently, the ESC Working Group on Myocardial and Pericardial Diseases proposed a definition of myocarditis as abnormal number of inflammatory infiltrates in myocardial tissue (≥14 leucocytes/mm2 including up to 4 monocytes/mm2 with the presence of ≥7 cells/mm2 CD3-positive T lymphocytes) (Caforio et al., 2013b).

Dilated cardiomyopathy (DCM) is referred to as left ventricular dilation associated with systolic dysfunction in the absence of coronary artery disease (Reichart et al., 2019). Histologically, it is manifested by extensive replacement of cardiac muscle cells with fibrotic tissue and collagen deposition (Jefferies and Towbin, 2010, Schultheiss et al., 2019). DCM patients develop not only

heart pump weakening, but also heart valve problems, blood clots, and arrhythmias leading to heart and secondary organ failures.

The etiology of myocarditis can be very diverse and can be divided into infective, immune related or toxic agents (Table 1) (Caforio et al., 2013a), being viral infection the most commonly diagnosed in Europe and North America. However, the most common cause worldwide is Chagas disease, an illness endemic to Central and South America that is due to infection by the protozoan *Trypanosoma cruzi* (Nunes et al., 2018). Heart-specific T cells and high titers of heart-specific autoantibodies have been identified in Chagastic patients (Cunha-Neto et al., 1996) as well as in experimental mouse models (Tibbetts et al., 1994, Rizzo et al., 1989).

Table 1. Etiopathogenetic agents associated with myocarditis/inflammatory cardiomyopathy.

1. Infective myocarditis	
Bacterial	Staphylococcus, Streptococcus, Pneumococcus, Meningococcus, Gonococcus, Salmonella, Corynebacterium diphtheriae, Haemophilus influenzae, Mycobacterium (tuberculosis), Mycoplasma pneumoniae, Brucella
Spirochetal	Borrelia (Lyme disease), Leptospira (Weil disease)
Fungal	Aspergillus, Actinomyces, Blastomyces, Candida, Coccidioides, Cryptococcus, Histoplasma, Mucormycoses, Nocardia, Sporothrix
Protozoal	Trypanosoma cruzi, Toxoplasma gondii, Entamoeba, Leishmania
Parasitic	Trichinella spiralis, Echinococcus granulosus, Tenia solium
Rickettsial	Coxiella burnetii (Q fever), R. rickettsii (Rocky Mountain spotted fever), R. tsutsugamuschi
Viral	Coxsackievirus A and B, echovirus, poliovirus, hepatitis viruses, influenza A and B viruses, adenovirus, respiratory syncytial virus, mumps virus, measles virus, rubella virus, dengue virus, chikungunya virus, yellow fever virus, Junin virus, Lassa fever virus, lymphocytic choriomeningitis virus, herpes simplex virus, varicella-zoster, human herpes virus-6, cytomegalovirus, Epstein-Barr virus, variola virus, vaccinia virus, parvovirus B19, rabies virus, human immunodeficiency virus-1
2. Immune-mediated myocarditis	
Allergens	Tetanus toxoid, vaccines, serum sickness
	Drugs: penicillin, cefaclor, colchicine, furosemide, isoniazid, lidocaine, tetracycline, sulfonamides, phenytoin, phenylbutazone, methyldopa, thiazide diuretics, amitriptyline
Alloantigens	Heart transplant rejection
Autoantigens	Idiopathic: Virus-negative lymphocytic, virus-negative giant cell
	Associated with autoimmune or immune-oriented disorders: systemic lupus erythematosus, rheumatoid arthritis, Churg-Strauss syndrome, Kawasaki's disease, inflammatory bowel disease, scleroderma, polymyositis, myasthenia gravis, insulin-dependent diabetes mellitus, thyrotoxicosis, sarcoidosis, Wegener's granulomatosis
3. Toxic myocarditis	
Drugs	Amphetamines, anthracyclines, cocaine, cyclophosphamide, ethanol, fluorouracil, lithium, catecholamines, hemetine, interleukin-2, trastuzumab, clozapine
Heavy metals	Copper, iron, lead
Miscellaneous	Scorpion sting, snake and spider bites, bee and wasp stings, carbon monoxide, inhalants, phosphorus, arsenic, sodium azide
Hormones	Pheochromocytoma, vitamins: beri–beri
Physical agents	Radiation, electric shock

Experimental autoimmune myocarditis (EAM) is a mouse model of myocarditis that can be induced in susceptible mouse strains by immunization with cardiac α-myosin heavy chain (MyHC-α)–derived peptides (Neu et al., 1987). In this regard, it has been shown that EAM is a $CD4^+$ T-cell–mediated disease which development depends critically on the interleukin (IL)-23–STAT4 axis, promoting the expansion of an autoreactive $CD4^+$ T-cell subset characterized by IL-17 production (Sonderegger et al., 2006) (Rangachari et al., 2006) (Liu et al., 2012). Mice lacking T-bet, a T-box transcription factor essential for Th1 lineage differentiation, develop a severe form of EAM with increased IL-17 release from heart-infiltrating cells (Rangachari et al., 2006). These findings further support the notion that IL-17 directly accounts for disease development. It has been reported that CD69 plays an important role in the control of the severity of myocarditis and subsequent dilated cardiomyopathy. *Cd69*$^{-/-}$ mice develop a severe form of autoimmune myocarditis that progresses to DCM and heart failure. This pathogenic effect is exerted mainly through an increased Th17-mediated inflammatory response (Cruz-Adalia et al., 2010).

6. Gut microbiota

The collection of microbial populations, including bacteria, fungi, parasites and viruses that colonize the skin and mucosal surfaces of vertebrates is commonly referred to as microbiota. In humans, more than 100 trillion microorganisms, mostly bacteria, colonize the oral–gastrointestinal tract, mainly the distal intestine. There is a mutualistic relationship between the microbiota and the host in which the host provides nutrients and niches for microbial survival and, in turn, the microbiota contributes to many host physiological processes, such as the digestion and fermentation of carbohydrates, the production of vitamins, the development of gut-associated lymphoid tissues (GALTs), the polarization of gut-specific immune responses and the prevention of colonization by exogenous pathogens (Hooper and Macpherson, 2010, Renz et al., 2011, Stecher and Hardt, 2011). However, when the mutualistic relationship between the host and microbiota is disrupted, the gut microbiota can cause or contribute to disease (Littman and Pamer, 2011, Honda and Littman, 2012).

The gut microbiome is acquired from the environment at the time of birth and its composition depends on many factors including the type of birth (caesarean or vaginal delivery (Jakobsson et al., 2014)), the diet and the environment (Tamburini et al., 2016, Rodriguez et al., 2015). The human gut microbiome is dominated by five phyla: Bacteroidetes, Firmicutes, Actinobacteria, Proteobacteria and Cerrucomicrobia. However, the most abundant groups in the healthy gut are Bacteroidetes (manly *Bacteroides* or *Prevotella* species) and Firmicutes (largely *Clostridium* and *Lactobacilli* species) (Arumugam et al., 2011, Sweeney and Morton, 2013)

6.1. Role of gut microbiota in immunity and autoimmune disorders

Resident microbiota modulates the development of specific lymphocyte subsets in the gut. Treg cells accumulate in the intestine, where they help to maintain gut homeostasis. The development of peripherally derived Treg cells is partly dependent on the gut microbiota, as the number of Treg cells is greatly decreased in the colonic lamina propria of germ-free mice (Atarashi et al., 2011, Geuking et al., 2011). *Clostridium* spp. clusters IV and XIVa, polysaccharide A (PSA)$^{+}$*Bacteroides fragilis* and other commensal bacteria promote the development and/or the activation of regulatory T cells (Atarashi et al., 2011, Geuking et al., 2011). In addition, it has been shown that in antibiotic-treated or germ free mice the presence of intestinal Th17 cells is greatly reduced (Shaw et al., 2012, Atarashi et al., 2008) which indicates that the microbiota has a crucial role in Th17 cell development. These cells, that have a role in the development of autoimmune disease, are induced by particular species of *Clostridia*-related bacteria, called segmented filamentous bacteria (SFB) (Ivanov et al., 2008, Ivanov et al., 2009, Gaboriau-Routhiau et al., 2009). The precise mechanism by which SFB promote Th17 cell development remains to be fully elucidated. The adhesion of SFB to the host epithelium upregulates serum amyloid A protein (SAA) production, which, in turn, promotes IL-6 and IL-23 production by CD11c^{+} lamina propria dendritic cells (DCs) and the subsequent induction of Th17 cell differentiation (Ivanov et al., 2009). These Th17 cells might migrate to the periphery to affect systemic and central nervous system (CNS) immunity promoting the depelopment of several immune disorders. Increased intestinal Th17 cells enhance the expansion of pathogenic autoantigen-specific T cells in the intestine and cause inflammation in the CNS. Disease symptoms of experimental autoimmune encephalomyelitis (EAE) are reduced in antibiotic treated or germ free mice (Ochoa-Reparaz et al., 2009, Lee et al., 2011, Berer et al., 2011) while are exacerbated after SFB monocolonization (Lee et al., 2011). By contrast Treg cell differentiation induced by *B. fragilis* can prevent EAE symptoms (Ochoa-Reparaz et al., 2010). Induced Th17 cells can also promote autoimmune arthritis by facilitating autoantibody production by B cells (Wu et al., 2010). In addition, microbiota-induced interleukin-1β (IL-1β) signalling participates in the development of rheumatoid arthritis through the induction of Th17 cells (Nakae et al., 2003).

Microbiota might also determine susceptibility to type 1 diabetes (T1D) an autoimmune disorder that results in the destruction of insulin-producing cells in the pancreas. A decreased Firmicutes/Bacteroides ratio on a phylum level is associated with lower risk of T1D in non-obese diabetic mice (Wen et al., 2008). Commensal bacteria also protects against allergic inflammation in the lungs through inhibition of IgE production in the gut (Hill et al., 2012)

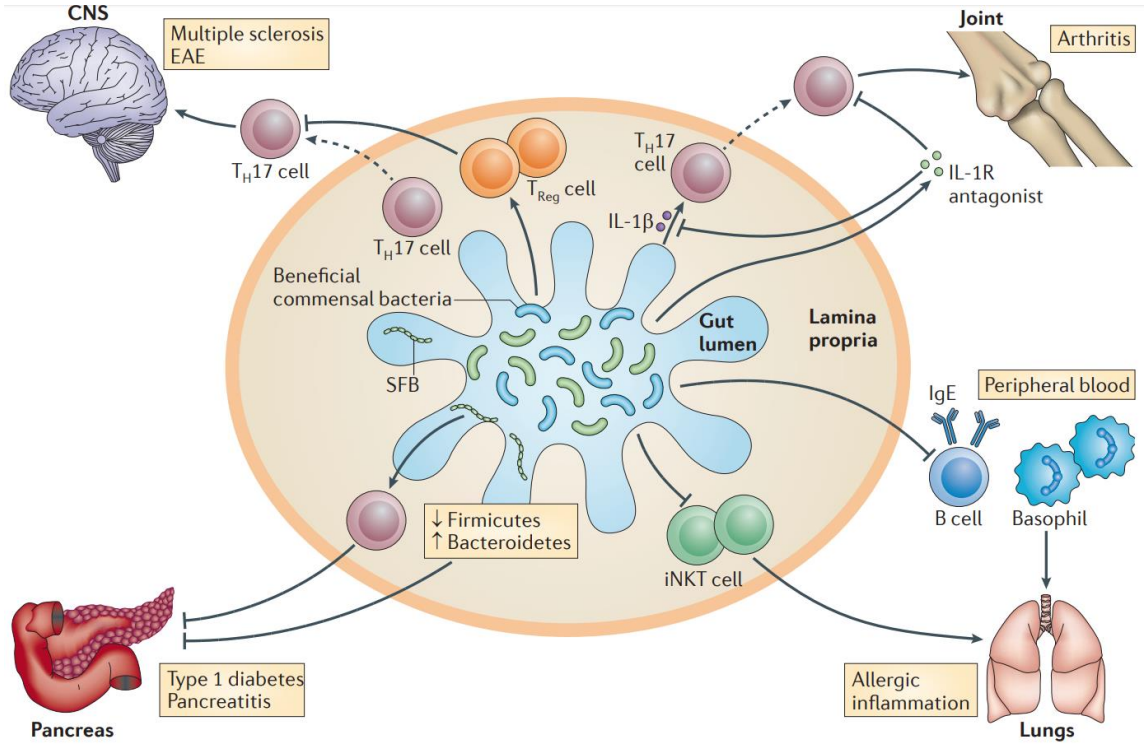

Figure 11. Gut microbiota affects autoimmune diseases. SFB induced Th17 cells can promote EAE and reumatoid arthritis development, while Treg cells induced by beneficial commensal bacteria reduce inflammation. Imbalance in the Firmicutes/Bacteroidetes ratio can promote T1D and allergic inflammation in the lungs can be reduced by inhibition of IgE production in the gut and decreased accumulation of iNKT cells due to exposure to microorganisms in neonatal life. SFB, Segmented Filamentous Bacteria. EAE, experimental autoimmune encephalomyelitis. T1D, Type 1 diabetes. (Kamada et al., 2013)

6.2. Gut microbiota and heart failure

There are many recent publications that associate the gut microbiota with heart disease, especially heart failure (Jie et al., 2017, Luedde et al., 2017, Nagatomo and Tang, 2015). Changes in the gut microbiota can lead to the development of risk factors for atherosclerotic vascular disease and directly influence the progression of the disease and heart failure.

Obesity, one of these risk factors for cardiovascular disease, is associated with changes in the relative abundance of Bacteroidetes and Firmicutes, with high Firmicutes levels (Ley et al., 2006). In addition, hypertension and diabetes have also been found to have associations with specific gut microbial patterns, and researchers have discovered certain links in the pathogenesis of these diseases and bacterial interactions (Pevsner-Fischer et al., 2017, Upadhyaya and Banerjee, 2015). Also, in patients with coronary heart disease (CHD), the proportion of the phylum Firmicutes was higher than in those without the disease (Cui et al., 2017).

Microbiota derived metabolites are also linked to increased cardiovascular risk. This is the case of trimethylamine–*N*-oxide (TMAO) produced after the metabolism of dietary L-carnitin and choline present at high levels foods rich in cholesterol and fat like red meat, liver and eggs (Wang et al., 2011, Tang et al., 2013). TMAO has been shown to affect cholesterol and sterol metabolism in animal models, enhancing macrophage cholesterol accumulation and atherosclerosis development. In multiple human studies, elevated TMAO has been associated with prevalent CVD and incident risks for MI, stroke, death, and revascularization (Li et al., 2017) (Schiattarella et al., 2017).

The gut microbiota is also implicated in the pathogenesis of heart failure (HF). In HF, due to reduced ejection fraction, there is a reduction in intestinal blood flow and low oxygen delivery that predisposes the gut to the growth of pathogenic types of anaerobic bacteria (Sandek et al., 2014). Patients with chronic HF also present bacterial overgrowth in the mucus layer adjacent to the apical surface of the colonic mucosa due to failure in the absorptive function of the gut. Increased intestinal permeability has been shown to correlate with right atrial pressure and C-reactive protein levels (Sandek et al., 2014) (Pasini et al., 2016).

There are also some evidences suggesting that gut dysbiosis is associated with myocarditis. Polyantibiotic treated mice are protected from EAM and fibrotic cardiac dysfunction in a Th17 dependent manner, as the same effect is not observed in *Il17RA*$^{-/-}$ treated animals (Barin et al., 2017). It has been reported that Th17 cells play a critical role in the development of cardiac inflammatory disease and heart failure and an important role for segmented filamentous bacteria (SFB) in eliciting Th17 responses from intestinal T cells has been also well-described. (Ivanov et al., 2009) (Ivanov and Honda, 2012) (Gaboriau-Routhiau et al., 2009), predicting that SFB colonization could contribute to susceptibility to autoimmune disease through the induction of Th17 cells (Lee et al., 2011; Wu et al., 2010).

OBJECTIVES

OBJECTIVES

In this doctoral Thesis the role of CD69 in innate and adaptive immune cells regulation, as well as in different animal models has been studied. Thus, the main objectives of this work can be divided in three different parts:

1. To study the role of CD69 in the regulation of "Natural Killer" (NK) cells receptors and activity in the context of innate immunity.

2. To study the role of CD69 in an "in vivo" model of atherosclerosis in the context of adaptive immunity.

3. To study the role of CD69 in the microbiota composition and the development of cardiomyopathy in germ free conditions.

MATERIALS AND METHODS

MATERIALS AND METHODS

1. Mice

CD69 deficient mice were generated in the 129/Sv background as described (Lauzurica et al., 2000) and backcrossed onto the C57BL/6 and BALB/c strain for at least 12 generations (Martin et al., 2010b)

ldlr$^{-/-}$ CD45.1+ mice were generated by crossing C57BL/6 -/-Ly5.1 mice (CD45.1+) from the Jackson Laboratory (B6.SJL-Ptprca Pepcb/BoyJ: 002014) with C57BL/6 129S7-Ldlrtm1Her/J mice from Charles River. This line was crossed with *Cd69*$^{-/-}$ or *Cd69*$^{+/+}$ C57BL/6 double reporter (dRep) for Treg cells (FIR mice, Foxp3–monomeric red fluorescent protein [mRFP]) and Th17 cells (IL-17A–IRES–enhanced green fluorescent protein [eGFP] (FoxP3-mRFP/IL17e-GFP), provided by Dr Richard Flavell (Yale University School of Medicine, 400 New Haven, CT). dRep mice allow us to monitor the presence of live Treg cells and Th17 cells by FACs throughout the experiment.

Rag2$^{-/-}$*γc*$^{-/-}$ (Rag2/Il2rg) mice were provided by the laboratory of M. L. Toribio (Centro de Biología Molecular, CSIC, Spain) and were intercrossed with *Cd69*$^{-/-}$ mice to generate *Il2rγ*$^{-/-}$*/Cd69*$^{-/-}$ mice.

Animals were housed and used under specific-pathogen-free (SPF) conditions at the Centro Nacional de Investigaciones Cardiovasculares (CNIC) animal facility. *Cd69*$^{-/-}$ BALB/c mice were re-derived into germ-free mice by 2-cell embryo transfer into germ-free recipient females at the Clean Mouse Facility of the University of Bern (Switzerland) and bred and maintained in flexible film isolators. These isolators were ventilated with HEPA-filtered sterile air under positive pressure and fitted with a side port containing a double door system to allow antiseptic connection of a transport drum to import sterile food, water and bedding. Germ-free mice were routinely monitored by culture-dependent and -independent methods and were independently confirmed to be pathogen-free.

All animal procedures were approved by the ethics committee of the Comunidad Autónoma de Madrid and conducted in accordance with the institutional guidelines that comply with European Institutes of Health directive 407 2010/63/UE of the European Parlament (Official Journal of the European Union, Vol. 53:33-79, 409, 2010).

2. Animal models and procedures

2.1. Graft versus host disease induction

2.1.1. T-cell isolation

Single-cell suspensions were obtained from spleen and incubated with the following biotinylated antibodies: CD8, CD19, B220, major histocompatibility complex (MHC) class II, CD11c, IgM, Dx5 and CD11b, followed by streptavidin Microbeads (MACS; Miltenyi Biotec). CD4+ T cells were negatively selected with a magnetic LS MACS column, according to the provider's instructions. The negative fraction was used for GvHD induction (adoptive transfer experiments).

2.1.2. Bone marrow transplantation

Recipient BALB/c ($H2^d$) WT or *Cd69*$^{-/-}$ mice were irradiated with 2 doses of 6.5 Gy 4 hours apart. Bone marrow cells were isolated from tibias and femurs of C57BL/6 donor mice, and were T-cell depleted by incubation with anti-CD3 biotinylated antibody, followed by streptavidin Microbeads (MACS; Miltenyi Biotec). T cells were positively selected with a magnetic LS MACS column, according to the provider's instructions, and the eluted fraction corresponded to T-cell depleted bone marrow cells. $1.5x10^6$ of these cells were intravenously injected to recipient mice together with $0.5x10^6$ splenic T-cells from C57BL/6 mice isolated as described. A total volume of 200µL was injected into each mouse. For anti-CD69 mAb-2.2 treatment the antibody was intravenously injected together with the naïve splenic T-cells three days after bone marrow transplant.

2.1.3. Clinical score assessment

Mice were monitored every day and a clinical score was assigned to each mouse as indicated in table 2 (Cooke et al., 1996).

Table 2. Assessment of Clinical GvHD in Transplanted Animals – adapted from (Cooke et al., 1996)

Criteria	Grade 0	Grade 1	Grade 2
Weight loss	<10%	>10% to <25%	>25%
Posture	Normal	Hunching noted only at rest	Severe hunching impairs movement
Activity	Normal	Mild to moderately decreased	Stationary unless simulated
Fur texture	Normal	Mild to moderate ruffling	Severe ruffling/poor grooming
Skin integrity	Normal	Scaling of paws/tail	Obvious areas of denude skin

2.2. Tumor growth in vivo

B16 melanoma cells resuspended in 200 µL of phosphate-buffered saline (PBS) were injected intravenously in *Rag2*$^{-/-}$*γc*$^{-/-}$ or *Rag2*$^{-/-}$*γc*$^{-/-}$ *Cd69*$^{-/-}$ mice together with 100 ug of anti-CD69 mAb-2.2 in the case of treated mice. A second intraperitoneal injection of 100 ug of anti-CD69 mAb-2.2 was performed five days after tumor injection. At 12 days lungs were collected and number of tumors were counted.

2.3. "In vivo" model of atherosclerosis

2.3.1. Atherosclerosis induction

To evaluate the influence of immune cell CD69 expression on atherosclerosis development, 5 week old male *Ldlr*$^{-/-}$ CD45.1+ mice were lethally irradiated with two doses of 6.5 Gy and reconstituted with 10^6 bone marrow precursors from *Cd69*$^{-/-}$ double reporter for Foxp3-mRFP and IL-17A-eGFP24 (*Cd69*$^{-/-}$dRep) mice or WT littermates (*Cd69*$^{+/+}$dRep), both CD45.2+. In addition, mixed bone marrow chimeras proficient or deficient for CD69 only in the lymphoid compartment were generated; *ldlr*$^{-/-}$ CD45.1+ mice were reconstituted with a mix of 75% CD45.2+ *Rag2*$^{-/-}$*γc*$^{-/-}$ BM plus 25% of either dRep or *Cd69*$^{-/-}$dRep BM (hereafter: LC *Cd69*$^{+/+}$ and LC *Cd69*$^{-/-}$ respectively). Myeloid chimeras in which CD69 is present or absent only in the myeloid compartment were also generated reconstituting *ldlr*$^{-/-}$ mice with a mix of 25% *Cd69*$^{+/+}$ BM cells plus 75% of either *Rag2*$^{-/-}$*γc*$^{-/-}$ *Cd69*$^{+/+}$ or *Rag2*$^{-/-}$*γc*$^{-/-}$ *Cd69*$^{-/-}$ BM cells. After 6 weeks, mice were checked to be fully reconstituted by phenotyping blood from the tail vein after surface staining with anti-CD45.1 (receptor cells) and CD45.2 (donor cells) antibodies and FACS analysis and were started on a high fat diet (SSNIFF, S9167-E010) until the indicated time points of sacrifice.

2.3.2. Monitoring of blood leukocyte subsets.

To assess the immune response, blood from the tail vein was collected and peripheral blood leukocytes (PBLs) were purified by Ficoll-Paque (GE healthcare) density gradient. Cells were stimulated in vitro with PMA and ionomycin in the presence of brefeldin A for 4 hours and stained with anti-CD4 APC antibody (BD pharmingen). The percentage of CD4+ IL-17-eGFP+ or CD4+ Foxp3-RFP+ cells was assessed by flow cytometry using a Fortessa (BD Biosciences) flow cytometer and subsequent analysis with the FlowJo software. The same procedure was followed at the endpoint of the experiment to evaluate the immune response in spleen, non-draining (axillary and inguinal) lymph nodes and draining (para-aortic) lymph nodes.

A different group of mice was studied to analyze the kinetics of all leukocyte subsets in blood during high fat diet administration. PBLs were purified as described above every two weeks until the end of the experiment and stimulated overnight with anti-CD3/CD28 (2µg/ml) for T cell activation or with LPS (100 ng/ml) for the rest of the cells. Surface staining with anti-CD44/CD62L was performed to distinguish naïve and memory CD4+ T cells and B220 to stain B cells. Myeloid cells were analyzed after surface staining with anti-CD11b, -CD11c, -Ly6G/C, - F4/80 and NK cells with anti–Nkp46. The expression of CD69 with anti-CD69 was analyzed after stimulation in all the leukocyte subsets by FACS.

2.4. Experimental Autoimmune Myocarditis (EAM) induction

Cd69$^{-/-}$ and control mice were immunized subcutaneously on days 0 and 7 with 100 µg/0.2 mL MyHC-α peptide (MyHC-$_{\alpha 614–629}$) Ac-RSLKLMATLFSTYASADR-OH emulsified 1:1 in PBS/complete Freund's adjuvant (1 mg/mL; H37Ra; Difco Laboratories, Detroit, Mich) (Neu et al., 1987). Myocarditis in α-MyHC/CFA immunized mice is characterized by massive infiltration of mainly myeloid cells together with CD4+ T cells and few B and CD8+ T lymphocytes, existing an acute Inflammation of cardiac tissue typically 14–21 days after the first immunization. Resolution of the inflammation is followed by the progressive accumulation of fibrotic tissue in the myocardium, ventricular dilatation and impaired heart function, allowing the study of dilated cardiomyopathy in the chronic phase between days 58 and 61 after induction (Baldeviano et al., 2010)

3. NK cell isolation

Single-cell suspensions were obtained from spleen and NK cells were isolated using an anti-Nkp46 microbead kit (Myltenyi) for further sorting in the AUTOMACs using Possel-ds program. The pooled cells were labeled with anti NKp46-FITC to check purity (higher than 85%) by FACs analysis and were frozen at -80ºC for further RNA isolation and RNAseq analysis.

4. Cell culture

All primary cell cultures were maintained in RPMI 1640 medium (SIGMA-ALDRICH) supplemented with 10% heat-inactivated calf serum (FCS, GibCo), 2 mM L-glutamine, 0.1 mM nonessential amino acids, 100mM sodium pyruvate, 0.05mM β-mercaptoethanol, 100 U/ml penicillin, and 100 µg/ml spreptomycin, at 37ºC, 5% CO2.

NKL cell line kindly given by Hugh Thombson Reyburn (Centro Nacional de Biotecnología, Madrid) were cultured in RPMI 1640 medium supplemented with 5% heat-inactivated calf serum (FCS,

GibCo), 5% heat-inactivated human serum (H4522 Sigma-Aldrich), 2 mM L-glutamine, 0.1 mM nonessential amino acids, 100mM sodium pyruvate, 0.05mM β-mercaptoethanol, 100 U/ml penicillin, and 100 µg/ml spreptomycin, and 50U/ml rh-IL2 (Peprotech) at 37ºC, 5% CO2.

5. RNA isolation and assessment of mRNA transcripts

RNA extraction from sorted cell pellets was performed using Trizol (TriReagent). Chloroform (200µl) was added, samples were mixed, and centrifuged (12,000 g, 15 min, 4°C). The upper aqueous phase was collected and RNA was precipitated with ice-cold isopropanol by centrifugation. The RNA pellet was washed with 75% ethanol, dried and resuspended in RNase-free water. DNAse treatment was carried out to eliminate genomic DNA with Turbo DNAse-free kit (Ambion).

Inverse transcription (RT-PCR) was done using High Capacity cDNA reverse transcription kit (Applied Biosystems) and mRNA expression levels was assessed by qPCR with design oligos and SYBR green PCR master mix (Applied Biosystems)

6. RNA-seq

Rag2$^{-/-}$, *Rag2*$^{-/-}$ *Cd69*$^{-/-}$ and *Rag2*$^{-/-}$ mice treated with 2.2 anti-CD69 mAb were challenged with allogenic cells injection as in an in vivo killing assay. After 4 hours NK cells were sorted from total splenocytes suspension. Three pools of NK cells obtained from 4 mice each were included in the The RNA integrity (RNA Integrity Score ≥ 6.8) and quantity was determined on the Agilent Bioanalyzer (Agilent Technologies Microarray Platform) following manufacturer's recommendation and subjected to cDNA synthesis. RNA-seq analysis using Illumina HiSeq 2500 platform (NGS) was performed by the CNIC Genomics Unit. Data was analyzed by the CNIC Bioinformatics Unit

7. Cell staining for Flow cytometry analysis

All superficial staining was performed in FACs Buffer (PBS, BSA 5%, EDTA 0.5 µM) with different mouse specific antibodies conjugated with different fluorochromes.

For NK cells staining: CD69, NK-p46, NKG2A/C/E (BD Bioscience); Ly49E/F, Ly49C/I/F/H, Ly49G2, CD94; Ly49H, Ly49D (Biologend); Ly49E/F, Ly49C/I/F/H, Ly49G2, CD94, NKG2D (eBioscience).

For assessment of chimerism and analysis of different subsets in peripheral blood and heart: CD45.1, CD45.2, CD4, CD8, CD11b, Ly6C (BD Bioscience); CD11c, CD27, F4/80 (Biolegend); Gr-1, B220 (BD Pharmingen).

For intracellular staining, after superficial staining cells were fixed with paraformaldehyde 2% in PBS and permeabilized in FACs buffer with 0.5% saponine. IL-17 and IFN-γ (BD-Bioscience) were diluted in FACs buffer with 0.5% saponine.

8. Mass cytometry

For Mass cytometry analysis five mice per strain were sacrificed and total blood, peripheric lymph nodes (axillary and inguinal lymph nodes), femur, mesenteric lymph nodes and spleen were collected. Cells were purified, stained with Cell-ID Cisplatin Viability Staining (Fluidigm) barcoded with the Cell-ID™ 20-Plex Pd Barcoding Kit (Fluidigm) following provider's instructions. Samples were subsequently pooled by organ and washed with Fluidigm-provided metal free buffers (Table 3). After superficial staining, intracellular staining and intercalation was performed according to the provider's instructions. Fixed samples were sent to the Flow Cytometry Core Facility of the Ecole Polytechnique Fédéral de Lausanne (EPFL)/Swiss Federal Institute of Technology (Switzerland), in collaboration with Miguel Toulson and Christoph Schwärzler. Samples were analyzed using a CyTOF2 (Helios) mass cytometer.

Table 3. Metal conjugatied antibodies and Fluidigm Buffers used for CyTOF experiment

Custom conjugations	Metal conjugated antibodies	Buffers
Anti- Mouse Ly49D 4E5-162Dy	Anti- Mouse CD45.2 (104) - 147Sm	Cell-ID Cisplatin, 100 µL
Anti- Mouse CD314 (NKG2D) CX5-156Gd	Anti- Mouse Nkp46 (29A1.4) -167Er	Cell-ID Intercalator-Ir - 500 µM
Anti- Mouse Ly49C/I/F/H 14B11-158Gd	Anti- Mouse NK1.1 (PK136) -170Er	Maxpar® Cell Staining Buffer - 500 mL
Anti- Mouse Ly49H 3D10-175Lu	Anti- Mouse CD3e (145-2C11)-152Sm	MaxPar® Fix I Buffer
Anti-Mouse Ly49G2 eBio4D11-153Eu	Anti- Mouse CD11b (M1/70)-148Nd	MaxPar® Perm-S Buffer
	Anti-Ms Perforin (OMAK-D)-172Yb	Maxpar® Fix and Perm Buffer - 100 mL
	Anti- Mouse IFNg (XMG1.2)-165Ho	Cell-ID 20-plex Pd Barcoding kit
	Anti- Mouse CD62L (MEL-14) -164Dy	
	Anti- Mouse CD19 (6D5) -149Sm	
	Anti- Mouse CD69 (H1.2F3)-145Nd	
	Anti-Human/Mouse CD27 (LG.3A10)-150Nd	
	Anti-Hu Granzyme B (GB11)-173Yb (100 Test)	

9. Bioinformatics analysis of mass cytometry

CyTOF experiment data has been analysed by Carlos Torroja form the Bioinfomatics Unit of CNIC following the R CyTOF workflow described by (Nowicka et al., 2017) with some modifications. Raw intensity data has been transformed and scaled with the arcsinh (hyperbolic inverse sine) function as implemented in the cytofAsinh method of the cytofkit R package (Chen et al., 2016). NK cells have been selected trough the following gating steps: 1) Standard gating to select real cells (Ce140Di [-Inf,4], Eu151Di [-Inf,4]) 2) B-cells and T-cells have been discarded based on has been applied and NK cells have been selected on have been removed based on CD3- and CD19- markers (CD19: [-Inf,1], CD3: [-Inf,1]). 3) Finally, NK cells were selected based on CD45+,Nkp46+ markers (CD45:[1,Inf], Nkp46:[0.5,Inf]). Unbiased cluster identification on NK cells was performed using the Phenograph algorithm (Levine et al., 2015) implemented in cytofkit R package and for visualization purposes t-stochastic neighbour embedding (t-SNE) (Van Der Maaten & Hinton, 2008) dimensionality reduction algorithm was used (Rtsne package, Jesse H. Krijthe 2015). Differential cell population abundances have been tested using a generalized linear mixed model with binomial likelihood and sample as a random variable, as described in (Nowicka et al., 2017). For differential marker expression between clusters, a linear mixed effect model has been applied.

10. anti-CD69 mAb-2.2 production

mAb-2.2 (IgG1-K) specific for mouse CD69, was generated as described in (Esplugues et al., 2005). The antibody was purified from concentrated hibridome supernatants using a G protein column (GE). It was further dialysate against PBS in PD10 column and its activity was tested by CD69 internalization assays in thymocytes with flow cytometry.

11. Co-Immunoprecipitation and Western Blot

Protein extracts from human NKL cells were prepared in buffer PD (Tris HC 40mM, ph 8.0; NaCl 0.5 M; EDTA 6 mM; EGTA 6 mM; 0.1% NP40) containing proteases inhibitors cocktail (Complete Mini, Roche). Extracts were incubated with a mix of mouse anti-human CD69 antibodies (TP1/55, TP1733, TP1/8; produced in the laboratory of Francisco Sánchez Madrid (Cebrian et al., 1988)). After that they were incubated with G protein Sepharose beads (GE Healthcare). Co-immunoprecipitated proteins were separated by SDS-PAGE in a 12% SDS-polyachrilamide gel in reduced conditions and transferred onto nitrocellulose membranes (BioRad). These membranes were blocked and incubated with rabbit anti-human NKG2D antibody (NBP2-43645, Novus Biologicals) diluted in PBS, 0.1% Tween. After incubation with secondary goat anti-rabbit antibody blots were scanned with an Odissey scanner and analysis was performed using Image Studio Lite v4.0 (LICOR).

12. Immunofluorescence microscopy

NKL cells were plated on poly-L-Lysine-coated coverslip. Cells were washed, fixed (2% PFA) and blocked in PHEM (1×), bovin serum albumin (BSA) 3%, human γ-globulin 100 μg/ ml, sodium azide 0.2%. Primary antibodies used were mouse anti-human TP1/8 or TP1/33 against CD69 and rabbit anti-human NKG2D antibody (NBP2-43645, Novus Biologicals). Secondary antibodies: anti-mouse-alexa 488 and anti-rabbit-alexa 568 were used. Coverslips were mounted on glass slides with Prolong mounting medium. Confocal laser-scanning microscope (Leica SP5).

13. Analysis of microbiota composition from mouse fecal samples

Fecal DNA was extracted from stool samples using Qiagen DNA stool kit. The V5/V6 region of 16 S rRNA genes was amplified with Invitrogen Platinum *Taq* DNA polymerase from 1,000–2,000 ng of DNA using a range of oligonucleotide primers specific for the domains V5 and V6 of rDNA bacteria. Each forward primer consists on an adaptor region and a unique barcode sequence that allow sample identification, being up to 96 different barcodes. The expected product length was ~350 base pairs including adaptors and barcodes. Bacteria-specific primers (forward 5'-CCATCTCATCCCTGCGTGTCTCCGACTCAGC-barcode-ATTAGATACCCYGGTAGTCC-3' and reverse 5'-CCTCTCTATGGGCAGTCGGTGATACGAGCTGACGACARCCATG-3') were used (Sundquist et al., 2007). PCR conditions consisted of an initial 5 min at 94 °C denaturation step, followed by 35 cycles of 1 min denaturation at 94 °C, 20 s annealing cycle at 46 °C and 30 s extension cycle at 72 °C, with a final extension for 7 min at 72 °C. Samples were kept at 4 °C until loading into a 2% agarose gel. Amplicons were purified using Gel Extraction Kit (Qiagen) and its concentration was evaluated by Qubit 3.0 Fluorometer (ThermoFisher). 26 pM of each sample was used to prepare the library. Sequencing was performed using the Ion Torrent NGS technology (Thermo Fiser).

14. Echocardiography and Magnetic Resonance Imaging

Mice were anaesthetized by inhalation of isoflurane/oxygen (1.25%/98.75%) and examined by a 30MHz transthoracic echocardiography probe. Images were obtained with VEVO 2100 (VisualSonics, Toronto, Canada) before EAM induction and during acute and chronic phases. From these images, left ventricle (LV) function was estimated by ejection fraction obtained from the M mode. Short-axis and long axis, BMode and 2D M-Mode views were obtained. From these images, left ventricle (LV) function was estimated by three validated methods as the shortening fraction (SF) and ejection fraction (EFm) obtained from the M mode, quantitative ejection fraction measured from the B mode (EFb), and visual assessment from the B mode by an expert in

echocardiography in a blind fashion. For SF measurements a long or short axis view of the heart was selected to obtain an M mode registration in a line perpendicular to the LV septum and posterior wall at the level of the mitral chordae tendinea. Diastolic and systolic manual segmentation of the LV endocardial edge in four chambers views of the heart was used to quantify EFb by the formula;

Ejection fraction from B Mode (EFb):

$$\frac{\text{Endocardial volumen (diastole)} - \text{endocardial volumen (sístole)}}{\text{Endocardial volumen (diastole)}} \times 100$$

LV regional and global function was scored as follows: normal (1), regional hypokinesia in more than one segment but not in all (2), regional akinesis in more than one segment (3), and global dysfunction in all segments (4). This method evaluates regional wall motion abnormalities globally and in greater detail compared to M mode and B mode. Regional kinetic abnormalities in mice with myocarditis in segments other than the LV septum and the postero-lateral wall are outside the region where FS and EFm are measured.

For Magnetic Resonance Imaging with T1 and T2 mapping, late gadolinium enhancement was used via intravenous injection. Up to 13 slices of each heart were imaged in a 7T MRI (Agilent-Varian) and myocardial water content was evaluated by averaging 3-5 ROI (brightness) values all along each myocardial slice and normalizing with the brightness of the gadolinium in the lumen of both left and right ventricles. Biomedical Imaging has been conducted at the Advanced Imaging Unit of the CNIC (Centro Nacional de Investigaciones Cardiovasculares Carlos III), Madrid, Spain. CNIC is founded by the Spanish Ministry of Science and Innovation, and by the Pro-CNIC Foundation

15. Histopathology analysis

Hearts were fixed in 10% phosphate-buffered formalin and embedded in paraffin. Sections were cut and stained with Haematoxilin-eosin to determine the level of inflammation and with Masson's trichrome to detect collagen deposition. H&E stained sections were scored for inflammation as follows: 0, no inflammatory infiltrates; 1, small foci of inflammatory cells; 2, larger foci of >100 inflammatory cells; 3, 10-30% of a cross section occupied by inflammatory cells; 4, >30% of a cross section occupied. Masson's trichrome stained sections were scored for myocardial fibrosis as follows: 0, no collagen deposits; 1, small areas of collagen deposits; 2, 10-30% of a cross section occupied by collagen deposits; 3, >30% of a cross section occupied by collagen deposits; 4, >50% of a cross section with collagen deposits.

16. Statistical analysis

In vivo experiments were performed according to a randomized complete block design (treatments and different time points have been taken into account) or a fully randomized design. Survival statistical analysis was tested with Log-rank (Mantel-Cox) test. To determine significant differences between 2 means, *P* values were calculated by unpaired *t* test or Mann-Whitney *U* test according to normality test, and differences among >2 means were analyzed by 1-way ANOVA or the Kruskal-Wallis test. To account for multiple comparisons, the Tukey or Bonferroni posttests were used to compare selected pairs of means and all pairs of means, respectively. Expression levels measured by qPCR were always considered in log2 scale to fulfil the normality assumption

In all cases, P values bellow 0.05 were considered significant, indicating statistical significance as *P < 0.05, **P < 0.01, ***P < 0.001, ****P < 0.0001. All statistical analyses were carried out with GraphPad Prism 5

RESULTS

RESULTS

1. Role of CD69 in the regulation of "natural killer" (NK) cells activity in the context of innate immunity.

NK cells have a critical role in the detection and elimination of infected or transformed cells. Previous work has shown that deficiency of CD69 confers protection to tumour growth in mice (Esplugues et al., 2003). In addition, treatment of wild type (WT) mice with a blocking monoclonal antibody for CD69 proved to be an effective therapeutic strategy, although no specific increase in cytotoxicity was observed for NK cells *in vivo* in those studies (Esplugues et al., 2005). Therefore, the first objective of this thesis was to decipher the mechanisms of CD69 to modulate NK cell cytotoxic activity.

1.1. Cd69$^{-/-}$ NK cells present an altered inhibitory/activating receptor repertoire

As the balance between activating and inhibitory receptor expression is pivotal for both tumor cell recognition and NK cell activation (Rahim and Makrigiannis, 2015), the first approach to our objectives was to examine whether lack of CD69 could lead to differences in the expression levels of said receptors. Here we applied mass cytometry (CyTOF) to precisely define NK cells in lymphoid organs from *Cd69*$^{+/+}$ and *Cd69*$^{-/-}$ C57BL/6 littermates. We examined maturation markers as well as NKG2D and Ly49 receptors expression on NK cells from blood, spleen, bone marrow (BM), peripheral (axillary and inguinal) lymph nodes and mesenteric lymph nodes. Single-cell analysis and unbiased clustering of the NKp46+ events showed a similar phenotype between *Cd69*$^{+/+}$ and *Cd69*$^{-/-}$ NK cells in the bone marrow (not shown), but differences in the blood (Figure 12A) and spleen (Figure 12B). Non-self and missing-self recognition receptors Ly49D (George et al., 1999) and Ly49G2 (Xie et al., 2009) were significantly upregulated, while Ly49H and NK1.1 were strongly downregulated in *Cd69* $^{-/-}$ NK cells. Mature CD27^{-}CD11b^{int} NK cells were similar between *Cd69*$^{+/+}$ and *Cd69*$^{-/-}$ in the C57BL/6 strain.

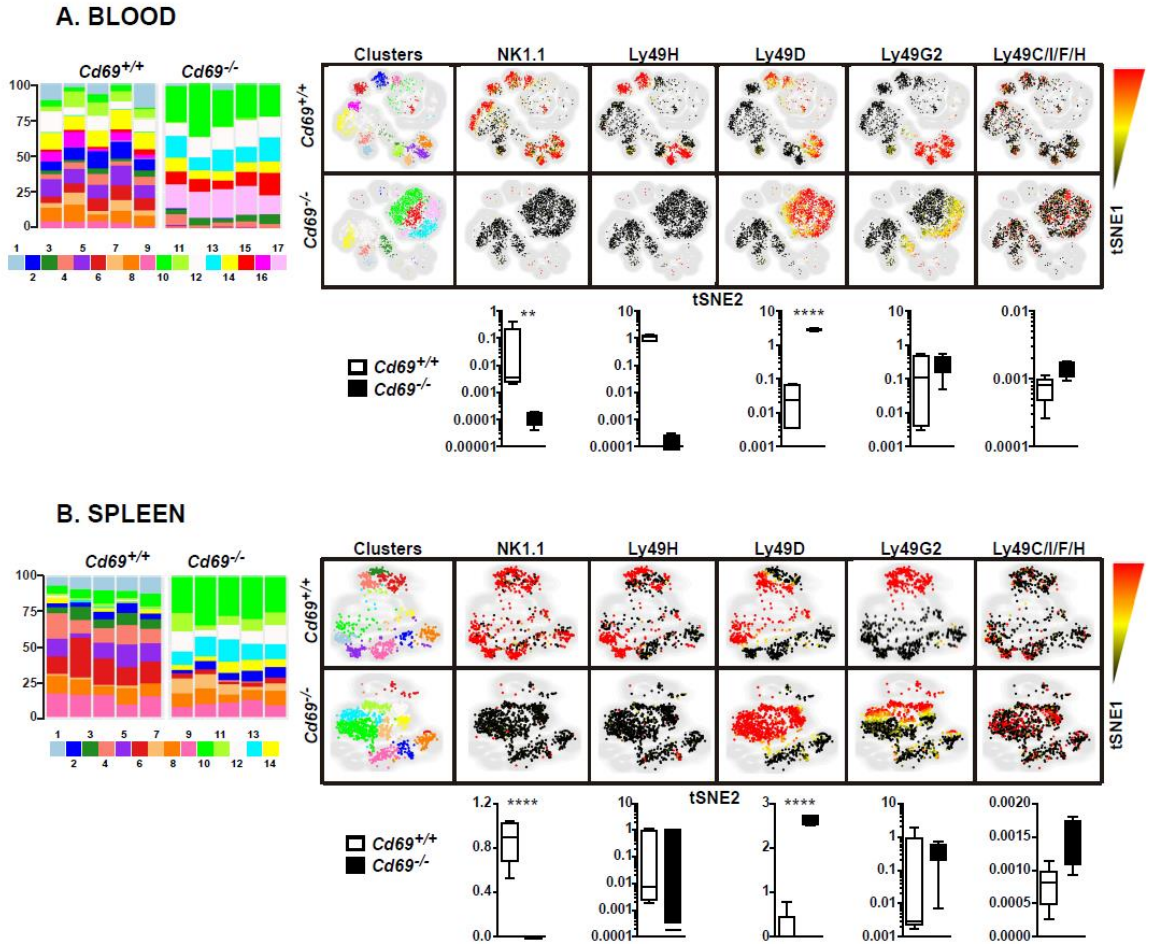

Figure 12. Unsupervised mass cytometry analysis of *Cd69*$^{+/+}$ and *Cd69*$^{-/-}$ NK cells. Cells from blood and spleen from five mice per group were stained with the extracellular panel (see Material and Methods). Left, frequency of significantly different clusters selected by phenotypic composition and generated by a statistical algorithm based on the expression of different markers by blood (A) or spleen (B) gated NKp46+ cells. Cluster numbers are identified in the color palette. Right, tSNE plots of the different clusters and relative expression of indicated NK cell markers (from maximum expression in red to minimum expression in dark green). For differential marker expression between clusters, a linear mixed effect model has been applied. **P* < 0.05, ***P* < 0.01, ****P* < 0.001, *****P* < 0.0001.

1.2. C57BL/6 *Cd69*$^{-/-}$ mice and anti-CD69mAb-treated littermates are highly susceptible to MCMV infection

Cd69$^{-/-}$ NK cells were recently shown to be more efficient in the control of Vaccinia virus infection, attributable to a lower cell death rate during the course of the infection (Notario et al., 2016). However, the molecular mechanisms for CD69 to control viral responses are unknown. Interestingly, we found an almost lack of expression of Ly49H in blood from *Cd69*$^{-/-}$NK cells. Ly49H on NK cells recognizes the m157 glycoprotein on the mouse cytomegalovirus (MCMV) capsid (Davis et al., 2008) and confers resistance to infection. To study the functional implication of the loss of

this receptor, *Cd69*$^{+/+}$ with or without anti-CD69mAb (Clone: 2.2) and *Cd69*$^{-/-}$ mice were infected with 10^5 PFUs of MCMV, administered intraperitoneally. Anti-CD69mAb 2.2 has been shown to downregulate the receptor inhibiting its downstream signaling (Esplugues et al., 2005). To evaluate the course of the infection, mice were weighted every day for 4 days, at which time point were sacrificed. *Cd69*$^{+/+}$ mice treated with anti-CD69mAb and *cd69*$^{-/-}$ mice lost significantly more weight after infection than non-mAb treated *cd69*$^{+/+}$ mice and harbored a higher viral load in both spleen and liver (Figure 13A). Consistently, organ damage was more extensive in mice with genetic ablation of CD69 and treated with 2.2 mAb, as assessed by histological analysis (Figure 13B). FACS analysis in peripheral blood of these mice 4 days after infection showed that Ly49H levels remained extremely low in *Cd69*$^{-/-}$ mice, and treatment with anti-CD69mAb brought about a significant downregulation of the receptor during the infection (Figure 13C). In agreement with previous reports on other types of viral infection (Du et al., 2010, Parsons et al., 2014), NKp46 levels were drastically downregulated during MCMV infection in all groups of mice (not shown). In summary, C*d69*$^{-/-}$ C57BL/6 mice are highly susceptible to MCMV infection due to the lack of the Ly49H receptor, and treatment of *Cd69*$^{+/+}$ littermates with anti-CD69mAb reproduces this phenotype.

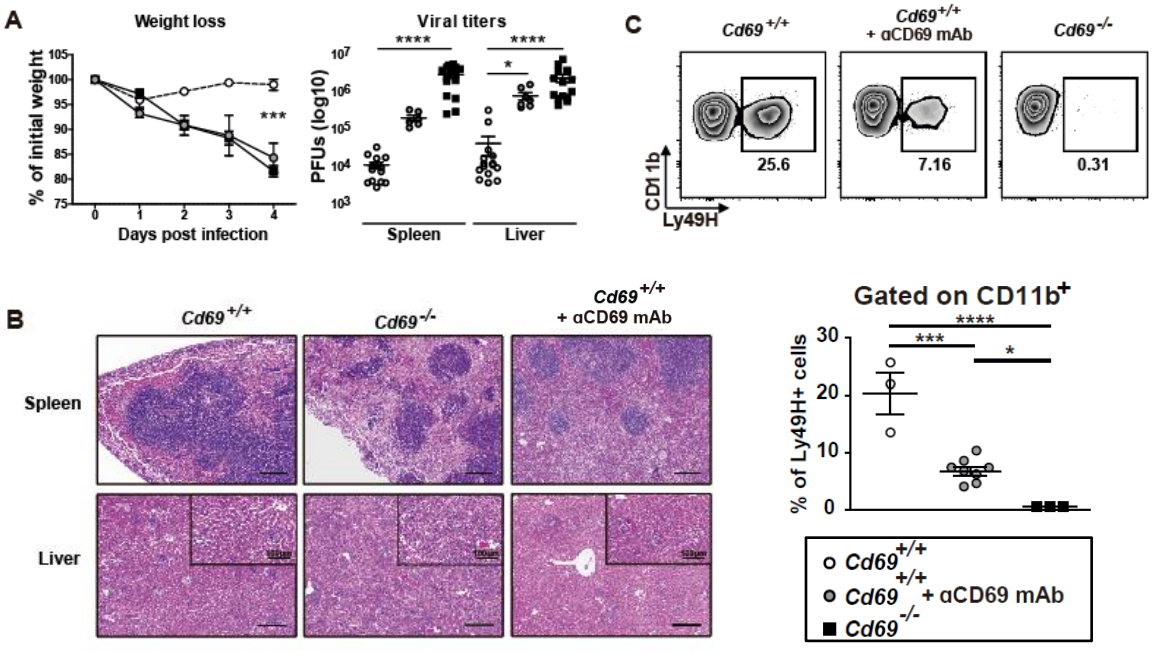

Figure 13. Genetic or pharmacologic ablation of CD69 renders C57BL/6 mice susceptible to MCMV infection. A. Weight loss and organ viral titers of the indicated experimental groups 4 days after MCMV infection. B. Histological evaluation of spleen (above) and liver (below) tissue 4 days after MCMV infection. Original magnification: 4x (inset: 10x). C. FACS plots and quantification of Ly49H expression in PBMC of the indicated experimental groups 4 days after MCMV infection. P-values were calculated with one-way ANOVA with Tukey post-test *P < 0.05, **P < 0.01, ***P < 0.001, ****P < 0.0001.

1.3. NK cell-targeted anti-CD69mAb treatment is efficient against a poorly immunogenic tumor

Cd69$^{-/-}$ mice appear to be resistant to tumor growth when injected with tumor cell lines that express high levels of MHC class I molecules, although this effect seems to be both NK- and CTL-dependent (Esplugues et al., 2003). Downregulation of said molecules is one of the main strategies of tumor cells for immune-evasion, and is associated with poor clinical prognosis (Garrido et al., 1997). To examine whether *Cd69*$^{-/-}$ NK cells could be efficient in the elimination of a poorly immunogenic tumor, which expresses low levels of MHC class I molecules, *Cd69*$^{+/+}$ and *Cd69*$^{-/-}$ littermates were injected intravenously with 5x10^5 B16F10 melanoma cells, which form metastases in the lungs (van Helden et al., 2015).

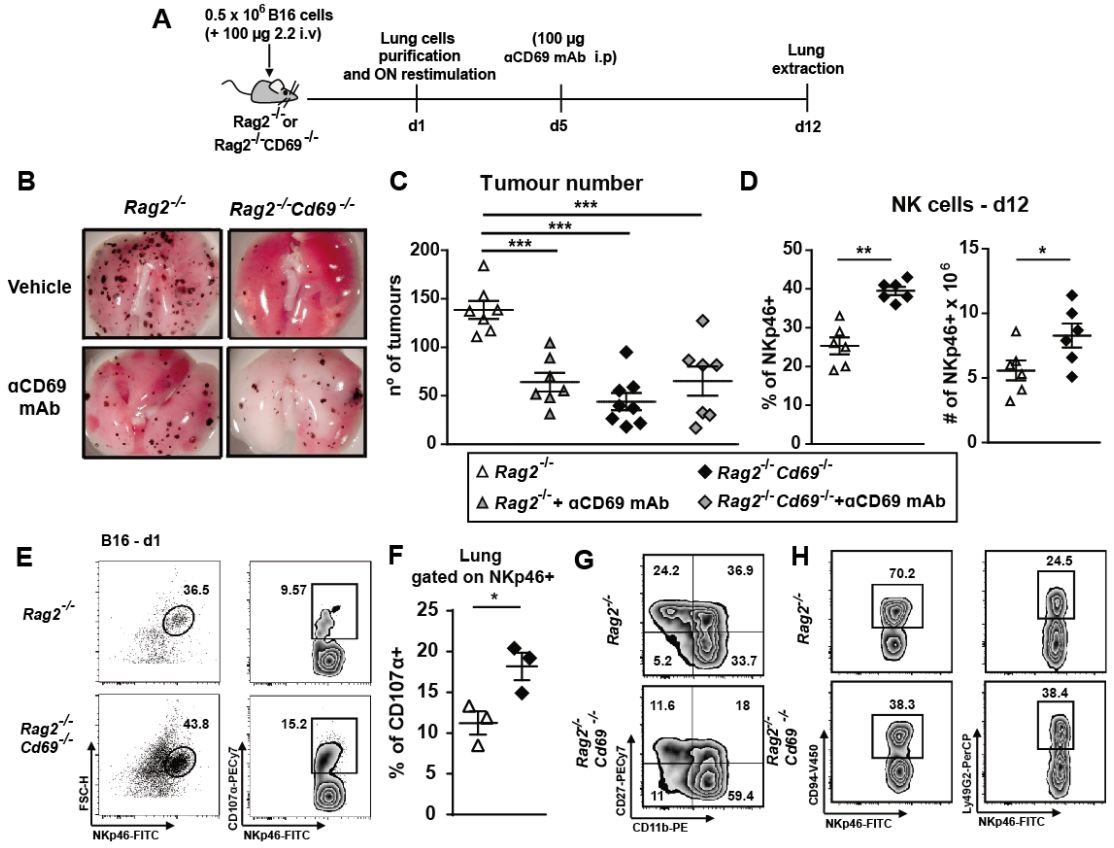

Figure 14. Genetic or pharmacologic ablation of CD69 specifically on NK cells impedes metastatic activity of poorly immunogenic tumors. A. Timeline of the experimental procedure (d: day). B. Representative lung pictures of one out of 7-9 mice/group. C. Quantification of B: single tumoral mass number 12 days after B16 injection. D. NK cells recruitment to the lungs of the indicated experimental groups 12 days after injection. Left: percentage, right: absolute numbers. E. Degranulation of NK cells 1 day after B16 injection. F. Quantification of E. G. Density plots showing percentages of mature NK cells (right lower quadrant) from peripheral blood of Rag2$^{-/-}$ and Rag2$^{-/-}$CD69$^{-/-}$ mice in steady state. Cells were gated as Nkp46$^+$. H. Phenotypic characterization of NK cells from peripheral blood of Rag2$^{-/-}$ and Rag2$^{-/-}$ CD69$^{-/-}$ mice in steady state. Frequencies of CD94+ and Ly49G2+ NKp46+ cells. P-values were calculated with one-way ANOVA with Tukey post-test in c and unpaired student's t test in d and f. **P* < 0.05, ***P* < 0.01, ****P* < 0.001, *****P* < 0.0001.

Contrary to previously reported with other tumor models, 12 days after injection *Cd69*$^{-/-}$ mice developed a significantly higher tumor number (not shown). To avoid interference from adaptive immune responses, the experiment was repeated in *Rag2*$^{-/-}$ background and *Rag2*$^{-/-}$*Cd69*$^{-/-}$ double knockout mice, in the presence or absence of anti-CD69mAb, according to the timeline shown in Figure 14A. In the absence of T and B cells, tumor growth was significantly inhibited after genetic or pharmacologic ablation of CD69 (Figures 14B and 14C). In parallel, percentage and absolute numbers of NK cells in the lungs 12 days after injection were significantly higher in *Rag2*$^{-/-}$*Cd69*$^{-/-}$ mice (Figure 14D). Moreover, degranulation after *in vitro* re-stimulation was also higher in *Rag2*$^{-/-}$ *Cd69*$^{-/-}$ NK cells, as assessed by CD107α exposure on the cell membrane (Figures 14E and 14F). In resting conditions, we observed a higher percentage of mature NK cells (CD27^{-}CD11b^{int}) in the absence of CD69 (Figure 14G), as well as higher Ly49G2 levels (Figure 14H), confirming the mass cytometry data (Figure 12). Moreover, expression levels of the inhibitory receptor CD94 were significantly lower in the absence of CD69 (Figure 14H). These data demonstrate that targeting NK cells with anti-CD69mAb could result an effective strategy to reduce metastases without the intervention of adaptive immune responses.

1.4. *Cd69*$^{-/-}$ mice are highly resistant to aGvHD after allogeneic HSCT

NK cells are one of the more resistant cell types to radiation and chemotherapy (Bogdandi et al., 2010) (Yang et al., 2014), playing an important role in the elimination of alloreactive T cells after allogenic transplants (Olson et al., 2010). Ly49G2 and Ly49D NK receptors mediate the rejection of MHC-I deficient BM grafts (Raziuddin et al., 1996, George et al., 1999, Raziuddin et al., 2000) and their expression was found higher in the membrane of CD69 deficient mice (Figure 12). Therefore, we wonder whether *Cd69*$^{-/-}$ mice were protected against graft versus host disease (GvHD) after allogeneic HSCT. Transfer of T cell-depleted bone marrow (TCD-BM) with $5x10^5$ splenic naïve CD4 T cells from C57BL/6 donors to lethally irradiated BALB/c hosts induced robust aGVHD disease in the *Cd69*$^{+/+}$ group, with high clinical scores (Cooke et al., 1996) and a mortality of 80% by day 10. On the contrary, 80-90% of the *Cd69*$^{-/-}$ hosts survived with significantly lower clinical scores (Figure 15A-C) and better appearance 25 days after treatment compared to the few *Cd69*$^{+/+}$ survivors (Figure 15D). Histologic evaluation of the main target organs of aGVHD (skin, lung, gut and liver) showed much more extensive damage in the *Cd69*$^{+/+}$ group compared to the *Cd69*$^{-/-}$ littermates (Figure 15E). Accordingly, CD4 T cells were significantly less abundant in blood and spleens of the *Cd69*$^{-/-}$ group, indicating a higher elimination rate of the alloreactive T cells by host NK cells in these mice.

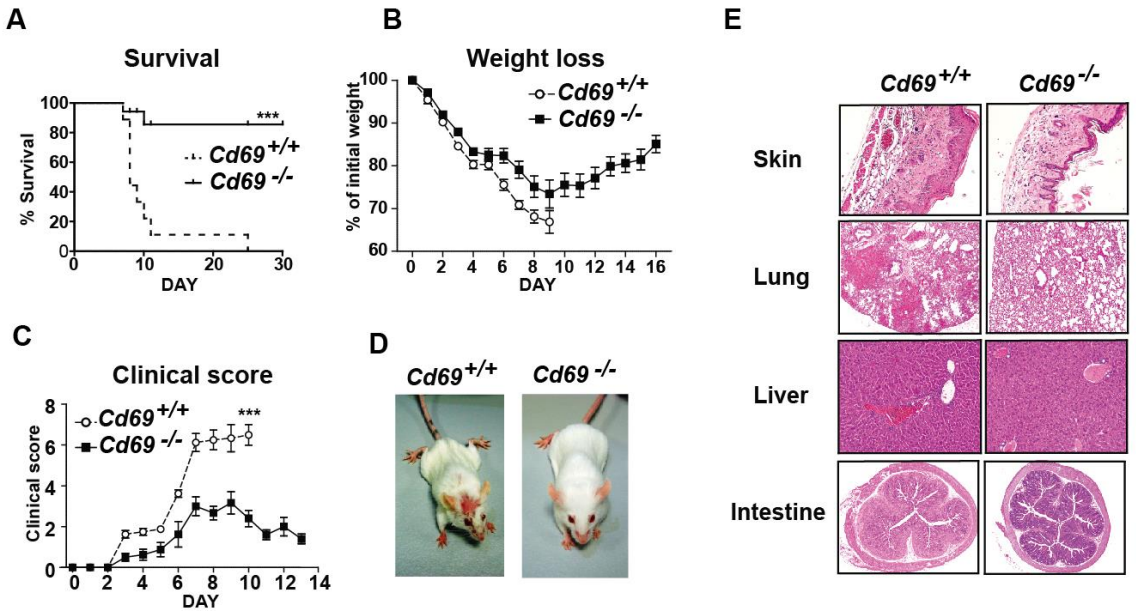

Figure 15. Increased survival and lower severity of GvHD in *Cd69*$^{-/-}$ mice. A-C Survival curve, weight curve (percentage of weight loss) and clinical score are shown. D. *Cd69*$^{+/+}$ and *Cd69*$^{-/-}$ mice at day 24 after transplant. E. Histology of organs affected by GvHD at d24 after transplant. Log-rank (Mantel-Cox) Test was used for survival statistical analysis. Two-way ANOVA with Bonferroni post-test for statistical analysis in panel b and c. (n=8). *P < 0.05, **P < 0.01, ***P < 0.001, ****P < 0.0001.

1.5. NK cells account for allogeneic killing in *Cd69*$^{-/-}$ hosts and anti-CD69mAb-treated littermates

To further analyze the contribution of other cell types in the observed phenotype shortly after transplant, we evaluated allogeneic cell killing *in vivo* in non-irradiated BALB/c, BALB/c *Cd69*$^{-/-}$, *Rag2*$^{-/-}$, *Rag2*$^{-/-}$*Cd69*$^{-/-}$, *Rag2*$^{-/-}$*γc*$^{-/-}$ and *Rag2*$^{-/-}$*γc*$^{-/-}$*Cd69*$^{-/-}$ recipients (Figure 16A). As expected, allogeneic cells were efficiently eliminated in the absence of T and B cells, and specific lysis was significantly augmented in the absence of CD69 independently of adaptive immune responses both by genetic ablation or pharmacological treatment (anti-CD69 mAb 2.2) (Figure 16B-C). *Rag2*$^{-/-}$*γc*$^{-/-}$ and *Rag2*$^{-/-}$*γc*$^{-/-}$*Cd69*$^{-/-}$ recipients, lacking NK cells, were unable to eliminate allogeneic splenocytes (Figure 16B), confirming that cells of myeloid origin are not involved in the observed phenotype independently of CD69 expression. Expression of Ly49G2 was significantly higher in *Cd69*$^{-/-}$ and anti-CD69mAb-treated *Cd69*$^{+/+}$ mice, while CD94 was downregulated in these two groups (Figure 16). Of note, 4 hours after in vivo challenge, the Ly49G2^{+}CD94^{-} subset also harbored slightly but significantly higher levels of the effector molecule granzyme B, indicating an increased cytolytic capacity of these cells. Taken together, this data indicates that genetic ablation or downregulation of CD69 on NK cells leads to a shift in receptor repertoire, increased cytolytic activity and highly

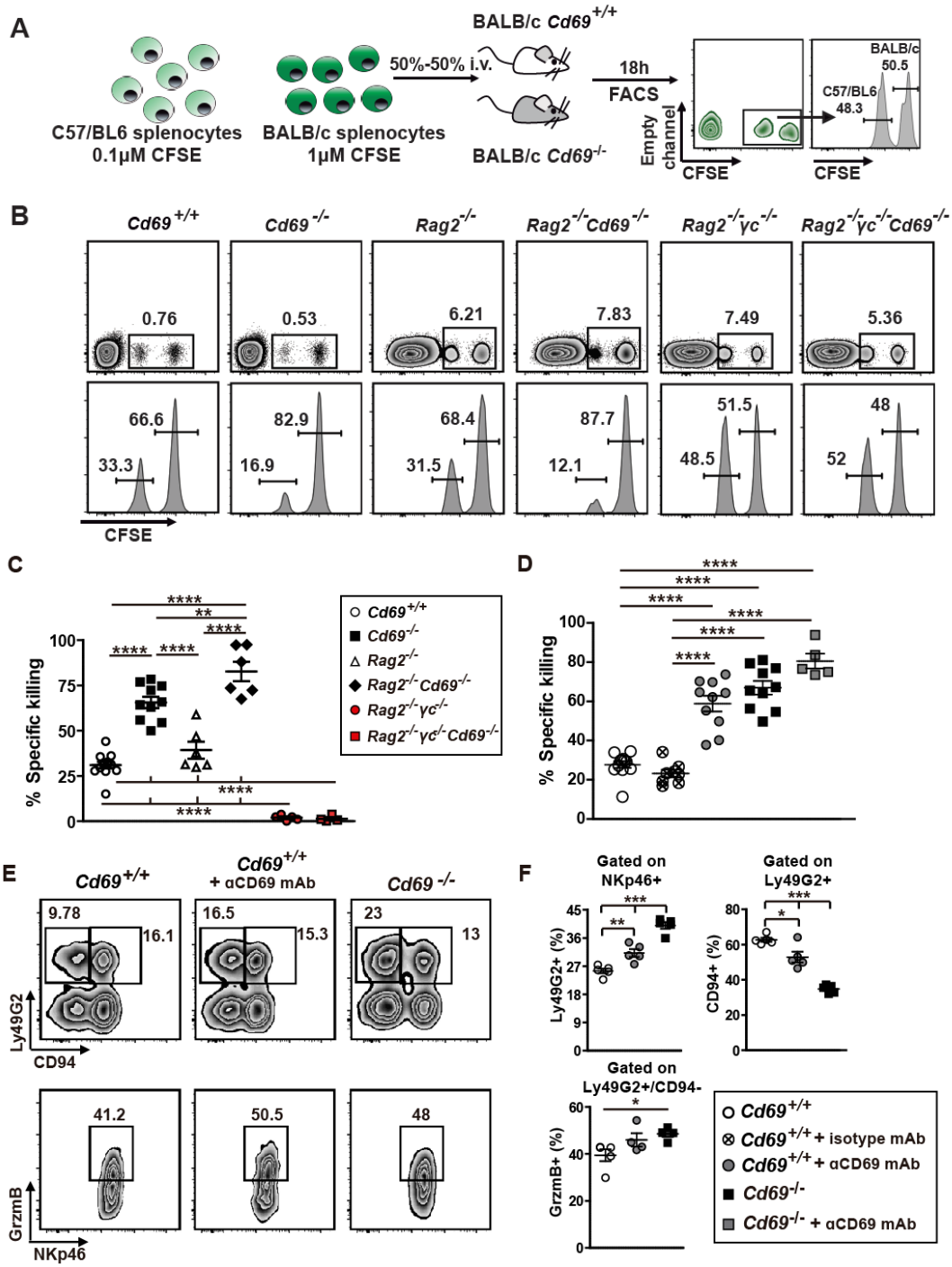

Figure 16. *Cd69*$^{-/-}$ mice exhibit higher NK activity against allogenic cells. A. Schematic diagram of the *in vivo* killing assay performed. B. CFSE histograms of isolated splenocytes (gated of CFSE+ cells) from BALB/c *Cd69*$^{+/+}$, *Cd69*$^{-/-}$ mice, *Rag2*$^{-/-}$ or *Rag2*$^{-/-}$ *Cd69*$^{-/-}$ mice. Histograms are representative of one experiment (n=6-9). C-D. Percentage of specific killing of allogenic cells by *Cd69*$^{+/+}$, *Cd69*$^{-/-}$ mice, *Rag2*$^{-/-}$ or *Rag2*$^{-/-}$ *Cd69*$^{-/-}$ mice (c) or *Cd69*$^{+/+}$ *and Cd69*$^{-/-}$ mice treated with an anti-CD69 mAb 2.2 (d). E. Representative dot plots of Ly49G2, CD94 and Granzyme B expression on NKp46+ cells. F. Percentages of Ly49G2+ cells gated on NKp46+ cells, CD94+ cells gated on Ly49G2+ NK cells and Granzyme B + cells gated on Ly49G2+/CD94. Statistical significance was determined by One-way ANOVA using Bonferroni post test. *P < 0.05, **P < 0.01, ***P < 0.001, ****P < 0.0001.

1.6. Ablation of CD69 renders NK cells resistant to apoptosis and enhances NK cell signaling during allogeneic cell elimination

To further address the mechanisms through which genetic or pharmacologic ablation of CD69 on NK cells increases allogeneic cell lysis, we performed RNAseq analyses on NK cells from *Rag2*$^{-/-}$, *Rag2*$^{-/-}$*Cd69*$^{-/-}$ or anti-CD69mAb treated *Rag2*$^{-/-}$ mice 4 hours after *in vivo* challenge with allogeneic splenocytes. We detected 2387 genes differentially expressed between the *Rag2*$^{-/-}$+anti-CD69mAb and the *Rag2*$^{-/-}$*Cd69*$^{-/-}$ groups compared to the *Rag2*$^{-/-}$ group (Figure 17A). These genes, similarly modulated in the former two groups (Figure 17B), are important in pathways related to apoptosis, phagosome maturation and NK cell signaling, among others (Figure 17C).

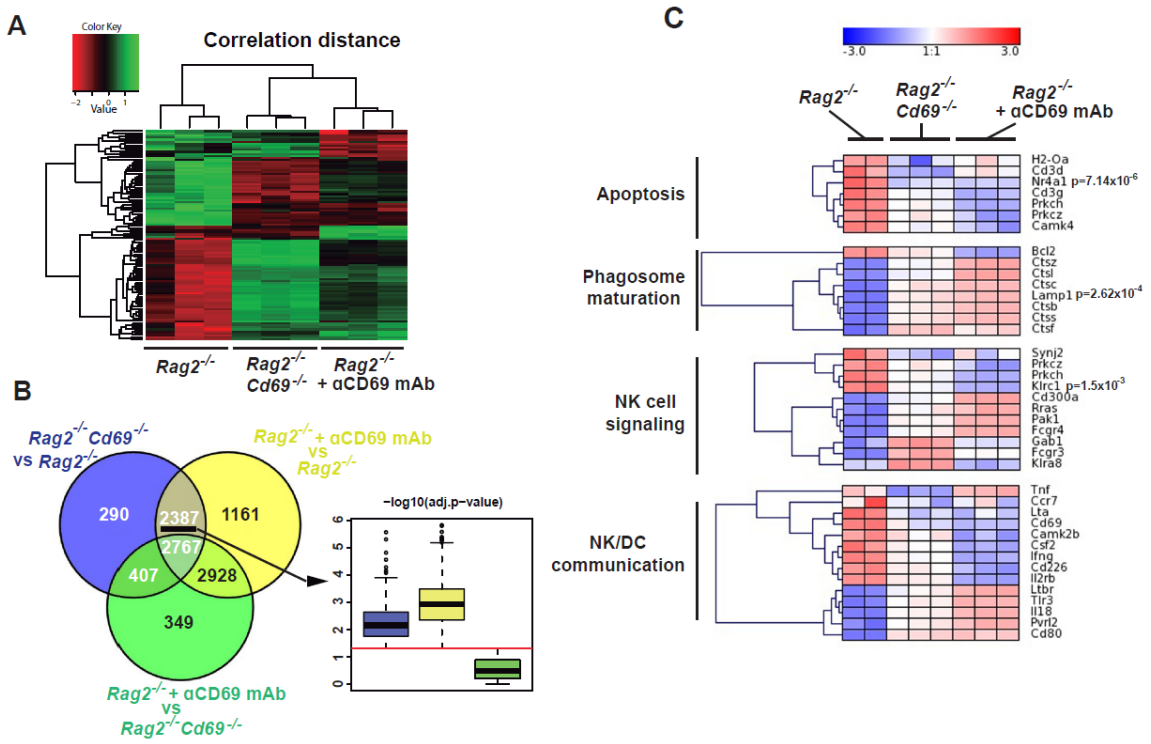

Figure 17. **RNAseq of NK cells from *Rag2*$^{-/-}$ and *Rag2*$^{-/-}$ *Cd69*$^{-/-}$ mice 4 hours after of allogenic challenge.** A. Hierarchical cluster analysis and heat map of the expression patterns of 104 genes from RNA-Seq data. Changes in expression levels are displayed from green (downregulated) to red (upregulated), as shown in the color gradient at the bottom left corner. Heat map was generated and hierarchical clustering was performed using Cluster 3.0. B. Venn diagram shows overlapping set of genes that are differentially expressed in the three conditions (*Rag2*$^{-/-}$, *Rag2*$^{-/-}$ *Cd69*$^{-/-}$ and *Rag2*$^{-/-}$ + anti-CD69 mAb) (with a p-value < 0.05). Box plot shows the p-value distribution (transform to log10 in negative values) of the 2.387 genes that are differentially expressed in the contrast *Rag2*$^{-/-}$ vs *Rag2*$^{-/-}$ *Cd69*$^{-/-}$ and *Rag2*$^{-/-}$ vs *Rag2*$^{-/-}$ + anti-CD69 mAb but not in *Rag2*$^{-/-}$ *Cd69*$^{-/-}$ vs *Rag2*$^{-/-}$ + anti-CD69 mAb. Red line corresponds to p-value = 0.05 (log10 = -1.3). C. Hierarchical cluster and heat map of the expression patterns of different relevant genes within the 2.387 genes differentially expressed and involved in different NK cell related pathways: apoptosis, phagosome maturation, NK cell signaling, NK/DC communication.

1.7. CD69 controls NKG2D expression, membrane clustering and signaling

Interestingly, one of the pathways modulated in the absence of CD69 was the signaling pathway downstream NKG2D stimulation (Figure 18A). NKG2D is a master regulator of activatory and inhibitory NK cell receptors and, therefore, one of the most interesting targets for us to study. A number of genes related to NKG2D activity, such as Dap10, Dap12, Zap70 and Vav1 among others, were found differentially expressed in NK cells from *Rag2*$^{-/-}$ vs *Rag2*$^{-/-}$ *Cd69*$^{-/-}$ and *Rag2*$^{-/-}$ vs *Rag2*$^{-/-}$ + anti-CD69 mAb mice. The upregulation of these genes was confirmed by qPCR (Figure 18B), suggesting that this signaling route was overactivated when CD69 is not present. CyTOF analysis showed that CD69 and NKG2D expression are located together within a specific cluster of cells, however, NKG2D expression in this cluster was lost in the absence of CD69, spreading among different clusters (Figure 18C). These data suggested some type of physical interaction between these two molecules. To test this hypothesis we performed Co-IP assays between CD69 and NKG2D that confirmed the interaction of the two receptors in the membrane of wild type NK cells (Figure 18D). Moreover, immunofluorescence assays showed that CD69 and NKG2D colocalize in the uropode of the cell after activation (Figure 18E).

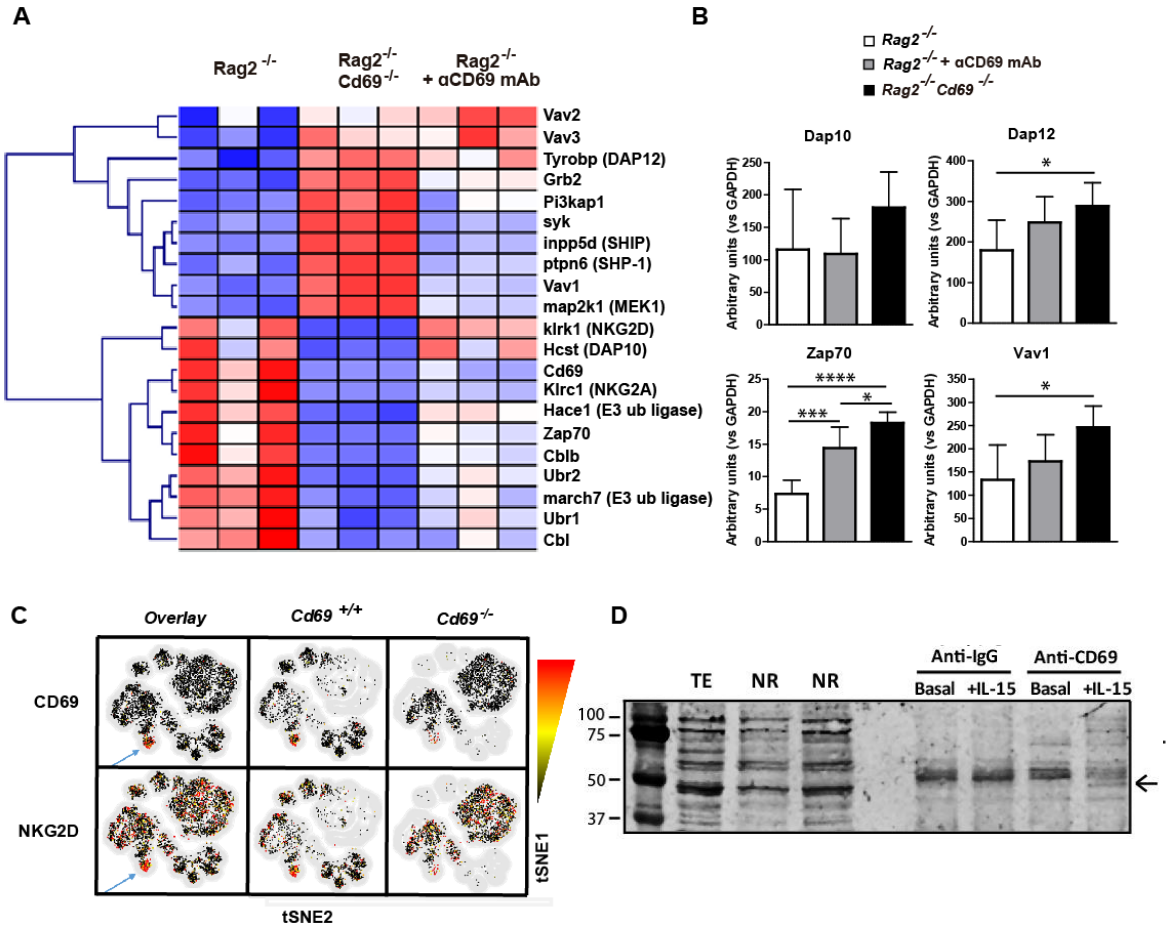

Figure 18. CD69 could be interacting with NKG2D and modulating its activity. (Next page)

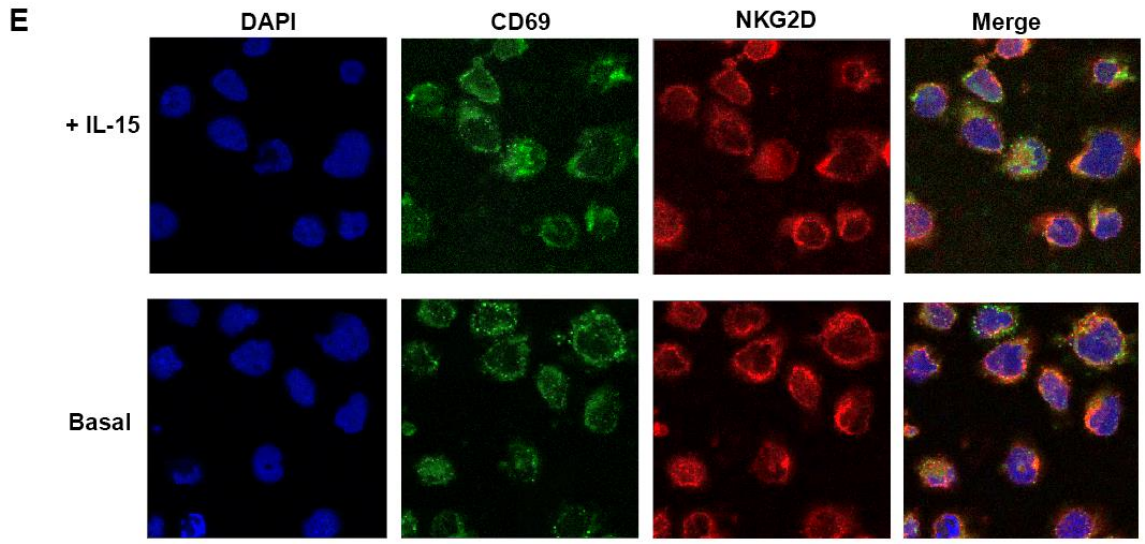

Figure 18. **CD69 interacts with NKG2D and modulates its expression and activity.** A. Hierarchical cluster analysis and heat map of the expression patterns of genes involved in NK cell signaling. Data obtained from RNA-Seq analysis. B. Validation of mRNA expression levels of genes involved in NKG2D signaling by qPCR. C. tSNE plots of CD69 and NKG2D expression on blood NKp46+ gated cells analyzed by CyTOF. D. Western Blot showing co-immunoprecipitation of NKG2D with CD69 in extracts obtained from NKL cells in basal conditions or after 24 hours with IL-15 stimulation. Black arrow indicates the band in the gel corresponding to NKG2D. E. Immunofluorescence of CD69 and NKG2D in NKL cells in resting conditions or after 24 hours with IL-15 stimulation. Statistical significance was determined by One-way ANOVA using Tukey post test. *P < 0.05, **P < 0.01, ***P < 0.001, ****P < 0.0001.

1.8. CD69 can be targeted to prevent aGVHD without compromising engraftment

Treatment with anti-CD69mAb reproduces the phenotype of *Cd69*$^{-/-}$ mice, eliminating cells of allogeneic origin more efficiently than non-treated littermates (Figure 16). We aimed to address the potential of anti-CD69 mAb as therapeutic agent to ameliorate aGVHD. BALB/c *Cd69*$^{+/+}$ mice were treated with anti-CD69mAb 24 hours before lethal irradiation, to inhibit CD69 upregulation on host NK cells. One day after irradiation, mice were transplanted with fully allogenic C57BL/6 TCD-BM. After allowing 3 days for engraftment, aGvHD was induced by C57BL/6 naïve T cell infusion, in the presence or absence of a second dose of anti-CD69 mAb. 5-7 days after aGvHD disease induction, mAb-treated *Cd69*$^{+/+}$ mice fared better than non-treated *Cd69*$^{+/+}$ littermates (Figure 19A), presenting a significantly lower clinical score and improved survival rate (Figure 19B). We also observed more robust NK cell populations in blood and spleens of CD69 deficient mice, which correlated with a much lower engraftment of allogeneic T cells at this time point (Figure 19C). Importantly, despite the efficient elimination of alloreactive T cells and the absence of aGvHD, reconstitution kinetics in the mAb-treated group were comparable to the non-treated *Cd69*$^{+/+}$ group, with a chimerism of around 95% already 14 days after aGvHD induction (Figure 19D). Thus,

it appears that mAb-treated host residual NK cells only eliminate highly alloreactive donor T cells shortly after infusion, while the rest of the graft successfully repopulates the host, and could efficiently maintain immunocompetence and the graft versus leukemia effect in a clinical setting.

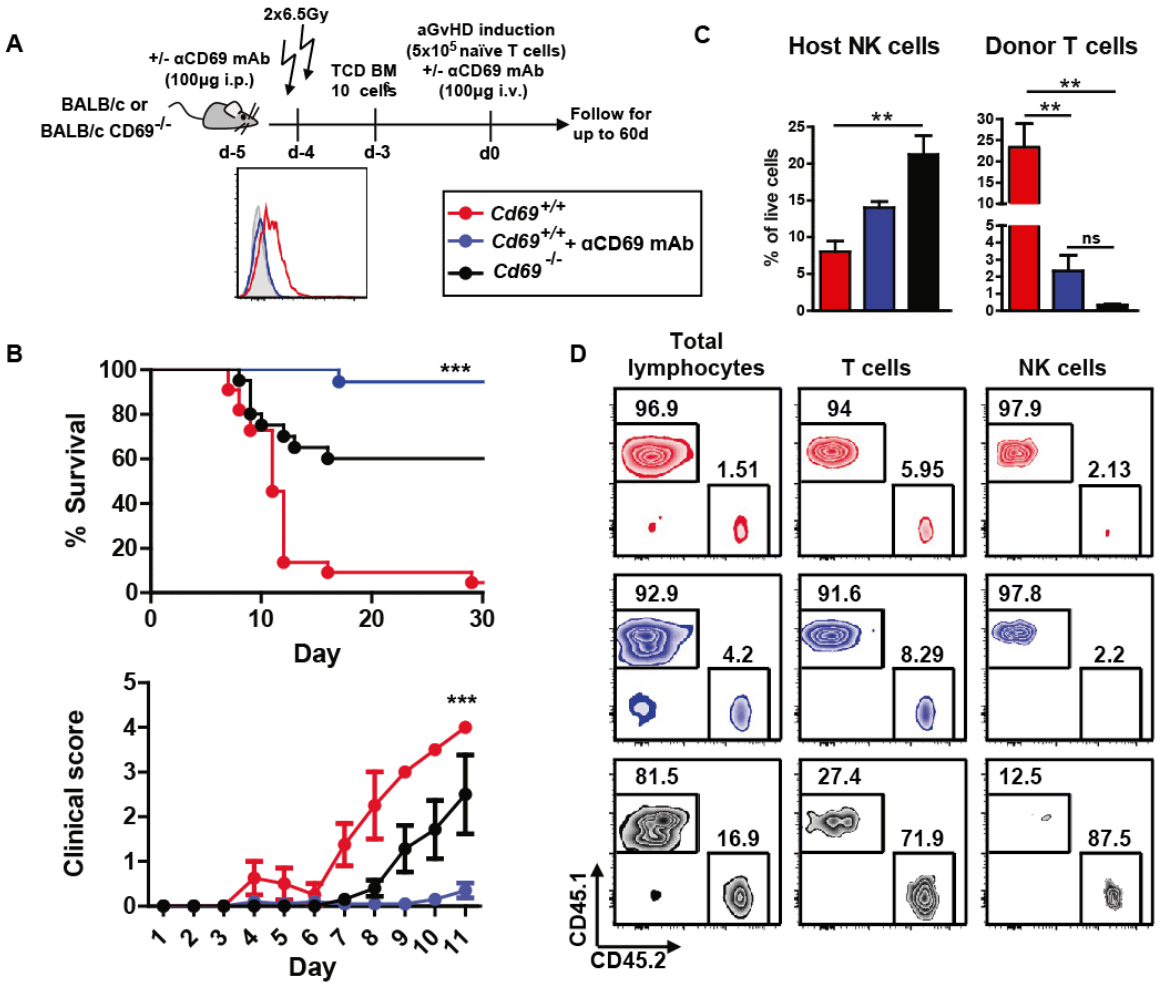

Figure 19. Anti-CD69 mAb treatment protects *Cd69*$^{+/+}$ mice from aGVHD without impairing engraftment. A. Schematic representation of the treatment strategy. Histogram overlay: expression of CD69 in the indicated experimental groups 1 day after irradiation. B. Survival rate (top) and clinical score (bottom) during aGvHD. C. Proportions of host NK cells (NKp46+ CD45.1-) and donor T cells (CD45.1+) that persist in spleen, 5 days after aGvHD induction. D. Reconstitution kinetics of the indicated experimental groups 14 days after transplant. One representative out of 9 mice/group. WT group: sole survivor. Statistical significance was determined by One-way ANOVA using Tukey post-test. *P < 0.05, **P < 0.01, ***P < 0.001, ****P < 0.0001. Log-rank (Mantel-Cox) Test was used to comparison of survival curves.

2. Role of CD69 in an "in vivo" model of atherosclerosis in the context of adaptive immunity.

In the last decade, the contribution of lymphocytes to atherosclerosis clinical manifestations has been highlighted. In vivo models of atherosclerosis suggest that regulatory T (Treg) cells suppress inflammatory responses and attenuate atherosclerosis (Ait-Oufella et al., 2006). This has been demonstrated by experimental therapies aimed to increase Treg proportions under high fat diet conditions (Dinh et al., 2012, Sasaki et al., 2009). However, the role of Th17 lymphocytes remains more controversial. Although genetic or pharmacological inhibition of interleukin (IL)-17 significantly ameliorates atherosclerosis (Ge et al., 2013) (Smith et al., 2010), concomitant increases in both IL-17 and IL-10 lead to smaller plaques (Taleb et al., 2009). Another study reports bigger plaques in *ApoE*$^{-/-}$*IL-17*$^{-/-}$ mice (Danzaki et al., 2012). A Th17/ Treg imbalance has been reported in patients with coronary artery atherosclerosis, with a significant increase in Th17 and a decrease in Treg cells (Potekhina et al., 2015) (Li et al., 2014). CD69 exerts a complex role in the modulation of the immune response and the inflammatory process by affecting the balance between Th17 and Treg cells. CD69-deficient mice present an exacerbated Th17 response and defective Treg cell function (Sanchez-Diaz et al., 2017) (Cortes et al., 2014), resulting in the inability to resolve inflammation or to maintain immune tolerance. This has been studied in different models of arthritis, asthma, contact dermatitis or myocarditis (Martin et al., 2010b, Cruz-Adalia et al., 2010, Sancho et al., 2003). CD69 deficiency was studied in the context of atherosclerosis using *Cd69*$^{-/-}$ *ApoE*$^{-/-}$ mice. However, no differences in the atheroma plaque formation was observed in these mice (Gomez et al., 2009).

One of the main objectives of this thesis was to study the role of CD69 expression on T cells in atherosclerosis development using a different mouse model in which the receptor for low-density lipoprotein (LDL) is absent (*Ldlr*$^{-/-}$ mice).

2.1. CD69 regulates adaptive immune responses in HFD conditions

To evaluate the influence of CD69 expression on immune cells in atherosclerosis development, 5 week old male *Ldlr*$^{-/-}$ CD45.1+ mice were irradiated and reconstituted with bone marrow from *Cd69*$^{-/-}$ double reporter for Foxp3-mRFP and IL-17A-eGFP24 (BM *Cd69*$^{-/-}$*)* mice or WT littermates (BM *Cd69*$^{+/+}$), both CD45.2+ (figure 20A). Mice were fed with high fat diet (HFD) and peripheral blood from the tail vein was collected every two weeks to analyse the immune response of these chimeric mice. In the absence of CD69 there was a polarization toward a proinflammatory phenotype as seen by an increased Th17/Treg ratio that was more evident at 13 weeks on HFD (Figure 20B). After 10 weeks of HFD, mice reconstituted with *Cd69*$^{-/-}$ dRep BM displayed a significantly high increase in IL-17–eGFP+ cells in para-aortic LNs, with higher absolute numbers

compared with BM *Cd69*$^{+/+}$ mice (Figure 20C and 20D). In agreement, the percentage but not cell numbers of Foxp3mRFP+ cells was significantly reduced in the absence of CD69 (Figure 20D), indicating that Treg cell recruitment to para-aortic LNs is not compromised.

The percentage of CD4+ IL-17–eGFP+ cells was increased in the aortic arc of BM *Cd69*$^{-/-}$chimeras, whereas there is a tendency for decreased CD4+ and FoxP3+ cells (Figure 20E and 20F). Collectively, flow cytometry data indicate that hyperlipidemia induces high proinflammatory activity and a disrupted Th17/Treg cells balance in the absence of CD69.

Histochemical analysis revealed more extensive lesions and necrotic cores in aortic valves from BM *Cd69*$^{-/-}$ chimeras compared with the BM *Cd69*$^{+/+}$ control group (Figure 20G and 20H). Atheroma plaques in both groups consisted mainly of F4/80+ foam cells, although a higher infiltration of CD3+ lymphocytes into atheroma plaques was found in the BM *Cd69*$^{-/-}$ group (Figure 20I and 20J).

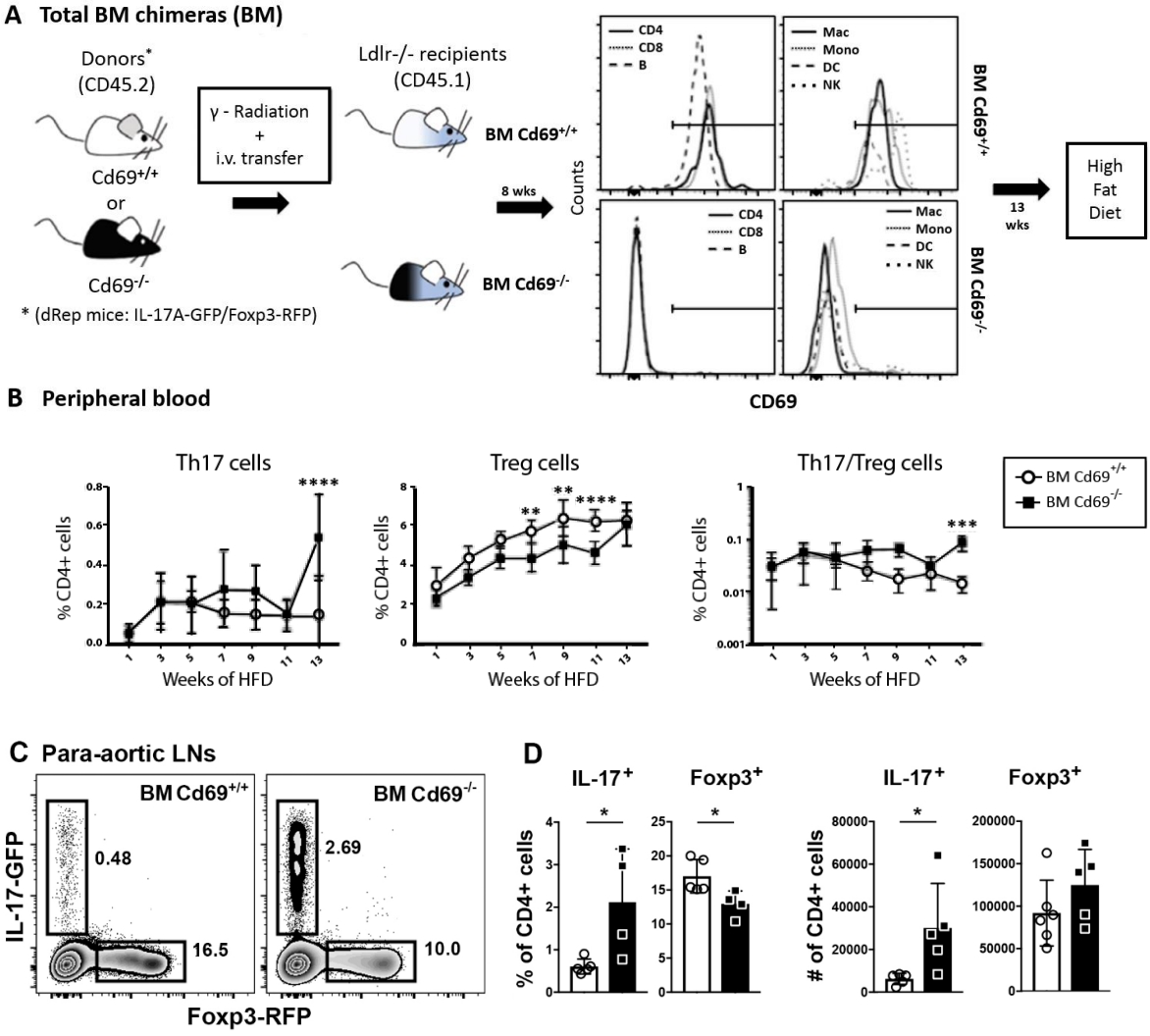

Figure 20. CD69 regulates adaptive immune responses in HFD conditions. (Next page)

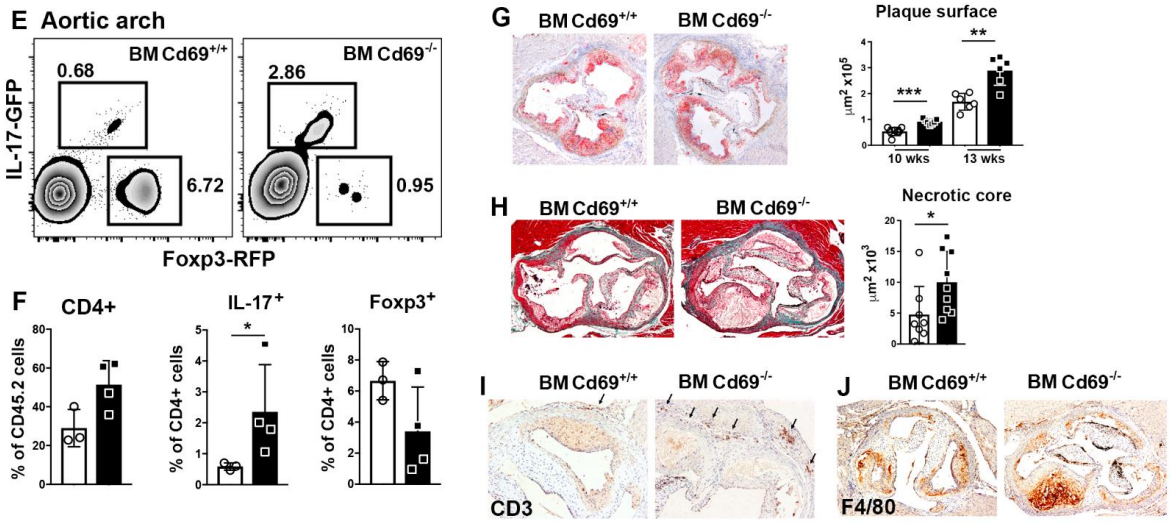

Figure 20. CD69 regulates adaptive immune responses in HFD conditions. A. *Ldlr*$^{-/-}$ mice were lethally irradiated and reconstituted with bone marrow from C57BL/6 *Cd69*$^{+/+}$ or *Cd69*$^{-/-}$ dRep mice. Eight weeks after reconstitution PBMCs were > 90% CD45.2+. Histograms show CD69 expression on CD4 and CD8 T cells, B cells (B), macrophages (Mac), monocytes (Mono), dendritic cells (DC) and natural killer cells (NK). PBMCs were stimulated with anti-CD3/CD28 for lymphoid cells and LPS for myeloid cells, of the indicated groups**. B**. Percentage of Th17 (IL-17-GFP+), Treg (Foxp3-RFP+) CD4+ T cells and Th17/Treg ratio in peripheral blood leukocytes of BM Cd69$^{+/+}$ and BM Cd69$^{-/-}$ mice at the indicated time points after HFD initiation. Error bars show SEM, **P < 0.01, ***P < 0.001, **** P < 0.0001. P values were calculated by 2-way repeated-measures ANOVA (Sidak´s post hoc test). **C**. Flow cytometry analysis of Th17 and Treg cells in para-aortic lymph nodes of BM *Cd69+/+* and BM *Cd69-/-* mice at 10 weeks after HFD administration, n=12 mice per group. **D**. Percentages and absolute numbers of Th17 and Treg cells from para-aortic lymph nodes of BM Cd69+/+ and BM Cd69-/- mice 10 weeks after HFD administration, n=12 mice per group. Error bars show SEM, *p<0.05, as determined by unpaired t-test or Mann-Whitney U test. **E**. Flow cytometry analysis of aortic arch 13 weeks after HFD initiation. **F**. Quantification and statistical analysis of data shown in E, n=7 mice per group, *P < 0.05, as determined by Mann-Whitney U test**. G**. Lack of CD69 on immune cells accelerates atheroma plaque formation. Oil Red O staining in aortic valves from BM *Cd69*$^{+/+}$ and BM *Cd69*$^{-/-}$ mice after 13 weeks of HFD (left) and quantification of plaque surface at the indicated time points (right), n=16 mice per group pooled from 3 different experiments. **H**. As before, Masson trichrome staining and quantification of fibrosis and necrotic core after 13 weeks of HFD, n=6 mice/group Error bars show SEM, *P < 0.05, **P < 0.01, ***P < 0.001, as determined by unpaired t-test**. I**. As before, F4/80 staining **J**. As before, CD3 staining, C and D. representative images of 6 mice/group. Original magnifications: A-C: 4x, D: 10x.

2.2. Analysis of blood leukocyte subsets during high fat diet

It has been reported an inverse correlation between myeloid dendritic cells and Tregs in human unstable atherosclerotic plaques (Rohm et al., 2015). Therefore, not only the Th17/Treg ratio but different population of lymphoid and myeloid peripheral blood leukocytes were analyzed during HFD administration with no significant changes between BM *Cd69*$^{+/+}$ and BM *Cd69*$^{-/-}$ mice (Figure 21A and 21B). Because CD69 has been reported to be critical for the generation and maintenance

of memory T helper lymphocytes (Shinoda et al., 2012), the CD44hi CD62Llo memory T-cell subset was also analyzed. Naïve T cells ($CD44^{lo}$ $CD62^{hi}$) decrease with HFD whereas memory T cells increase in both chimeric mice, suggesting that CD69 is not playing a role in the maintenance of T-helper memory cells in this model (Figure 21C). Moreover, we found that the ratio between dendritic cells and Treg cells during HFD remains equal in both chimeric mice (Figure 21D). These data suggest that Th17 and Treg cell proportions are altered under the course of HFD in BM *Cd69*$^{-/-}$ chimeric mice, whereas the other leukocyte subsets remained unaltered.

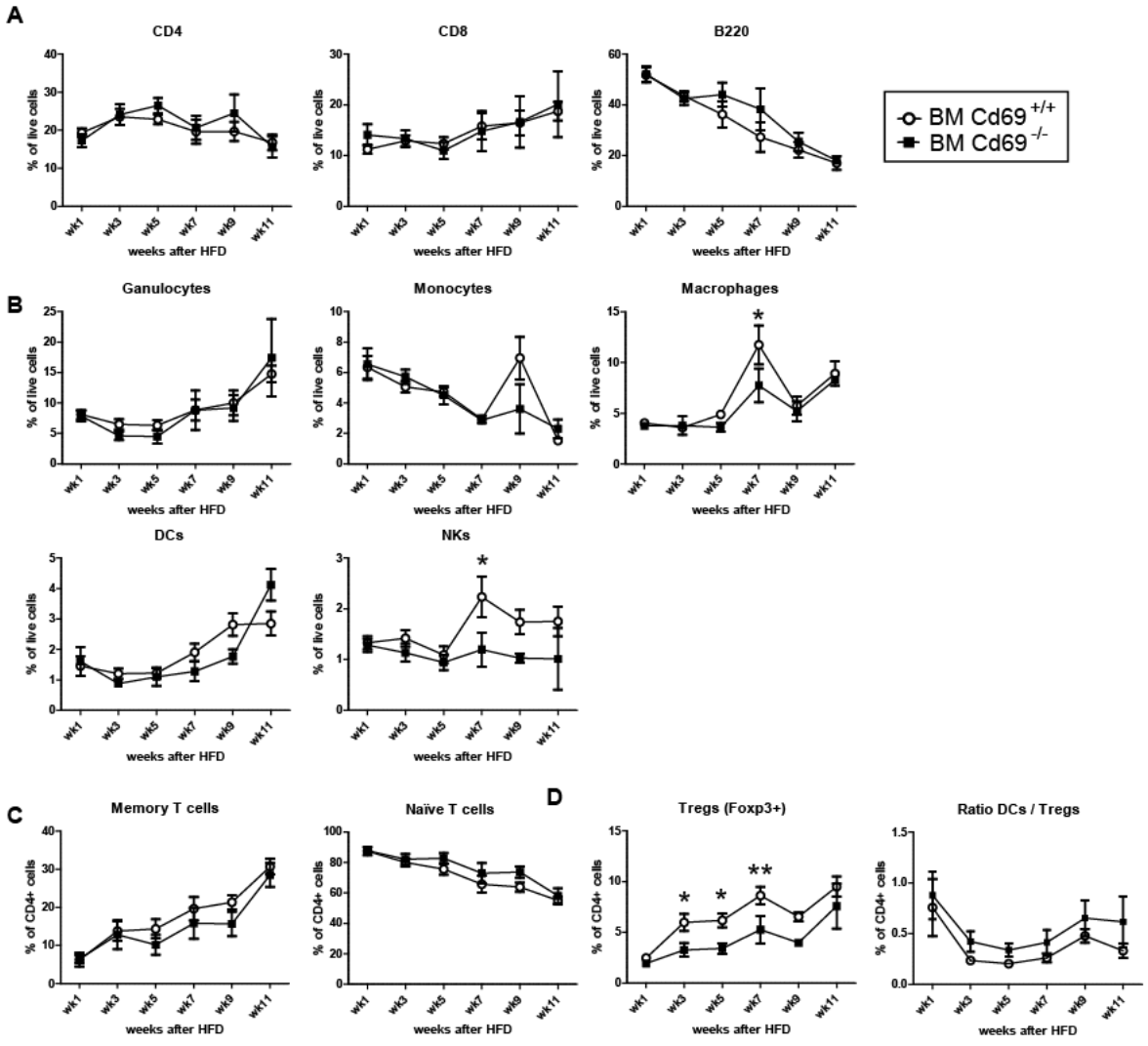

Figure 21. Analysis of blood leukocyte subsets during high fat diet. A. Analysis of lymphoid CD4+, CD8+ T cells and B cells (B220) was performed by FACS. B. Myeloid cells were analysed after surface staining with anti-CD11b, -CD11c, -Ly6G/C, -F4/80 and NK cells with anti–Nkp46. The percentages of granulocytes, monocytes, macrophages, natural killer cells (NKs) and dendritic cells (DCs) are shown. C. Surface staining with anti-CD44/CD62L was performed to distinguish naïve (CD62Lhi CD44lo) and memory (CD62Llo CD44hi) CD4+ T cells. D. Percentages of Tregs (Foxp3+) and the ratio between DCs and Tregs is shown. n= 15 BM *Cd69*$^{+/+}$ and n=13 BM Cd69-/-chimeric mice. Error bars show SEM, *P < 0.05, **P < 0.01. P values were calculated by 2-way ANOVA (Sidak´s post hoc test).

2.3. CD69 deficiency in lymphoid cells aggravates atherosclerosis

To address whether the observed phenotype in BM *Cd69*$^{-/-}$ mice is specific to the lymphoid compartment (LC) mixed BM chimeras proficient or deficient for CD69 in either the LC (LC *Cd69*$^{+/+}$ and LC *Cd69*$^{-/-}$ groups) were generated and the specific deletion of CD69 on lymphocytes was confirmed by flow cytometry analysis in the blood of hyperlipidemic mice (Figure 22A). It was observed a significantly enhanced plateau of Th17 response in the peripheral blood of the LC *Cd69*$^{-/-}$ group after HFD, whereas percentages of Foxp3 cells were significantly decreased compared with the Cd69+/+ group (Figure 22B and 22C). On observation that peripheral Th17 responses started to diminish in the LC *Cd69*$^{-/-}$ group after week 16 on HFD (Figure 22C), mice were euthanized, and immune responses and plaque formation were assessed. IL-17–eGFP+ cells in para-aortic LNs from LC *Cd69*$^{-/-}$ mice were once again increased, whereas the percentages of Foxp3mRFP+ cells were comparable in the 2 groups (Figure 22D). However, the absolute number of Treg cells was significant decreased, with a significant increase in the number of Th17 cells (Figure 22D). Finally, atherosclerotic lesions were significantly more advanced with more extensive necrotic cores in the LC *Cd69*$^{-/-}$ group as assessed by Oil Red O and Masson trichrome staining (Figure 22E and 22F).

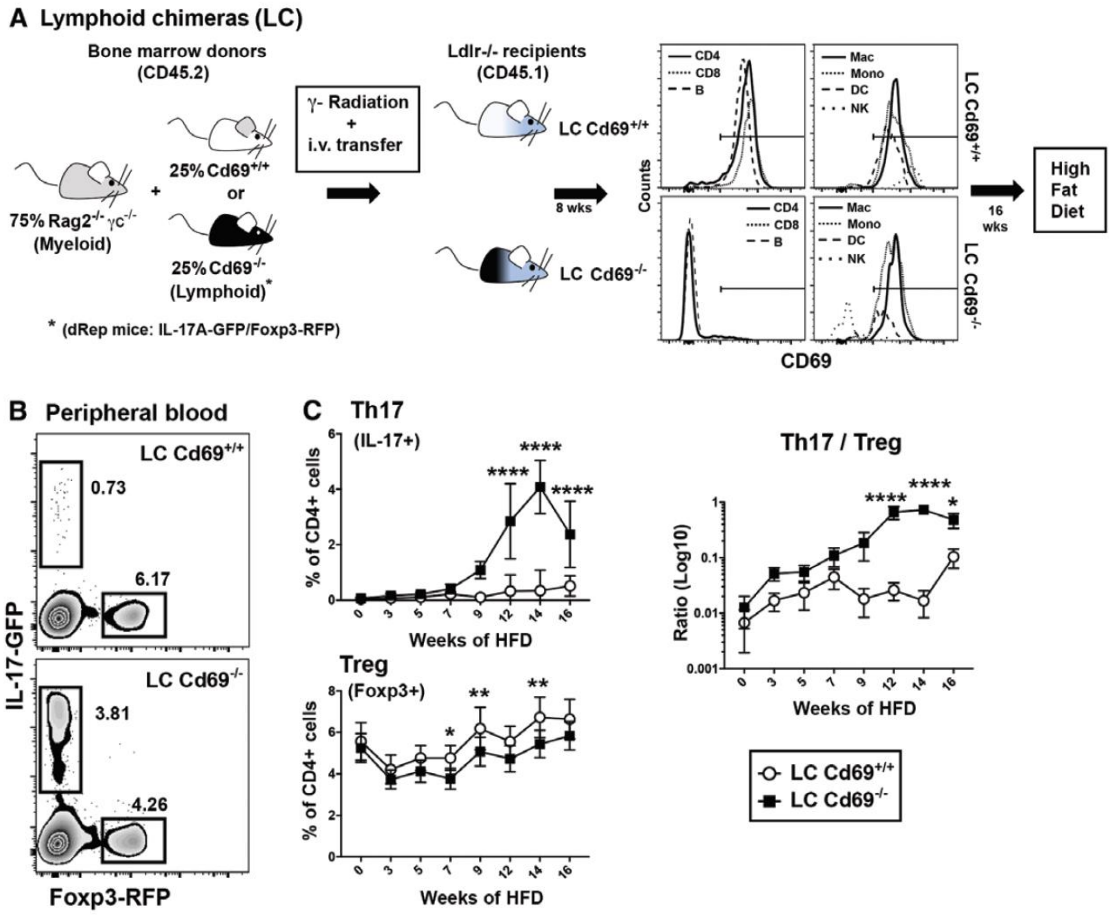

Figure 22. CD69 deficiency in lymphoid cells aggravates atherosclerosis (Next page)

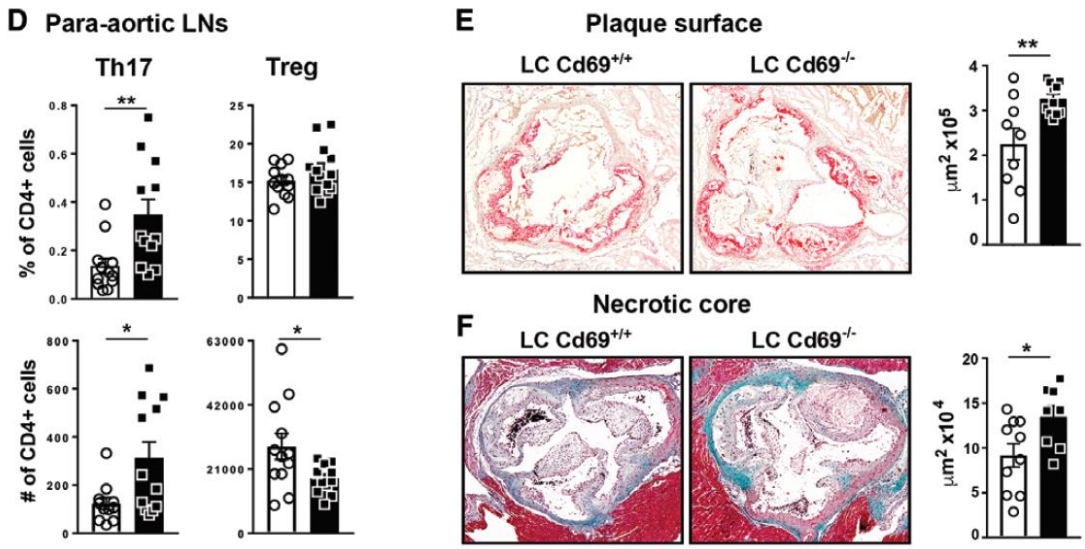

Figure 22. CD69 deficiency in lymphoid cells aggravates atherosclerosis. A, Schematic illustrating the generation of lymphoid chimeras (LCs). *Ldlr*$^{-/-}$ (CD45.1+) mice were lethally irradiated and reconstituted with mixed bone marrow (BM) from *Rag2*$^{-/-}$*γc*$^{-/-}$ plus BM from C57BL/6-Cd69$^{+/+}$ (LC *Cd69*$^{+/+}$) or C57BL/6-*Cd69*$^{-/-}$ (LC *Cd69*$^{-/-}$) (double-reporter [dRep]; mice at a 3:1 ratio, respectively. Reconstitution of the lymphoid and myeloid compartments of CD45.2+ cells was assessed by fluorescence-activated cell sorting. Peripheral blood mononuclear cells (PBMCs) after 8 weeks of reconstitution were >90% CD45.2+. Histograms show CD69 expression on CD4 and CD8 T cells, B cells (B), macrophages (Mac), monocytes (Mono), dendritic cells (DCs), and natural killer cells (NKs). PBMCs were stimulated overnight with anti–CD3/CD28 for lymphoid cells and lipopolysaccharide for myeloid cells of the indicated groups. B, Flow cytometry analysis of IL-17–GFP+ and Foxp3-RFP+ CD4 T cells in peripheral blood of LC CD69$^{+/+}$ and LC *Cd69*$^{-/-}$ mice after 14 weeks of a high fat diet (HFD). C, Percentage of Th17 (IL-17–GFP+), regulatory T (Treg; Foxp3-RFP+) CD4+ T cells, and Th17/Treg ratio in peripheral blood leukocytes of LC *Cd69*$^{+/+}$ and LC *Cd69*$^{-/-}$ mice at the indicated time points after HFD initiation. n=15 mice per group (pooled from 3 independent experiments; error bars show SEM). P values were calculated by 2-way repeated-measures ANOVA (Sidak post hoc test). *P<0,05. **P<0,01. ***P<0,001. ****P<0,0001. D, Percentage and absolute numbers of IL-17–GFP+, Foxp3-RFP+ CD4 T cells in para-aortic lymph nodes (LN). n=12 mice per group. E. Oil Red O staining and quantification of plaque and necrotic core surface in aortic valves from LC Cd69$^{+/+}$ and LC Cd69$^{-/-}$ mice after 16 weeks of HFD. n= 8 mice/group. F, As in E, Masson trichrome staining and fibrosis quantification. n=7 mice per group Original magnification ×4. In D through F, error bars show SEM. *P<0,05. **P<0,01. as determined by unpaired t test or Mann-Whitney U test.

2.4. CD69 deficiency in myeloid cells does not influence atherosclerosis development

As myeloid cells are pivotal for atherosclerosis development (Cimen et al., 2016) (Warnatsch et al., 2015), the absence of CD69 in the myeloid compartment was studied by generation of mixed BM chimeras proficient or deficient for CD69 in the MC (MC *Cd69*$^{+/+}$ and MC *Cd69*$^{-/-}$; Figure 23A). However, no differences were detected during HFD in Th17 or Treg cell dynamics in the periphery, at the site of inflammation (para-aortic LNs; Figure 23B through 23D), or in atheroma plaque formation (Figure 23E and 23F).

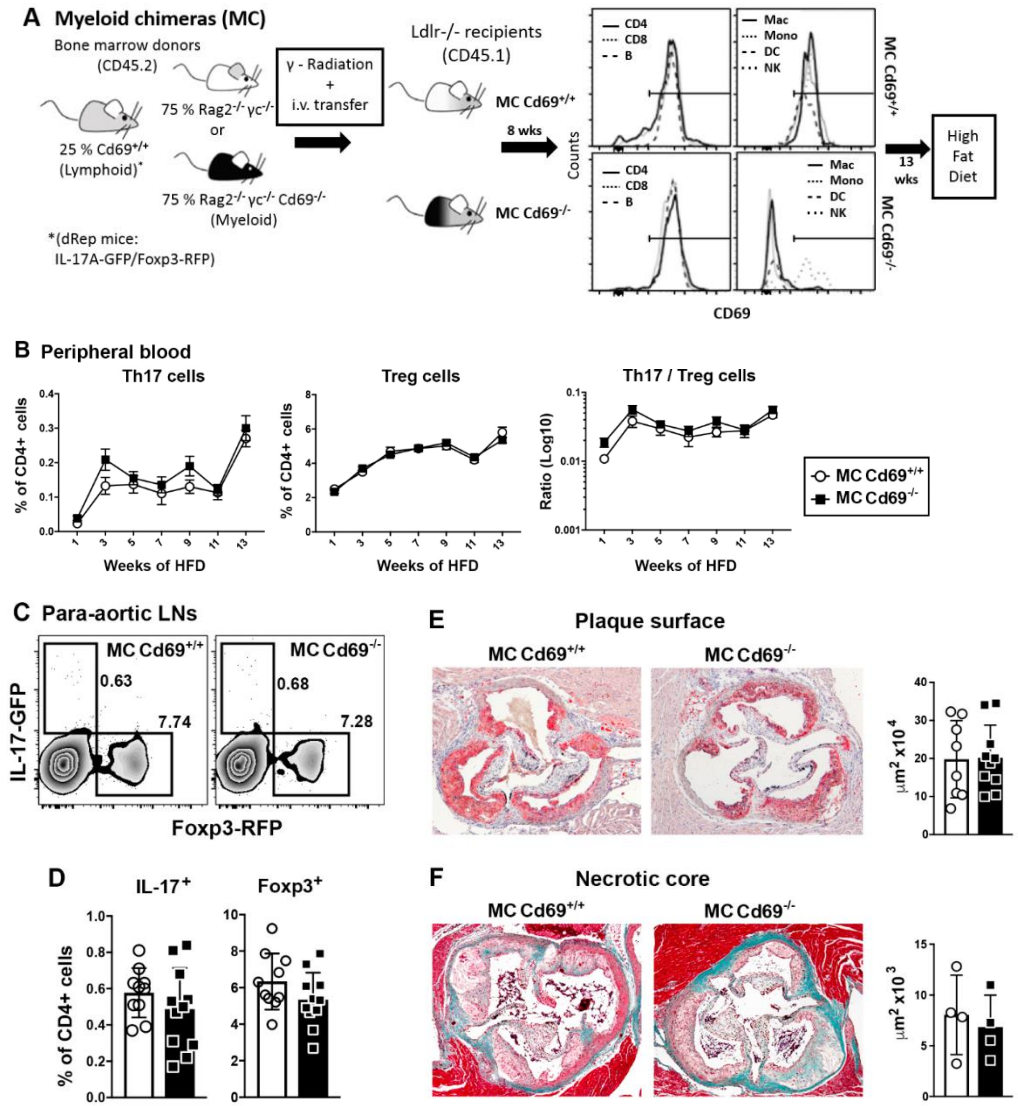

Figure 23. CD69 deficiency in myeloid cells does not influence atherosclerosis development. A. Scheme illustrating the generation of myeloid chimeras (MC). Ldlr-/- mice were lethally irradiated and reconstituted with mixed bone marrow, from *Rag2*$^{-/-}$*γc*$^{-/-}$ or *Rag2*$^{-/-}$*γc*$^{-/-}$ *Cd69*$^{-/-}$ plus bone marrow from C57BL/6-*CD69*$^{+/+}$ (double-reporter dRep: IL-17-GFP+ / Foxp3 RFP+) at a 3:1 ratio, respectively. Eight weeks after reconstitution PBMCs were > 90% CD45.2+. Reconstitution of lymphoid and myeloid compartments of CD45.2+ cells was assessed by FACS. Histograms show CD69 expression on CD4 and CD8 T cells, B cells (B), macrophages (Mac), monocytes (Mono), dendritic cells (DC) and natural killer cells (NK). PBMCs were stimulated with anti CD3/CD28 for lymphoid cells and LPS for myeloid cells, of the indicated groups. B. Kinetics of the adaptive immune response in peripheral blood for Th17 (IL-17 GFP+), Treg (Foxp3-RFP+) CD4+ T cells and Th17/Treg ratio in peripheral blood leukocytes after HFD, n=11 mice/group, C. Flow cytometry analysis of Foxp3 mRFP+ and IL-17-eGFP+ CD4 T cells in para-aortic LNs of MC *Cd69*$^{+/+}$ and MC *Cd69*$^{-/-}$ mice after 13 weeks of HFD, D. Quantification and statistical analysis of data shown in C, n=12 mice per group, E. Oil Red O staining and quantification of plaque in aortic valves from MC *Cd69*$^{+/+}$ and MC *Cd69*$^{-/-}$ mice after 13 weeks of HFD, n= 8-10 mice/group, F. As in E., Masson trichrome staining and necrotic core quantification, n=8-10 mice/group Original magnifications: 4x. Error bars show SEM. No significant differences were observed between groups as determined by two-way repeated-measures ANOVA (Sidak´s multiple comparisons post hoc tests) (B), unpaired t-test and Mann-Whitney U test (D-F) as appropriate.

2.5. Analysis of circulating lipids in mice subjected to HFD

All the CD69-proficient and -deficient groups gained similar amounts of weight throughout the experiment. However, the circulating levels of lipids (free fatty acids, triglycerides, high-density lipoprotein, LDL, and cholesterol) were lower in LC *Cd69*$^{-/-}$ compared with LC *Cd69*$^{+/+}$, suggesting that the enhanced plaque formation in LC *Cd69*$^{-/-}$ was not attributable to a metabolic defect (Figure 24). We conclude that specific CD69 deletion in the LC accounts for the increased proinflammatory phenotype and the enhanced atheroma plaque formation.

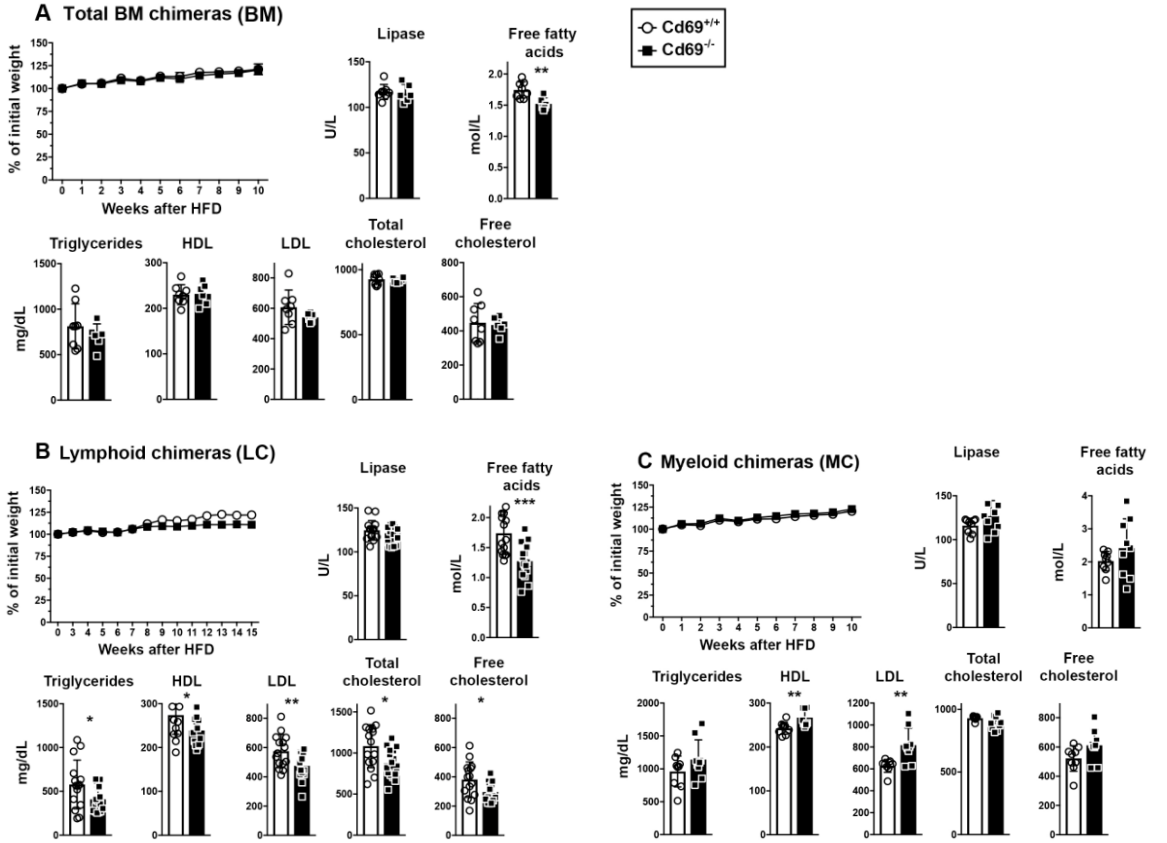

Figure 24. Analysis of circulating lipids in mice lacking CD69 in total immune, lymphoid or myeloid compartments. Weight gain, lipase activity, free fatty acids, triglyceride and cholesterol levels of the indicated experimental groups were measured. **A**. Weight curve and biochemical profile of chimeric BM *Cd69*$^{+/+}$ and BM *Cd69*$^{-/-}$ mice, n=6-8 mice/group. **B**. as in a, for LC *Cd69*$^{+/+}$ and LC *Cd69*$^{-/-}$ mice, n=15-16 mice/group. **C**. as in A for MC *Cd69*$^{+/+}$ and MC *Cd69*$^{-/-}$ mice, n=9 mice/group. No significant differences were observed in weight gain between groups as determined by two-way repeated-measures ANOVA (Sidak´s multiple comparisons post hoc tests). Error bars show SEM. *P < 0.05, **P < 0.01, ***P < 0.001, as determined by unpaired t-test and Mann-Whitney U test as appropriate.

3. Role of CD69 in the development of cardiomyopathy in the absence of microbiota.

Recent studies have shown that the gut microbiota interacts with the host contributing to many physiological processes. However, the mutualistic relationship between these commensal bacteria can also be involved in the development of several intra and extra-intestinal pathologies. There is an association between gut microbiota metabolism and composition and cardiovascular diseases and heart failure. Moreover, several autoimmune disorders have been related with alterations in gut microbiota and high autoimmunity due to bacterial induced Th17 cells. However, there is no clear link between microbiota composition and heart function in the context of autoimmune myocarditis.

3.1. CD69 deficient mice exhibit different gut microbiota composition.

Previous studies of the group showed that experimental autoimmune myocarditis (EAM) progression is Th17-dependent and that CD69 limits the severity of cardiomyopathy, being CD69 deficient mice more susceptible to develop exacerbated Th17 responses and severe myocarditis (Cruz-Adalia et al., 2010). As it has been reported that gut microbiota can induce systemic Th17 responses we hypothesized whether commensal bacteria could be playing a role in the observed phenotype. A 16S rRNA analysis of fecal contents revealed that gut microbiota composition differs between *Cd69*$^{-/-}$ mice and their wild type littermates (Figure 25), existing also differences among the two mouse strains. The different microbiota composition could explain the differences observed in both genotypes, in particular Verrucomicrobia phylum that contribute to intestinal health and glucose homeostasis, is apparently mostly absent in Cd69$^{-/-}$ mice from BALB/c background, the strain susceptible of EAM. This data could indicate that Cd69$^{-/-}$ have a less healthy gut microbiota composition.

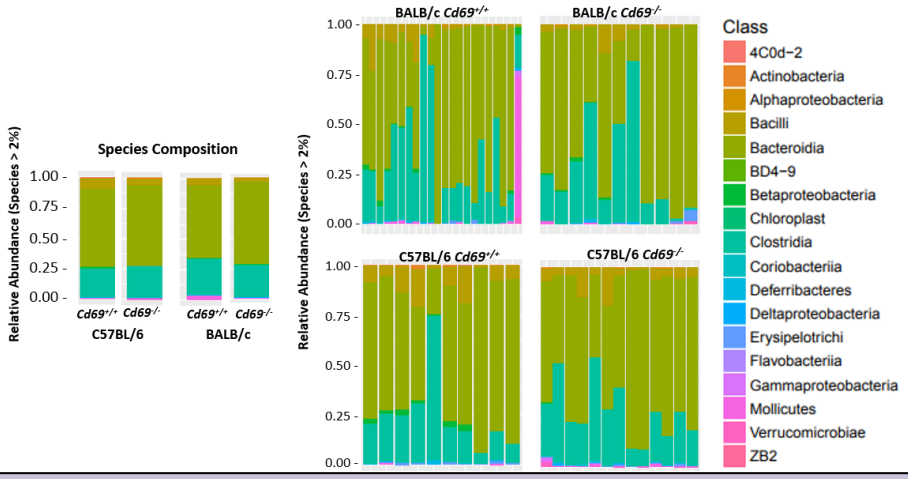

Figure 25. Gut microbiota composition of BALB/c and C57BL/6 mice proficient or deficient for CD69. On the left is represented the mean relative abundance of different species in all the mice analyzed. On the right each animal is shown individually.

3.2. Antibiotics treatment reduce heart failure after myocarditis induction

To analyze the role of microbiota in the development of myocarditis, we aimed to explore the onset and course of the disease after dampening gut bacteria what allowed us to study the role of CD69 without that variable. In order to deplete gut microbiota, a cocktail of antibiotics (Vancomycin, Puromycin, Neomyicin and Metronidazol) was given to C57BL/6 mice in drinking water. After four weeks, there was no apparent cultivable bacteria in the feces of these animals and myocarditis was induced, maintaining antibiotic treatment until the end of the experiment (Figure 26A).

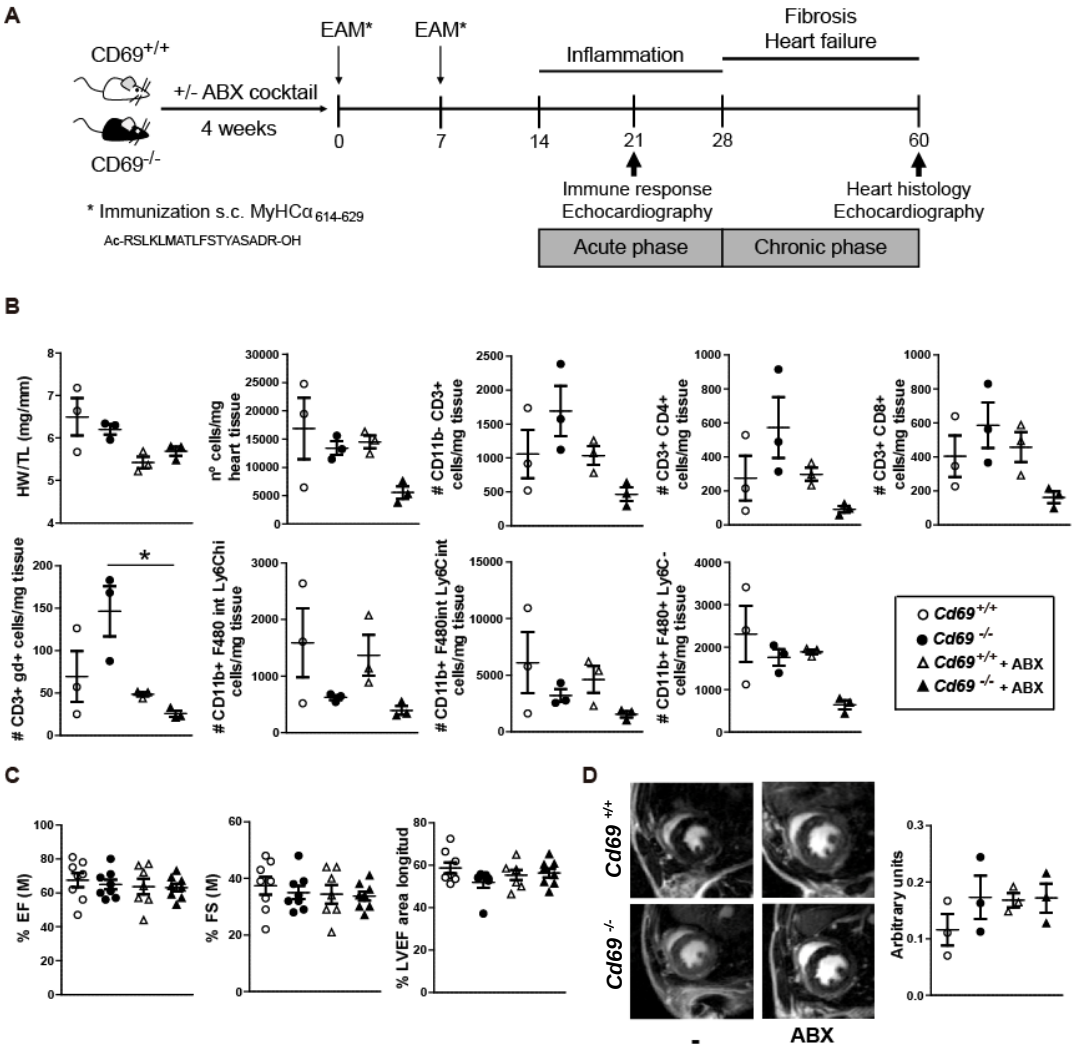

Figure 26. Myocarditis development in antibiotic-treated mice (Acute phase). A. Scheme of experimental workflow. B. Cardiomyopathy and heart infiltration of different lymphoid and myeloid subsets, 21 days after myocarditis induction. Lymphoid cells are gated on CD11b- population and myeloid cells on CD11b+ population. C. Echocardiography analysis at d20 after induction. D. Representative cardiac magnetic resonance imaging (MRI) images of each group and quantification. HW/TL (Heart weight/Tibial length), %EF (% Ejection Fraction M-mode), % FS (%Fractional Sortening M-mode), LVEF (Left Ventricule Ejection Fraction B-mode). Statistical significance was determined by Kruskall-Wallis test and Dunn's Multiple Comparison Test, not assuming normal distribution. *P < 0.05, **P < 0.01, ***P < 0.001, ****P < 0.0001.

21 days after myocarditis induction, during the acute phase of the disease, it becomes apparent that leukocyte infiltration in the heart was reduced in antibiotic-treated mice, in particular in *Cd69*$^{-/-}$ mice in comparison with *Cd69*$^{-/-}$ with regular water (Figure 26B). Echocardiography study did not reveal great differences between groups but this is quite normal in the acute phase of the disease when inflammation is high and heart function is still minimally affected (Figure 26C). Magnetic resonance imaging (MRI) was performed and, surprisingly, we found that hearts from animals presented more edematous zones when treated with the antibiotics cocktail (Figure 26D), although the *Cd69*$^{-/-}$ mice do not have enhanced edema compared to wild-type in this group. However, in the chronic phase of the disease, 60 days after induction, as previously reported, there was a drop in heart function parameters in CD69 deficient mice that is recovered in mice treated with antibiotics (Figure 27A). In addition, histological analysis revealed that hearts from CD69 deficient mice presented higher fibrotic areas compared to their wild type littermates while this increase is not observed in the antibiotic-treated CD69 deficient animals (Figure 27B). These data point to a role of microbiota in the development of severe myocarditis, however, the ABX treatment is not able to eliminate all the gut microbiota and given that, *Cd69*$^{+/+}$ and *Cd69*$^{-/-}$ have different microbiota composition, that could be influencing the response and the course of the disease.

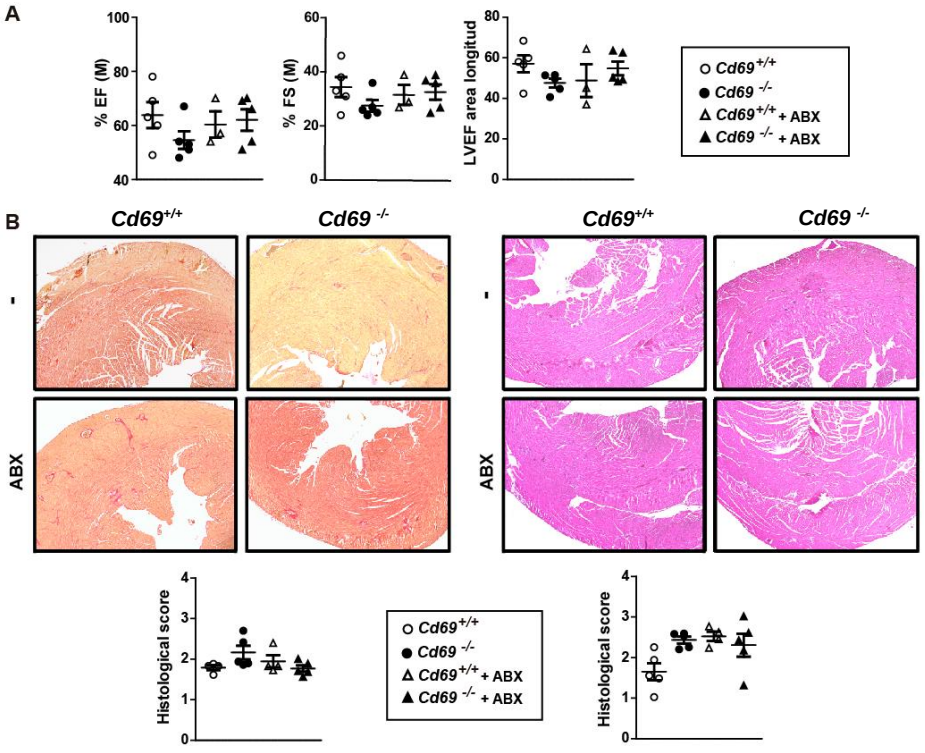

Figure 27. Myocarditis induction in antibiotic treated mice (Chronic phase). A. Echocardiography analysis at d60 after myocarditis induction. B. Representative images of Picrosirius Red staining (left) for collagen fibrosis and Hematoxilin&Eosin staining (right) for inflammation of paraffin embedded heart sections. Statistical significance was determined by Kruskall-Wallis test and Dunn's Multiple Comparison Test, not assuming normal distribution. *P < 0.05, **P < 0.01, ***P < 0.001, ****P < 0.0001

3.3. Systemic inflammation and autoimmune myocarditis are abrogated in the absence of microbiota.

To further confirm that gut microbiota was playing a role in the development of myocarditis and dilated cardiomyopathy, EAM induction was performed in the Germ Free facility of the University of Bern in collaboration with Dr. MacPhersons´s group, where animals were housed completely sterile. In parallel, the same experiment was carried out in specific pathogen free conditions (SPF) at CNIC. According to the results obtained with the antibiotic cocktail, germ free mice did not present heart infiltration and in contrast to what happens in SPF conditions, there was complete lack of Th17 responses in the heart of germ free mice (Figure 28A). In SPF conditions CD69 deficient mice behaves as previously reported, presented an exacerbated systemic inflammation characterized by strong IL-17 and IFNγ responses (Figure 28B).

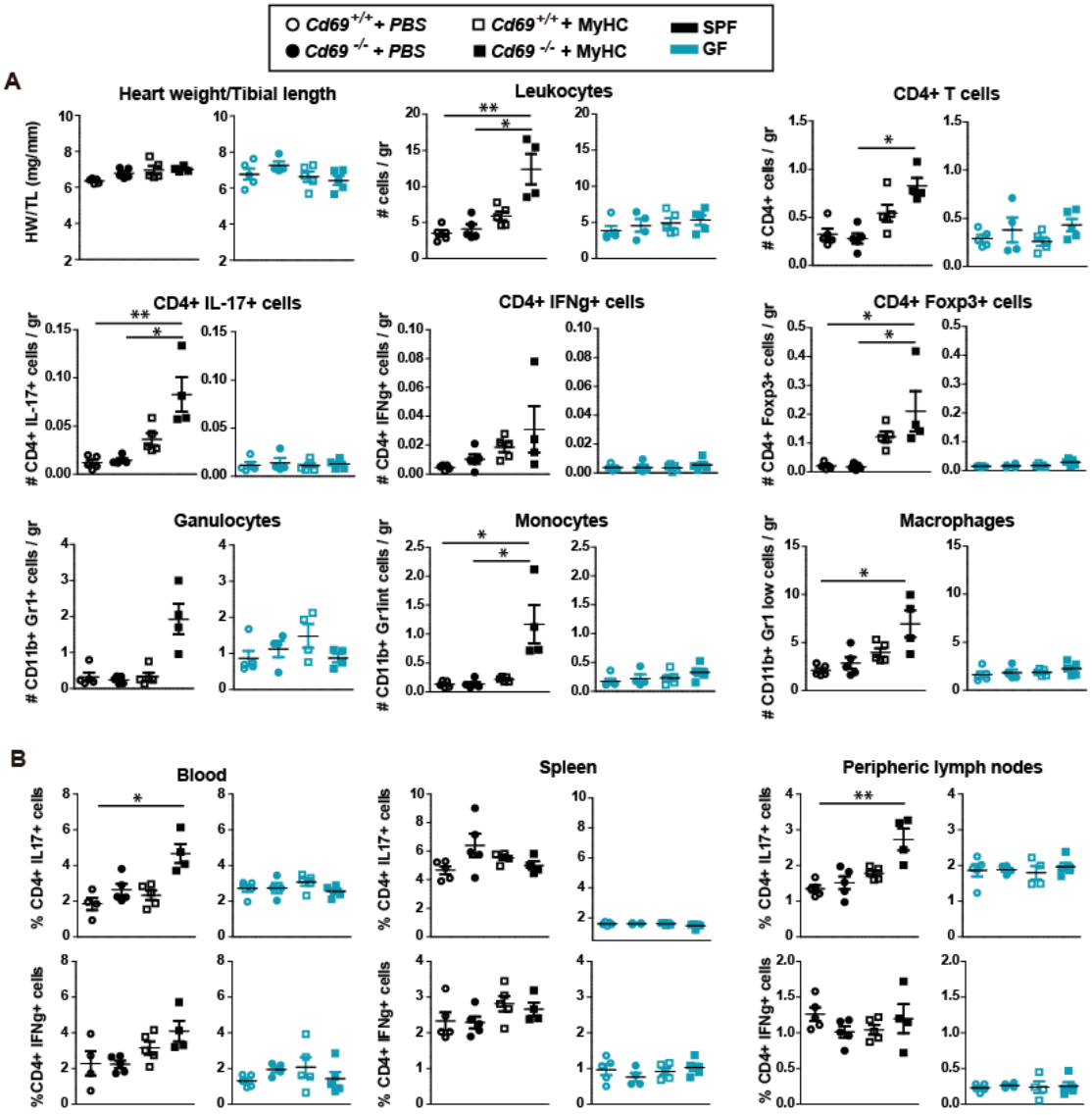

Figure 28. Heart failure after myocarditis induction is abrogated in the absence of microbiota.

Figure 28. Heart failure after myocarditis induction is abrogated in the absence of microbiota. B. Percentages of CD4+ IL17+ cells (up) and CD4+ IFNg+ cells (down) in peripheral blood, spleen and peripheric (inguinal and axillary) lymph nodes. Statistical significance was determined by Kruskall-Wallis test and Dunn's Multiple Comparison Test, not assuming normal distribution. *P < 0.05, **P < 0.01, ***P < 0.001, ****P < 0.0001.

In germ free conditions there was not apparent activation of the immune system after myocarditis induction (Figure 28) and therefore, there was not triggering of Th17 responses (Figure 29). Consequently, the heart function was maintained unaltered 60 days after peptide injection in germ free conditions. However, as previously described, under SPF, CD69 deficient mice presented a severe heart failure, with decreased ejection fraction and fractional shortening and increased left ventricular mass (Figure 29A-B). These data clearly indicated that the presence of microbiota seems to be essential for the development of Th17 responses that drive heart inflammation and subsequent cardiomyopathy after challenge with immunogenic peptides towards heart myosin heavy chain. Moreover, microbiota is also needed to trigger the severe myocarditis in the absence of CD69, suggesting an interaction between this receptor and gut bacteria essential to exert its function. To further confirm that myocarditis is not taking place in germ-free animals, we aimed to address the infiltration and fibrosis of chronic phase by histological analyses after H&E and Masson trichromic staining, respectively. The histology revealed great affected areas in CD69 deficient hearts under SPF with extensive fibrotic and infiltrated areas (Figure 29C and D) confirming the data by flow cytometry and echocardiography, whereas mice under germ free conditions do not showed neither inflammation nor fibrosis. These data are the first that firmly demonstrate that gut microbiota is needed for the development of myocarditis and dilated cardiomyopathy and also contributes to the regulation of the disease by interacting with the CD69 immune-receptors pathway.

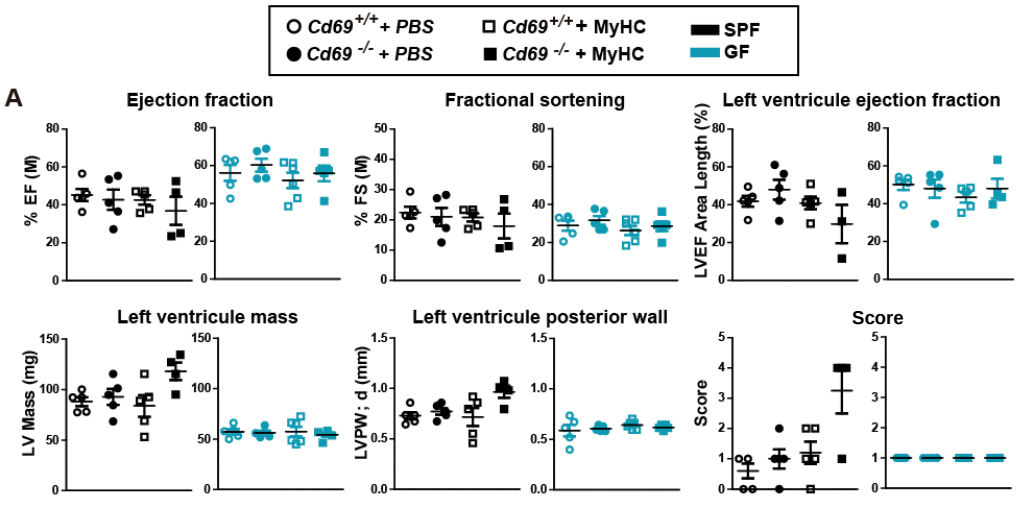

Figure 29. In the absence of microbiota, heart failure after myocarditis induction is abrogated.

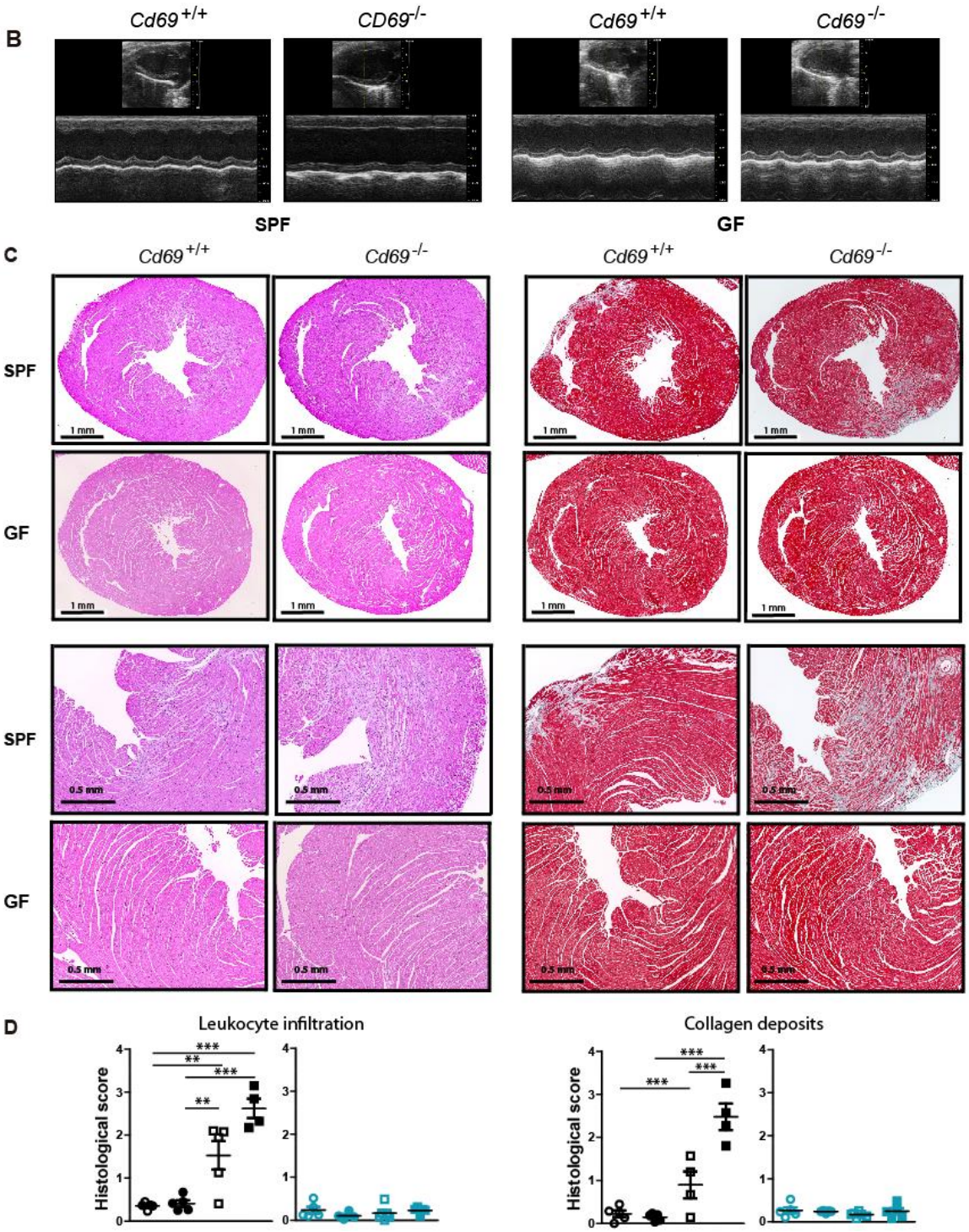

Figure 29. In the absence of microbiota, heart failure after myocarditis induction is abrogated. A. Echocardiography analysis at d60 after myocarditis induction. Score: B. Representative images of echocardiography showing ejection fraction (contraction) of the heart along long axis. Statistical significance was determined by Kruskall-Wallis test and Dunn's Multiple Comparison Test, not assuming normal distribution. *P < 0.05, **P < 0.01, ***P < 0.001, ****P < 0.000. C. Representative images of hematoxilin & eosin staining (left) and Masson trichromic staining (right) of paraffin embedded heart sections. Top: 2.5x magnification. Bottom: 5x magnification. D. Quantification of infiltration (left) and fibrosis (right) as described in materials and methods. P-values were calculated with one-way ANOVA with Tukey post-test *P < 0.05, **P < 0.01, ***P < 0.001, ****P < 0.0001.

DISCUSSION

DISCUSSION

1. CD69 as an immunomodulatory molecule

In the last decades, different studies have proven the complex role of CD69 in the modulation of both innate and adaptive immune responses. CD69 deficiency in the lymphoid compartment increases inflammation in different models of chronic inflammation like arthritis (Sancho et al., 2003) allergic asthma and contact dermatitis (Martin et al., 2010b), autoimmune myocarditis (Cruz-Adalia et al., 2010) or colitis (Radulovic et al., 2012). In all those cases CD69 deficient mice present exacerbated Th17 responses. Therefore, CD69 can be defined as negatively regulator of inflammation through the regulation of the balance between Th17 and regulatory T lymphocytes.

In this study we have addressed the role of CD69 in the context of innate immune NK cells, revealing that CD69 can modulate NK cell activity through clustering organization of the different NK cell receptors. CD69 deficient NK cells present higher cytotoxic activity against tumors and allogenic cells allowing resistance to graft versus host disease development after HSCT. We have also studied the role of CD69 in the context of adaptive immune responses in cardiovascular diseases such as atherosclerosis and myocarditis. Taking advantage of chimeric *Ldlr*$^{-/-}$ mice under HFD as atherosclerosis model, we show that CD69 depletion on the lymphoid compartment leads to an altered Th17/Treg equilibrium and a consequent exacerbated increase in atheroma plaque during disease progression. Nowadays it is known that gut microbiota is involved in the modulation of local and systemic inflammation in several diseases, including cardiovascular pathologies. Here we have demonstrated that CD69 can influence Th17 responses in heart and the composition of gut microbiota affecting the severity of autoimmune myocarditis. And finally, in this study we show that gut microbiota is required for the progression of the autoimmune myocarditis to the development of dilated cardiomyopathy.

2. Role of CD69 in the regulation of "natural killer" (NK) cells activity in the context of innate immunity.

CD69 has been well studied in the context of adaptive immune response and its role in the development of several immune disorders is well documented. There are also studies in which CD69 function is studied in the context of innate immunity and NK cells. These early studies postulated CD69 as a stimulatory receptor for NK cells that can be blocked by CD94 (Moretta et al., 1991) (Zingoni et al., 2000). Moreover, in vitro studies suggested that CD69 is a pro activator molecule in all leukocytes, including NK cells (Testi et al., 1994) (Cebrian et al., 1988). However, recent studies indicate that CD69 exerts a down-regulatory role in vivo in the immune system, as CD69 deficient

mice exhibit a potent immune response against tumor cells (Esplugues et al., 2003) and the treatment with anti-CD69 antibodies induces strong tumor NK-cell immunity against tumors (Esplugues el al,Blood 2005). However, the molecular mechanism/s explaining the enhanced activation of NK cells in the absence of CD69 are still not elucidated. But the activatory/inhibitory status of the NK cells very much depends on the expression of a plethora of different NK receptors in the membrane of the cells. NK cell education and differentiation, including acquisition of both activating and inhibitory receptors, occurs primarily in the bone marrow. The process of receptor acquisition and NK cell education remains poorly understood. However, it is known that terminal NK cell differentiation usually occurs when the cells present $CD94^{low}$ and $CD56^{dim}$ expression (Yu et al., 2010) and is characterized by the appearance of CD57, decreased proliferation and increased cytolytic activity (Moussa et al., 2012). It has been shown here that CD69 deficient NK cells present lower expression of CD94 and higher cytolytic activity than control cells, suggesting a more activated phenotype. In line with previous reports (Yu et al., 2009), and in agreement with the notion of a functional dichotomy of NK cells between cytokine production and cytotoxicity (Colucci et al., 2001, Mondelli et al., 2012, Rajagopalan et al., 2001), the lower levels of CD94 in *Cd69*$^{-/-}$ mice resulted in lower IFN-γ production in all tested contexts (not shown). These cells also have a different expression pattern of several activating and inhibitory NK cell receptors, with higher expression of the activating receptor Ly49D but lower expression of the activating receptor Ly49H and the inhibitory receptors Ly49A and Ly49E. Ly49H directly binds the m157 glycoprotein encoded by murine cytomegalovirus (MCMV) on infected cells (Adams et al., 2007), while Ly49D recognizes the MHC-I molecule H2-Dd and is responsible for the rejection of bone marrow allografts in C57BL/6 recipient mice (George et al., 1999), though Ly49 gene haplotypes differ between mouse strains and BALB/c mice don't possess Ly49H or Ly49D. Thus, the exact mechanism by which BALB/c NK cells recognize allogenic cells is still unclear. Interestingly, Ly49H expression is dampened in *Cd69*$^{-/-}$ C57BL/6 mice that are highly susceptible to MCMV infection confirming that the absence of CD69 in NK cells induced different repertoire of receptors in the membrane of these cells.

Data obtained in this Thesis support the idea of CD69 as a negative regulator of the immune response in NK cells. In this work it has been observed that *Cd69*$^{-/-}$ NK cells were more efficient in the elimination of a poorly immunogenic tumor in vivo. To study the role of NK cells in the tumor response, avoiding the effect of CD8+ T cells anti-tumor responses, we have analyzed Rag2KO mice that lack T or B lymphocytes. Increased NK cell percentage and absolute numbers in the lungs, where the tumors grow, were reported in *Rag2*$^{-/-}$*Cd69*$^{-/-}$ mice and degranulation after *in vitro* re-stimulation was also higher in *Rag2*$^{-/-}$*Cd69*$^{-/-}$ NK cells, accounting for the increased cytotoxicity in these mice. Moreover, *Rag2*$^{-/-}$*γc*$^{-/-}$ and *Rag2*$^{-/-}$*γc*$^{-/-}$*Cd69*$^{-/-}$ recipients, lacking NK cells, were unable to

eliminate allogeneic splenocytes, confirming that other cells of lymphoid or myeloid origin are not involved in the observed phenotype that is driven by NK cells, independently of CD69 expression. We have found that NK cells from $Cd69^{-/-}$ mice with tumors are more mature and have inhibited expression of inhibitory CD94 in the membrane, again indicating a different repertoire of receptors compared to wild type NK cells.

NK cells have to stay tolerant to healthy tissues and they express at least one inhibitory receptor specific for self MHC as a means to prevent NK cell autoreactivity (Joncker and Raulet, 2008), this is known as NK cell education. While there is no doubt that MHC class I molecules play a critical role in NK cell education, there is considerable debate regarding the types of cell interactions (or lack thereof) that influence this process. One hypothesis proposed is the tuning model which postulates that each NK cell, depending on the inhibitory (and stimulatory) receptors expressed, and the MHC genotype of the animal, receives a varying amount of stimulation and inhibition when encountering neighboring cells. Stimulatory and inhibitory signals are thought to be integrated by the NK cell. The model proposes further that depending on the net stimulation received, the NK cell assumes a quantitatively appropriate responsiveness state. Strong net stimulation (e.g. steady state stimulation without opposing inhibition) drives the NK cell to its lowest responsive state, whereas weak (or no) net stimulation drives the cell to its highest responsive state. Ly49G2 is an inhibitory receptor that recognize self MHC I molecules. This receptor is overexpressed in CD69 deficient NK cells compared to CD69 proficient cells. According to this theory, CD69 deficient NK cells would had received weak stimulation during their education process, driving the cells to a higher responsive state (Shifrin et al., 2014) (Joncker et al., 2009)

The cytolytic capacity of human and mouse NK cells appears to be directly related to KIR and NKp46 expression levels, respectively (Garcia-Iglesias et al., 2009, Glasner et al., 2017, Sivori et al., 1999). Of note, mean fluorescence intensity for NKp46 was significantly increased both in the $Cd69^{-/-}$ and the mAb-treated $Cd69^{+/+}$ groups compared to the non-treated $Cd69^{+/+}$ mice.

Hematopoietic stem cell transplantation (HSCT) has proven to be an effective treatment for a wide range of hematologic malignancies and some solid tumors (Copelan, 2006) (Ljungman et al., 2010). However, in most cases it is impossible to find a donor with identical major histocompatibility complex (MHC) proteins and up to 80% of patients in mismatch settings develop graft-versus host disease (GvHD) (Perez-Simon et al., 2006).

It has been previously reported that NK cells may promote transplant tolerance by killing donor antigen-presenting cells (Yu et al., 2006). Moreover, prior studies have demonstrated that NK cells are resistant to ionizing radiation (Bogdandi et al., 2010) (Yang et al., 2014). Here it has been

confirmed that NK cells are resistant to lethal doses of myeloablative ionizing radiation. Importantly, 6-8 weeks after reconstitution, chimerism was complete in the *Cd69*$^{-/-}$ mice, indicating that host NK cells do not fully eliminate the graft, which is important to maintain the graft versus leukemia effects, and they do not persist in the host in the long run. Although radiotherapy-resistant T cells made up a small percentage of residual host cells, roughly 85% of these cells were eliminated 7 days after transplant, whereas 70-80% of host NK cells were still present at this time point. Thus, it appears that residual NK cells protect *Cd69*$^{-/-}$ hosts from aGVHD development by reacting against allogenic T cells, decreasing the T-cell mediated host tissue damage after allogenic stem cell transplant.

NKG2D is the best-characterized activating NK cell receptor. It recognizes "induced-self" ligands – molecules that are not expressed or are expressed at low levels on most healthy cells, but that can be induced by hyper-proliferation and transformation, as well as when cells are infected by pathogens. Thus, the NKG2D pathway serves a mechanism for the immune system to detect and eliminate cells that have undergone "stress" (Raulet, 2003, Lanier, 2005, Raulet et al., 2013). NKG2D recognizes an extensive repertoire of ligands including MICA/MICB and ULBP1–6 in humans, and MULT1, RAE-1α-ε, and H60a–c in mice (Raulet et al., 2013). NKG2D recognition of target cells is a major mode of natural killing of tumor cells (Jamieson et al., 2002), and has been implicated in some autoimmune diseases as well (Schleinitz et al., 2010) (Schleinitz et al., 2010). Recent studies suggest that this receptor may mediates NK cell education in the bone marrow and peripheral tolerance upon chronic ligand exposure mediating its own downregulation and subsequent hypo-responsiveness to stimulation. Chronic NKG2D ligand recognition mediates downregulation of the receptor and reduce NK cell responsiveness. Under physiological conditions, this process is thought to prevent NK cell hyper-responsiveness against peripheral ligands for which education in the bone marrow is incomplete (Groh et al., 2002) (Mincheva-Nilsson et al., 2006) (Cox et al., 2015).

In this work we hypothesized that CD69 and NKG2D could be interacting in the membrane of NK cells, based in our unbiased mass cytometry and RNAseq analysis. Chronic NKG2D engagement by NK cells results in reduced responsiveness of multiple receptors other than NKG2D. This mechanism could explain the differences in the expression pattern of membrane receptors in CD69 deficient NK cells. In this work, it has been demonstrated that CD69 and NKG2D cluster together and interacts in the cell membrane. In the absence of CD69, NKG2D expression-cluster population disappears and the expression of the receptor dilutes in different cell clusters. Therefore, these data indicate that CD69-NKG2D interaction may be necessary for the fine downmodulation of NKG2D upon chronic engagement, as, in the absence of CD69, NKG2D remains active in NK cell membrane, driving the cell to a hyper-responsiveness state (Figure 30). This type of membrane regulation/stabilization of

other receptors by CD69 has been described. For example, it associates with the aromatic-amino-acid-transporter complex LAT1-CD98 on the plasma membrane of activated T cells and regulates its surface expression and uptake of L-tryptophan (L-Trp) (Cibrian et al., 2016). CD69 also associates with of S1P(1) receptors in the membrane of leukocytes and inhibits their function by inducing its internalization and degradation, this mechanism is the responsible for the modulation of T cell egression from lymph nodes (Bankovich et al., 2010) (Shiow et al., 2006).

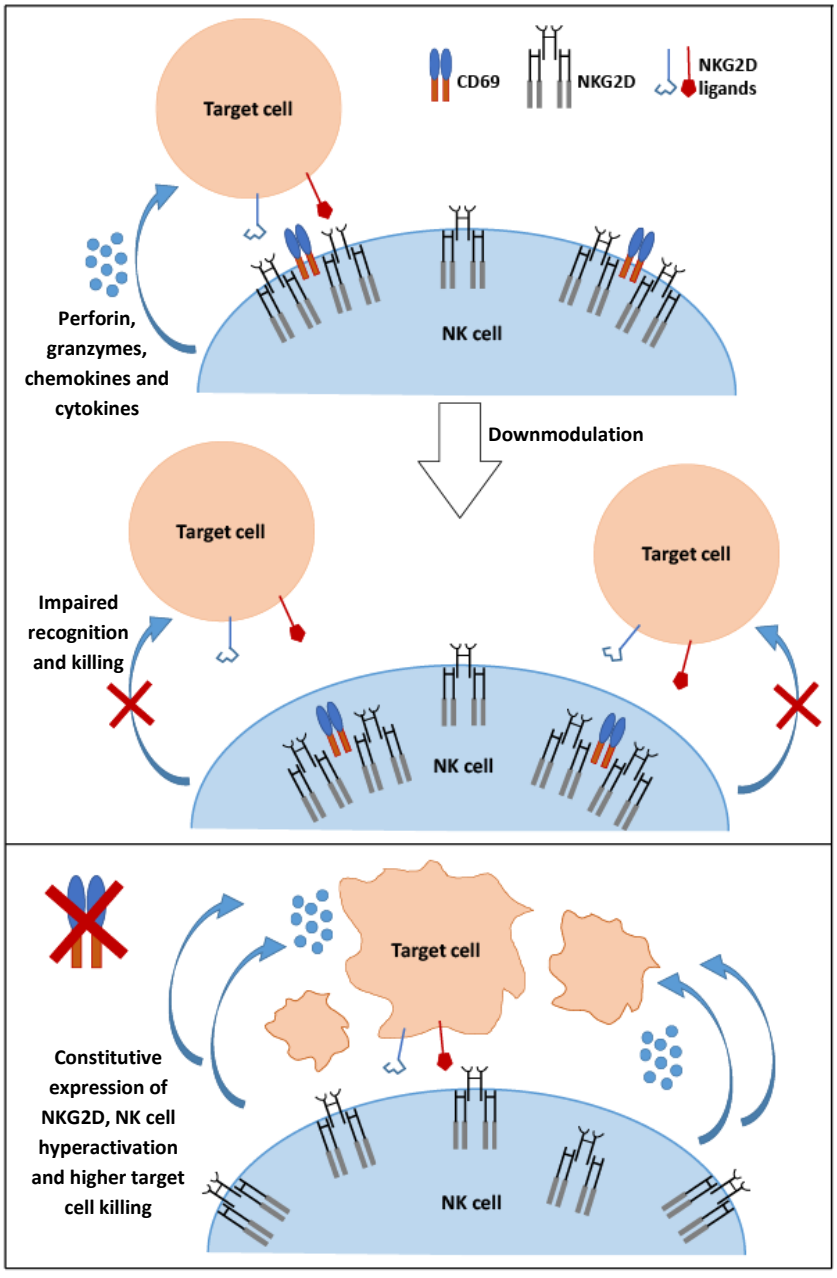

Figure 30. Hypothesis of CD69-NKG2D interaction. Upper. CD69 would interact with NKG2D in the membrane facilitating its stabilization in the membrane and allowing NKG2D downregulation after chronic stimulus. Lower. In the absence of CD69, NKG2D is not downregulated and it is constitutively expressed in the cell membrane leading NK cell to a hyperactivated state with higher target cell killing. Adapted from (Molfetta et al., 2016)

Cell therapy with NK cells has been proposed to prevent GvHD as it has been proved that administration of activated NK cells resulted in GvHD inhibition and higher Graft versus tumor effects after allogeneic bone marrow transplant (Asai et al., 1998) (Murphy and Longo, 1997) (Olson et al., 2010). In all those cases the authors study the possibility of injecting donor activated NK cells at the time of HSCT. Here we proposed that enhancement of cytolytic activity of the recipient NK cells could also be useful in the clinic for prevention of GvHD. This enhancement could be achieved by pharmacological blockade of CD69, although more research is still needed to confirm this hypothesis.

Concomitant injection of anti-CD69 mAb with the allogenic T cell depleted BM and naïve T cells led to the complete elimination of the graft in the mAb-treated mice and high mortality due to lack of BM engraftment (not shown). Previous work on both animal models and clinical trials has shown that injection of T Cell depleted BM and subsequent infusions of donor T cells is a valid option that successfully restores host immunocompetence and maintains the graft versus leukemia (GvL) effect. However, risk of aGvHD is high in these protocols (Collins et al., 1997, Drobyski et al., 1993, Johnson et al., 1993). Here the aGvHD induction protocol was adapted to match these clinical settings, inducing aGvHD with allogenic T cell infusion together with a second dose of anti-CD69 mAb 3 days after reconstitution with T cell depleted bone marrow to allow a good engraftment.

Irradiation is not the treatment of choice for malignant bone marrow elimination in the clinics. Preliminary results not shown in this thesis have indicated that on day 0 after chemotherapy mostly cells of myeloid origin persist in the host. However, a clear lymphocytic subset is detectable and within this population, a $CD56^{dim}CD16^{+}$ NK cell subset is present in varying percentages in the $CD3^{-}$ compartment. In line with data from the mouse model, residual host $CD56^{dim}CD16^{+}$ NK cells expressed high levels of CD69 after chemotherapy. This was not the case for other persisting immune cell subsets like T cells or granulocytes, nor for the $CD56^{bright}CD16^{-}$ subset of NK cells. However, CD69 levels gradually diminish as donor cells expand and repopulate the host. After 7 days only a small percentage of host NK cells persist in some patients, which could be responsible for the remaining $CD69^{+}$ cells within this subset.

Taken together, our data so far indicates that pharmacological targeting of CD69 on human NK cells, could increase their cytolytic capacity, modulate activating/inhibitory receptor repertoire, and contribute to the control of alloreactive donor T cell clonal expansion in the early stages after transplant. Although more research regarding CD69 expression in patients after HSCT and its correlation with graft versus host disease development and progression is needed.

3. Role of CD69 in the progression of atherosclerosis in the context of adaptive immunity.

CD69 controls inflammatory processes through modulation of Treg/Th17 responses. In this work it has been shown that the absence of CD69 in the lymphoid compartment results in larger atheroma plaque formation in *Ldlr*$^{-/-}$ deficient mice subjected to high fat diet. This could be associated, at least in part, with defects in Treg cell differentiation. It has been well documented that Treg cells exert an atheroprotective function through the suppression of T-cell proliferation and secretion of anti-inflammatory cytokines, playing a protective role during the initial phases of atherosclerosis not only by reducing atherosclerotic plaque formation but also by improving stabilization of the atherosclerotic lesions (Butcher et al., 2016) (Mallat et al., 2007) (Foks et al., 2011). On the other side, CD69 also controls Th17 differentiation through the association of its cytoplasmic tail with the Jak3/Stat5 signaling pathway, regulating RAR-related orphan receptor-γ transcription and differentiation toward the Th17 lineage (Martin et al., 2010a).

The role of IL-17 in atherosclerosis is not so clear, as recent evidence has indicated both proatherogenic and antiatherogenic roles for this cytokine (Gistera et al., 2013) (Erbel et al., 2014). Under HFD, *Ldlr*$^{-/-}$ mice deficient for CD69 in the lymphoid compartment developed exacerbated Th17 responses and more severe atherosclerotic lesions, supporting the role of IL-17 as a proatherogenic molecule. Despite previous reports supporting that IL-17 can either stabilize the plaque through collagen production or enhance the recruitment of proatherogenic cells through CXCL1 upregulation (Danzaki et al., 2012) (Erbel et al., 2014), the former seems not to be the case in our model. Increased amounts of IL-17 seem to stabilize plaque formation when levels of IL-10 are also higher, namely in the presence of a proper regulatory response (Gistera et al., 2013). In our model, however, we have a concomitant increase of IL-17 and defective Treg development and function.

Previous results indicated that the regulatory action of CD69 during atherosclerosis was lost in ApoE$^{-/-}$ mice because, compared with the double-knockout group (*Cd69*$^{-/-}$*ApoE*$^{-/-}$), no significant difference was observed in plaque formation (Gomez et al., 2009). *Ldlr*$^{-/-}$ and *ApoE*$^{-/-}$ mice have been extensively used to study the mechanisms of atherosclerosis development but feature important differences, for example, in plasma proteins. The major accumulating lipoprotein in the plasma of *Ldlr* $^{-/-}$ mice fed a high-cholesterol diet is LDL. Conversely, *ApoE*$^{-/-}$ mice accumulate cholesterol mostly in the very-low-density lipoprotein and chylomicron fractions (Getz and Reardon, 2016) (Emini Veseli et al., 2017). This is a very important issue to be considered that could account for the differences observed between *Cd69*$^{-/-}$*/ApoE*$^{-/-}$ and *CD69*$^{-/-}$*/Ldlr*$^{-/-}$ models. Additional data from the group (not shown in this thesis) identified the functional interaction

between CD69 and oxLDL as the mechanism responsible for the observed phenotype, exerting an immune-regulatory function during atherosclerosis development (Tsilingiri et al., 2019). This work shows that binding of oxLDL to CD69 induces the expression of NR4A receptors 1 and 3 that have been implicated in Treg differentiation (Sekiya et al., 2013).

In the ApoE knockout model, the levels of LDL may not have reached the threshold that is required for signaling through CD69. An additional difference that should be taken into consideration is that *Ldlr*$^{-/-}$ lesions have higher T-cell density than the ApoE model (Roselaar et al., 1996), meaning that *Ldlr*$^{-/-}$ mice have more T cells that could express CD69 to exert their function. Finally, *ApoE*$^{-/-}$ mice on an HFD develop plaques more rapidly and exhibit larger aortic lesions with larger necrotic cores than *Ldlr*$^{-/-}$ mice (Libby, 2017) (Emini Veseli et al., 2017); therefore, this high-intensity model could be masking the differences between the CD69-expressing and CD69-deficient animals. Clinical data has shown a downregulation of CD69 expression in peripheral leucocytes of subjects with subclinical atherosclerosis compared with individuals without atherosclerosis (Tsilingiri et al., 2019). This finding was in agreement with the experimental evidence showing a downregulation of CD69 expression on T lymphocytes in mice on exposure to HFD. Despite a suggested role for oxLDL in adaptive immune responses, a putative receptor on T lymphocytes has remained elusive (van Bruggen and Ouyang, 2014). This study demonstrates that binding of oxLDL to CD69 in human T cells has a protective effect against the inflammatory response, downregulating proinflammatory cytokines and promoting Treg differentiation.

The chimeric *ldlr*$^{-/-}$ mouse models used shed light on the role of CD69/oxLDL functional interaction in lymphocytes and on the maintenance of immune homeostasis to protect medium and large arteries from severe atheroma plaque formation over time. Further studies of the new regulatory oxLDL/CD69 pair in human lymphoid cells during atherosclerotic disease progression will provide novel insight into targeting these pathways for the prognosis/treatment of cardiovascular diseases.

Recent data emphasized the link between the inflammatory response and atherosclerotic risk in the clinical arena (Ridker et al., 2017). However, the complex interplay between lipid metabolism and immune responses remains to be fully disclosed. Collectively, the in vivo data obtained in this study strongly indicate an important role for CD69 expression on lymphocytes during atherosclerosis development. CD69 expression was assessed in peripheral blood lymphocytes from a cohort of subjects with thoroughly characterized subclinical atherosclerosis from the PESA study fully asymptomatic and free of cardiac events (Tsilingiri et al., 2019). The profile of CD69 expression detected in human samples was very similar to that observed in the in vivo model. Considering focal disease and generalized disease as different stages with the same pathology, this data indicate that

expression of CD69 gradually declines as disease progresses. CD69 remained significally associated with the extent of the disease when comparing subjects free of disease versus those with established but yet subclinical atherosclerosis or generalized subclinical disease, more closely resembling the animal experiments. This finding underscores the putative role of CD69 as a potential marker for the detection of atherosclerosis at a preclinical stage.

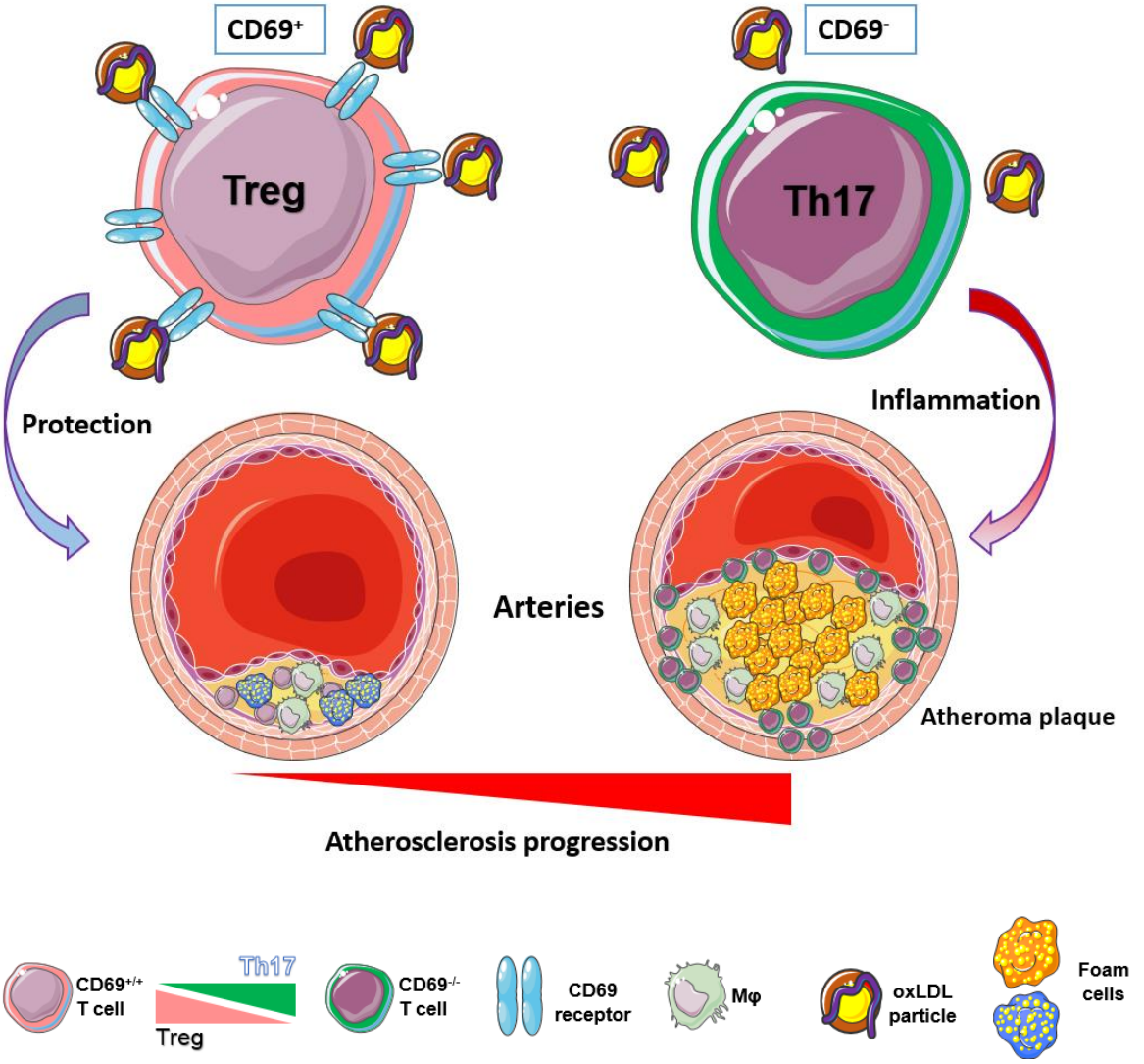

Figure 31. Scheme of the role of CD69 in atherosclerosis. Figure despites the regulatory role of CD69 in T cell responses and in the formation of atheroma plaque and disease progression. CD69 binds oxLDL particles in the membrane of circulating lymphocytes, conferring and immunomodulatory phenotype to the CD4+ T cells that modulates atheroma plaque formation.

4. Role of CD69 in the development of cardiomyopathy in the absence of microbiota

The mammal's immune system has evolved to maintain a symbiotic relationship with the highly diverse microbial community that inhabits the gut. This complex host-microbiota interaction is necessary for the correct development of the immune system. Commensal microorganisms are required for the maturation of the immune system, which "learns" to differentiate between commensal bacteria (which are becoming almost quasi-self and tolerated antigens) and pathogenic bacteria (Thaiss et al., 2016) (Nakanishi et al., 2015). Gut microbiota has been shown to modulate neutrophil migration and function (Owaga et al., 2015) and to affect the differentiation of T cell populations into different types of helper cells Th1, Th2, and Th17 or into regulatory T cells (Tregs) (Francino, 2014).

It has been documented that this microbiota may be necessary to enhance the priming of autoimmune adaptive responses at extra-intestinal sites. For example, several groups have demonstrated that in the absence of microbiota (by antibiotics treatment (Ochoa-Reparaz et al., 2009) or under germ free conditions (Lee et al., 2011)) mice present reduced induction of experimental autoimmune encephalitis (EAE). Recolonization of germ-free mice with SFB alone enhances central nervous system neurodegeneration upon EAE induction by promotion of Th17 cells differentiation in the gut (Lee et al., 2011). In addition, germ-free K/BxN mice are resistant to the development of autoimmune arthritis, while SFB mono-colonization restores the disease through the activation of Th17 cells in the intestine which then traffic to the spleen to aid in germinal center formation and the production of autoantibodies (Wu et al., 2010). More recently, SFB colonization in K/BxN mice was found to induce the activation of follicular helper T cells (Tfh) in the PPs, which subsequently egress to the spleen and aid in the production of auto-antibodies (Teng et al., 2016).

Myocarditis can be defined as the inflammatory process affecting the muscular tissues of the heart (myocardium) and is an important cause of sudden death by heart failure in young adults (Feldman and McNamara, 2000). Etiology of the disease can be very vary, being autoimmunity the cause of some types of myocarditis. In this case, tolerance disruption leads to an uncontrolled T cell response in the heart that promotes inflammation and tissue damage. Clinical practice has shown that myocarditis is a rare extraintestinal complication of inflammatory bowel disease (Hyttinen et al., 2003) (Leuschner et al., 2009). However, little is known about the role of microbiota in the development of this disease.

There are some evidences suggesting that gut dysbiosis is associated with myocarditis. A recent study has shown an increase in microbial richness and diversity in myocarditis mice, with an

increased Firmicutes/Bacteroidetes ratio. Restored of Bacteroidetes population diminished inflammatory infiltration in the EAM mouse model, attenuating myocarditis. (Hu et al., 2019). A previous study comparing animals from different sources (Jackson Labs and Taconic Farms) with different microbiota composition demonstrated variable susceptibility to the disease, finding more abundant RORγt$_+$ Th17 cells, as well as neutrophils and Ly6C^{hi} inflammatory monocytes in the hearts of BALB/cJ animals. Moreover, polyantibiotic dysbiosis protected mice from EAM and fibrotic cardiac dysfunction, while this antibiotic treatment failed to suppress the development of myocarditis in *Il17RA*$^{-/-}$ animals (Barin et al., 2017). It has been reported that Th17 cells play a critical role in the development of cardiac inflammatory disease and heart failure and an important role for segmented filamentous bacteria (SFB) in eliciting Th17 responses from intestinal T cells has been also well-described. (Ivanov et al., 2009) (Ivanov and Honda, 2012) (Gaboriau-Routhiau et al., 2009), predicting that SFB colonization could contribute to susceptibility to autoimmune disease through the induction of Th17 cells (Lee et al., 2011; Wu et al., 2010). However, SFB colonization had neither protective nor pathogenic effects on development of EAM (Barin et al., 2017).

Treatment with broad-spectrum antibiotics is commonly used to deplete the gut microbiota of mice, and can be applied to any genotype or condition of mouse. Due to differences in mechanism of action, antibiotics can selectively deplete different members of the microbiota. For example, metronidazole and clindamycin both target anaerobes, vancomycin is only effective against gram-positive bacteria, and polymyxin B specifically targets gram-negative bacteria (Brandl et al., 2008) (Schubert et al., 2015). A cocktail of different classes of antibiotics can be used to broadly deplete the gut microbiota. However, there are reports of mice avoiding water and becoming dehydrated when provided antibiotics in this manner (Hill et al., 2010) (Reikvam et al., 2011) (Zakostelska et al., 2016). This was the case of BALB/c mice and that is the reason why antibiotic depletion experiments in this thesis were done with C57BL/6 mice instead of BALB/c mice despite the higher susceptibility of the later ones to EAM induction. These experiment showed that polyantibiotic dysbiosis reduces EAM severity in C57BL/6 mice. Moreover, the effect of these antibiotics seem to depend on the genotype and the initial microbiota composition as myocarditis reduction is even higher in the CD69 deficient mice. These crosstalk between CD69 and microbiota point to a possible ligand for the receptor in the gut flora. This interaction, that has previously reported for other C-type lectins and microbiota (Martinez-Lopez et al., 2019), could explain the regulation of Th17 responses by CD69 and the different microbiota composition of these animals, as a consequence.

With cocktail antibiotic treatment there is a nearly total depletion of the gut flora, however there could be still some resistant commensals that could account for the results obtained. The best way to study the effect of microbiota in the development of the disease is by the use of germ-free mice. These mice are bred in isolators which fully block exposure to microorganisms, with the intent of keeping them free of detectable bacteria, viruses, and eukaryotic microbes. Adaptive immune responses are compromised in germ free mice. Indeed, Th17 cells are absent in these mice and can be reconstituted by mono-colonization with SFB (Ivanov et al., 2009). Here it has been described that 21 days after EAM induction Th17 levels remain low, in contrast to what happens in SPF conditions. According to the fact that myocarditis development and cardiomyopathy progression is dependent on Th17 responses, germ free mice preserve heart function and do not present leukocyte infiltration in the heart, indicating that gut microbiota is necessary for the development of autoimmune myocarditis and the subsequent progression to dilated cardiomyopathy. This may be independent of genotype as the presence or absence of CD69 does not seem to alter the results.

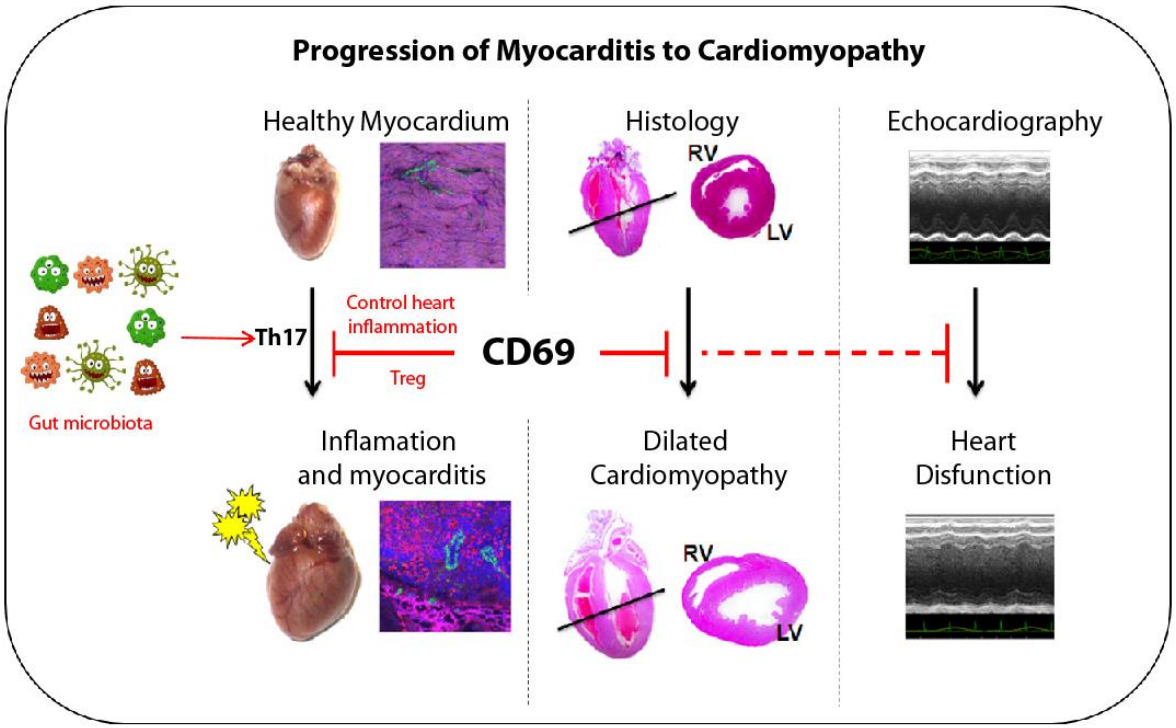

Figure 32. Myocarditis and subsequent progression to Cardiomyopathy are dependent on Th17 responses produced by gut microbiota.

In summary, the results obtained in this Thesis have revealed a new role for CD69 in the regulation of NK cell activation and function by modulation of NKG2D receptor. These data shed light on the development of a new therapy for graft versus host disease after hematopoietic stem cell transplant and a potential role for immunotherapy in cancer. Moreover, CD69 has been identified as a new modulator for cardiovascular diseases, with a role in the maintenance of immune tolerance during atherosclerosis progression that controls the atheroma plaque formation. These data has provided the basis for new studies in humans with CD69 as a possible predictor of cardiovascular disease, one of the main cause of death in Europe and America. Finally, in this work it has been described for the first time, the role of microbiota in the development of autoimmune myocarditis and dilated cardiomyopathy, creating a new important field of investigation for a disease with no specific treatment at the moment

CONCLUSIONS

CONCLUSIONS

1. *Cd69*$^{-/-}$ NK cells present an altered inhibitory/activating receptor repertoire with higher levels of non-self and missing self-recognition receptors: Ly49H, Ly49G2, Ly49D. This phenotype increases NK cell cytolytic capacity against tumors and allogenic cells.

2. *Cd69*$^{-/-}$ mice are highly resistant to aGvHD after allogeneic HSCT due to higher levels of Ly49G2 and Ly49D receptors and lower expression of CD94 than wild type mice mice.

3. CD69 interacts with NKG2D receptors in the membrane of NK cells and regulates the activation state of the molecule and, therefore, NK cell activity through modulation of the different NK cell membrane receptors.

4. Anti-CD69mAb treatment enhance anti-allogeneic activity of NK cells in vivo, revealing as a putative therapeutic agent in the clinics to reduce GvH effects potentially maintaining GvL effects.

5. CD69 deficiency in hyperlipidemic mice increases the proinflammatory Th17 cell subset and diminishes regulatory T cell responses.

6. The depletion of CD69 in the lymphoid compartment accounts for the proinflammatory phenotype.

7. Lack of CD69 in the lymphoid compartment aggravates atherosclerosis progression, with exacerbated Th17 responses and more severe atherosclerotic lesions, supporting the role of IL-17 as a proatherogenic molecule.

8. CD69 depletion alters the composition of the gut microbiota.

9. Heart infiltration and systemic inflammation after experimental autoimmune myocarditis induction is dampened in the absence of microbiota, both by antibiotics depletion or in germ free conditions.

10. Gut microbiota is required for the development of Th17 responses, autoimmune myocarditis and the subsequent progression to dilated cardiomyopathy.

CONCLUSIONES

CONCLUSIONES

1. Las células NK deficientes en CD69 expresan en su membrana un repertorio de receptores activadores e inhibidores distinto al que presentan las células silvestres, presentando una mayor expresión de receptores implicados en el reconocimiento de antígenos del complejo mayor de histocompatibilidad no propios, como son los receptores Ly49H, Ly49G2 y Ly49D. Dicho fenotipo provoca un aumento en la capacidad citolítica estas células NK frente a tumores y células alogénicas.

2. Los ratones deficientes en CD69 son resistentes a la enfermedad injerto contra huésped después de un trasplante alogénico de células madre hematopoyéticas. Esto es debido a la mayor expresión de los receptores Ly49G2 y Ly49D y la menor expresión del receptor CD94 en la superficie de las células NK de estos ratones comparado con los animales silvestres.

3. CD69 interacciona con el receptor NKG2D en la membrana de las células NK regulando el estado de activación de dicha molécula y, por lo tanto, la actividad de la célula NK mediante la modulación de la expresión de diferentes receptores en la membrana.

4. La administración de un anticuerpo monoclonal frente a CD69 incrementa la actividad citolítica de las células NK frente a células alogénicas *in vivo*. Dicho tratamiento podría ser empleado en la clínica para reducir el efecto “injerto contra huésped” manteniendo los efectos “injerto contra leucemia”.

5. La deficiencia de CD69 en ratones con hiperlipidemia genera una mayor respuesta pro-inflamatoria caracterizada por células Th17 mientras que disminuye la respuesta supresora de las células T reguladoras.

6. La depleción de CD69 específicamente en el compartimento linfoide conlleva la aparición de dicho fenotipo proinflamatorio.

7. La deficiencia de CD69 en el compartimento linfoide agrava la progresión de aterosclerosis, provocando respuestas Th17 exacerbadas y un incremento en la formación de la placa de ateroma tras la administración de dieta rica en grasa, demostrando la implicación de la interleucina 17 como una molécula pro-aterogénica.

8. La ausencia de CD69 altera la composición de la microbiota intestinal.

9. En ausencia de microbiota, ya sea por su depleción mediante el uso de antibióticos o mediante la estabulación de los ratones en condiciones libres de gérmenes, disminuye la infiltración leucocitaria en el corazón y la inflamación sistémica tras la inducción de miocarditis autoinmune.

10. La microbiota intestinal es esencial en la generación de la respuesta Th17 responsable de la inducción de miocarditis autoinmune y su progresión hacia una cardiomiopatía dilatada.

REFERENCES

REFERENCES

ADAMS, E. J., JUO, Z. S., VENOOK, R. T., BOULANGER, M. J., ARASE, H., LANIER, L. L. & GARCIA, K. C. 2007. Structural elucidation of the m157 mouse cytomegalovirus ligand for Ly49 natural killer cell receptors. *Proc Natl Acad Sci U S A,* 104**,** 10128-33.

AIT-OUFELLA, H., SALOMON, B. L., POTTEAUX, S., ROBERTSON, A. K., GOURDY, P., ZOLL, J., MERVAL, R., ESPOSITO, B., COHEN, J. L., FISSON, S., FLAVELL, R. A., HANSSON, G. K., KLATZMANN, D., TEDGUI, A. & MALLAT, Z. 2006. Natural regulatory T cells control the development of atherosclerosis in mice. *Nat Med,* 12**,** 178-80.

AMADEI, B., URBANI, S., CAZALY, A., FISICARO, P., ZERBINI, A., AHMED, P., MISSALE, G., FERRARI, C. & KHAKOO, S. I. 2010. Activation of natural killer cells during acute infection with hepatitis C virus. *Gastroenterology,* 138**,** 1536-45.

ARETZ, H. T., BILLINGHAM, M. E., EDWARDS, W. D., FACTOR, S. M., FALLON, J. T., FENOGLIO, J. J., JR., OLSEN, E. G. & SCHOEN, F. J. 1987. Myocarditis. A histopathologic definition and classification. *Am J Cardiovasc Pathol,* 1**,** 3-14.

ARUMUGAM, M., RAES, J., PELLETIER, E., LE PASLIER, D., YAMADA, T., MENDE, D. R., FERNANDES, G. R., TAP, J., BRULS, T., BATTO, J. M., BERTALAN, M., BORRUEL, N., CASELLAS, F., FERNANDEZ, L., GAUTIER, L., HANSEN, T., HATTORI, M., HAYASHI, T., KLEEREBEZEM, M., KUROKAWA, K., LECLERC, M., LEVENEZ, F., MANICHANH, C., NIELSEN, H. B., NIELSEN, T., PONS, N., POULAIN, J., QIN, J., SICHERITZ-PONTEN, T., TIMS, S., TORRENTS, D., UGARTE, E., ZOETENDAL, E. G., WANG, J., GUARNER, F., PEDERSEN, O., DE VOS, W. M., BRUNAK, S., DORE, J., META, H. I. T. C., ANTOLIN, M., ARTIGUENAVE, F., BLOTTIERE, H. M., ALMEIDA, M., BRECHOT, C., CARA, C., CHERVAUX, C., CULTRONE, A., DELORME, C., DENARIAZ, G., DERVYN, R., FOERSTNER, K. U., FRISS, C., VAN DE GUCHTE, M., GUEDON, E., HAIMET, F., HUBER, W., VAN HYLCKAMA-VLIEG, J., JAMET, A., JUSTE, C., KACI, G., KNOL, J., LAKHDARI, O., LAYEC, S., LE ROUX, K., MAGUIN, E., MERIEUX, A., MELO MINARDI, R., M'RINI, C., MULLER, J., OOZEER, R., PARKHILL, J., RENAULT, P., RESCIGNO, M., SANCHEZ, N., SUNAGAWA, S., TORREJON, A., TURNER, K., VANDEMEULEBROUCK, G., VARELA, E., WINOGRADSKY, Y., ZELLER, G., WEISSENBACH, J., EHRLICH, S. D. & BORK, P. 2011. Enterotypes of the human gut microbiome. *Nature,* 473**,** 174-80.

ASAI, O., LONGO, D. L., TIAN, Z. G., HORNUNG, R. L., TAUB, D. D., RUSCETTI, F. W. & MURPHY, W. J. 1998. Suppression of graft-versus-host disease and amplification of graft-versus-tumor effects by activated natural killer cells after allogeneic bone marrow transplantation. *J Clin Invest,* 101**,** 1835-42.

ATARASHI, K., NISHIMURA, J., SHIMA, T., UMESAKI, Y., YAMAMOTO, M., ONOUE, M., YAGITA, H., ISHII, N., EVANS, R., HONDA, K. & TAKEDA, K. 2008. ATP drives lamina propria T(H)17 cell differentiation. *Nature,* 455**,** 808-12.

ATARASHI, K., TANOUE, T., SHIMA, T., IMAOKA, A., KUWAHARA, T., MOMOSE, Y., CHENG, G., YAMASAKI, S., SAITO, T., OHBA, Y., TANIGUCHI, T., TAKEDA, K., HORI, S., IVANOV, II, UMESAKI, Y., ITOH, K. & HONDA, K. 2011. Induction of colonic regulatory T cells by indigenous Clostridium species. *Science,* 331**,** 337-41.

BALDEVIANO, G. C., BARIN, J. G., TALOR, M. V., SRINIVASAN, S., BEDJA, D., ZHENG, D., GABRIELSON, K., IWAKURA, Y., ROSE, N. R. & CIHAKOVA, D. 2010. Interleukin-17A is dispensable for myocarditis but essential for the progression to dilated cardiomyopathy. *Circ Res,* 106**,** 1646-55.

BANKOVICH, A. J., SHIOW, L. R. & CYSTER, J. G. 2010. CD69 suppresses sphingosine 1-phosophate receptor-1 (S1P1) function through interaction with membrane helix 4. *J Biol Chem,* 285**,** 22328-37.

BARIN, J. G., TALOR, M. V., DINY, N. L., ONG, S., SCHAUB, J. A., GEBREMARIAM, E., BEDJA, D., CHEN, G., CHOI, H. S., HOU, X., WU, L., CARDAMONE, A. B., PETERSON, D. A., ROSE, N. R. & CIHAKOVA, D. 2017. Regulation of autoimmune myocarditis by host responses to the microbiome. *Exp Mol Pathol,* 103**,** 141-152.

BAUER, S., GROH, V., WU, J., STEINLE, A., PHILLIPS, J. H., LANIER, L. L. & SPIES, T. 1999. Activation of NK cells and T cells by NKG2D, a receptor for stress-inducible MICA. *Science,* 285**,** 727-9.

BEDOYA, S. K., LAM, B., LAU, K. & LARKIN, J., 3RD 2013. Th17 cells in immunity and autoimmunity. *Clin Dev Immunol,* 2013**,** 986789.

BENEDETTI, G. & MIOSSEC, P. 2014. Interleukin 17 contributes to the chronicity of inflammatory diseases such as rheumatoid arthritis. *Eur J Immunol,* 44**,** 339-47.

BERER, K., MUES, M., KOUTROLOS, M., RASBI, Z. A., BOZIKI, M., JOHNER, C., WEKERLE, H. & KRISHNAMOORTHY, G. 2011. Commensal microbiota and myelin autoantigen cooperate to trigger autoimmune demyelination. *Nature,* 479**,** 538-41.

BIASSONI, R., CANTONI, C., PENDE, D., SIVORI, S., PAROLINI, S., VITALE, M., BOTTINO, C. & MORETTA, A. 2001. Human natural killer cell receptors and co-receptors. *Immunol Rev,* 181**,** 203-14.

BOGDANDI, E. N., BALOGH, A., FELGYINSZKI, N., SZATMARI, T., PERSA, E., HILDEBRANDT, G., SAFRANY, G. & LUMNICZKY, K. 2010. Effects of low-dose radiation on the immune system of mice after total-body irradiation. *Radiat Res,* 174**,** 480-9.

BOIERI, M., ULVMOEN, A., SUDWORTH, A., LENDREM, C., COLLIN, M., DICKINSON, A. M., KVEBERG, L. & INNGJERDINGEN, M. 2017. IL-12, IL-15, and IL-18 pre-activated NK cells target resistant T cell acute lymphoblastic leukemia and delay leukemia development in vivo. *Oncoimmunology,* 6**,** e1274478.

BORREGO, F., ULBRECHT, M., WEISS, E. H., COLIGAN, J. E. & BROOKS, A. G. 1998. Recognition of human histocompatibility leukocyte antigen (HLA)-E complexed with HLA class I signal sequence-derived peptides by CD94/NKG2 confers protection from natural killer cell-mediated lysis. *J Exp Med,* 187**,** 813-8.

BRANDL, K., PLITAS, G., MIHU, C. N., UBEDA, C., JIA, T., FLEISHER, M., SCHNABL, B., DEMATTEO, R. P. & PAMER, E. G. 2008. Vancomycin-resistant enterococci exploit antibiotic-induced innate immune deficits. *Nature,* 455**,** 804-7.

BRYCESON, Y. T., MARCH, M. E., LJUNGGREN, H. G. & LONG, E. O. 2006. Synergy among receptors on resting NK cells for the activation of natural cytotoxicity and cytokine secretion. *Blood,* 107**,** 159-66.

BUONO, C., BINDER, C. J., STAVRAKIS, G., WITZTUM, J. L., GLIMCHER, L. H. & LICHTMAN, A. H. 2005. T-bet deficiency reduces atherosclerosis and alters plaque antigen-specific immune responses. *Proc Natl Acad Sci U S A,* 102**,** 1596-601.

BUTCHER, M. J., FILIPOWICZ, A. R., WASEEM, T. C., MCGARY, C. M., CROW, K. J., MAGILNICK, N., BOLDIN, M., LUNDBERG, P. S. & GALKINA, E. V. 2016. Atherosclerosis-Driven Treg Plasticity Results in Formation of a Dysfunctional Subset of Plastic IFNgamma+ Th1/Tregs. *Circ Res,* 119**,** 1190-1203.

CAFORIO, A. L., MARCOLONGO, R., JAHNS, R., FU, M., FELIX, S. B. & ILICETO, S. 2013a. Immune-mediated and autoimmune myocarditis: clinical presentation, diagnosis and management. *Heart Fail Rev,* 18**,** 715-32.

CAFORIO, A. L., PANKUWEIT, S., ARBUSTINI, E., BASSO, C., GIMENO-BLANES, J., FELIX, S. B., FU, M., HELIO, T., HEYMANS, S., JAHNS, R., KLINGEL, K., LINHART, A., MAISCH, B., MCKENNA, W., MOGENSEN, J., PINTO, Y. M., RISTIC, A., SCHULTHEISS, H. P., SEGGEWISS, H., TAVAZZI, L., THIENE, G., YILMAZ, A., CHARRON, P., ELLIOTT, P. M., EUROPEAN SOCIETY OF CARDIOLOGY WORKING GROUP ON, M. & PERICARDIAL, D. 2013b. Current state of knowledge on aetiology, diagnosis, management, and therapy of myocarditis: a position statement of the European Society of Cardiology Working Group on Myocardial and Pericardial Diseases. *Eur Heart J,* 34**,** 2636-48, 2648a-2648d.

CALIGIURI, G., RUDLING, M., OLLIVIER, V., JACOB, M. P., MICHEL, J. B., HANSSON, G. K. & NICOLETTI, A. 2003. Interleukin-10 deficiency increases atherosclerosis, thrombosis, and low-density lipoproteins in apolipoprotein E knockout mice. *Mol Med,* 9**,** 10-7.

CARAYANNOPOULOS, L. N., NAIDENKO, O. V., FREMONT, D. H. & YOKOYAMA, W. M. 2002. Cutting edge: murine UL16-binding protein-like transcript 1: a newly described transcript encoding a high-affinity ligand for murine NKG2D. *J Immunol,* 169**,** 4079-83.

CARLYLE, J. R., MESCI, A., FINE, J. H., CHEN, P., BELANGER, S., TAI, L. H. & MAKRIGIANNIS, A. P. 2008. Evolution of the Ly49 and Nkrp1 recognition systems. *Semin Immunol,* 20**,** 321-30.

CEBRIAN, M., YAGUE, E., RINCON, M., LOPEZ-BOTET, M., DE LANDAZURI, M. O. & SANCHEZ-MADRID, F. 1988. Triggering of T cell proliferation through AIM, an activation inducer molecule expressed on activated human lymphocytes. *J Exp Med,* 168**,** 1621-37.

CEDENO-LAURENT, F., OPPERMAN, M., BARTHEL, S. R., KUCHROO, V. K. & DIMITROFF, C. J. 2012. Galectin-1 triggers an immunoregulatory signature in Th cells functionally defined by IL-10 expression. *J Immunol,* 188**,** 3127-37.

CERWENKA, A., BAKKER, A. B., MCCLANAHAN, T., WAGNER, J., WU, J., PHILLIPS, J. H. & LANIER, L. L. 2000. Retinoic acid early inducible genes define a ligand family for the activating NKG2D receptor in mice. *Immunity,* 12**,** 721-7.

CIBRIAN, D., SAIZ, M. L., DE LA FUENTE, H., SANCHEZ-DIAZ, R., MORENO-GONZALO, O., JORGE, I., FERRARINI, A., VAZQUEZ, J., PUNZON, C., FRESNO, M., VICENTE-MANZANARES, M., DAUDEN, E., FERNANDEZ-SALGUERO, P. M., MARTIN, P. & SANCHEZ-MADRID, F. 2016. CD69 controls the uptake of L-tryptophan through LAT1-CD98 and AhR-dependent secretion of IL-22 in psoriasis. *Nat Immunol,* 17**,** 985-96.

CIMEN, I., KOCATURK, B., KOYUNCU, S., TUFANLI, O., ONAT, U. I., YILDIRIM, A. D., APAYDIN, O., DEMIRSOY, S., AYKUT, Z. G., NGUYEN, U. T., WATKINS, S. M., HOTAMISLIGIL, G. S. & ERBAY, E. 2016. Prevention of atherosclerosis by bioactive palmitoleate through suppression of organelle stress and inflammasome activation. *Sci Transl Med,* 8**,** 358ra126.

COLUCCI, F., ROSMARAKI, E., BREGENHOLT, S., SAMSON, S. I., DI BARTOLO, V., TURNER, M., VANES, L., TYBULEWICZ, V. & DI SANTO, J. P. 2001. Functional dichotomy in natural killer cell signaling: Vav1-dependent and -independent mechanisms. *J Exp Med,* 193**,** 1413-24.

COLLINS, R. H., JR., SHPILBERG, O., DROBYSKI, W. R., PORTER, D. L., GIRALT, S., CHAMPLIN, R., GOODMAN, S. A., WOLFF, S. N., HU, W., VERFAILLIE, C., LIST, A., DALTON, W., OGNOSKIE, N., CHETRIT, A., ANTIN, J. H. & NEMUNAITIS, J. 1997. Donor leukocyte infusions in 140 patients with relapsed malignancy after allogeneic bone marrow transplantation. *J Clin Oncol,* 15**,** 433-44.

COOKE, K. R., GERBITZ, A., CRAWFORD, J. M., TESHIMA, T., HILL, G. R., TESOLIN, A., ROSSIGNOL, D. P. & FERRARA, J. L. 2001. LPS antagonism reduces graft-versus-host disease and preserves graft-versus-leukemia activity after experimental bone marrow transplantation. *J Clin Invest,* 107**,** 1581-9.

COOKE, K. R., KOBZIK, L., MARTIN, T. R., BREWER, J., DELMONTE, J., JR., CRAWFORD, J. M. & FERRARA, J. L. 1996. An experimental model of idiopathic pneumonia syndrome after bone marrow transplantation: I. The roles of minor H antigens and endotoxin. *Blood,* 88**,** 3230-9.

COPELAN, E. A. 2006. Hematopoietic stem-cell transplantation. *N Engl J Med,* 354**,** 1813-26.

CORTES, J. R., SANCHEZ-DIAZ, R., BOVOLENTA, E. R., BARREIRO, O., LASARTE, S., MATESANZ-MARIN, A., TORIBIO, M. L., SANCHEZ-MADRID, F. & MARTIN, P. 2014. Maintenance of immune tolerance by Foxp3+ regulatory T cells requires CD69 expression. *J Autoimmun,* 55**,** 51-62.

COSTANTINO, C. M., BAECHER-ALLAN, C. & HAFLER, D. A. 2008. Multiple sclerosis and regulatory T cells. *J Clin Immunol,* 28**,** 697-706.

COX, S. T., LAZA-BRIVIESCA, R., PEARSON, H., SORIA, B., GIBSON, D., GOMEZ, S., MADRIGAL, J. A. & SAUDEMONT, A. 2015. Umbilical cord blood plasma contains soluble NKG2D ligands that mediate loss of natural killer cell function and cytotoxicity. *Eur J Immunol,* 45**,** 2324-34.

CRUZ-ADALIA, A., JIMENEZ-BORREGUERO, L. J., RAMIREZ-HUESCA, M., CHICO-CALERO, I., BARREIRO, O., LOPEZ-CONESA, E., FRESNO, M., SANCHEZ-MADRID, F. & MARTIN, P. 2010. CD69 limits the severity of cardiomyopathy after autoimmune myocarditis. *Circulation,* 122**,** 1396-404.

CUA, D. J., SHERLOCK, J., CHEN, Y., MURPHY, C. A., JOYCE, B., SEYMOUR, B., LUCIAN, L., TO, W., KWAN, S., CHURAKOVA, T., ZURAWSKI, S., WIEKOWSKI, M., LIRA, S. A., GORMAN, D., KASTELEIN, R. A. & SEDGWICK, J. D. 2003. Interleukin-23 rather than interleukin-12 is the critical cytokine for autoimmune inflammation of the brain. *Nature,* 421**,** 744-8.

CUI, L., ZHAO, T., HU, H., ZHANG, W. & HUA, X. 2017. Association Study of Gut Flora in Coronary Heart Disease through High-Throughput Sequencing. *Biomed Res Int,* 2017**,** 3796359.

CUNHA-NETO, E., COELHO, V., GUILHERME, L., FIORELLI, A., STOLF, N. & KALIL, J. 1996. Autoimmunity in Chagas' disease. Identification of cardiac myosin-B13 Trypanosoma cruzi protein crossreactive T cell clones in heart lesions of a chronic Chagas' cardiomyopathy patient. *J Clin Invest,* 98**,** 1709-12.

CHEN, H., LAU, M. C., WONG, M. T., NEWELL, E. W., POIDINGER, M. & CHEN, J. 2016. Cytofkit: A Bioconductor Package for an Integrated Mass Cytometry Data Analysis Pipeline. *PLoS Comput Biol,* 12**,** e1005112.

CHEN, J., LIAO, M. Y., GAO, X. L., ZHONG, Q., TANG, T. T., YU, X., LIAO, Y. H. & CHENG, X. 2013. IL-17A induces pro-inflammatory cytokines production in macrophages via MAPKinases, NF-kappaB and AP-1. *Cell Physiol Biochem,* 32**,** 1265-74.

CHENG, X., YU, X., DING, Y. J., FU, Q. Q., XIE, J. J., TANG, T. T., YAO, R., CHEN, Y. & LIAO, Y. H. 2008. The Th17/Treg imbalance in patients with acute coronary syndrome. *Clin Immunol,* 127**,** 89-97.

CHILDS, R. A., GALUSTIAN, C., LAWSON, A. M., DOUGAN, G., BENWELL, K., FRANKEL, G. & FEIZI, T. 1999. Recombinant soluble human CD69 dimer produced in Escherichia coli: reevaluation of saccharide binding. *Biochem Biophys Res Commun,* 266**,** 19-23.

DANZAKI, K., MATSUI, Y., IKESUE, M., OHTA, D., ITO, K., KANAYAMA, M., KUROTAKI, D., MORIMOTO, J., IWAKURA, Y., YAGITA, H., TSUTSUI, H. & UEDE, T. 2012. Interleukin-17A deficiency accelerates unstable atherosclerotic plaque formation in apolipoprotein E-deficient mice. *Arterioscler Thromb Vasc Biol,* 32**,** 273-80.

DAVIS, A. H., GUSEVA, N. V., BALL, B. L. & HEUSEL, J. W. 2008. Characterization of murine cytomegalovirus m157 from infected cells and identification of critical residues mediating recognition by the NK cell receptor Ly49H. *J Immunol,* 181**,** 265-75.

DE LA FUENTE, H., CRUZ-ADALIA, A., MARTINEZ DEL HOYO, G., CIBRIAN-VERA, D., BONAY, P., PEREZ-HERNANDEZ, D., VAZQUEZ, J., NAVARRO, P., GUTIERREZ-GALLEGO, R., RAMIREZ-HUESCA, M., MARTIN, P. & SANCHEZ-MADRID, F. 2014. The leukocyte activation receptor CD69 controls T cell differentiation through its interaction with galectin-1. *Mol Cell Biol,* 34**,** 2479-87.

DIEFENBACH, A., JAMIESON, A. M., LIU, S. D., SHASTRI, N. & RAULET, D. H. 2000. Ligands for the murine NKG2D receptor: expression by tumor cells and activation of NK cells and macrophages. *Nat Immunol,* 1**,** 119-26.

DINH, T. N., KYAW, T. S., KANELLAKIS, P., TO, K., TIPPING, P., TOH, B. H., BOBIK, A. & AGROTIS, A. 2012. Cytokine therapy with interleukin-2/anti-interleukin-2 monoclonal antibody complexes expands CD4+CD25+Foxp3+ regulatory T cells and attenuates development and progression of atherosclerosis. *Circulation,* 126**,** 1256-66.

DOMINGUEZ-VILLAR, M., BAECHER-ALLAN, C. M. & HAFLER, D. A. 2011. Identification of T helper type 1-like, Foxp3+ regulatory T cells in human autoimmune disease. *Nat Med,* 17**,** 673-5.

DOMINGUEZ-VILLAR, M. & HAFLER, D. A. 2018. Regulatory T cells in autoimmune disease. *Nat Immunol,* 19**,** 665-673.

DRANOFF, G. 2004. Cytokines in cancer pathogenesis and cancer therapy. *Nat Rev Cancer,* 4**,** 11-22.

DROBYSKI, W. R., KEEVER, C. A., ROTH, M. S., KOETHE, S., HANSON, G., MCFADDEN, P., GOTTSCHALL, J. L., ASH, R. C., VAN TUINEN, P., HOROWITZ, M. M. & ET AL. 1993. Salvage immunotherapy using donor leukocyte infusions as treatment for relapsed chronic myelogenous leukemia after allogeneic bone marrow transplantation: efficacy and toxicity of a defined T-cell dose. *Blood,* 82**,** 2310-8.

DU, N., ZHOU, J., LIN, X., ZHANG, Y., YANG, X., WANG, Y. & SHU, Y. 2010. Differential activation of NK cells by influenza A pseudotype H5N1 and 1918 and 2009 pandemic H1N1 viruses. *J Virol,* 84**,** 7822-31.

DZAU, V. J., BRAUN-DULLAEUS, R. C. & SEDDING, D. G. 2002. Vascular proliferation and atherosclerosis: new perspectives and therapeutic strategies. *Nat Med,* 8**,** 1249-56.

EID, R. E., RAO, D. A., ZHOU, J., LO, S. F., RANJBARAN, H., GALLO, A., SOKOL, S. I., PFAU, S., POBER, J. S. & TELLIDES, G. 2009. Interleukin-17 and interferon-gamma are produced concomitantly by human coronary artery-infiltrating T cells and act synergistically on vascular smooth muscle cells. *Circulation,* 119**,** 1424-32.

EMINI VESELI, B., PERROTTA, P., DE MEYER, G. R. A., ROTH, L., VAN DER DONCKT, C., MARTINET, W. & DE MEYER, G. R. Y. 2017. Animal models of atherosclerosis. *Eur J Pharmacol,* 816**,** 3-13.

ERBEL, C., AKHAVANPOOR, M., OKUYUCU, D., WANGLER, S., DIETZ, A., ZHAO, L., STELLOS, K., LITTLE, K. M., LASITSCHKA, F., DOESCH, A., HAKIMI, M., DENGLER, T. J., GIESE, T., BLESSING, E., KATUS, H. A. & GLEISSNER, C. A. 2014. IL-17A influences essential functions of the monocyte/macrophage lineage and is involved in advanced murine and human atherosclerosis. *J Immunol,* 193**,** 4344-55.

ERBEL, C., CHEN, L., BEA, F., WANGLER, S., CELIK, S., LASITSCHKA, F., WANG, Y., BOCKLER, D., KATUS, H. A. & DENGLER, T. J. 2009. Inhibition of IL-17A attenuates atherosclerotic lesion development in apoE-deficient mice. *J Immunol,* 183**,** 8167-75.

ESPLUGUES, E., SANCHO, D., VEGA-RAMOS, J., MARTINEZ, C., SYRBE, U., HAMANN, A., ENGEL, P., SANCHEZ-MADRID, F. & LAUZURICA, P. 2003. Enhanced antitumor immunity in mice deficient in CD69. *J Exp Med,* 197**,** 1093-106.

ESPLUGUES, E., VEGA-RAMOS, J., CARTOIXA, D., VAZQUEZ, B. N., SALAET, I., ENGEL, P. & LAUZURICA, P. 2005. Induction of tumor NK-cell immunity by anti-CD69 antibody therapy. *Blood,* 105**,** 4399-406.

FABRE, A. & SHEPPARD, M. N. 2006. Sudden adult death syndrome and other non-ischaemic causes of sudden cardiac death. *Heart,* 92**,** 316-20.

FELDMAN, A. M. & MCNAMARA, D. 2000. Myocarditis. *N Engl J Med,* 343**,** 1388-98.

FOKS, A. C., FRODERMANN, V., TER BORG, M., HABETS, K. L., BOT, I., ZHAO, Y., VAN ECK, M., VAN BERKEL, T. J., KUIPER, J. & VAN PUIJVELDE, G. H. 2011. Differential effects of regulatory T cells on the initiation and regression of atherosclerosis. *Atherosclerosis,* 218**,** 53-60.

FONTENOT, J. D., GAVIN, M. A. & RUDENSKY, A. Y. 2003. Foxp3 programs the development and function of CD4+CD25+ regulatory T cells. *Nat Immunol,* 4**,** 330-6.

FRANCINO, M. P. 2014. Early development of the gut microbiota and immune health. *Pathogens,* 3**,** 769-90.

FUKAURA, H., KENT, S. C., PIETRUSEWICZ, M. J., KHOURY, S. J., WEINER, H. L. & HAFLER, D. A. 1996. Induction of circulating myelin basic protein and proteolipid protein-specific transforming growth factor-beta1-secreting Th3 T cells by oral administration of myelin in multiple sclerosis patients. *J Clin Invest,* 98**,** 70-7.

GABORIAU-ROUTHIAU, V., RAKOTOBE, S., LECUYER, E., MULDER, I., LAN, A., BRIDONNEAU, C., ROCHET, V., PISI, A., DE PAEPE, M., BRANDI, G., EBERL, G., SNEL, J., KELLY, D. & CERF-BENSUSSAN, N. 2009. The key role of segmented filamentous bacteria in the coordinated maturation of gut helper T cell responses. *Immunity,* 31**,** 677-89.

GALKINA, E. & LEY, K. 2007. Leukocyte influx in atherosclerosis. *Curr Drug Targets,* 8**,** 1239-48.

GARCIA-IGLESIAS, T., DEL TORO-ARREOLA, A., ALBARRAN-SOMOZA, B., DEL TORO-ARREOLA, S., SANCHEZ-HERNANDEZ, P. E., RAMIREZ-DUENAS, M. G., BALDERAS-PENA, L. M., BRAVO-CUELLAR, A., ORTIZ-LAZARENO, P. C. & DANERI-NAVARRO, A. 2009. Low NKp30, NKp46 and NKG2D expression and reduced cytotoxic activity on NK cells in cervical cancer and precursor lesions. *BMC Cancer,* 9**,** 186.

GARRIDO, F., RUIZ-CABELLO, F., CABRERA, T., PEREZ-VILLAR, J. J., LOPEZ-BOTET, M., DUGGAN-KEEN, M. & STERN, P. L. 1997. Implications for immunosurveillance of altered HLA class I phenotypes in human tumours. *Immunol Today,* 18**,** 89-95.

GE, S., HERTEL, B., KOLTSOVA, E. K., SORENSEN-ZENDER, I., KIELSTEIN, J. T., LEY, K., HALLER, H. & VON VIETINGHOFF, S. 2013. Increased atherosclerotic lesion formation and vascular leukocyte accumulation in renal impairment are mediated by interleukin-17A. *Circ Res,* 113**,** 965-74.

GEORGE, T. C., MASON, L. H., ORTALDO, J. R., KUMAR, V. & BENNETT, M. 1999. Positive recognition of MHC class I molecules by the Ly49D receptor of murine NK cells. *J Immunol,* 162**,** 2035-43.

GETZ, G. S. & REARDON, C. A. 2016. Do the Apoe-/- and Ldlr-/- Mice Yield the Same Insight on Atherogenesis? *Arterioscler Thromb Vasc Biol,* 36**,** 1734-41.

GEUKING, M. B., CAHENZLI, J., LAWSON, M. A., NG, D. C., SLACK, E., HAPFELMEIER, S., MCCOY, K. D. & MACPHERSON, A. J. 2011. Intestinal bacterial colonization induces mutualistic regulatory T cell responses. *Immunity,* 34**,** 794-806.

GISTERA, A., ROBERTSON, A. K., ANDERSSON, J., KETELHUTH, D. F., OVCHINNIKOVA, O., NILSSON, S. K., LUNDBERG, A. M., LI, M. O., FLAVELL, R. A. & HANSSON, G. K. 2013. Transforming growth factor-beta signaling in T cells promotes stabilization of atherosclerotic plaques through an interleukin-17-dependent pathway. *Sci Transl Med,* 5**,** 196ra100.

GLASNER, A., ISAACSON, B., VIUKOV, S., NEUMAN, T., FRIEDMAN, N., MANDELBOIM, M., SEXL, V., HANNA, J. H. & MANDELBOIM, O. 2017. Increased NK cell immunity in a transgenic mouse model of NKp46 overexpression. *Sci Rep,* 7**,** 13090.

GOLUBOVSKAYA, V. & WU, L. 2016. Different Subsets of T Cells, Memory, Effector Functions, and CAR-T Immunotherapy. *Cancers (Basel),* 8.

GOMEZ, M., SANZ-GONZALEZ, S. M., ABU NABAH, Y. N., LAMANA, A., SANCHEZ-MADRID, F. & ANDRES, V. 2009. Atherosclerosis development in apolipoprotein E-null mice deficient for CD69. *Cardiovasc Res,* 81**,** 197-205.

GONG, F., LIU, Z., LIU, J., ZHOU, P., LIU, Y. & LU, X. 2015. The paradoxical role of IL-17 in atherosclerosis. *Cell Immunol,* 297**,** 33-9.

GONZALEZ-AMARO, R., CORTES, J. R., SANCHEZ-MADRID, F. & MARTIN, P. 2013. Is CD69 an effective brake to control inflammatory diseases? *Trends Mol Med,* 19**,** 625-32.

GROH, V., RHINEHART, R., RANDOLPH-HABECKER, J., TOPP, M. S., RIDDELL, S. R. & SPIES, T. 2001. Costimulation of CD8alphabeta T cells by NKG2D via engagement by MIC induced on virus-infected cells. *Nat Immunol,* 2**,** 255-60.

GROH, V., WU, J., YEE, C. & SPIES, T. 2002. Tumour-derived soluble MIC ligands impair expression of NKG2D and T-cell activation. *Nature,* 419**,** 734-8.

GRONBERG, C., NILSSON, J. & WIGREN, M. 2017. Recent advances on CD4(+) T cells in atherosclerosis and its implications for therapy. *Eur J Pharmacol,* 816**,** 58-66.

HILL, D. A., HOFFMANN, C., ABT, M. C., DU, Y., KOBULEY, D., KIRN, T. J., BUSHMAN, F. D. & ARTIS, D. 2010. Metagenomic analyses reveal antibiotic-induced temporal and spatial changes in intestinal microbiota with associated alterations in immune cell homeostasis. *Mucosal Immunol,* 3**,** 148-58.

HILL, D. A., SIRACUSA, M. C., ABT, M. C., KIM, B. S., KOBULEY, D., KUBO, M., KAMBAYASHI, T., LAROSA, D. F., RENNER, E. D., ORANGE, J. S., BUSHMAN, F. D. & ARTIS, D. 2012. Commensal bacteria-derived signals regulate basophil hematopoiesis and allergic inflammation. *Nat Med,* 18**,** 538-46.

HO, E. L., CARAYANNOPOULOS, L. N., POURSINE-LAURENT, J., KINDER, J., PLOUGASTEL, B., SMITH, H. R. & YOKOYAMA, W. M. 2002. Costimulation of multiple NK cell activation receptors by NKG2D. *J Immunol,* 169**,** 3667-75.

HONDA, K. & LITTMAN, D. R. 2012. The microbiome in infectious disease and inflammation. *Annu Rev Immunol,* 30**,** 759-95.

HOOPER, L. V. & MACPHERSON, A. J. 2010. Immune adaptations that maintain homeostasis with the intestinal microbiota. *Nat Rev Immunol,* 10**,** 159-69.

HORI, S., NOMURA, T. & SAKAGUCHI, S. 2003. Control of regulatory T cell development by the transcription factor Foxp3. *Science,* 299**,** 1057-61.

HU, X. F., ZHANG, W. Y., WEN, Q., CHEN, W. J., WANG, Z. M., CHEN, J., ZHU, F., LIU, K., CHENG, L. X., YANG, J. & SHU, Y. W. 2019. Fecal microbiota transplantation alleviates myocardial damage in myocarditis by restoring the microbiota composition. *Pharmacol Res,* 139**,** 412-421.

HYTTINEN, L., KAIPIAINEN-SEPPANEN, O. & HALINEN, M. 2003. Recurrent myopericarditis in association with Crohn's disease. *J Intern Med,* 253**,** 386-8.

IVANOV, II, ATARASHI, K., MANEL, N., BRODIE, E. L., SHIMA, T., KARAOZ, U., WEI, D., GOLDFARB, K. C., SANTEE, C. A., LYNCH, S. V., TANOUE, T., IMAOKA, A., ITOH, K., TAKEDA, K., UMESAKI, Y., HONDA, K. & LITTMAN, D. R. 2009. Induction of intestinal Th17 cells by segmented filamentous bacteria. *Cell,* 139**,** 485-98.

IVANOV, II, FRUTOS RDE, L., MANEL, N., YOSHINAGA, K., RIFKIN, D. B., SARTOR, R. B., FINLAY, B. B. & LITTMAN, D. R. 2008. Specific microbiota direct the differentiation of IL-17-producing T-helper cells in the mucosa of the small intestine. *Cell Host Microbe,* 4**,** 337-49.

IVANOV, II & HONDA, K. 2012. Intestinal commensal microbes as immune modulators. *Cell Host Microbe,* 12**,** 496-508.

JAECKEL, E., MPOFU, N., SAAL, N. & MANNS, M. P. 2008. Role of regulatory T cells for the treatment of type 1 diabetes mellitus. *Horm Metab Res,* 40**,** 126-36.

JAKOBSSON, H. E., ABRAHAMSSON, T. R., JENMALM, M. C., HARRIS, K., QUINCE, C., JERNBERG, C., BJORKSTEN, B., ENGSTRAND, L. & ANDERSSON, A. F. 2014. Decreased gut microbiota diversity, delayed Bacteroidetes colonisation and reduced Th1 responses in infants delivered by caesarean section. *Gut,* 63**,** 559-66.

JAMIESON, A. M., DIEFENBACH, A., MCMAHON, C. W., XIONG, N., CARLYLE, J. R. & RAULET, D. H. 2002. The role of the NKG2D immunoreceptor in immune cell activation and natural killing. *Immunity,* 17**,** 19-29.

JEFFERIES, J. L. & TOWBIN, J. A. 2010. Dilated cardiomyopathy. *Lancet,* 375**,** 752-62.

JIE, Z., XIA, H., ZHONG, S. L., FENG, Q., LI, S., LIANG, S., ZHONG, H., LIU, Z., GAO, Y., ZHAO, H., ZHANG, D., SU, Z., FANG, Z., LAN, Z., LI, J., XIAO, L., LI, J., LI, R., LI, X., LI, F., REN, H., HUANG, Y., PENG, Y., LI, G., WEN, B., DONG, B., CHEN, J. Y., GENG, Q. S., ZHANG, Z. W., YANG, H., WANG, J., WANG, J., ZHANG, X., MADSEN, L., BRIX, S., NING, G., XU, X., LIU, X., HOU, Y., JIA, H., HE, K. & KRISTIANSEN, K. 2017. The gut microbiome in atherosclerotic cardiovascular disease. *Nat Commun,* 8**,** 845.

JOHNSON, B. D., DROBYSKI, W. R. & TRUITT, R. L. 1993. Delayed infusion of normal donor cells after MHC-matched bone marrow transplantation provides an antileukemia reaction without graft-versus-host disease. *Bone Marrow Transplant,* 11**,** 329-36.

JONCKER, N. T., FERNANDEZ, N. C., TREINER, E., VIVIER, E. & RAULET, D. H. 2009. NK cell responsiveness is tuned commensurate with the number of inhibitory receptors for self-MHC class I: the rheostat model. *J Immunol,* 182**,** 4572-80.

JONCKER, N. T. & RAULET, D. H. 2008. Regulation of NK cell responsiveness to achieve self-tolerance and maximal responses to diseased target cells. *Immunol Rev,* 224**,** 85-97.

JONJIC, S., POLIC, B. & KRMPOTIC, A. 2008. Viral inhibitors of NKG2D ligands: friends or foes of immune surveillance? *Eur J Immunol,* 38**,** 2952-6.

JOVANOVIC, D. V., DI BATTISTA, J. A., MARTEL-PELLETIER, J., JOLICOEUR, F. C., HE, Y., ZHANG, M., MINEAU, F. & PELLETIER, J. P. 1998. IL-17 stimulates the production and expression of proinflammatory cytokines, IL-beta and TNF-alpha, by human macrophages. *J Immunol,* 160**,** 3513-21.

KAMADA, N., SEO, S. U., CHEN, G. Y. & NUNEZ, G. 2013. Role of the gut microbiota in immunity and inflammatory disease. *Nat Rev Immunol,* 13**,** 321-35.

KANEGANE, H. & TOSATO, G. 1996. Activation of naive and memory T cells by interleukin-15. *Blood,* 88**,** 230-5.

LANIER, L. L. 1998. NK cell receptors. *Annu Rev Immunol,* 16**,** 359-93.

LANIER, L. L. 2005. NK cell recognition. *Annu Rev Immunol,* 23**,** 225-74.

LANIER, L. L., BUCK, D. W., RHODES, L., DING, A., EVANS, E., BARNEY, C. & PHILLIPS, J. H. 1988. Interleukin 2 activation of natural killer cells rapidly induces the expression and phosphorylation of the Leu-23 activation antigen. *J Exp Med,* 167**,** 1572-85.

LAUZURICA, P., SANCHO, D., TORRES, M., ALBELLA, B., MARAZUELA, M., MERINO, T., BUEREN, J. A., MARTINEZ, A. C. & SANCHEZ-MADRID, F. 2000. Phenotypic and functional characteristics of hematopoietic cell lineages in CD69-deficient mice. *Blood,* 95**,** 2312-20.

LE BERT, N. & GASSER, S. 2014. Advances in NKG2D ligand recognition and responses by NK cells. *Immunol Cell Biol,* 92**,** 230-6.

LEE, Y. K., MENEZES, J. S., UMESAKI, Y. & MAZMANIAN, S. K. 2011. Proinflammatory T-cell responses to gut microbiota promote experimental autoimmune encephalomyelitis. *Proc Natl Acad Sci U S A,* 108 Suppl 1**,** 4615-22.

LEUSCHNER, F., KATUS, H. A. & KAYA, Z. 2009. Autoimmune myocarditis: past, present and future. *J Autoimmun,* 33**,** 282-9.

LEVINE, J. H., SIMONDS, E. F., BENDALL, S. C., DAVIS, K. L., AMIR EL, A. D., TADMOR, M. D., LITVIN, O., FIENBERG, H. G., JAGER, A., ZUNDER, E. R., FINCK, R., GEDMAN, A. L., RADTKE, I., DOWNING, J. R., PE'ER, D. & NOLAN, G. P. 2015. Data-Driven Phenotypic Dissection of AML Reveals Progenitor-like Cells that Correlate with Prognosis. *Cell,* 162**,** 184-97.

LEVINGS, M. K. & RONCAROLO, M. G. 2000. T-regulatory 1 cells: a novel subset of CD4 T cells with immunoregulatory properties. *J Allergy Clin Immunol,* 106**,** S109-12.

LEY, R. E., TURNBAUGH, P. J., KLEIN, S. & GORDON, J. I. 2006. Microbial ecology: human gut microbes associated with obesity. *Nature,* 444**,** 1022-3.

LI, Q., WANG, Y., WANG, Y., CHEN, K., ZHOU, Q., WEI, W. & WANG, Y. 2014. Treg/Th17 ratio acts as a novel indicator for acute coronary syndrome. *Cell Biochem Biophys,* 70**,** 1489-98.

LI, X. S., OBEID, S., KLINGENBERG, R., GENCER, B., MACH, F., RABER, L., WINDECKER, S., RODONDI, N., NANCHEN, D., MULLER, O., MIRANDA, M. X., MATTER, C. M., WU, Y., LI, L., WANG, Z., ALAMRI, H. S., GOGONEA, V., CHUNG, Y. M., TANG, W. H., HAZEN, S. L. & LUSCHER, T. F. 2017. Gut microbiota-dependent trimethylamine N-oxide in acute coronary syndromes: a prognostic marker for incident cardiovascular events beyond traditional risk factors. *Eur Heart J,* 38**,** 814-824.

LIBBY, P. 2017. Interleukin-1 Beta as a Target for Atherosclerosis Therapy: Biological Basis of CANTOS and Beyond. *J Am Coll Cardiol,* 70**,** 2278-2289.

LIM, H., KIM, Y. U., SUN, H., LEE, J. H., REYNOLDS, J. M., HANABUCHI, S., WU, H., TENG, B. B. & CHUNG, Y. 2014. Proatherogenic conditions promote autoimmune T helper 17 cell responses in vivo. *Immunity,* 40**,** 153-65.

LIN, C. R., WEI, T. Y., TSAI, H. Y., WU, Y. T., WU, P. Y. & CHEN, S. T. 2015. Glycosylation-dependent interaction between CD69 and S100A8/S100A9 complex is required for regulatory T-cell differentiation. *FASEB J,* 29**,** 5006-17.

LITTMAN, D. R. & PAMER, E. G. 2011. Role of the commensal microbiota in normal and pathogenic host immune responses. *Cell Host Microbe,* 10**,** 311-23.

LIU, Y., ZHU, H., SU, Z., SUN, C., YIN, J., YUAN, H., SANDOGHCHIAN, S., JIAO, Z., WANG, S. & XU, H. 2012. IL-17 contributes to cardiac fibrosis following experimental autoimmune myocarditis by a PKCbeta/Erk1/2/NF-kappaB-dependent signaling pathway. *Int Immunol,* 24**,** 605-12.

LJUNGMAN, P., BREGNI, M., BRUNE, M., CORNELISSEN, J., DE WITTE, T., DINI, G., EINSELE, H., GASPAR, H. B., GRATWOHL, A., PASSWEG, J., PETERS, C., ROCHA, V., SACCARDI, R., SCHOUTEN, H., SUREDA, A., TICHELLI, A., VELARDI, A., NIEDERWIESER, D., EUROPEAN GROUP FOR, B. & MARROW, T. 2010. Allogeneic and autologous transplantation for haematological diseases, solid tumours and immune disorders: current practice in Europe 2009. *Bone Marrow Transplant,* 45**,** 219-34.

LOPEZ-CABRERA, M., MUNOZ, E., BLAZQUEZ, M. V., URSA, M. A., SANTIS, A. G. & SANCHEZ-MADRID, F. 1995. Transcriptional regulation of the gene encoding the human C-type lectin leukocyte receptor AIM/CD69 and functional characterization of its tumor necrosis factor-alpha-responsive elements. *J Biol Chem,* 270**,** 21545-51.

LOPEZ-CABRERA, M., SANTIS, A. G., FERNANDEZ-RUIZ, E., BLACHER, R., ESCH, F., SANCHEZ-MATEOS, P. & SANCHEZ-MADRID, F. 1993. Molecular cloning, expression, and chromosomal localization of the human earliest lymphocyte activation antigen AIM/CD69, a new member of the C-type animal lectin superfamily of signal-transmitting receptors. *J Exp Med,* 178**,** 537-47.

LUEDDE, M., WINKLER, T., HEINSEN, F. A., RUHLEMANN, M. C., SPEHLMANN, M. E., BAJROVIC, A., LIEB, W., FRANKE, A., OTT, S. J. & FREY, N. 2017. Heart failure is associated with depletion of core intestinal microbiota. *ESC Heart Fail,* 4**,** 282-290.

LLODRA, J., ANGELI, V., LIU, J., TROGAN, E., FISHER, E. A. & RANDOLPH, G. J. 2004. Emigration of monocyte-derived cells from atherosclerotic lesions characterizes regressive, but not progressive, plaques. *Proc Natl Acad Sci U S A,* 101**,** 11779-84.

MAIOLINO, G., ROSSITTO, G., CAIELLI, P., BISOGNI, V., ROSSI, G. P. & CALO, L. A. 2013. The role of oxidized low-density lipoproteins in atherosclerosis: the myths and the facts. *Mediators Inflamm,* 2013**,** 714653.

MALLAT, Z., AIT-OUFELLA, H. & TEDGUI, A. 2007. Regulatory T-cell immunity in atherosclerosis. *Trends Cardiovasc Med,* 17**,** 113-8.

MANDELBOIM, O., LIEBERMAN, N., LEV, M., PAUL, L., ARNON, T. I., BUSHKIN, Y., DAVIS, D. M., STROMINGER, J. L., YEWDELL, J. W. & PORGADOR, A. 2001. Recognition of haemagglutinins on virus-infected cells by NKp46 activates lysis by human NK cells. *Nature,* 409**,** 1055-60.

MARTIN, P., GOMEZ, M., LAMANA, A., CRUZ-ADALIA, A., RAMIREZ-HUESCA, M., URSA, M. A., YANEZ-MO, M. & SANCHEZ-MADRID, F. 2010a. CD69 association with Jak3/Stat5 proteins regulates Th17 cell differentiation. *Mol Cell Biol,* 30**,** 4877-89.

MARTIN, P., GOMEZ, M., LAMANA, A., MATESANZ MARIN, A., CORTES, J. R., RAMIREZ-HUESCA, M., BARREIRO, O., LOPEZ-ROMERO, P., GUTIERREZ-VAZQUEZ, C., DE LA FUENTE, H., CRUZ-ADALIA, A. & SANCHEZ-MADRID, F. 2010b. The leukocyte activation antigen CD69 limits allergic asthma and skin contact hypersensitivity. *J Allergy Clin Immunol,* 126**,** 355-65, 365 e1-3.

MARTIN, P. & SANCHEZ-MADRID, F. 2011. CD69: an unexpected regulator of TH17 cell-driven inflammatory responses. *Sci Signal,* 4**,** pe14.

MARTINEZ-LOPEZ, M., IBORRA, S., CONDE-GARROSA, R., MASTRANGELO, A., DANNE, C., MANN, E. R., REID, D. M., GABORIAU-ROUTHIAU, V., CHAPARRO, M., LORENZO, M. P., MINNERUP, L., SAZ-LEAL, P., SLACK, E., KEMP, B., GISBERT, J. P., DZIONEK, A., ROBINSON, M. J., RUPEREZ, F. J., CERF-BENSUSSAN, N., BROWN, G. D., BERNARDO, D., LEIBUNDGUT-LANDMANN, S. & SANCHO, D. 2019. Microbiota Sensing by Mincle-Syk Axis in Dendritic Cells Regulates Interleukin-17 and -22 Production and Promotes Intestinal Barrier Integrity. *Immunity,* 50**,** 446-461 e9.

MASON, L. H., GOSSELIN, P., ANDERSON, S. K., FOGLER, W. E., ORTALDO, J. R. & MCVICAR, D. W. 1997. Differential tyrosine phosphorylation of inhibitory versus activating Ly-49 receptor proteins and their recruitment of SHP-1 phosphatase. *J Immunol,* 159**,** 4187-96.

MCVICAR, D. W., TAYLOR, L. S., GOSSELIN, P., WILLETTE-BROWN, J., MIKHAEL, A. I., GEAHLEN, R. L., NAKAMURA, M. C., LINNEMEYER, P., SEAMAN, W. E., ANDERSON, S. K., ORTALDO, J. R. & MASON, L. H. 1998. DAP12-mediated signal transduction in natural killer cells. A dominant role for the Syk protein-tyrosine kinase. *J Biol Chem,* 273**,** 32934-42.

MINCHEVA-NILSSON, L., NAGAEVA, O., CHEN, T., STENDAHL, U., ANTSIFEROVA, J., MOGREN, I., HERNESTAL, J. & BARANOV, V. 2006. Placenta-derived soluble MHC class I chain-related molecules down-regulate NKG2D receptor on peripheral blood mononuclear cells during human pregnancy: a possible novel immune escape mechanism for fetal survival. *J Immunol,* 176**,** 3585-92.

MOHTY, M. & APPERLEY, J. F. 2010. Long-term physiological side effects after allogeneic bone marrow transplantation. *Hematology Am Soc Hematol Educ Program,* 2010**,** 229-36.

MOLFETTA, R., QUATRINI, L., ZITTI, B., CAPUANO, C., GALANDRINI, R., SANTONI, A. & PAOLINI, R. 2016. Regulation of NKG2D Expression and Signaling by Endocytosis. *Trends Immunol,* 37**,** 790-802.

MONDELLI, M. U., OLIVIERO, B., MELE, D., MANTOVANI, S., GAZZABIN, C. & VARCHETTA, S. 2012. Natural killer cell functional dichotomy: a feature of chronic viral hepatitis? *Front Immunol,* 3**,** 351.

MORETTA, A., BIASSONI, R., BOTTINO, C., PENDE, D., VITALE, M., POGGI, A., MINGARI, M. C. & MORETTA, L. 1997. Major histocompatibility complex class I-specific receptors on human natural killer and T lymphocytes. *Immunol Rev,* 155**,** 105-17.

MORETTA, A., POGGI, A., PENDE, D., TRIPODI, G., ORENGO, A. M., PELLA, N., AUGUGLIARO, R., BOTTINO, C., CICCONE, E. & MORETTA, L. 1991. CD69-mediated pathway of lymphocyte activation: anti-CD69 monoclonal antibodies trigger the cytolytic activity of different lymphoid effector cells with the exception of cytolytic T lymphocytes expressing T cell receptor alpha/beta. *J Exp Med,* 174**,** 1393-8.

MOUSSA, P., MARTON, J., VIDAL, S. M. & FODIL-CORNU, N. 2012. Genetic dissection of NK cell responses. *Front Immunol,* 3**,** 425.

MURPHY, W. J. & LONGO, D. L. 1997. The potential role of NK cells in the separation of graft-versus-tumor effects from graft-versus-host disease after allogeneic bone marrow transplantation. *Immunol Rev,* 157**,** 167-76.

NAGATOMO, Y. & TANG, W. H. 2015. Intersections Between Microbiome and Heart Failure: Revisiting the Gut Hypothesis. *J Card Fail,* 21**,** 973-80.

NAKAE, S., SAIJO, S., HORAI, R., SUDO, K., MORI, S. & IWAKURA, Y. 2003. IL-17 production from activated T cells is required for the spontaneous development of destructive arthritis in mice deficient in IL-1 receptor antagonist. *Proc Natl Acad Sci U S A,* 100**,** 5986-90.

NAKANISHI, Y., SATO, T. & OHTEKI, T. 2015. Commensal Gram-positive bacteria initiates colitis by inducing monocyte/macrophage mobilization. *Mucosal Immunol,* 8**,** 152-60.

NEU, N., ROSE, N. R., BEISEL, K. W., HERSKOWITZ, A., GURRI-GLASS, G. & CRAIG, S. W. 1987. Cardiac myosin induces myocarditis in genetically predisposed mice. *J Immunol,* 139**,** 3630-6.

NEWBY, A. C. 2008. Metalloproteinase expression in monocytes and macrophages and its relationship to atherosclerotic plaque instability. *Arterioscler Thromb Vasc Biol,* 28**,** 2108-14.

NG, K. K., PARK-SNYDER, S. & WEIS, W. I. 1998. Ca2+-dependent structural changes in C-type mannose-binding proteins. *Biochemistry,* 37**,** 17965-76.

NOTARIO, L., ALARI-PAHISSA, E., DE MOLINA, A. & LAUZURICA, P. 2016. CD69 Deficiency Enhances the Host Response to Vaccinia Virus Infection through Altered NK Cell Homeostasis. *J Virol,* 90**,** 6464-6474.

NOWICKA, M., KRIEG, C., CROWELL, H. L., WEBER, L. M., HARTMANN, F. J., GUGLIETTA, S., BECHER, B., LEVESQUE, M. P. & ROBINSON, M. D. 2017. CyTOF workflow: differential discovery in high-throughput high-dimensional cytometry datasets. *F1000Res,* 6**,** 748.

NUNES, M. C. P., BEATON, A., ACQUATELLA, H., BERN, C., BOLGER, A. F., ECHEVERRIA, L. E., DUTRA, W. O., GASCON, J., MORILLO, C. A., OLIVEIRA-FILHO, J., RIBEIRO, A. L. P., MARIN-NETO, J. A., AMERICAN HEART ASSOCIATION RHEUMATIC FEVER, E., KAWASAKI DISEASE COMMITTEE OF THE COUNCIL ON CARDIOVASCULAR DISEASE IN THE, Y., COUNCIL ON, C., STROKE, N. & STROKE, C. 2018. Chagas Cardiomyopathy: An Update of Current Clinical Knowledge and Management: A Scientific Statement From the American Heart Association. *Circulation,* 138**,** e169-e209.

OCHOA-REPARAZ, J., MIELCARZ, D. W., DITRIO, L. E., BURROUGHS, A. R., FOUREAU, D. M., HAQUE-BEGUM, S. & KASPER, L. H. 2009. Role of gut commensal microflora in the development of experimental autoimmune encephalomyelitis. *J Immunol,* 183**,** 6041-50.

OCHOA-REPARAZ, J., MIELCARZ, D. W., WANG, Y., BEGUM-HAQUE, S., DASGUPTA, S., KASPER, D. L. & KASPER, L. H. 2010. A polysaccharide from the human commensal Bacteroides fragilis protects against CNS demyelinating disease. *Mucosal Immunol,* 3**,** 487-95.

OGASAWARA, K., BENJAMIN, J., TAKAKI, R., PHILLIPS, J. H. & LANIER, L. L. 2005. Function of NKG2D in natural killer cell-mediated rejection of mouse bone marrow grafts. *Nat Immunol,* 6**,** 938-45.

OLSON, J. A., LEVESON-GOWER, D. B., GILL, S., BAKER, J., BEILHACK, A. & NEGRIN, R. S. 2010. NK cells mediate reduction of GVHD by inhibiting activated, alloreactive T cells while retaining GVT effects. *Blood,* 115**,** 4293-301.

OWAGA, E., HSIEH, R. H., MUGENDI, B., MASUKU, S., SHIH, C. K. & CHANG, J. S. 2015. Th17 Cells as Potential Probiotic Therapeutic Targets in Inflammatory Bowel Diseases. *Int J Mol Sci,* 16**,** 20841-58.

PARK, H., LI, Z., YANG, X. O., CHANG, S. H., NURIEVA, R., WANG, Y. H., WANG, Y., HOOD, L., ZHU, Z., TIAN, Q. & DONG, C. 2005. A distinct lineage of CD4 T cells regulates tissue inflammation by producing interleukin 17. *Nat Immunol,* 6**,** 1133-41.

PARSONS, M. S., TANG, C. C., JEGASKANDA, S., CENTER, R. J., BROOKS, A. G., STRATOV, I. & KENT, S. J. 2014. Anti-HIV antibody-dependent activation of NK cells impairs NKp46 expression. *J Immunol,* 192**,** 308-15.

PASINI, E., AQUILANI, R., TESTA, C., BAIARDI, P., ANGIOLETTI, S., BOSCHI, F., VERRI, M. & DIOGUARDI, F. 2016. Pathogenic Gut Flora in Patients With Chronic Heart Failure. *JACC Heart Fail,* 4**,** 220-7.

PEREZ-SIMON, J. A., SANCHEZ-ABARCA, I., DIEZ-CAMPELO, M., CABALLERO, D. & SAN MIGUEL, J. 2006. Chronic graft-versus-host disease: Pathogenesis and clinical management. *Drugs,* 66**,** 1041-57.

PEVSNER-FISCHER, M., BLACHER, E., TATIROVSKY, E., BEN-DOV, I. Z. & ELINAV, E. 2017. The gut microbiome and hypertension. *Curr Opin Nephrol Hypertens,* 26**,** 1-8.

PINDERSKI, L. J., FISCHBEIN, M. P., SUBBANAGOUNDER, G., FISHBEIN, M. C., KUBO, N., CHEROUTRE, H., CURTISS, L. K., BERLINER, J. A. & BOISVERT, W. A. 2002. Overexpression of interleukin-10 by activated T lymphocytes inhibits atherosclerosis in LDL receptor-deficient Mice by altering lymphocyte and macrophage phenotypes. *Circ Res,* 90**,** 1064-71.

POTEKHINA, A. V., PYLAEVA, E., PROVATOROV, S., RULEVA, N., MASENKO, V., NOEVA, E., KRASNIKOVA, T. & AREFIEVA, T. 2015. Treg/Th17 balance in stable CAD patients with different stages of coronary atherosclerosis. *Atherosclerosis,* 238**,** 17-21.

RADULOVIC, K., MANTA, C., ROSSINI, V., HOLZMANN, K., KESTLER, H. A., WEGENKA, U. M., NAKAYAMA, T. & NIESS, J. H. 2012. CD69 regulates type I IFN-induced tolerogenic signals to mucosal CD4 T cells that attenuate their colitogenic potential. *J Immunol,* 188**,** 2001-13.

RAHIM, M. M. & MAKRIGIANNIS, A. P. 2015. Ly49 receptors: evolution, genetic diversity, and impact on immunity. *Immunol Rev,* 267**,** 137-47.

RAJAGOPALAN, S., FU, J. & LONG, E. O. 2001. Cutting edge: induction of IFN-gamma production but not cytotoxicity by the killer cell Ig-like receptor KIR2DL4 (CD158d) in resting NK cells. *J Immunol,* 167**,** 1877-81.

RANGACHARI, M., MAUERMANN, N., MARTY, R. R., DIRNHOFER, S., KURRER, M. O., KOMNENOVIC, V., PENNINGER, J. M. & ERIKSSON, U. 2006. T-bet negatively regulates autoimmune myocarditis by suppressing local production of interleukin 17. *J Exp Med,* 203**,** 2009-19.

RAPHAEL, I., NALAWADE, S., EAGAR, T. N. & FORSTHUBER, T. G. 2015. T cell subsets and their signature cytokines in autoimmune and inflammatory diseases. *Cytokine,* 74**,** 5-17.

RAULET, D. H. 2003. Roles of the NKG2D immunoreceptor and its ligands. *Nat Rev Immunol,* 3**,** 781-90.

RAULET, D. H., GASSER, S., GOWEN, B. G., DENG, W. & JUNG, H. 2013. Regulation of ligands for the NKG2D activating receptor. *Annu Rev Immunol,* 31**,** 413-41.

RAZIUDDIN, A., BENNETT, M., WINKLER-PICKETT, R., ORTALDO, J. R., LONGO, D. L. & MURPHY, W. J. 2000. Synergistic effects of in vivo depletion of Ly-49A and Ly-49G2 natural killer cell subsets in the rejection of H2(b) bone marrow cell allografts. *Blood,* 95**,** 3840-4.

RAZIUDDIN, A., LONGO, D. L., MASON, L., ORTALDO, J. R. & MURPHY, W. J. 1996. Ly-49 G2+ NK cells are responsible for mediating the rejection of H-2b bone marrow allografts in mice. *Int Immunol,* 8**,** 1833-9.

REICHART, D., MAGNUSSEN, C., ZELLER, T. & BLANKENBERG, S. 2019. Dilated Cardiomyopathy - From Epidemiologic to Genetic Phenotypes A Translational Review of Current Literature. *J Intern Med*.

REIKVAM, D. H., EROFEEV, A., SANDVIK, A., GRCIC, V., JAHNSEN, F. L., GAUSTAD, P., MCCOY, K. D., MACPHERSON, A. J., MEZA-ZEPEDA, L. A. & JOHANSEN, F. E. 2011. Depletion of murine intestinal microbiota: effects on gut mucosa and epithelial gene expression. *PLoS One,* 6**,** e17996.

RENZ, H., BRANDTZAEG, P. & HORNEF, M. 2011. The impact of perinatal immune development on mucosal homeostasis and chronic inflammation. *Nat Rev Immunol,* 12**,** 9-23.

RIDKER, P. M., EVERETT, B. M., THUREN, T., MACFADYEN, J. G., CHANG, W. H., BALLANTYNE, C., FONSECA, F., NICOLAU, J., KOENIG, W., ANKER, S. D., KASTELEIN, J. J. P., CORNEL, J. H., PAIS, P., PELLA, D., GENEST, J., CIFKOVA, R., LORENZATTI, A., FORSTER, T., KOBALAVA, Z., VIDA-SIMITI, L., FLATHER, M., SHIMOKAWA, H., OGAWA, H., DELLBORG, M., ROSSI, P. R. F., TROQUAY, R. P. T., LIBBY, P., GLYNN, R. J. & GROUP, C. T. 2017. Antiinflammatory Therapy with Canakinumab for Atherosclerotic Disease. *N Engl J Med,* 377**,** 1119-1131.

RIZZO, L. V., CUNHA-NETO, E. & TEIXEIRA, A. R. 1989. Autoimmunity in Chagas' disease: specific inhibition of reactivity of CD4+ T cells against myosin in mice chronically infected with Trypanosoma cruzi. *Infect Immun,* 57**,** 2640-4.

ROBINSON, D. S. 2009. Regulatory T cells and asthma. *Clin Exp Allergy,* 39**,** 1314-23.

RODRIGUEZ, J. M., MURPHY, K., STANTON, C., ROSS, R. P., KOBER, O. I., JUGE, N., AVERSHINA, E., RUDI, K., NARBAD, A., JENMALM, M. C., MARCHESI, J. R. & COLLADO, M. C. 2015. The composition of the gut microbiota throughout life, with an emphasis on early life. *Microb Ecol Health Dis,* 26**,** 26050.

ROHM, I., ATISKOVA, Y., DROBNIK, S., FRITZENWANGER, M., KRETZSCHMAR, D., PISTULLI, R., ZANOW, J., KRONERT, T., MALL, G., FIGULLA, H. R. & YILMAZ, A. 2015. Decreased regulatory T cells in vulnerable atherosclerotic lesions: imbalance between pro- and anti-inflammatory cells in atherosclerosis. *Mediators Inflamm,* 2015**,** 364710.

ROSELAAR, S. E., KAKKANATHU, P. X. & DAUGHERTY, A. 1996. Lymphocyte populations in atherosclerotic lesions of apoE -/- and LDL receptor -/- mice. Decreasing density with disease progression. *Arterioscler Thromb Vasc Biol,* 16**,** 1013-8.

SAKAGUCHI, S., SAKAGUCHI, N., ASANO, M., ITOH, M. & TODA, M. 1995. Immunologic self-tolerance maintained by activated T cells expressing IL-2 receptor alpha-chains (CD25). Breakdown of a single mechanism of self-tolerance causes various autoimmune diseases. *J Immunol,* 155**,** 1151-64.

SAKAKURA, K., NAKANO, M., OTSUKA, F., LADICH, E., KOLODGIE, F. D. & VIRMANI, R. 2013. Pathophysiology of atherosclerosis plaque progression. *Heart Lung Circ,* 22**,** 399-411.

SANCHEZ-DIAZ, R., BLANCO-DOMINGUEZ, R., LASARTE, S., TSILINGIRI, K., MARTIN-GAYO, E., LINILLOS-PRADILLO, B., DE LA FUENTE, H., SANCHEZ-MADRID, F., NAKAGAWA, R., TORIBIO, M. L. & MARTIN, P. 2017. Thymus-Derived Regulatory T Cell Development Is Regulated by C-Type Lectin-Mediated BIC/MicroRNA 155 Expression. *Mol Cell Biol,* 37.

SANCHEZ-MATEOS, P. & SANCHEZ-MADRID, F. 1991. Structure-function relationship and immunochemical mapping of external and intracellular antigenic sites on the lymphocyte activation inducer molecule, AIM/CD69. *Eur J Immunol,* 21**,** 2317-25.

SANCHO, D., GOMEZ, M., VIEDMA, F., ESPLUGUES, E., GORDON-ALONSO, M., GARCIA-LOPEZ, M. A., DE LA FUENTE, H., MARTINEZ, A. C., LAUZURICA, P. & SANCHEZ-MADRID, F. 2003. CD69 downregulates autoimmune reactivity through active transforming growth factor-beta production in collagen-induced arthritis. *J Clin Invest,* 112**,** 872-82.

SANDEK, A., SWIDSINSKI, A., SCHROEDL, W., WATSON, A., VALENTOVA, M., HERRMANN, R., SCHERBAKOV, N., CRAMER, L., RAUCHHAUS, M., GROSSE-HERRENTHEY, A., KRUEGER, M.,

VON HAEHLING, S., DOEHNER, W., ANKER, S. D. & BAUDITZ, J. 2014. Intestinal blood flow in patients with chronic heart failure: a link with bacterial growth, gastrointestinal symptoms, and cachexia. *J Am Coll Cardiol,* 64**,** 1092-102.

SASAKI, N., YAMASHITA, T., TAKEDA, M., SHINOHARA, M., NAKAJIMA, K., TAWA, H., USUI, T. & HIRATA, K. 2009. Oral anti-CD3 antibody treatment induces regulatory T cells and inhibits the development of atherosclerosis in mice. *Circulation,* 120**,** 1996-2005.

SCHIATTARELLA, G. G., SANNINO, A., TOSCANO, E., GIUGLIANO, G., GARGIULO, G., FRANZONE, A., TRIMARCO, B., ESPOSITO, G. & PERRINO, C. 2017. Gut microbe-generated metabolite trimethylamine-N-oxide as cardiovascular risk biomarker: a systematic review and dose-response meta-analysis. *Eur Heart J,* 38**,** 2948-2956.

SCHLEINITZ, N., VELY, F., HARLE, J. R. & VIVIER, E. 2010. Natural killer cells in human autoimmune diseases. *Immunology,* 131**,** 451-8.

SCHROEDER, M. A. & DIPERSIO, J. F. 2011. Mouse models of graft-versus-host disease: advances and limitations. *Dis Model Mech,* 4**,** 318-33.

SCHUBERT, A. M., SINANI, H. & SCHLOSS, P. D. 2015. Antibiotic-Induced Alterations of the Murine Gut Microbiota and Subsequent Effects on Colonization Resistance against Clostridium difficile. *MBio,* 6**,** e00974.

SCHULTHEISS, H. P., FAIRWEATHER, D., CAFORIO, A. L. P., ESCHER, F., HERSHBERGER, R. E., LIPSHULTZ, S. E., LIU, P. P., MATSUMORI, A., MAZZANTI, A., MCMURRAY, J. & PRIORI, S. G. 2019. Dilated cardiomyopathy. *Nat Rev Dis Primers,* 5**,** 32.

SEKIYA, T., KASHIWAGI, I., YOSHIDA, R., FUKAYA, T., MORITA, R., KIMURA, A., ICHINOSE, H., METZGER, D., CHAMBON, P. & YOSHIMURA, A. 2013. Nr4a receptors are essential for thymic regulatory T cell development and immune homeostasis. *Nat Immunol,* 14**,** 230-7.

SETOGUCHI, R. 2016. IL-15 boosts the function and migration of human terminally differentiated CD8+ T cells by inducing a unique gene signature. *Int Immunol,* 28**,** 293-305.

SHAW, M. H., KAMADA, N., KIM, Y. G. & NUNEZ, G. 2012. Microbiota-induced IL-1beta, but not IL-6, is critical for the development of steady-state TH17 cells in the intestine. *J Exp Med,* 209**,** 251-8.

SHIFRIN, N., RAULET, D. H. & ARDOLINO, M. 2014. NK cell self tolerance, responsiveness and missing self recognition. *Semin Immunol,* 26**,** 138-44.

SHINODA, K., TOKOYODA, K., HANAZAWA, A., HAYASHIZAKI, K., ZEHENTMEIER, S., HOSOKAWA, H., IWAMURA, C., KOSEKI, H., TUMES, D. J., RADBRUCH, A. & NAKAYAMA, T. 2012. Type II membrane protein CD69 regulates the formation of resting T-helper memory. *Proc Natl Acad Sci U S A,* 109**,** 7409-14.

SHIOW, L. R., ROSEN, D. B., BRDICKOVA, N., XU, Y., AN, J., LANIER, L. L., CYSTER, J. G. & MATLOUBIAN, M. 2006. CD69 acts downstream of interferon-alpha/beta to inhibit S1P1 and lymphocyte egress from lymphoid organs. *Nature,* 440**,** 540-4.

SIVORI, S., PENDE, D., BOTTINO, C., MARCENARO, E., PESSINO, A., BIASSONI, R., MORETTA, L. & MORETTA, A. 1999. NKp46 is the major triggering receptor involved in the natural cytotoxicity of fresh or cultured human NK cells. Correlation between surface density of NKp46 and natural cytotoxicity against autologous, allogeneic or xenogeneic target cells. *Eur J Immunol,* 29**,** 1656-66.

SMITH, E., PRASAD, K. M., BUTCHER, M., DOBRIAN, A., KOLLS, J. K., LEY, K. & GALKINA, E. 2010. Blockade of interleukin-17A results in reduced atherosclerosis in apolipoprotein E-deficient mice. *Circulation,* 121**,** 1746-55.

SMITH, K. M., WU, J., BAKKER, A. B., PHILLIPS, J. H. & LANIER, L. L. 1998. Ly-49D and Ly-49H associate with mouse DAP12 and form activating receptors. *J Immunol,* 161**,** 7-10.

SONDEREGGER, I., ROHN, T. A., KURRER, M. O., IEZZI, G., ZOU, Y., KASTELEIN, R. A., BACHMANN, M. F. & KOPF, M. 2006. Neutralization of IL-17 by active vaccination inhibits IL-23-dependent autoimmune myocarditis. *Eur J Immunol,* 36**,** 2849-56.

STECHER, B. & HARDT, W. D. 2011. Mechanisms controlling pathogen colonization of the gut. *Curr Opin Microbiol,* 14**,** 82-91.

STEINBERG, C., EISENACHER, K., GROSS, O., REINDL, W., SCHMITZ, F., RULAND, J. & KRUG, A. 2009. The IFN regulatory factor 7-dependent type I IFN response is not essential for early resistance against murine cytomegalovirus infection. *Eur J Immunol,* 39**,** 1007-18.

SUNDQUIST, A., BIGDELI, S., JALILI, R., DRUZIN, M. L., WALLER, S., PULLEN, K. M., EL-SAYED, Y. Y., TASLIMI, M. M., BATZOGLOU, S. & RONAGHI, M. 2007. Bacterial flora-typing with targeted, chip-based Pyrosequencing. *BMC Microbiol,* 7**,** 108.

SWEENEY, T. E. & MORTON, J. M. 2013. The human gut microbiome: a review of the effect of obesity and surgically induced weight loss. *JAMA Surg,* 148**,** 563-9.

TALEB, S., ROMAIN, M., RAMKHELAWON, B., UYTTENHOVE, C., PASTERKAMP, G., HERBIN, O., ESPOSITO, B., PEREZ, N., YASUKAWA, H., VAN SNICK, J., YOSHIMURA, A., TEDGUI, A. & MALLAT, Z. 2009. Loss of SOCS3 expression in T cells reveals a regulatory role for interleukin-17 in atherosclerosis. *J Exp Med,* 206**,** 2067-77.

TALEB, S., TEDGUI, A. & MALLAT, Z. 2015. IL-17 and Th17 cells in atherosclerosis: subtle and contextual roles. *Arterioscler Thromb Vasc Biol,* 35**,** 258-64.

TAMBURINI, S., SHEN, N., WU, H. C. & CLEMENTE, J. C. 2016. The microbiome in early life: implications for health outcomes. *Nat Med,* 22**,** 713-22.

TANG, W. H., WANG, Z., LEVISON, B. S., KOETH, R. A., BRITT, E. B., FU, X., WU, Y. & HAZEN, S. L. 2013. Intestinal microbial metabolism of phosphatidylcholine and cardiovascular risk. *N Engl J Med,* 368**,** 1575-84.

TENG, F., KLINGER, C. N., FELIX, K. M., BRADLEY, C. P., WU, E., TRAN, N. L., UMESAKI, Y. & WU, H. J. 2016. Gut Microbiota Drive Autoimmune Arthritis by Promoting Differentiation and Migration of Peyer's Patch T Follicular Helper Cells. *Immunity,* 44**,** 875-88.

TESTI, R., D'AMBROSIO, D., DE MARIA, R. & SANTONI, A. 1994. The CD69 receptor: a multipurpose cell-surface trigger for hematopoietic cells. *Immunol Today,* 15**,** 479-83.

TESTI, R., PHILLIPS, J. H. & LANIER, L. L. 1988. Constitutive expression of a phosphorylated activation antigen (Leu 23) by CD3bright human thymocytes. *J Immunol,* 141**,** 2557-63.

THAISS, C. A., ZMORA, N., LEVY, M. & ELINAV, E. 2016. The microbiome and innate immunity. *Nature,* 535**,** 65-74.

TIBBETTS, R. S., MCCORMICK, T. S., ROWLAND, E. C., MILLER, S. D. & ENGMAN, D. M. 1994. Cardiac antigen-specific autoantibody production is associated with cardiomyopathy in Trypanosoma cruzi-infected mice. *J Immunol,* 152**,** 1493-9.

TOMASELLO, E., BLERY, M., VELY, F. & VIVIER, E. 2000. Signaling pathways engaged by NK cell receptors: double concerto for activating receptors, inhibitory receptors and NK cells. *Semin Immunol,* 12**,** 139-47.

TSILINGIRI, K., DE LA FUENTE, H., RELANO, M., SANCHEZ-DIAZ, R., RODRIGUEZ, C., CRESPO, J., SANCHEZ-CABO, F., DOPAZO, A., ALONSO-LEBRERO, J. L., VARA, A., VAZQUEZ, J., CASASNOVAS, J. M., ALFONSO, F., IBANEZ, B., FUSTER, V., MARTINEZ-GONZALEZ, J., MARTIN, P. & SANCHEZ-MADRID, F. 2019. Oxidized Low-Density Lipoprotein Receptor in Lymphocytes Prevents Atherosclerosis and Predicts Subclinical Disease. *Circulation,* 139**,** 243-255.

UNUTMAZ, D., PILERI, P. & ABRIGNANI, S. 1994. Antigen-independent activation of naive and memory resting T cells by a cytokine combination. *J Exp Med,* 180**,** 1159-64.

UPADHYAYA, S. & BANERJEE, G. 2015. Type 2 diabetes and gut microbiome: at the intersection of known and unknown. *Gut Microbes,* 6**,** 85-92.

USUI, F., KIMURA, H., OHSHIRO, T., TATSUMI, K., KAWASHIMA, A., NISHIYAMA, A., IWAKURA, Y., ISHIBASHI, S. & TAKAHASHI, M. 2012. Interleukin-17 deficiency reduced vascular inflammation and development of atherosclerosis in Western diet-induced apoE-deficient mice. *Biochem Biophys Res Commun,* 420**,** 72-7.

VAN BRUGGEN, N. & OUYANG, W. 2014. Th17 cells at the crossroads of autoimmunity, inflammation, and atherosclerosis. *Immunity,* 40**,** 10-2.

VAN ES, T., VAN PUIJVELDE, G. H., FOKS, A. C., HABETS, K. L., BOT, I., GILBOA, E., VAN BERKEL, T. J. & KUIPER, J. 2010. Vaccination against Foxp3(+) regulatory T cells aggravates atherosclerosis. *Atherosclerosis,* 209**,** 74-80.

VAN HELDEN, M. J., GOOSSENS, S., DAUSSY, C., MATHIEU, A. L., FAURE, F., MARCAIS, A., VANDAMME, N., FARLA, N., MAYOL, K., VIEL, S., DEGOUVE, S., DEBIEN, E., SEUNTJENS, E., CONIDI, A., CHAIX, J., MANGEOT, P., DE BERNARD, S., BUFFAT, L., HAIGH, J. J., HUYLEBROECK, D., LAMBRECHT, B. N., BERX, G. & WALZER, T. 2015. Terminal NK cell maturation is controlled by concerted actions of T-bet and Zeb2 and is essential for melanoma rejection. *J Exp Med,* 212**,** 2015-25.

VANCE, R. E., KRAFT, J. R., ALTMAN, J. D., JENSEN, P. E. & RAULET, D. H. 1998. Mouse CD94/NKG2A is a natural killer cell receptor for the nonclassical major histocompatibility complex (MHC) class I molecule Qa-1(b). *J Exp Med,* 188**,** 1841-8.

VIVIER, E. & DAERON, M. 1997. Immunoreceptor tyrosine-based inhibition motifs. *Immunol Today,* 18**,** 286-91.

VIVIER, E., RAULET, D. H., MORETTA, A., CALIGIURI, M. A., ZITVOGEL, L., LANIER, L. L., YOKOYAMA, W. M. & UGOLINI, S. 2011. Innate or adaptive immunity? The example of natural killer cells. *Science,* 331**,** 44-9.

VIVIER, E., TOMASELLO, E., BARATIN, M., WALZER, T. & UGOLINI, S. 2008. Functions of natural killer cells. *Nat Immunol,* 9**,** 503-10.

VIVIER, E., UGOLINI, S., BLAISE, D., CHABANNON, C. & BROSSAY, L. 2012. Targeting natural killer cells and natural killer T cells in cancer. *Nat Rev Immunol,* 12**,** 239-52.

WANG, Z., KLIPFELL, E., BENNETT, B. J., KOETH, R., LEVISON, B. S., DUGAR, B., FELDSTEIN, A. E., BRITT, E. B., FU, X., CHUNG, Y. M., WU, Y., SCHAUER, P., SMITH, J. D., ALLAYEE, H., TANG, W. H., DIDONATO, J. A., LUSIS, A. J. & HAZEN, S. L. 2011. Gut flora metabolism of phosphatidylcholine promotes cardiovascular disease. *Nature,* 472**,** 57-63.

WARNATSCH, A., IOANNOU, M., WANG, Q. & PAPAYANNOPOULOS, V. 2015. Inflammation. Neutrophil extracellular traps license macrophages for cytokine production in atherosclerosis. *Science,* 349**,** 316-20.

WEINER, H. L. 2001. Induction and mechanism of action of transforming growth factor-beta-secreting Th3 regulatory cells. *Immunol Rev,* 182**,** 207-14.

WEN, L., LEY, R. E., VOLCHKOV, P. Y., STRANGES, P. B., AVANESYAN, L., STONEBRAKER, A. C., HU, C., WONG, F. S., SZOT, G. L., BLUESTONE, J. A., GORDON, J. I. & CHERVONSKY, A. V. 2008. Innate immunity and intestinal microbiota in the development of Type 1 diabetes. *Nature,* 455**,** 1109-13.

WENSVEEN, F. M., JELENCIC, V. & POLIC, B. 2018. NKG2D: A Master Regulator of Immune Cell Responsiveness. *Front Immunol,* 9**,** 441.

WIGREN, M., KOLBUS, D., DUNER, P., LJUNGCRANTZ, I., SODERBERG, I., BJORKBACKA, H., FREDRIKSON, G. N. & NILSSON, J. 2011. Evidence for a role of regulatory T cells in mediating the atheroprotective effect of apolipoprotein B peptide vaccine. *J Intern Med,* 269**,** 546-56.

WORKMAN, C. J., SZYMCZAK-WORKMAN, A. L., COLLISON, L. W., PILLAI, M. R. & VIGNALI, D. A. 2009. The development and function of regulatory T cells. *Cell Mol Life Sci,* 66**,** 2603-22.

WU, H. J., IVANOV, II, DARCE, J., HATTORI, K., SHIMA, T., UMESAKI, Y., LITTMAN, D. R., BENOIST, C. & MATHIS, D. 2010. Gut-residing segmented filamentous bacteria drive autoimmune arthritis via T helper 17 cells. *Immunity,* 32**,** 815-27.

WU, J., SONG, Y., BAKKER, A. B., BAUER, S., SPIES, T., LANIER, L. L. & PHILLIPS, J. H. 1999. An activating immunoreceptor complex formed by NKG2D and DAP10. *Science,* 285**,** 730-2.

XIE, X., STADNISKY, M. D. & BROWN, M. G. 2009. MHC class I Dk locus and Ly49G2+ NK cells confer H-2k resistance to murine cytomegalovirus. *J Immunol,* 182**,** 7163-71.

YANG, G., KONG, Q., WANG, G., JIN, H., ZHOU, L., YU, D., NIU, C., HAN, W., LI, W. & CUI, J. 2014. Low-dose ionizing radiation induces direct activation of natural killer cells and provides a novel approach for adoptive cellular immunotherapy. *Cancer Biother Radiopharm,* 29**,** 428-34.

YEN, D., CHEUNG, J., SCHEERENS, H., POULET, F., MCCLANAHAN, T., MCKENZIE, B., KLEINSCHEK, M. A., OWYANG, A., MATTSON, J., BLUMENSCHEIN, W., MURPHY, E., SATHE, M., CUA, D. J., KASTELEIN, R. A. & RENNICK, D. 2006. IL-23 is essential for T cell-mediated colitis and promotes inflammation via IL-17 and IL-6. *J Clin Invest,* 116**,** 1310-6.

YOKOYAMA, W. M. & PLOUGASTEL, B. F. 2003. Immune functions encoded by the natural killer gene complex. *Nat Rev Immunol,* 3**,** 304-16.

YU, G., XU, X., VU, M. D., KILPATRICK, E. D. & LI, X. C. 2006. NK cells promote transplant tolerance by killing donor antigen-presenting cells. *J Exp Med,* 203**,** 1851-8.

YU, J., MAO, H. C., WEI, M., HUGHES, T., ZHANG, J., PARK, I. K., LIU, S., MCCLORY, S., MARCUCCI, G., TROTTA, R. & CALIGIURI, M. A. 2010. CD94 surface density identifies a functional intermediary between the CD56bright and CD56dim human NK-cell subsets. *Blood,* 115**,** 274-81.

YU, J., WEI, M., MAO, H., ZHANG, J., HUGHES, T., MITSUI, T., PARK, I. K., HWANG, C., LIU, S., MARCUCCI, G., TROTTA, R., BENSON, D. M., JR. & CALIGIURI, M. A. 2009. CD94 defines phenotypically and functionally distinct mouse NK cell subsets. *J Immunol,* 183**,** 4968-74.

ZAFIROVA, B., WENSVEEN, F. M., GULIN, M. & POLIC, B. 2011. Regulation of immune cell function and differentiation by the NKG2D receptor. *Cell Mol Life Sci,* 68**,** 3519-29.

ZAKOSTELSKA, Z., MALKOVA, J., KLIMESOVA, K., ROSSMANN, P., HORNOVA, M., NOVOSADOVA, I., STEHLIKOVA, Z., KOSTOVCIK, M., HUDCOVIC, T., STEPANKOVA, R., JUZLOVA, K., HERCOGOVA, J., TLASKALOVA-HOGENOVA, H. & KVERKA, M. 2016. Intestinal Microbiota Promotes Psoriasis-Like Skin Inflammation by Enhancing Th17 Response. *PLoS One,* 11**,** e0159539.

ZENG, H., ZHANG, R., JIN, B. & CHEN, L. 2015. Type 1 regulatory T cells: a new mechanism of peripheral immune tolerance. *Cell Mol Immunol,* 12**,** 566-71.

ZHANG, Z., ZHENG, M., BINDAS, J., SCHWARZENBERGER, P. & KOLLS, J. K. 2006. Critical role of IL-17 receptor signaling in acute TNBS-induced colitis. *Inflamm Bowel Dis,* 12**,** 382-8.

ZHU, S. & QIAN, Y. 2012. IL-17/IL-17 receptor system in autoimmune disease: mechanisms and therapeutic potential. *Clin Sci (Lond),* 122**,** 487-511.

ZIEGLER, S. F., LEVIN, S. D., JOHNSON, L., COPELAND, N. G., GILBERT, D. J., JENKINS, N. A., BAKER, E., SUTHERLAND, G. R., FELDHAUS, A. L. & RAMSDELL, F. 1994. The mouse CD69 gene. Structure, expression, and mapping to the NK gene complex. *J Immunol,* 152**,** 1228-36.

ZINGONI, A., PALMIERI, G., MORRONE, S., CARRETERO, M., LOPEZ-BOTEL, M., PICCOLI, M., FRATI, L. & SANTONI, A. 2000. CD69-triggered ERK activation and functions are negatively regulated by CD94 / NKG2-A inhibitory receptor. *Eur J Immunol,* 30**,** 644-51.

ANNEX

ANNEX INDEX

Published articles related to this thesis

Tsilingiri K, de la Fuente H*,* ***Relaño M****, Sánchez-Díaz R, Rodríguez C, Crespo J, Sánchez-Cabo F, Dopazo A, Alonso-Lebrero JL, Vara A, Vázquez J, Casasnovas JM, Alfonso F, Ibáñez B, Fuster V, Martínez-González J, Martín P, Sánchez-Madrid F. "****Oxidized Low-Density Lipoprotein Receptor in Lymphocytes Prevents Atherosclerosis and Predicts Subclinical Disease".** *Circulation. 2019 Jan 8;139(2):243-255. doi: 10.1161/CIRCULATIONAHA.118.034326.*

Circulation

ORIGINAL RESEARCH ARTICLE

Oxidized Low-Density Lipoprotein Receptor in Lymphocytes Prevents Atherosclerosis and Predicts Subclinical Disease

BACKGROUND: Although the role of Th17 and regulatory T cells in the progression of atherosclerosis has been highlighted in recent years, their molecular mediators remain elusive. We aimed to evaluate the association between the CD69 receptor, a regulator of Th17/regulatory T cell immunity, and atherosclerosis development in animal models and in patients with subclinical disease.

METHODS: Low-density lipoprotein receptor–deficient chimeric mice expressing or not expressing CD69 on either myeloid or lymphoid cells were subjected to a high fat diet. In vitro functional assays with human T cells were performed to decipher the mechanism of the observed phenotypes. Expression of CD69 and NR4A nuclear receptors was evaluated by reverse transcription–polymerase chain reaction in 305 male participants of the PESA study (Progression of Early Subclinical Atherosclerosis) with extensive (n=128) or focal (n=55) subclinical atherosclerosis and without disease (n=122).

RESULTS: After a high fat diet, mice lacking CD69 on lymphoid cells developed large atheroma plaque along with an increased Th17/regulatory T cell ratio in blood. Oxidized low-density lipoprotein was shown to bind specifically and functionally to CD69 on human T lymphocytes, inhibiting the development of Th17 cells through the activation of NR4A nuclear receptors. Participants of the PESA study with evidence of subclinical atherosclerosis displayed a significant CD69 and NR4A1 mRNA downregulation in peripheral blood leukocytes compared with participants without disease. The expression of CD69 remained associated with the risk of subclinical atherosclerosis in an adjusted multivariable logistic regression model (odds ratio, 0.62; 95% CI, 0.40–0.94; *P*=0.006) after adjustment for traditional risk factors, the expression of NR4A1, the level of oxidized low-density lipoprotein, and the counts of different leucocyte subsets.

CONCLUSIONS: CD69 depletion from the lymphoid compartment promotes a Th17/regulatory T cell imbalance and exacerbates the development of atherosclerosis. CD69 binding to oxidized low-density lipoprotein on T cells induces the expression of anti-inflammatory transcription factors. Data from a cohort of the PESA study with subclinical atherosclerosis indicate that CD69 expression in PBLs inversely correlates with the presence of disease. The expression of CD69 remained an independent predictor of subclinical atherosclerosis after adjustment for traditional risk factors.

Katerina Tsilingiri, PhD*
Hortensia de la Fuente, MD, PhD*
Marta Relaño, MSc
Raquel Sánchez-Díaz, PhD
Cristina Rodríguez, PhD
Javier Crespo, PhD
Fátima Sánchez-Cabo, PhD
Ana Dopazo, PhD
José L. Alonso-Lebrero, PhD
Alicia Vara, BSc
Jesús Vázquez, PhD
José M. Casasnovas, PhD
Fernando Alfonso, MD, PhD
Borja Ibáñez, MD, PhD
Valentín Fuster, MD, PhD
José Martínez-González, PhD
Pilar Martín, PhD
Francisco Sánchez-Madrid, PhD

*Drs Tsilingiri and de la Fuente contributed equally.

Key Words: atherosclerosis ■ CD69 antigen ■ oxidized low density lipoprotein ■ regulatory T lymphocytes ■ Th17 cells

Sources of Funding, see page 254

Clinical Perspective

What Is New?

- This study identifies CD69 as an oxidized low-density lipoprotein receptor in T lymphocytes that contributes to the regulatory action of the adaptive immune system, preventing atherosclerosis development.
- CD69 controls the onset and progression of atherosclerosis, and its mRNA expression is an independent marker of early subclinical disease in humans.
- Data from a cohort of asymptomatic individuals indicate that CD69 expression in circulating T cells correlates inversely with the presence and extension of subclinical atherosclerosis.
- The expression of CD69 remained associated with the risk of subclinical atherosclerosis after adjustment for traditional cardiovascular risk factors.

What Are the Clinical Implications?

- Oxidized low-density lipoprotein binding to CD69 confers a regulatory phenotype to human and mouse T cells, dampening Th17 responses and ameliorating atherosclerosis.
- Expression of CD69 in circulating cells might serve as a new biomarker for the presence of subclinical atherosclerosis.

Although lipid deposition in the vessel wall is the hallmark of atherosclerosis, for many years, it has been recognized that inflammation also plays a crucial role in the genesis and progression of the disease and the appearance of clinical manifestations (infarction, stroke).[1] Recently, it has been demonstrated that the modulation of the inflammatory response is a valid target to reduce the risk of atherothrombotic events in high-risk patients.[2] The interplay between lipid metabolism and immune response is not completely understood. In the last decade, the contribution of lymphocytes to atherosclerosis clinical manifestations has been highlighted, and effector T-cell responses seem to be exacerbated in hyperlipidemia.[3,4]

In vivo models of atherosclerosis suggest that regulatory T (Treg) cells suppress inflammatory responses and attenuate atherosclerosis.[5] Experimental therapies aimed to increase Treg cell population under high fat diet (HFD) conditions have conclusively demonstrated an important role for this T-cell subset in atherosclerosis attenuation.[6,7] The role of Th17 lymphocytes is more controversial. Although genetic or pharmacological inhibition of interleukin (IL)-17 significantly ameliorates atherosclerosis,[8,9] concomitant increases in both IL-17 and IL-10 lead to smaller plaques.[10] Another study reports bigger plaques in *ApoE*$^{-/-}$*IL-17*$^{-/-}$ mice.[11] A Th17/Treg imbalance has been reported in patients with coronary artery atherosclerosis, with a significant increase in Th17 and a decrease in Treg cells.[12,13]

The early lymphocyte activation antigen CD69 regulates Th17 and Treg cell differentiation. CD69-deficient mice display enhanced Th17 differentiation and defective Treg cell function,[14–16] resulting in an inability to resolve inflammation or to maintain immune tolerance in diseases such as arthritis, asthma, contact dermatitis, or myocarditis.[17–19] However, no differences were observed in the atheroma plaque formation in CD69$^{-/-}$ ApoE$^{-/-}$ mice.[20]

A key event in the process of atheroma plaque formation is low-density lipoprotein (LDL) peroxidation, which generates highly inflammatory and immunogenic oxidized LDL (oxLDL).[21] However, oxLDL can also elicit anti-inflammatory responses by activating peroxisome proliferator-activated receptor-γ[22] and liver X receptor or by upregulating transcription factors with anti-inflammatory activity such as NR4A nuclear receptors.[23,24]

The main objectives of this work were to analyze the role of CD69 lymphocyte expression in atherosclerosis development, the immune mechanisms involved, and its relation with human disease. Using chimeric *ldlr*$^{-/-}$ mice subjected an HFD as atherosclerosis model, we show that CD69 deficiency specifically on lymphocytes leads to an altered Th17/Treg equilibrium and a consequent increase in atheroma plaque size during an HFD. In vitro assays in human T cells showed that the interaction between oxLDL and CD69 activates the expression of *NR4A* transcription factors, skewing T cells toward a regulatory phenotype and dampening Th17 and Th1 responses. Thus, we describe an unexpected regulatory mechanism of the adaptive immune system that delays atherosclerosis development in hyperlipidemic conditions. Remarkably, our data from participants in the PESA (Progression of Early Subclinical Atherosclerosis) cohort[25] were in agreement with these results in that downregulated CD69 expression in peripheral blood leukocytes (PBLs) is associated with subclinical atherosclerosis in an adjusted multivariable logistic regression model.

METHODS

The data, methods, and study material will be available to other researchers for purposes of reproducing the results or replicating the procedures by contacting the corresponding authors.

Study Design

To analyze the role of CD69 during atherosclerosis development, we used chimeras from ldlr$^{-/-}$ CD45.1^{+} mice (the line was obtained in house by crossing and subsequent selection by genotype of B6;129S7-*Ldlr*^{tm1Her}/J with B6.SJL-Ptprc^{a}Pepc^{b}/BoyCrl, from Jackson and Charles River, respectively) and CD69$^{-/-}$ or CD69$^{+/+}$ B6 double reporter (dRep) for Treg cells (FIR mice, Foxp3–monomeric red fluorescent protein [mRFP])

and Th17 cells (IL-17A–IRES–enhanced green fluorescent protein [eGFP]), hereafter *cd69*$^{-/-}$*dRep* and *cd69*$^{+/+}$*dRep*, respectively. dRep mice allow us to monitor the presence of live Treg cells and Th17 cells throughout the experiment. To evaluate the influence of immune cell CD69 expression during atherosclerosis development, Ldlr$^{-/-}$ mice were irradiated and reconstituted with bone marrow (BM) from *cd69*$^{-/-}$*dRep* mice or *cd69*$^{+/+}$*dRep*. Next, atherosclerosis development was evaluated in mice proficient or deficient for CD69 only in the myeloid compartment (MC; hereafter MC *cd69*$^{+/+}$ and MC *cd69*$^{-/-}$) or lymphoid compartment (LC; hereafter LC *cd69*$^{+/+}$ and LC *cd69*$^{-/-}$). For a detailed description of chimeric mice design, see the online-only Data Supplement. After 6 weeks of BM reconstitution, mice were placed on an HFD (SSNIFF, S9167-E010) for 10 to 16 weeks. Immune response was evaluated in peripheral blood, draining (para-aortic) lymph nodes (LNs), nondraining (inguinal, axillary, mesenteric) LNs, and spleen by flow cytometry and quantitative polymerase chain reaction (PCR). All animal procedures were approved by the ethics committee of the Comunidad Autónoma de Madrid and conducted in accordance with the institutional guidelines that comply with the European Institutes of Health directives (2010/63/EU of the European Parliament and the Council on the Protection of Animals Used for Scientific Purposes [*Official Journal of the European Union*, 2010:53:33–79]).

Quantification of CD69 and NR4A Gene Expression in the PESA Study

Expression of CD69 and nuclear receptors NR4A1 was evaluated by reverse transcription PCR with Taqman probes in PBLs of a subset of the participants from the PESA study.[25] This study prospectively enrolled 4184 asymptomatic participants 40 to 54 years of age to evaluate the systemic extent of atherosclerosis in the carotid, abdominal aortic, and iliofemoral territories by 2-dimensional/3-dimensional ultrasound and coronary artery calcification by computed tomography at baseline and 3 and 6 years after enrollment for follow-up studies. Participants were then defined as free of atherosclerosis (no disease; no presence of plaque and a coronary artery calcium score of zero) or with evidence of focal (1 site affected) or generalized (4–6 sites affected) subclinical atherosclerotic disease.[25] Following a general study strategy (ie, not for this specific analysis), 480 individuals of the whole cohort were retrospectively selected on the basis of the extent of subclinical atherosclerosis to perform molecular tests. Individuals were included in this subcohort, prioritizing those with more territories with evidence of plaque at baseline. For those presenting a tie, individuals with coronary artery calcification score ≥1 were included. Control subjects were then selected from those individuals without plaques and matched with the chosen cases on the basis of age, sex, family history of cardiovascular disease, dyslipidemia, and hypertension. From this subpopulation of 480 individuals, we selected 305 male participants classified as without disease (n=122) or with focal (n=55) or generalized (n=128) disease to test the expression of CD69 and NR4A1 by reverse transcription PCR. General characteristics of this specific subcohort are shown in Table I in the online-only Data Supplement.

Monitoring Th17 and Treg Cells in the In Vivo Model

To assess the immune response, the percentages of IL-17–eGFP^{+} or Foxp3-RFP^{+} cells in peripheral blood CD4^{+} T cells were monitored throughout the experiment by flow cytometry. The presence of Th17 and Treg cells was also evaluated at the end point of the experiment in aortic arch, spleen, nondraining (axillary) LNs, and draining (para-aortic) LNs.

OxLDL Binding Assays

Jurkat T (JK) cells or rat basophilic leukemia (RBL) cells stably transfected or not with CD69 were incubated with 1,1′-dioctadecyl-3,3,3′,3′-tetramethylindo-carbocyanine perchlorate–labeled (DiI) LDL in their native and oxidized form in the presence or not of unlabeled lipoproteins. Lipoprotein binding was determined with flow cytometry. In some cases, blocking anti-CD69 antibody was added.

Human CD4^{+} T Cell Polarization

For human Th1, Th17, and Treg cell polarization, CD4^{+} T cells were purified from peripheral blood of healthy donors and incubated with a specific cocktail of recombinant cytokines. After the indicated days of culture, cells were analyzed in a FACSCanto Flow Cytometer. When indicated, oxLDL (50 μg/mL) and anti-CD69 (20 μg/mL) were added to the cultures.

Assessment of CD69 and NR4A Transcripts

Expression of mRNA levels of CD69 and NR4A nuclear receptors was analyzed in PBLs from patients with subclinical atherosclerosis and healthy subjects with reverse transcription PCR with Taqman probes (Applied Biosystems). Expression of NR4A receptors was also assessed in Jurkat T cells and human primary lymphocytes in the presence or not of oxLDL. When indicated, blocking anti-CD69 antibodies were also added. NR4A and CD69 mRNA expression was also determined in para-aortic LNs and peripheral blood lymphocytes from mice.

Tissue Processing and Immunohistochemistry

For plaque area assessment, 5-μm-thick sections at 100-μm intervals were collected starting at the origin of the aortic valve cusps. Sections were stained with Oil Red O staining, (Sigma-Aldrich) and hematoxylin, and lesion size was analyzed with ImageJ software. For Masson trichrome staining, 7-μm-thick sections at 100-μm intervals were collected. Sections were stained with the Masson-Goldner staining kit (Merck). For specific staining, anti-F480 antibody was purchased from Abcam (ab6640) and anti-CD3 from Santa Cruz Biotechnology (sc-1127). OxLDL was detected by immunofluorescence with rabbit anti-mouse oxLDL from Abcris.

Statistical Analysis

In vivo experiments were performed according to a randomized complete block design (treatments and different

time points have been taken into account) or a fully randomized design. To determine significant differences between 2 means, *P* values were calculated by unpaired *t* test or Mann-Whitney *U* test according to normality test, and differences among >2 means were analyzed by 1-way ANOVA or the Kruskal-Wallis test. To account for multiple comparisons, the Tukey or Bonferroni posttests were used to compare selected pairs of means and all pairs of means, respectively. When indicated, the Wilcoxon signed-rank test was used to analyze paired data. For differences in human T-cell differentiation assays, data were analyzed with the Friedman test and the Dunn multiple-comparison test. In kinetic experiments with the same mice, 2-way repeated-measures ANOVA with the Sidak multiple-comparison post hoc test was performed. Differences were considered significant at $P<0.05$.

Table I in the online-only Data Supplement shows demographics and cardiovascular risk factor statistics of the PESA subcohort selected for the quantitative PCR assay. Statistics were calculated with Stata (StataCorp, College Station, TX). Data are expressed as mean±SD, median and interquartile range, or number (percent). *P* values are derived from ANOVA for log-transformed continuous variables and χ^2 for categorical variables, except for those variables with n<6, for which the Fisher test was used.

The Cuzick extension of the Wilcoxon rank-sum test was used to assess the significance of the trend in the quantitative PCR data across the 3 ordinal groups allowing for ties. After that, 1-way ANOVA followed by the Tukey posttest was used to identify significant differences between each stage of subclinical atherosclerosis and baseline. Expression levels measured by quantitative PCR were normalized and considered in the log2 scale to fulfill the normality assumption. We then focused on the 2 most extreme groups (no disease versus generalized disease) and used a multivariable logistic regression model to assess the association of CD69 with subclinical atherosclerosis independently of known cardiovascular risk factors (age, smoking, family history of cardiovascular disease, dyslipidemia, hypertension, diabetes mellitus), the expression of NR4A1, oxLDL levels, and volume of different leukocyte subsets. These variables included in the model were found to be statistically significant with a value of $P<0.1$ in a univariable logistic regression model. Odds ratio, 95% CI, and *P* value are reported. Traditional cardiovascular risk factors were determined from blood samples and interviews as follows: (1) diabetes mellitus: fasting plasma glucose ≥126 mg/dL or treatment with insulin or oral hypoglycemic medication; (2) arterial hypertension: systolic blood pressure ≥140 mm Hg, diastolic blood pressure ≥90 mm Hg, or use of antihypertensive medication; (3) hypercholesterolemia: total cholesterol ≥240 mg/dL, LDL cholesterol ≥160 mg/dL, high-density lipoprotein cholesterol <40 mg/dL, or use of lipid-lowering drugs; (4) smoking: current smoking status and a lifetime consumption of >100 cigarettes; and (5) family history of cardiovascular disease: first-degree relative diagnosed with atherosclerosis before 55 years of age in men and 65 years of age in women. Linear regression models were used to assess the correlation between the expression levels of CD69 with NR4A1 receptors. All these analyses were implemented with the R statistical software (www.r-project.org).

RESULTS

Lack of CD69 on Lymphocytes Exacerbates Atherosclerotic Plaque Formation

To evaluate the role of CD69 expression on BM-derived cells in the development of atherosclerosis, male Ldlr$^{-/-}$ mice were irradiated and reconstituted with BM from *cd69*$^{-/-}$ dRep for Foxp3-mRFP and IL-17A–eGFP[26] mice (BM *Cd69*$^{-/-}$) or WT-dRep littermates (BM *Cd69*$^{+/+}$; Figure IA in the online-only Data Supplement). From week 13 on, we found increased Th17/Treg cells ratio in PBLs of chimeric mice (Figure IB in the online-only Data Supplement), indicating a polarization toward proinflammatory phenotype in the absence of CD69. After 10 weeks of HFD, mice reconstituted with *cd69*$^{-/-}$*dRep* BM displayed a significantly high increase in IL-17–eGFP^{+} cells in para-aortic LNs, with higher absolute numbers compared with BM *Cd69*$^{+/+}$ mice (Figure IC and ID in the online-only Data Supplement). In agreement, the percentage but not cell numbers of Foxp3mRFP^{+} cells was significantly reduced in the absence of CD69 (Figure ID in the online-only Data Supplement), indicating that Treg cell recruitment to para-aortic LNs is not compromised. The percentage of CD4^{+} IL-17–eGFP^{+} cells was increased in the aortic arc of BM *Cd69*$^{-/-}$chimeras, whereas there is a tendency for decreased CD4^{+} and FoxP3^{+} cells (Figure IE and IF in the online-only Data Supplement). Collectively, flow cytometry data indicate that hyperlipidemia induces high proinflammatory activity and a disrupted Th17/Treg cells balance in the absence of CD69. Histochemical studies revealed more extensive lesions and necrotic cores in aortic valves from BM *Cd69*$^{-/-}$ chimeras compared with the BM *Cd69*$^{+/+}$ control group (Figure IG and IH in the online-only Data Supplement). Atheroma plaques in both groups consisted mainly of F4/80^{+} foam cells, although we found a higher infiltration of CD3^{+} lymphocytes into atheroma plaques in the BM *Cd69*$^{-/-}$ group (Figure II and IJ in the online-only Data Supplement). Peripheral blood leukocytes were analyzed during an HFD with no significant changes between BM *Cd69*$^{+/+}$ and BM *Cd69*$^{-/-}$ mice (Figure IIA and IIB in the online-only Data Supplement). Because CD69 has been also related to the maintenance of T-cell helper memory,[27] the CD44^{hi} CD62L^{lo} memory T-cell subset was also analyzed. Naïve T cells decrease with an HFD whereas memory T cells increase in both chimeric mice, suggesting that CD69 is not playing a role in the maintenance of T-helper memory cells in this model (Figure IIC in the online-only Data Supplement). Moreover, we found that the ratio between dendritic cells and Treg cells during HFD remains equal in both chimeric mice (Figure IID in the online-only Data Supplement). These data suggest that Th17 and Treg cell proportions are altered under the

course of HFD in BM Cd69$^{-/-}$ chimeric mice, whereas the other leukocyte subsets remained unaltered.

To address whether the observed phenotype in BM *Cd69*$^{-/-}$ mice is specific to the LC or MC, we generated mixed BM chimeras proficient or deficient for CD69 in either the LC (LC *Cd69*$^{+/+}$ and LC *Cd69*$^{-/-}$ groups) or MC (Figure 1A and Figure III in the online-only Data Supplement). The specific deletion of CD69 on lymphocytes and myeloid cells was confirmed by flow cytometry analysis in the blood of hyperlipidemic mice (Figure 1A). We observed a significantly enhanced plateau of Th17 response in the peripheral blood of the *LC Cd69*$^{-/-}$ group after HFD, whereas percentages of Foxp3 cells were significantly decreased compared with the *Cd69*$^{+/+}$ group (Figure 1B and 1C). On observation that peripheral Th17 responses started to diminish in the *LC Cd69*$^{-/-}$ group after week 16 on HFD (Figure 1C), mice were euthanized, and immune responses and plaque formation were assessed. IL-17–eGFP^{+} cells in para-aortic LNs from *LC Cd69*$^{-/-}$ mice were once again increased, whereas the percentages of Foxp3mRFP^{+} cells were comparable in the 2 groups (Figure 1D). However, the absolute number of Treg cells was significant decreased, with a significant increase in the number of Th17 cells (Figure 1D). Finally, atherosclerotic lesions were significantly more advanced with more extensive necrotic cores in the *LC Cd69*$^{-/-}$ group as assessed by Oil Red O and Masson trichrome staining (Figure 1E and 1F).

Myeloid cells are pivotal for atherosclerosis development.[28,29] We next performed mixed BM chimeras proficient or deficient for CD69 in the MC (MC *Cd69*$^{+/+}$ and MC *Cd69*$^{-/-}$; Figure IIIA in the online-only Data Supplement). We did not detect differences during HFD in Th17 or Treg cell dynamics in the periphery, at the site of inflammation (para-aortic LNs; Figure IIIB through IIID in the online-only Data Supplement), or in atheroma plaque formation (Figure IIIE and IIIF in the online-only Data Supplement). All the CD69-proficient and -deficient groups gained similar amounts of weight throughout the experiment. However, the circulating levels of lipids (free fatty acids, triglycerides, high-density lipoprotein, LDL, and cholesterol) were lower in LC *Cd69*$^{-/-}$ compared with LC *Cd69*$^{+/+}$, suggesting that the enhanced plaque formation in LC *Cd69*$^{-/-}$ was not attributable to a metabolic defect (Figure IVA through IVC in the online-only Data Supplement).

We conclude that specific CD69 deletion in the LC accounts for the increased proinflammatory phenotype and the enhanced atheroma plaque formation.

OxLDL Binds to CD69 on T Lymphocytes

The main receptor of oxLDL on vascular cells is lectin-like oxLDL receptor-1 (LOX-1), located in the same chromosomal locus immediately upstream to CD69. The LOX-1 and CD69 C-type lectin-like domains form very similar dimers (Figure 2A, left), unlike other C-type lectins such as dectin-1 or the macrophage mannose receptor (Figure V in the online-only Data Supplement). In LOX-1, the oxLDL-binding surface is located at the top of the dimer and contains a unique basic "spine" formed by the diagonal arrangement of arginine residues across the dimer surface (Figure 2A, top right).[30,31] Electrostatic surface representation of the CD69 C-type lectin-like domain dimer indicated that 4 arginine residues cluster at the center of the dimer and form a basic spine, similar to that of LOX-1 (Figure 2A, bottom right). Because this structural feature is proposed to be important for oxLDL recognition,[30] we hypothesized that CD69 binding to oxLDL particles could account for the phenotype observed in vivo.

Transfected Jurkat T cells stably expressing CD69 (JKCD69) on their surface bound oxLDL-DiI much more efficiently than untransfected JK (JKwt) cells (Figure 2B and 2C). JKCD69 cells bound oxLDL in a dose-dependent manner and showed a weaker binding of native LDL (Figure 2D). This binding was able to induce CD69 internalization in JKCD69 cells (Figure 2E). The specificity of oxLDL binding to CD69 was confirmed in blocking assays with anti-CD69 antibodies (Figure 2F).

CD69/oxLDL Binding Controls Th17/Treg Equilibrium and Expression of NR4A Nuclear Receptors

OxLDL exposure significantly reduced the mRNA levels of IL-8 and interferon-γ (IFN-γ) produced by JKCD69 cells but not in JKwt cells after activation (Figure 3A). Because of the role of CD69 in effector T-cell differentiation,[16] we evaluated human T-cell differentiation to effector phenotypes. Challenge of human CD4^{+} T cells with oxLDL diminished the percentage of IL-17^{+} and IFN-γ^{+} cells generated in response to Th17- or Th1-polarizing stimuli (Figure 3B and 3C) and favored Treg differentiation (Figure 3D). This effect was dependent on CD69, as demonstrated by the blockade with anti-CD69 antibodies (Figure 3B through 3D).

The NR4A orphan nuclear receptors have emerged as key regulators of the immune response, controlling the magnitude of the inflammatory processes; *NR4A1* and *NR4A3* are crucial for Treg cell development.[23,24] We assessed whether oxLDL regulates the expression of NR4A nuclear receptors (*NR4A1* and *NR4A3*) in human CD4^{+} T cells. As shown in Figure 3E, oxLDL enhanced *NR4A1* and *NR4A3* mRNA expression in T-cell receptor–activated human primary CD4^{+} T cells. An early induction of *NR4A3* was also evoked by oxLDL in JKCD69 cells but not in JKwt cells (Figure 3F), which was blocked by preincubation with anti-CD69 antibodies (Figure 3G) or shRNA, confirming the CD69-dependent effect of oxLDL (Figure 3H).

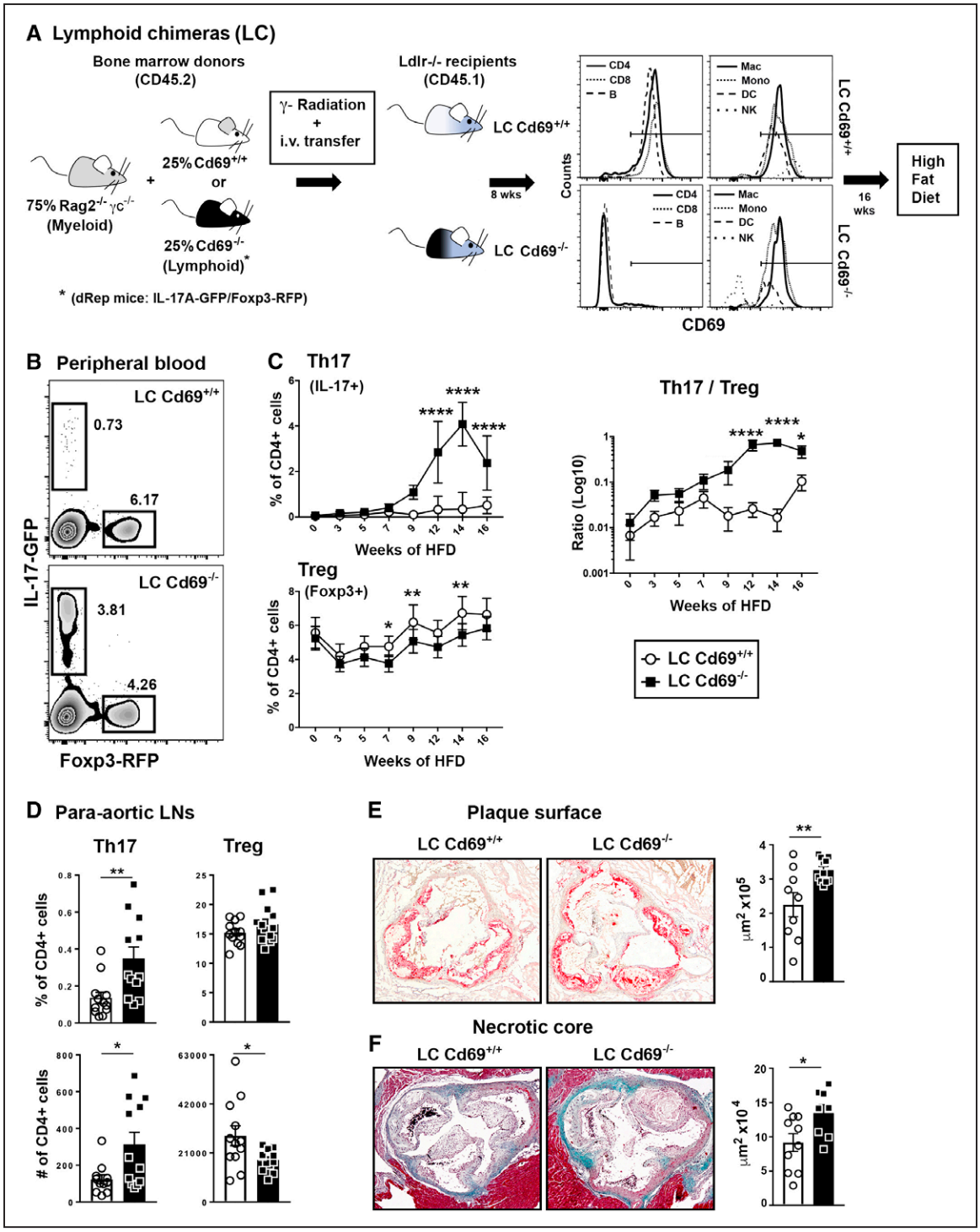

Figure 1. CD69 deficiency in lymphoid cells aggravates atherosclerosis.
A, Schematic illustrating the generation of lymphoid chimeras (LCs). Ldlr$^{-/-}$ (CD45.1^{+}) mice were lethally irradiated and reconstituted with mixed bone marrow (BM) from Rag2$^{-/-}$γc$^{-/-}$ plus BM from C57BL/6-Cd69$^{+/+}$ (LC *Cd69*$^{+/+}$) or C57BL/6-Cd69$^{-/-}$ (LC *Cd69*$^{-/-}$) (double-reporter [dRep]; interleukin [IL]-17–green fluorescent protein [GFP]$^{+}$/Foxp3–monomeric red fluorescent protein [RFP]$^{+}$) mice at a 3:1 ratio, respectively. Reconstitution of the lymphoid and myeloid compartments of CD45.2^{+} cells was assessed by fluorescence-activated cell sorting. Peripheral blood mononuclear cells (PBMCs) after 8 weeks of reconstitution were >90% CD45.2^{+}. Histograms show CD69 expression on CD4 and CD8 T cells, B cells (B), macrophages (Mac), monocytes (Mono), dendritic cells (DCs), and natural killer cells (NKs). PBMCs were stimulated overnight with anti–CD3/CD28 for lymphoid cells and lipopolysaccharide for myeloid cells of the indicated groups. **B**, Flow cytometry analysis of IL-17–GFP^{+} and Foxp3-RFP^{+} CD4 T cells in peripheral blood of LC CD69$^{+/+}$ and LC CD69$^{-/-}$ mice after 14 weeks of a high fat diet (HFD). **C**, Percentage of Th17 (IL-17–GFP^{+}), regulatory T (Treg; Foxp3-RFP^{+}) CD4^{+} T cells, and Th17/Treg ratio in peripheral blood leukocytes of LC *Cd69*$^{+/+}$ and LC *Cd69*$^{-/-}$ mice at the indicated time points after HFD initiation. n=15 mice per group (pooled from 3 independent experiments; error bars show SEM). *P* values were calculated by 2-way repeated-measures ANOVA (Sidak post hoc test). **P*<0.05. ***P*<0.01. **** *P*<0.0001. **D**, Percentage and absolute numbers of IL-17–GFP^{+}, Foxp3-RFP^{+} CD4 T cells in para-aortic lymph nodes (LN). n=12 mice per group. **E**. Oil Red O staining and quantification of plaque and necrotic core surface in aortic valves from LC *Cd69*$^{+/+}$ and LC *Cd69*$^{-/-}$ mice after 16 weeks of HFD. n= 8 mice/group. **F**, As in **E**, Masson trichrome staining and fibrosis quantification. n=7 mice per group Original magnification ×4. In **D** through **F**, error bars show SEM. **P*<0.05, ***P*<0.01 as determined by unpaired *t* test or Mann-Whitney *U* test.

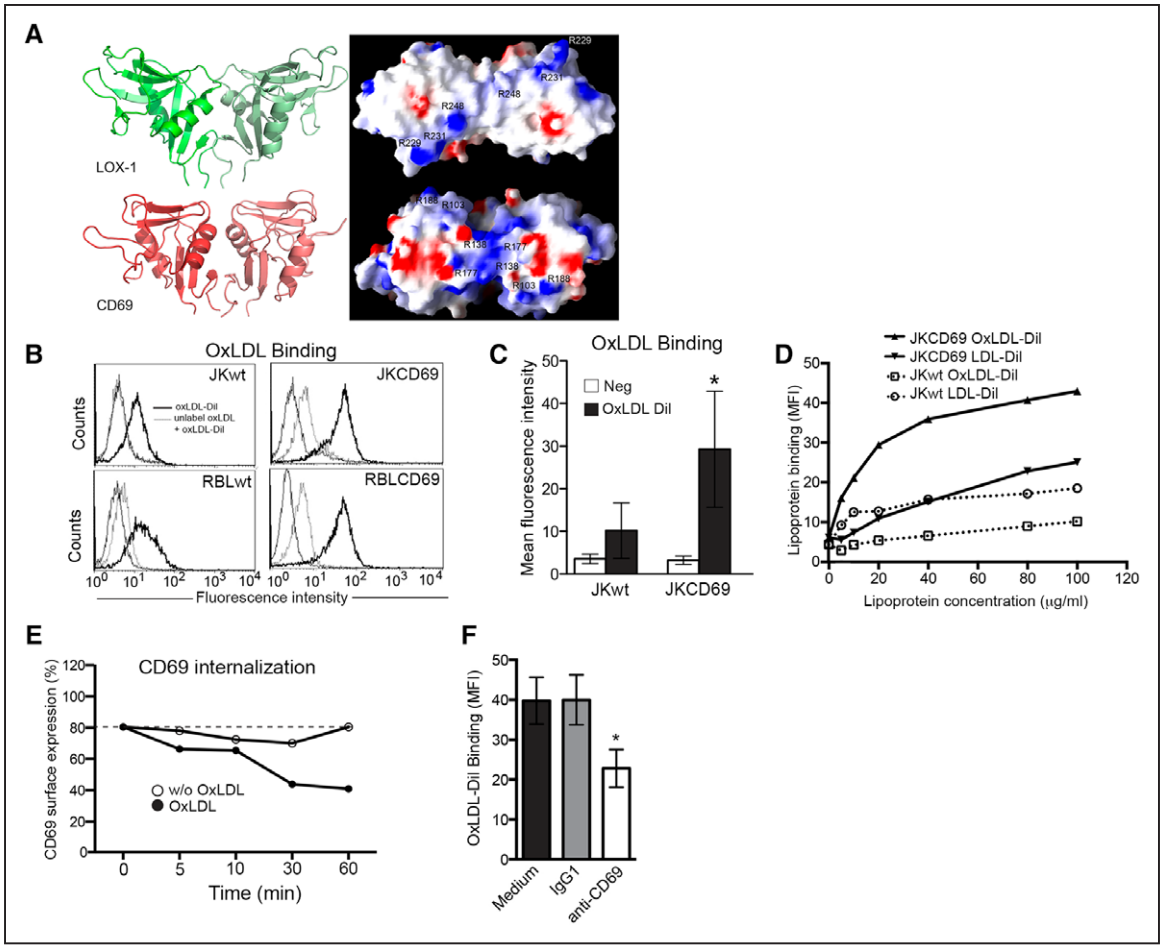

Figure 2. CD69 binding to oxidized low-density lipoprotein (oxLDL).
A, The LOX-1 and CD69 dimeric structures and their ligand-binding surfaces. Ribbon representations of the LOX-1 (Protein Data Bank code 1YXK) and CD69 (Protein Data Bank code 1E8i) C-type lectin-like domain (CTLD) structures (**left**; side views, prepared with PyMOL). Top views of the dimers with their surface charge distributions are shown on the **right** (prepared with GRASP). Arginine residues that form a basic "spine" across the dimer surface are labeled. **B**, Histograms show the binding of DiI-labeled oxLDL (solid line) to Jurkat T cells stably expressing CD69 (JKCD69) or rat basophilic leukemia cells (RBLCD69). Dotted line indicates the displacement of DiI-OxLDL by unlabeled lipoprotein. **C**, OxLDL binding to untransfected Jurkat T (JKwt) and JKCD69 cells (mean±SD from 10 independent experiments). *P<0.05 by Mann Whitney U test in both cell lines. **D**, Dose-response curves of oxLDL and native low-density lipoprotein (LDL) binding to JKwt and JKCD69 cells. **E**, CD69 internalization induced by oxLDL. JKCD69 cells were incubated with unlabeled oxLDL, and membrane-surface CD69 expression was analyzed by flow cytometry at the indicated times. Graph is representative of 1 of 3 experiments. **F**, Anti-CD69 antibodies inhibit the binding of oxLDL to JKCD69 cells (mean±SD from 4 experiments; *P<0.05). IgG1 indicates immunoglobulin G1; and MFI, mean fluorescence intensity.

In the in vivo model of atherosclerosis, the reporter GFP$^+$ Th17 cells and oxLDL localized closely at the atheroma plaque. Moreover, CD3$^+$ T cells and oxLDL colocalized at atheroma plaque (Figure VIA and VIB in the online-only Data Supplement). *NR4A1* and *NR4A3* mRNA expression was decreased in para-aortic LNs from BM *Cd69*$^{-/-}$ mice after 13 weeks of HFD (Figure 3I). Moreover, PBL expression of CD69 and *NR4A1* transcripts gradually declined in *ldlr*$^{-/-}$ mice during HFD administration (Figure 3J), indicating that these receptors are dynamically regulated in PBLs under these conditions.

CD69 Expression Is an Early Predictor of Subclinical Atherosclerosis

The PESA study is a prospective study that uses advanced imaging techniques to assess the presence of atheroma plaque in the main arteries of healthy individuals. Having observed a significant downregulation of CD69 as plaque formation progressed in mice, we compared CD69 and NR4A1 mRNA expression in PBLs from PESA participants with focal (1 affected site, n=55) or generalized (4–6 affected sites, n=128) subclinical atherosclerosis with that of PESA participants without any evidence of subclinical atherosclerosis (n=122; Table I in the online-only Data Supplement). The extent of subclinical atherosclerosis was assessed with advanced imaging techniques.[25] There is a gradient in CD69 expression across atherosclerosis extension stages; that is, CD69 expression decreases as disease progresses (trend test, P=0.006; Figure 4A). The same is true for NR4A1 (trend test, P=0.003; Figure 4A). These differences were particularly significant for the generalized subclinical disease group (Figure 4B and 4C). Thus, we focused on

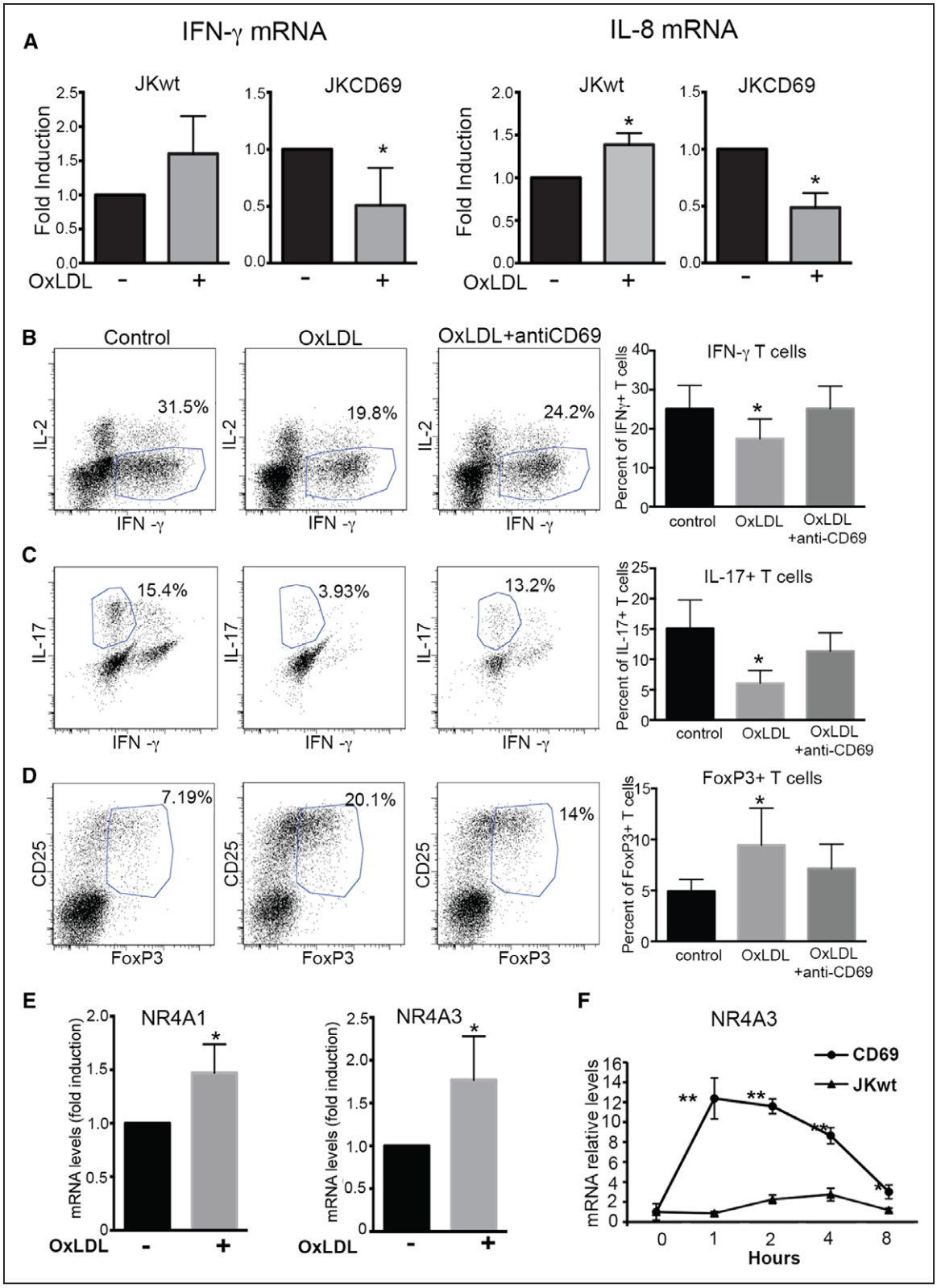

Figure 3. Oxidized low-density lipoprotein (OxLDL) binding to CD69 regulates the expression of NR4A receptors and cytokines in T cells.
A, OxLDL effect on phorbol 12-myristate 13-acetate/ionomycin-induced expression of interferon-γ(IFN-γ) and interleukin (IL)-8 in untransfected Jurkat T (JKwt) and Jurkat T cells stably expressing CD69 (JKCD69) cells. Data correspond to fold induction of mRNA levels (IFN-γ, n=6; IL-8, n=4) analyzed with the Wilcoxon signed-rank test. *P<0.05. **B** through **D**, Binding of oxLDL to CD69 blocks Th1 and Th17 differentiation and promotes regulatory T (Treg) cells. Human CD4⁺ T-cell differentiation was carried out in the absence (control) or presence of oxLDL (50 μg/mL) or oxLDL+anti-CD69. After corresponding days of culture, the percent of IFN-γ⁺ T cells (**B**), percent of IL-17⁺ T cells (**C**), and percent of CD25⁺Foxp3⁺ T cells (**D**) were determined by flow cytometry. Data correspond to 4 independent experiments, and bars represent mean±SEM of percent of positive cells. Data were analyzed with the Friedman test and Dunn posttest. *P<0.05 vs control. **E**, OxLDL induces NR4A1 and NR4A3 expression in activated human CD4⁺ T cells. Wilcoxon signed-rank test, *P<0.05 (n=4). **F**, Expression of NR4A3 in JKCD69 and JKwt cells treated (*Continued*)

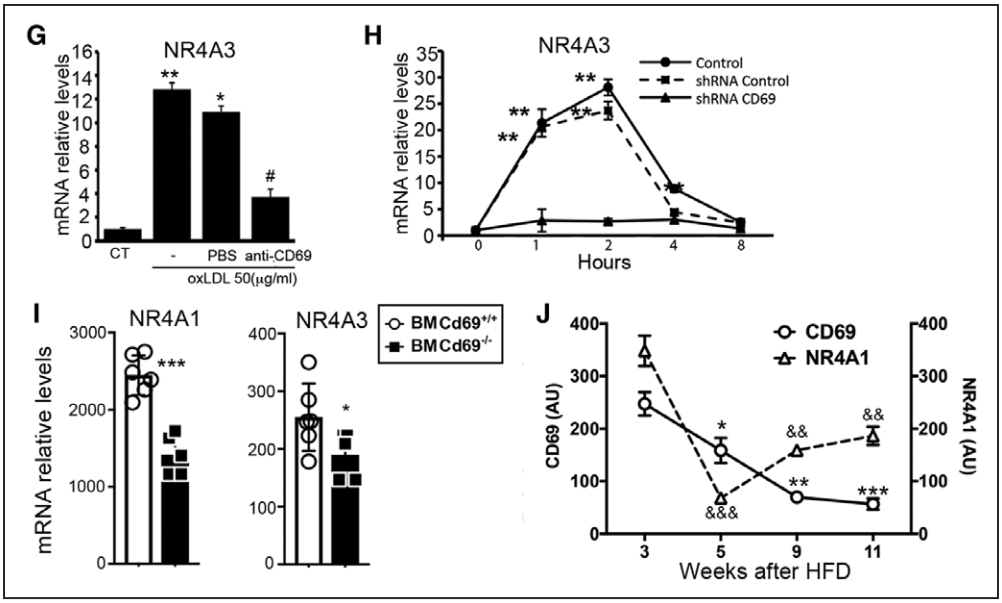

Figure 3 Continued. with oxLDL. Fold induction vs baseline (t=0). Data are mean±SD (n= 6) and were analyzed with 2-way ANOVA. ** *P*<0.0001, * *P*<0.01 vs JKwt at each time. **G**, Anti-CD69 inhibits oxLDL-induced NR4A3 expression in JKCD69 cells. Data are mean±SD (n= 6). Differences among groups were tested with the Kruskal-Wallis test. ***P*<0.001, **P*<0.01 vs control. #*P*<0.02 vs oxLDL. **H**, shRNA silencing of CD69 expression blocks oxLDL-induced NR4A3 expression in JKCD69 cells. Data are mean±SD (n= 6). Data were analyzed with 2-way ANOVA. ** *P*<0.0001 vs shRNA CD69. **I**, mRNA levels of the indicated nuclear receptors in para-aortic lymph nodes from total bone marrow (BM) chimeras at 13 weeks after a high fat diet (HFD). n=5 mice per group. Error bars show SEM. **P*<0.05, ****P*<0.001 as determined by unpaired *t* test. **J**, CD69 and NR4A1 mRNA relative expression in blood lymphocytes from *ldlr*$^{-/-}$ mice at different weeks after an HFD. Error bars show SEM. */&*P*<0.05, **/&&*P*<0.01, ***/&&&*P*<0.001 as determined by 1-way repeated-measures ANOVA. The Dunnett multiple-comparison test was performed between values at 5 to 11 weeks after an HFD vs 3 weeks after an HFD for CD69 (*) and NR4A1 (&) individually. AU indicates arbitrary units.

the control group (no disease) versus generalized disease group and examined whether CD69 can be used as independent marker for subclinical atherosclerosis. After a univariable logistic regression analysis (Table II in the online-only Data Supplement) of relevant variables (known cardiovascular risk factors: age, smoking, BMI, hypercholesterolemia, hypertension, diabetes mellitus, family history of cardiovascular disease; peripheral count of different subsets of leucocytes; expression of NR4A1 and the levels of oxLDL and C-reactive protein), a multivariable logistic regression analysis determined that CD69 expression remained an independent predictor of atherosclerosis at an early stage (odds ratio, 0.62; *P*=0.0056; Table). Furthermore, CD69 levels correlated significantly with NR4A1 levels (Figure 4D and Table III in the online-only Data Supplement), supporting the notion of a common regulation pathway.

DISCUSSION

Our findings indicate that the absence of CD69 in the LC results in larger atheroma plaque formation in *ldlr*$^{-/-}$ deficient mice subjected to an HFD. We identify the functional interaction between CD69 and oxLDL as the mechanism responsible for the observed phenotype. Our clinical data support this concept because CD69 expression in peripheral leucocytes of subjects with subclinical atherosclerosis is downregulated compared with individuals without atherosclerosis. This finding was in agreement with the experimental evidence showing a downregulation of CD69 expression on T lymphocytes in mice on exposure to HFD. Despite a suggested role for oxLDL in adaptive immune responses, a putative receptor on T lymphocytes has remained elusive.[32] Our study demonstrates that binding of oxLDL to CD69 in human T cells has a protective effect against the inflammatory response through the expression of NR4A nuclear receptors, downregulating proinflammatory cytokines and promoting Treg differentiation.

Although the classic view is that oxLDL induces the recruitment of inflammatory cells to the subendothelial space, cells and tissues also respond to oxLDL through the inhibition of proinflammatory signaling pathways.[33,34] The NR4A subfamily of human nuclear receptors (NR4A1 [Nur77], NR4A2 [Nurr1] and NR4A3 [NOR-1]) can be induced in endothelial and smooth muscle cells by a range of stimuli (including oxLDL), regulating the expression of different molecules involved in the immune response.[35] NR4A overexpression decreases the levels of IL-1β, IL-8, and monocyte chemoattractant protein-1 inflammatory cytokines. Furthermore, NR4A1 and NR4A3 have been implicated in Treg differentiation.[23,24] Our data show that binding of oxLDL to CD69 in human T cells induces the expression of NR4A receptors. Moreover, the absence of CD69 during atherosclerosis development results in a lower expression of NR4A1 and NR4A3 in both PBLs and para-aortic LNs. The observation of the regulatory effect of CD69/oxLDL interaction in human Treg differentiation, together with the loss of Treg responses

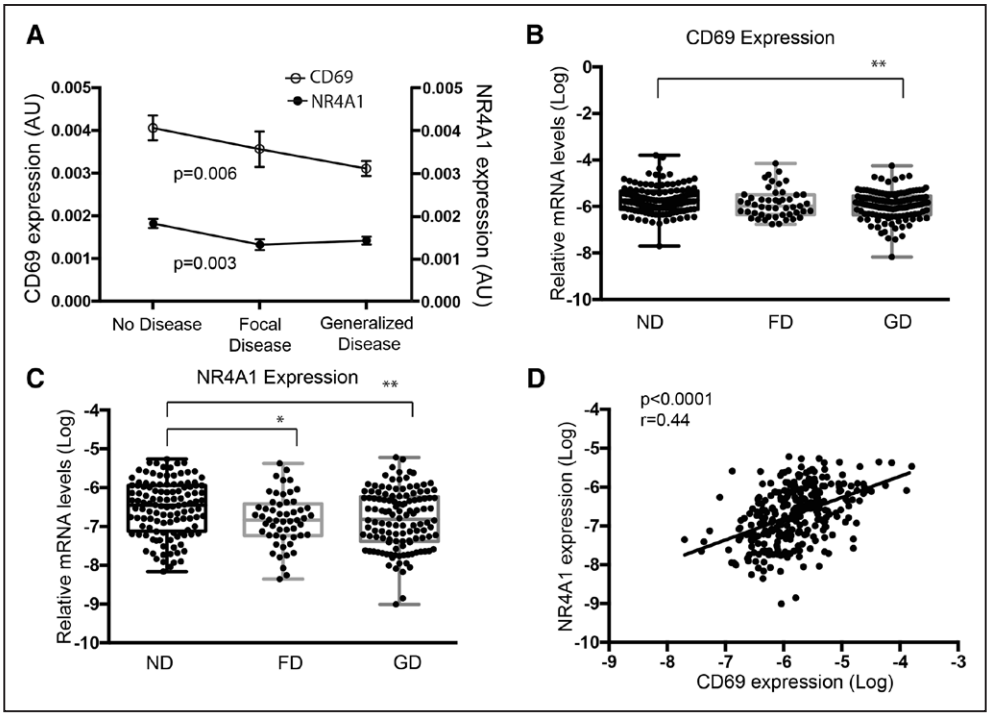

Figure 4. Individuals with subclinical atherosclerosis express low levels of CD69 and NR4A1.
A, mRNA expression of CD69 and NR4A1 is presented as mean±SEM in linear scale. Significance of the trend across groups was calculated with the Cuzick extension of the Wilcoxon rank-sum test to assess the significance of the trend across the 3 ordinal groups allowing for ties. **B**, mRNA levels of CD69 in peripheral blood leukocytes from healthy subjects (no disease [ND], n=122) and individuals with subclinical atherosclerosis (focal disease [FD], n=55; generalized disease [GD], n=128). **C**, mRNA levels of NR4A1 as in **B**. Data are expressed in log2 scale and were analyzed with 1-way ANOVA followed by Tukey posttests. * *P*<0.05. ***P*<0.005. **D**, Correlation between the expression of CD69 and NR4A1. The Pearson correlation test was used.

observed in lymphocyte CD69-deficient mice during atherosclerosis development, suggests that the modulation of NR4A nuclear receptors could participate in CD69 signaling/Treg differentiation. The more extensive atherosclerosis developed in the absence of CD69 could be associated, at least in part, with defects in Treg cell differentiation. Treg cells exert an atheroprotective function through the suppression of T-cell proliferation and secretion of anti-inflammatory cytokines and are protective during the initial phases of atherosclerosis not only by reducing atherosclerotic plaque formation but also by improving stabilization of the atherosclerotic lesions.[36–38]

Besides promoting Treg cell function, CD69 controls Th17 differentiation through the association of its cytoplasmic tail with the Jak3/Stat5 signaling pathway, regulating RAR-related orphan receptor-γ transcription and differentiation toward the Th17 lineage.[15] Recent evidence for the role of IL-17 in atherosclerosis has shed little light on the subject in both proatherogenic and antiatherogenic roles.[39,40] Under HFD, *ldlr*$^{-/-}$ mice deficient for CD69 in the LC developed exacerbated Th17 responses and more severe atherosclerotic lesions, supporting the role of IL-17 as a proatherogenic molecule. Despite previous reports supporting that IL-17 can either stabilize the plaque through collagen production or enhance the recruitment of proatherogenic cells through CXCL1 upregulation,[11,40] the former seems not to be the case in our model. Increased amounts of IL-17 seem to stabilize plaque formation when levels of IL-10 are also higher, namely in the presence of a proper

Table. Multivariable Logistic Regression Comparing Individuals With Generalized Subclinical Atherosclerosis and Individuals With No Disease

	Odds Ratio (95% CI)	*P* Value
log2(CD69)	0.62 (0.40–0.94)	0.0056
log2(NR4A1)	1.12 (0.80–1.58)	0.0441
Age	1.21 (1.11–1.33)	0.0000
Familial hypercholesterolemia	2.06 (0.90–4.87)	0.0630
Hypercholesterolemia	1.13 (0.58–2.22)	0.1168
Smoking	2.16 (1.00–4.87)	0.0027
Monocytes	0.06 (0.00–1.61)	0.4733
Lymphocytes	1.57 (0.66 –3.82)	0.0025
Leukocytes	1.61 (1.11–2.41)	0.0079
Diabetes mellitus*	Not applicable	0.0246
Oxidized low-density lipoprotein	1.02 (1.00–1.04)	0.0457

All covariates with a value of *P*<0.1 in the univariable analysis (Table II in the online-only Data Supplement) were considered.

**P* values were calculated with the likelihood ratio test to accommodate groups with 0 counts (diabetes mellitus), for which odds ratio estimates could not be calculated. Odds ratio and CIs were estimated with a generalized linear model.

regulatory response.[39] In our model, however, we have a concomitant increase of IL-17 and defective Treg development and function.

Previous results indicated that the regulatory action of CD69 during atherosclerosis was lost in *ApoE*$^{-/-}$ mice because, compared with the double-knockout group (*Cd69*$^{-/-}$*ApoE*$^{-/-}$), no significant difference was observed in plaque formation.[20] LDLr$^{-/-}$ and ApoE$^{-/-}$ mice have been extensively used to study the mechanisms of atherosclerosis development but feature important differences, for example, in plasma proteins. The major accumulating lipoprotein in the plasma of LDLr$^{-/-}$ mice fed a high-cholesterol diet is LDL. Conversely, ApoE$^{-/-}$ mice accumulate cholesterol mostly in the very-low-density lipoprotein and chylomicron fractions.[41,42] This is a very important issue to be considered that could account for the differences observed between CD69$^{-/-}$/apoE$^{-/-}$ and CD69$^{-/-}$/Ldlr$^{-/-}$ models. Our data show that oxLDL binding to CD69 exerts an immune-regulatory function during atherosclerosis development. In the ApoE knockout model, the levels of LDL may not have reached the threshold that is required for signaling through CD69. An additional difference that should be taken into consideration is that Ldlr$^{-/-}$ lesions have higher T-cell density than the ApoE model,[43] meaning that Ldlr$^{-/-}$ mice have more T cells that could express CD69 to exert their function. Finally, ApoE$^{-/-}$ mice on an HFD develop plaques more rapidly and exhibit larger aortic lesions with larger necrotic cores than Ldldr$^{-/-}$ mice[41,42]; therefore, this high-intensity model could be masking the differences between the CD69-expressing and CD69-deficient animals. We found a significant decrease in the blood lipid profile of free fatty acids, triglycerides, high-density lipoprotein, LDL, and cholesterol in the *Cd69*$^{-/-}$ lymphoid chimeras. This "dissociation" of the immune profile of the organism from the metabolic parameters is quite intriguing; it seems to occur via mechanisms related mainly to the adaptive immune responses (in this case, lack of CD69 and Th17 propensity). Our data pave the way for further research on mechanisms that could contribute to atherogenesis.

Our results describe for the first time an oxLDL receptor on lymphocytes with an important function in the regulation of the adaptive immune response and atheroma plaque formation during an HFD. The chimeric *ldlr*$^{-/-}$ mouse models used shed light on the role of CD69/oxLDL functional interaction in lymphocytes and on the maintenance of immune homeostasis to protect medium and large arteries from severe atheroma plaque formation over time. Further studies of the new regulatory oxLDL/CD69 pair in human lymphoid cells during atherosclerotic disease progression will provide novel insight into targeting these pathways for the prognosis/treatment of cardiovascular diseases.

Recent data emphasized the link between the inflammatory response and atherosclerotic risk in the clinical arena.[2] However, the complex interplay between lipid metabolism and immune responses remains to be fully disclosed. Collectively, our in vivo data strongly indicate an important role for CD69 expression on lymphocytes during atherosclerosis development. To validate this new paradigm in humans, we assessed the expression of CD69 and NR4A in PBLs from a cohort of subjects with thoroughly characterized subclinical atherosclerosis. It is important to point out that all PESA participants included in the study were asymptomatic and free of events. The profile of CD69 expression detected in human samples was very similar to that observed in the in vivo model. If we consider focal disease and generalized disease as different stages with the same pathology, our data indicate that expression of CD69 gradually declines as disease progresses. Hence, we focused on the generalized disease group, which is still preclinical, to assess the association of the expression of CD69 with subclinical atherosclerosis, accounting for the effect of traditional risk factors, peripheral counts of different subsets of leucocytes, expression of NR4A1, and levels of oxLDL. The proof of clinical study more closely resembling the animal experiments was to compare subjects free of disease or no disease versus those with established but yet subclinical atherosclerosis or generalized subclinical disease. CD69 remained significantly associated with the extent of the disease after adjustment for risk factors. This finding underscores the putative role of CD69 as a potential marker for the detection of atherosclerosis at a preclinical stage.

The fact that atherosclerosis presence is well identified in a context different from acute conditions (eg, myocardial infarction) supports the causative role of CD69 expression on atherosclerosis development rather than a consequence of an acute event.

ARTICLE INFORMATION

Received February 13, 2018; accepted July 20, 2018.

The online-only Data Supplement is available with this article at https://www.ahajournals.org/doi/suppl/10.1161/circulationaha.118.034326.

Correspondence

Francisco Sánchez-Madrid, PhD, Immunology Department, Hospital Universitario de la Princesa, Diego de León 62, 28006 Madrid, Spain, or Pilar Martin, Vascular Pathophysiology Area, Centro Nacional de Investigaciones Cardiovasculares, Melchor Fernández Almagro 3, 28029 Madrid, Spain. Email fsmadrid@salud.madrid.org or pmartinf@cnic.es

Affiliations

Vascular Pathophysiology Area (K.T., M.R., R.S.-D., V.F., P.M., F.S.-M.), Bioinformatics Unit (F.S.-C.), Genomics Unit (A.D.), Proteomics Unit (J.V.), and Myocardial Pathophysiology Area (B.I.), Centro Nacional de Investigaciones Cardiovasculares Carlos III, Madrid, Spain. Department of Immunology (H.d.L.F., J.L.A.-L., A.V., F.S.-M.) and Department of Cardiology (F.A.), Instituto de Investigación Sanitaria Hospital de la Princesa, IIS-IP, Madrid, Spain. Instituto de Investigacio-

nes Biomédicas de Barcelona, IIB-Sant Pau, Spain (J.M.-G.). Institut de Recerca del Hospital de la Santa Creu i Sant Pau-Programa ICCC, IIB-Sant Pau, Barcelona, Spain (C.R., J.C.). Centro Nacional de Biotecnología, Madrid, Spain (J.M.C.). IIS-Fundación Jiménez Díaz University Hospital, Madrid, Spain (B.I.). Cardiovascular Institute, Icahn School of Medicine at Mount Sinai, New York, NY (V.F.). CIBER de Enfermedades Cardiovasculares, Madrid, Spain (H.d.L.F., R.S.-D., C.R., J.V., B.I., J.M.-G, P.M., F.S.-M.).

Acknowledgments

The authors are grateful to Irene García Fernández for technical assistance and Belén Oliva for statistical support. The authors thank the group of Prof Almudena Ramiro for constructive comments and technology transfer. Finally, they thank Dr Richard Flavell for the dRep mice and Dr Miguel Vicente-Manzanares for critical reading and editing of the manuscript.

Sources of Funding

Funding was provided by the Spanish Ministry of Economy and Competitiveness: Plan Nacional de Salud SAF2017-82886-R to Dr Sánchez-Madrid, SAF2015-64767-R to Dr Martínez-González; Instituto de Salud Carlos III (AES 2016): PI16/01956 to Dr Martin, Centro de Investigación Biomédica en Red de Enfermedades Cardiovasculares; European Research Council, ERC-2011-AdG294340-GENTRIS to Dr Sánchez-Madrid; Proyecto Integrado de Excelencia PIE13/041 and Fundació La Marató TV3 (20152330 31); and Comunidad Autónoma de Madrid CAM (S2017/BMD-3671) to Drs Martin and Sánchez-Madrid. Dr Tsilingiri is cofunded by the European Union Marie Curie Program. M. Relaño is supported by a Contratos Predoctorales Severo Ochoa para la formación de doctores (BES-2015–072625) from the Spanish Ministry of Economy and Competitiveness. This research has been cofinanced by Fondo Europeo de Desarrollo Regional. Centro Nacional de Investigaciones Cardiovasculares (CNIC), Madrid, Spain, is supported by the Ministerio de Ciencia, Innovación y Universidades, and the Pro CNIC Foundation and is a Severo Ochoa Center of Excellence (SEV-2015-0505). The PESA study is cofunded equally by the Pro CNIC Foundation and Banco Santander, Madrid, Spain.

Disclosures

None.

REFERENCES

1. Libby P. Interleukin-1 beta as a target for atherosclerosis therapy: biological basis of CANTOS and beyond. *J Am Coll Cardiol*. 2017;70:2278–2289. doi: 10.1016/j.jacc.2017.09.028
2. Ridker PM, Everett BM, Thuren T, MacFadyen JG, Chang WH, Ballantyne C, Fonseca F, Nicolau J, Koenig W, Anker SD, Kastelein JJP, Cornel JH, Pais P, Pella D, Genest J, Cifkova R, Lorenzatti A, Forster T, Kobalava Z, Vida-Simiti L, Flather M, Shimokawa H, Ogawa H, Dellborg M, Rossi PRF, Troquay RPT, Libby P, Glynn RJ; CANTOS Trial Group. Antiinflammatory therapy with canakinumab for atherosclerotic disease. *N Engl J Med*. 2017;377:1119–1131. doi: 10.1056/NEJMoa1707914
3. Lim H, Kim YU, Sun H, Lee JH, Reynolds JM, Hanabuchi S, Wu H, Teng BB, Chung Y. Proatherogenic conditions promote autoimmune T helper 17 cell responses in vivo. *Immunity*. 2014;40:153–165. doi: 10.1016/j.immuni.2013.11.021
4. Frangogiannis NG. The inflammatory response in myocardial injury, repair, and remodelling. *Nat Rev Cardiol*. 2014;11:255–265. doi: 10.1038/nrcardio.2014.28
5. Ait-Oufella H, Salomon BL, Potteaux S, Robertson AK, Gourdy P, Zoll J, Merval R, Esposito B, Cohen JL, Fisson S, Flavell RA, Hansson GK, Klatzmann D, Tedgui A, Mallat Z. Natural regulatory T cells control the development of atherosclerosis in mice. *Nat Med*. 2006;12:178–180. doi: 10.1038/nm1343
6. Dinh TN, Kyaw TS, Kanellakis P, To K, Tipping P, Toh BH, Bobik A, Agrotis A. Cytokine therapy with interleukin-2/anti-interleukin-2 monoclonal antibody complexes expands CD4+CD25+Foxp3+ regulatory T cells and attenuates development and progression of atherosclerosis. *Circulation*. 2012;126:1256–1266. doi: 10.1161/CIRCULATIONAHA.112.099044
7. Sasaki N, Yamashita T, Takeda M, Shinohara M, Nakajima K, Tawa H, Usui T, Hirata K. Oral anti-CD3 antibody treatment induces regulatory T cells and inhibits the development of atherosclerosis in mice. *Circulation*. 2009;120:1996–2005. doi: 10.1161/CIRCULATIONAHA.109.863431
8. Ge S, Hertel B, Koltsova EK, Sörensen-Zender I, Kielstein JT, Ley K, Haller H, von Vietinghoff S. Increased atherosclerotic lesion formation and vascular leukocyte accumulation in renal impairment are mediated by interleukin-17A. *Circ Res*. 2013;113:965–974. doi: 10.1161/CIRCRESAHA.113.301934
9. Smith E, Prasad KM, Butcher M, Dobrian A, Kolls JK, Ley K, Galkina E. Blockade of interleukin-17A results in reduced atherosclerosis in apolipoprotein E-deficient mice. *Circulation*. 2010;121:1746–1755. doi: 10.1161/CIRCULATIONAHA.109.924886
10. Taleb S, Romain M, Ramkhelawon B, Uyttenhove C, Pasterkamp G, Herbin O, Esposito B, Perez N, Yasukawa H, Van Snick J, Yoshimura A, Tedgui A, Mallat Z. Loss of SOCS3 expression in T cells reveals a regulatory role for interleukin-17 in atherosclerosis. *J Exp Med*. 2009;206:2067–2077. doi: 10.1084/jem.20090545
11. Danzaki K, Matsui Y, Ikesue M, Ohta D, Ito K, Kanayama M, Kurotaki D, Morimoto J, Iwakura Y, Yagita H, Tsutsui H, Uede T. Interleukin-17A deficiency accelerates unstable atherosclerotic plaque formation in apolipoprotein E-deficient mice. *Arterioscler Thromb Vasc Biol*. 2012;32:273–280. doi: 10.1161/ATVBAHA.111.229997
12. Potekhina AV, Pylaeva E, Provatorov S, Ruleva N, Masenko V, Noeva E, Krasnikova T, Arefieva T. Treg/Th17 balance in stable CAD patients with different stages of coronary atherosclerosis. *Atherosclerosis*. 2015;238:17–21. doi: 10.1016/j.atherosclerosis.2014.10.088
13. Li Q, Wang Y, Wang Y, Chen K, Zhou Q, Wei W, Wang Y. Treg/Th17 ratio acts as a novel indicator for acute coronary syndrome. *Cell Biochem Biophys*. 2014;70:1489–1498. doi: 10.1007/s12013-014-9993-5
14. Sanchez-Diaz R, Blanco-Dominguez R, Lasarte S, Tsilingiri K, Martin-Gayo E, Linillos-Pradillo B, de la Fuente H, Sanchez-Madrid F, Nakagawa R, Toribio ML, Martin P. Thymus-derived regulatory t cell development is regulated by C-type lectin-mediated Bic/microRNA 155 expression. *Mol Cell Biol*. 2017;37: e00341–e00346.
15. Martín P, Gómez M, Lamana A, Cruz-Adalia A, Ramírez-Huesca M, Ursa MA, Yáñez-Mo M, Sánchez-Madrid F. CD69 association with Jak3/Stat5 proteins regulates Th17 cell differentiation. *Mol Cell Biol*. 2010;30:4877–4889. doi: 10.1128/MCB.00456-10
16. Cortés JR, Sánchez-Díaz R, Bovolenta ER, Barreiro O, Lasarte S, Matesanz-Marín A, Toribio ML, Sánchez-Madrid F, Martín P. Maintenance of immune tolerance by Foxp3+ regulatory T cells requires CD69 expression. *J Autoimmun*. 2014;55:51–62. doi: 10.1016/j.jaut.2014.05.007
17. Martín P, Gómez M, Lamana A, Matesanz Marín A, Cortés JR, Ramírez-Huesca M, Barreiro O, López-Romero P, Gutiérrez-Vázquez C, de la Fuente H, Cruz-Adalia A, Sánchez-Madrid F. The leukocyte activation antigen CD69 limits allergic asthma and skin contact hypersensitivity. *J Allergy Clin Immunol*. 2010;126:355–365, 365.e1. doi: 10.1016/j.jaci.2010.05.010
18. Cruz-Adalia A, Jiménez-Borreguero LJ, Ramírez-Huesca M, Chico-Calero I, Barreiro O, López-Conesa E, Fresno M, Sánchez-Madrid F, Martín P. CD69 limits the severity of cardiomyopathy after autoimmune myocarditis. *Circulation*. 2010;122:1396–1404. doi: 10.1161/CIRCULATIONAHA.110.952820
19. Sancho D, Gómez M, Viedma F, Esplugues E, Gordón-Alonso M, García-López MA, de la Fuente H, Martínez-A C, Lauzurica P, Sánchez-Madrid F. CD69 downregulates autoimmune reactivity through active transforming growth factor-beta production in collagen-induced arthritis. *J Clin Invest*. 2003;112:872–882. doi: 10.1172/JCI19112
20. Gómez M, Sanz-González SM, Abu Nabah YN, Lamana A, Sánchez-Madrid F, Andrés V. Atherosclerosis development in apolipoprotein E-null mice deficient for CD69. *Cardiovasc Res*. 2009;81:197–205. doi: 10.1093/cvr/cvn227
21. Witztum JL, Lichtman AH. The influence of innate and adaptive immune responses on atherosclerosis. *Annu Rev Pathol*. 2014;9:73–102. doi: 10.1146/annurev-pathol-020712-163936
22. Ricote M, Huang J, Fajas L, Li A, Welch J, Najib J, Witztum JL, Auwerx J, Palinski W, Glass CK. Expression of the peroxisome proliferator-activated receptor gamma (PPARgamma) in human atherosclerosis and regulation in macrophages by colony stimulating factors and oxidized low density lipoprotein. *Proc Natl Acad Sci USA*. 1998;95:7614–7619.
23. Sekiya T, Kashiwagi I, Yoshida R, Fukaya T, Morita R, Kimura A, Ichinose H, Metzger D, Chambon P, Yoshimura A. Nr4a receptors are essential for thymic regulatory T cell development and immune homeostasis. *Nat Immunol*. 2013;14:230–237. doi: 10.1038/ni.2520
24. Calvayrac O, Rodríguez-Calvo R, Martí-Pamies I, Alonso J, Ferrán B, Aguiló S, Crespo J, Rodríguez-Sinovas A, Rodríguez C, Martínez-González J. NOR-1 modulates the inflammatory response of vascular smooth muscle cells by preventing NFκB activation. *J Mol Cell Cardiol*. 2015;80:34–44. doi: 10.1016/j.yjmcc.2014.12.015

25. Fernández-Friera L, Peñalvo JL, Fernández-Ortiz A, Ibañez B, López-Melgar B, Laclaustra M, Oliva B, Mocoroa A, Mendiguren J, Martínez de Vega V, García L, Molina J, Sánchez-González J, Guzmán G, Alonso-Farto JC, Guallar E, Civeira F, Sillesen H, Pocock S, Ordovás JM, Sanz G, Jiménez-Borreguero LJ, Fuster V. Prevalence, vascular distribution, and multiterritorial extent of subclinical atherosclerosis in a middle-aged cohort: the PESA (Progression of Early Subclinical Atherosclerosis) Study. *Circulation*. 2015;131:2104–2113. doi: 10.1161/CIRCULATIONAHA.114.014310
26. Esplugues E, Huber S, Gagliani N, Hauser AE, Town T, Wan YY, O'Connor W Jr, Rongvaux A, Van Rooijen N, Haberman AM, Iwakura Y, Kuchroo VK, Kolls JK, Bluestone JA, Herold KC, Flavell RA. Control of TH17 cells occurs in the small intestine. *Nature*. 2011;475:514–518. doi: 10.1038/nature10228
27. Shinoda K, Tokoyoda K, Hanazawa A, Hayashizaki K, Zehentmeier S, Hosokawa H, Iwamura C, Koseki H, Tumes DJ, Radbruch A, Nakayama T. Type II membrane protein CD69 regulates the formation of resting T-helper memory. *Proc Natl Acad Sci USA*. 2012;109:7409–7414. doi: 10.1073/pnas.1118539109
28. Çimen I, Kocatürk B, Koyuncu S, Tufanlı Ö, Onat UI, Yıldırım AD, Apaydın O, Demirsoy Ş, Aykut ZG, Nguyen UT, Watkins SM, Hotamışlıgil GS, Erbay E. Prevention of atherosclerosis by bioactive palmitoleate through suppression of organelle stress and inflammasome activation. *Sci Transl Med*. 2016;8:358ra126. doi: 10.1126/scitranslmed.aaf9087
29. Warnatsch A, Ioannou M, Wang Q, Papayannopoulos V. Inflammation. Neutrophil extracellular traps license macrophages for cytokine production in atherosclerosis. *Science*. 2015;349:316–320. doi: 10.1126/science.aaa8064
30. Ohki I, Ishigaki T, Oyama T, Matsunaga S, Xie Q, Ohnishi-Kameyama M, Murata T, Tsuchiya D, Machida S, Morikawa K, Tate S. Crystal structure of human lectin-like, oxidized low-density lipoprotein receptor 1 ligand binding domain and its ligand recognition mode to OxLDL. *Structure*. 2005;13:905–917. doi: 10.1016/j.str.2005.03.016
31. Llera AS, Viedma F, Sánchez-Madrid F, Tormo J. Crystal structure of the C-type lectin-like domain from the human hematopoietic cell receptor CD69. *J Biol Chem*. 2001;276:7312–7319. doi: 10.1074/jbc.M008573200
32. van Bruggen N, Ouyang W. Th17 cells at the crossroads of autoimmunity, inflammation, and atherosclerosis. *Immunity*. 2014;40:10–12. doi: 10.1016/j.immuni.2013.12.006
33. Bochkov VN, Leitinger N. Anti-inflammatory properties of lipid oxidation products. *J Mol Med (Berl)*. 2003;81:613–626. doi: 10.1007/s00109-003-0467-2
34. Wigren M, Bengtsson D, Dunér P, Olofsson K, Björkbacka H, Bengtsson E, Fredrikson GN, Nilsson J. Atheroprotective effects of Alum are associated with capture of oxidized LDL antigens and activation of regulatory T cells. *Circ Res*. 2009;104:e62–e70. doi: 10.1161/CIRCRESAHA.109.196667
35. Hamers AA, Hanna RN, Nowyhed H, Hedrick CC, de Vries CJ. NR4A nuclear receptors in immunity and atherosclerosis. *Curr Opin Lipidol*. 2013;24:381–385. doi: 10.1097/MOL.0b013e3283643eac
36. Butcher MJ, Filipowicz AR, Waseem TC, McGary CM, Crow KJ, Magilnick N, Boldin M, Lundberg PS, Galkina EV. Atherosclerosis-driven Treg plasticity results in formation of a dysfunctional subset of plastic IFNγ+ Th1/Tregs. *Circ Res*. 2016;119:1190–1203. doi: 10.1161/CIRCRESAHA.116.309764
37. Mallat Z, Ait-Oufella H, Tedgui A. Regulatory T-cell immunity in atherosclerosis. *Trends Cardiovasc Med*. 2007;17:113–118. doi: 10.1016/j.tcm.2007.03.001
38. Foks AC, Frodermann V, ter Borg M, Habets KL, Bot I, Zhao Y, van Eck M, van Berkel TJ, Kuiper J, van Puijvelde GH. Differential effects of regulatory T cells on the initiation and regression of atherosclerosis. *Atherosclerosis*. 2011;218:53–60. doi: 10.1016/j.atherosclerosis.2011.04.029
39. Gisterå A, Robertson AK, Andersson J, Ketelhuth DF, Ovchinnikova O, Nilsson SK, Lundberg AM, Li MO, Flavell RA, Hansson GK. Transforming growth factor-β signaling in T cells promotes stabilization of atherosclerotic plaques through an interleukin-17-dependent pathway. *Sci Transl Med*. 2013;5:196ra100. doi: 10.1126/scitranslmed.3006133
40. Erbel C, Akhavanpoor M, Okuyucu D, Wangler S, Dietz A, Zhao L, Stellos K, Little KM, Lasitschka F, Doesch A, Hakimi M, Dengler TJ, Giese T, Blessing E, Katus HA, Gleissner CA. IL-17A influences essential functions of the monocyte/macrophage lineage and is involved in advanced murine and human atherosclerosis. *J Immunol*. 2014;193:4344–4355. doi: 10.4049/jimmunol.1400181
41. Getz GS, Reardon CA. Do the Apoe-/- and Ldlr-/- mice yield the same insight on atherogenesis? *Arterioscler Thromb Vasc Biol*. 2016;36:1734–1741. doi: 10.1161/ATVBAHA.116.306874
42. Emini Veseli B, Perrotta P, De Meyer GRA, Roth L, Van der Donckt C, Martinet W, De Meyer GRY. Animal models of atherosclerosis. *Eur J Pharmacol*. 2017;816:3–13. doi: 10.1016/j.ejphar.2017.05.010
43. Roselaar SE, Kakkanathu PX, Daugherty A. Lymphocyte populations in atherosclerotic lesions of apoE -/- and LDL receptor -/- mice: decreasing density with disease progression. *Arterioscler Thromb Vasc Biol*. 1996;16:1013–1018.

SUPPLEMENTAL MATERIAL.

Mice and atherosclerosis induction.

To evaluate the influence of immune cell CD69 expression on atherosclerosis development, 5 week old male Ldlr-/- CD45.1$^+$ mice were irradiated and reconstituted with bone marrow from *cd69*$^{-/-}$ double reporter for Foxp3-mRFP and IL-17A-eGFP[24] (*Cd69*$^{-/-}$*dRep)* mice or WT littermates (*Cd69*$^{+/+}$*dRep*), both CD45.2$^+$. In addition, we generated mixed bone marrow chimeras proficient or deficient for CD69 only in the myeloid or lymphoid compartment; *ldlr*$^{-/-}$ CD45.1$^+$ mice were reconstituted with a mix of 75% CD45.2$^+$ *Rag2*$^{-/-}$*γc*$^{-/-}$ BM plus 25% of either *dRep* or *cd69*$^{-/-}$*dRep* BM (hereafter: LC *Cd69*$^{+/+}$ and LC *Cd69*$^{-/-}$ respectively). After 6 weeks, mice were deemed to be fully reconstituted by phenotyping blood from the tail vein after surface staining with anti-CD45.1 and –CD45.2 antibodies and FACS analysis and were started on a high fat diet (SSNIFF, S9167-E010). Mice were sacrificed at the indicated time points. All animal procedures were approved by the ethics committee of the Comunidad Autónoma de Madrid and conducted in accordance with the institutional guidelines that comply with the European Institutes of Health´s; Directive 2010/63/EU of the European Parliament and the Council on the Protection of Animals Used for Scientific Purposes (Official Journal of the European Union. Vol. 53:33-79, 2010).

Monitoring blood Th17, Treg cells and all leukocyte subsets.

To assess the immune response, blood from the tail vein was collected and peripheral blood leukocytes (PBLs) were purified by Ficoll (GE healthcare) gradient. Cells were stimulated in vitro with PMA and ionomycin in the presence

of brefeldin for 4 hours and stained with anti-CD4 APC antibody (BD pharmingen). The percentage of IL-17-eGFP+ or Foxp3-RFP+ cells in the CD4+ population was assessed using a Fortessa (BD Biosciences) flow cytometer, analyses were performed with the FlowJo software. A different group of mice was studied to analyze the kinetics of all leukocyte subsets in blood during high fat diet. PBLs were stimulated overnight with anti-CD3/CD28 for T cell activation or with LPS for the rest. Surface staining with anti-CD44/CD62L was performed to distinguish naïve and memory CD4+ T cells and B220 to stain B cells. Myeloid cells were analysed after surface staining with anti-CD11b, -CD11c, -Ly6G/C, -F4/80 and NK cells with anti–Nkp46. The expression of CD69 with anti-CD69 was analysed after stimulation in all the leukocyte subsets by FACS. At the endpoint of the experiment the same process was followed for cells from spleen, non-draining (axillary) lymph nodes and draining (para-aortic) lymph nodes.

LDL isolation, characterization and oxidation. LDL were isolated from pooled plasma of healthy blood volunteers. Plasma was centrifuged to remove chylomicrons, and LDL (d=1.019-1.063 g/mL) were isolated by potassium bromide density-gradient ultracentifugation (36,000 rpm [using a 50.2 Ti rotor, Beckman Coulter] for 18 h at 4 ºC). OxLDL were prepared by exposing native LDL (nLDL) to 10 μM $CuSO_4$ at 37 ºC. The degree of oxidation was monitored by fluorescent emission at 234 nm. Thiobarbituric acid-reactive substances (TBARS) content was used as an indirect evaluation of lipid peroxidation (nLDL<1.0 nmol malondialdehyde (MDA)/mg of LDL protein; oxLDL>20 nmol MDA/mg LDL protein). The absence of contamination by other lipoproteins was determined by electrophoresis on agarose gels (Paragon Electrophoresis system, Beckman). The content of protein (BCA protein assay) and cholesterol

(Cholesterol assay kit, RefLab) was determined by colorimetric assays. LDL were sterilized by filtration through a low protein-binding non-pyrogenic filter. Endotoxin contamination was discarded by the chromogenic Limulus amebocyte assay. Lipoproteins were stored under N2 at 4 ºC in the dark. Fluorescent labelling of the lipid moiety of lipoproteins was performed by incubating lipoproteins with DiI (1,1'-dioctadecyl-3,3,3',3'-tetramethylindo-carbocyanine perchlorate) at 37 ºC for 8 h. Labelled lipoproteins were re-floated by ultracentrifugation, dialyzed and sterilized.

Lipoprotein Binding and Internalization Assays. Binding and cell association of DiI-labeled lipoproteins to Jurkat (JKwt Vs JKCD69) and RBL-2H3 (RBLwt Vs RBLCD69) cells were performed by incubating $5x10^5$ cells with 10 μg/ml of DiI-labeled lipoprotein in culture medium supplemented with 10% (v/v) fetal bovine serum deprived of lipoproteins (LPDS) for 2h at 4ºC (binding) or 37ºC (cell association). After incubation, cells were washed in cold PBS and analyzed by fluorescence flow cytometry using a FACScalibur® cytofluorometer (Becton Dickinson, Mountain View, CA). For blocking assays, unlabeled-lipoprotein or purified antibodies (50 μg/ml) were pre-incubated for 30 min in incomplete medium supplemented with 10 % (v/v) LPDS. For internalization assays, Jurkat cells (JKwt and JKCD69) were incubated with unlabelled oxLDL (50 μg/ml) at different time points (10, 30, 60, 90, 120 and 240 minutes) in culture medium supplemented with 10% (v/v) LPDS and CD69 expression on membrane surface was analyzed by flow cytometry.

RT-PCR. Jurkat cells (JKwt and JKCD69) $1x10^6$/ml were incubated in the presence of PMA (50 μg/ml) and ionomycin (0.5 μg/ml) for 4 h, then cells were washed twice and incubated in the presence or absence of oxLDL (50 μg/ml)

during 2 h. Cells were then harvested and processed for RNA isolation. Total RNA was isolated with a QIAGEN RNeasy Kit (QIAGEN). Then 1μg/ml of total RNA was reverse transcripted into cDNA, PCR were performed using SYBR Green. Data were normalized using GAPDH expression. Data were analyzed using 2-ΔΔCt method. GADPH forward: 5'-GCC CAA TAC GAC CAA ATC C-3'; GAPDH reverse: 5' AGC CAC ATC GCT CAG ACA C3'. IL-8 forward: 5'-TCT GTG TGA AGG TGC AGT TTT G-3'; IL8 reverse: 5'-GGG GTG GAA AGG TTT GGA GT-3'. For the expression of NR4A nuclear receptors, Jurkat cells (JKwt and JKCD69) $1x10^6$ cell/ml were incubated with oxLDL (50μg/ml) at different time points. For blocking assays, cells were pre-incubated with anti-CD69 (20μg/ml) during 45 min. RT-PCR for human and mouse NR4A receptors was performed using Taqman assays (Applied Biosystems).

Human CD4+ T cell polarization. For human Th1, Th17 and Treg polarization, CD4+ T cells were purified by immunomagnetic depletion with the human CD4+ T Cell Isolation Kit II (Miltenyi Biotec, CA, USA) with a purity >96%. Th17 cells were polarized as described. For Th1 polarization CD4+ T cells (1 x 106), were incubated with IL-2 (20 U/ml) and IL-12 (20 ng/ml), while for Treg polarization cells were cultured with TGF-b (5 ng/ml) and IL-2 (20 U/ml) (all cytokines from R&D systems). After 5 days of culture, percentage of IFN-g and IL-2 producing cells (Th1) and Foxp3+ CD25+ cell (Treg) was analyzed in a FACS Canto Cytometer and analyzed with FlowJo software. Where indicated, oxLDL (50 ug/ml) and anti-CD69 (20 μg/ml) were added to the cultures.

Tissue processing and immunohistochemistry

For plaque area assessment, 5 μm thick sections at 100 μm intervals were collected starting at the origin of the aortic valve cusps. Sections were stained

with Oil Red O (ORO) staining, (Sigma-Aldrich) and hematoxylin, and lesion size was analyzed with ImageJ software. For Masson trichrome staining 7 μm thick sections at 100μm intervals were collected. Sections were stained with the Masson-Goldner staining kit (Merck). For specific staining, anti-F480 antibody was purchased from Abcam (ab6640) and anti-CD3 from Santa Cruz Biotechnology (sc-1127).

Supplementary Table 1: Demographic characteristics and cardiovascular risk factors.

	Total	No Atherosclerosis	Focal Disease	Generalized Disease	P-value
	(n=305)	(n=122)	(n=55)	(n=128)	
Age (years)	48,58 ± 3,9	46,66 ± 3,5	50,84 ± 2,2	49,46 ± 4	<0,001
Sex (men)	308 (100)	122 (100)	55 (100)	128 (100)	-
Family history of CVD	54 (17,5)	17 (13,9)	6 (10,9)	31 (24,2)	0,02
Smoking	84 (27,3)	24 (19,7)	10 (18,2)	49 (38,3)	<0,001
BMI (Kg/m2)	27,46 ± 3,3	27,46 ± 3,4	27,21 ± 3,4	27,52 ± 3,3	0,485
Weight (kg)	83,5 ± 12,1	84,19 ± 12,6	82,28 ± 11,2	83,02 ± 12,1	0,749
Height (cm)	174,2 ± 6,6	174,9 ± 7	173,9 ± 6,7	173,5 ± 5,9	0,095
Obesity	60 (19,5)	24 (19,7)	10 (18,2)	25 (19,5)	0,993
Hypertension	78 (25,3)	27 (22,1)	12 (21,8)	37 (28,9)	0,19
SBP (mmHg)	121,8 ± 12,5	121,1 ± 13,7	119,1 ± 10,9	123,7 ± 11,4	0,005
DBP (mmHg)	76,13 ± 9,1	75,3 ± 10,6	75,47 ± 8,6	77,18 ± 7,5	0,033
Diabetes	13 (4,2)	0 (0)	1 (1,8)	11 (8,6)	<0,001
Fasting glucose (mg/dL)	93 [87 - 100]	93 [87 - 97]	93 [88 - 99]	94 [87 - 103]	0,068
HbA1c (%)	5,5 [5,3 - 5,8]	5,5 [5,2 - 5,7]	5,4 [5,3 - 5,8]	5,5 [5,3 - 5,9]	0,004
Insulin (uU/mL)	6,2 [4,2 - 9,2]	5,9 [4,1 - 9,1]	6,4 [4,6 - 9,3]	6,35 [4,2 - 9,5]	0,887
Dyslipidemia	196 (63,6)	71 (58,2)	34 (61,8)	89 (69,5)	0,059
Total cholesterol (mg/dL)	202,1 ± 32,7	199,8 ± 28,9	200,5 ± 38,5	205,8 ± 33	0,151
LDL-C (mg/dL)	136,2 ± 27,8	135,1 ± 24,6	135,7 ± 32,8	138,2 ± 28,3	0,411
HDL-C (mg/dL)	42,79 ± 9,6	42,63 ± 9,3	44,11 ± 9,1	42,51 ± 9,9	0,71
Triglycerides (mg/dL)	97 [73 - 139]	91 [69 - 139]	89 [71 - 122]	106 [75 - 144]	0,017
Oxidized LDL-C(mg/dL)	54,13 ± 16,1	52,11 ± 13,9	52,35 ± 18,4	56,86 ± 16,8	0,027
Lipoprotein a (mg/dL)	16,6 [6,64 - 38,6]	12,4 [4,76 - 27,4]	15,4 [8,13 - 40]	20,6 [7,92 - 45,5]	0,016
Creatinine (mg/dL)	0,89 ± 0,1	0,91 ± 0,1	0,91 ± 0,1	0,86 ± 0,1	0,005
Cystatin C (mg/L)	0,78 ± 0,1	0,78 ± 0,1	0,79 ± 0,1	0,77 ± 0,1	0,226
Fibrinogen (mg/dL)	265,6 ± 45,2	256 ± 36,7	263,4 ± 45,2	274,5 ± 50,2	0,248
P-Selectin (ng/mL)	140,3 ± 43,3	136,8 ± 40,8	142,4 ± 39,2	142,3 ± 47	0,001
hs-CRP (mg/mL)	0,13 [0,07 - 0,22]	0,13 [0,06 - 0,20]	0,13 [0,08 - 0,21]	0,135 [0,07 - 0,124]	0,364
VCAM-1 (ng/mL)	620 [494,8 - 760,6]	620 [505 - 763]	672 [520,5 - 841,5]	612,8 [483,1 - 725,4]	0,277
PREDIMED	4,92 ± 1,42	4,83 ± 1,48	5,15 ± 1,33	4,90 ± 1,40	0,711
MVPA	51,48 ± 21,41	49,50 ± 18,83	57,25 ± 24,89	50,94 ± 21,90	0,632

Data are expressed as mean±SD, median and IQR or n (%). P-values are derived from Anova for log-transformed continuous variables and chi-square for categorical variables, except for those variables with n<6 for which Fisher Test was used. BMI: Body mass index. CVD: Cardiovascular Disease; SBP: Systolic blood pressure; DBP: Diastolic blood pressure; LDL-C: Low-density lipoprotein cholesterol; HDL-C: High-density lipoprotein cholesterol. MVPA: Moderate to Vigorous Physical Activity. In bold, variables included in the multivariable model.

Supplementary Table 2: Univariable logistic regression to compare individuals with “Generalized subclinical atherosclerosis” to individuals with “no disease”.

	OR (95% CI)	P Value
log2(CD69)	0.63(0.46-0.85)	0.0035
log2(NR4A1)	0.69(0.53-0.88)	0.0031
Age	1.21(1.13-1.31)	0.0000
FH	1.97(1.04-3.86)	0.0412
Smoking	2.53(1.44-4.54)	0.0014
Hypercholesterolemia	1.64(0.98-2.77)	0.0628
Hypertension	1.43(0.81-2.56)	0.2209
Diabetes*	NA	0.0001
BMI	1.01(0.93-1.08)	0.8928
Monocytes	11.57(1.61-89.99)	0.0168
Lymphocytes	3.08(1.8-5.5)	0.0001
Leukocytes	1.66(1.37-2.04)	0.0000
Neutrophils	1.91(1.47-2.55)	0.0000
oxLDL	1.02(1-1.04)	0.0170

*For diabetes, no OR could be estimated due to the lack of individuals with diabetes in the “No disease” group (see Supplementary Table 1). P-value for diabetes was estimated using the likelihood ratio test.

Supplementary Table 3. Correlation between the expression level of CD69 (log2 scaled) and a set of relevant molecular and clinical variables.

	Estimate*	P Value
log2(NR4A1)	0.36	0.0000
Age	0.00	0.9170
FH	-0.09	0.5190
Smoking	-0.28	0.0266
Hypercholesterolemia	-0.08	0.4930
Hypertension	0.00	0.9950
Diabetes	-0.35	0.1970
BMI	-0.02	0.3660
Monocytes	0.13	0.7720
Lymphocytes	0.16	0.1390
Leukocytes	-0.03	0.3950
Neutrophils	-0.09	0.0564
oxLDL	-0.01	0.0520
CRP	0.03	0.9190
FH10Y	-1.32	0.2650

* For continuous independent variables the *Estimate* represents the slope of the linear regression fit. For discrete independent variables the *Estimate* represents the difference in expression between the groups.

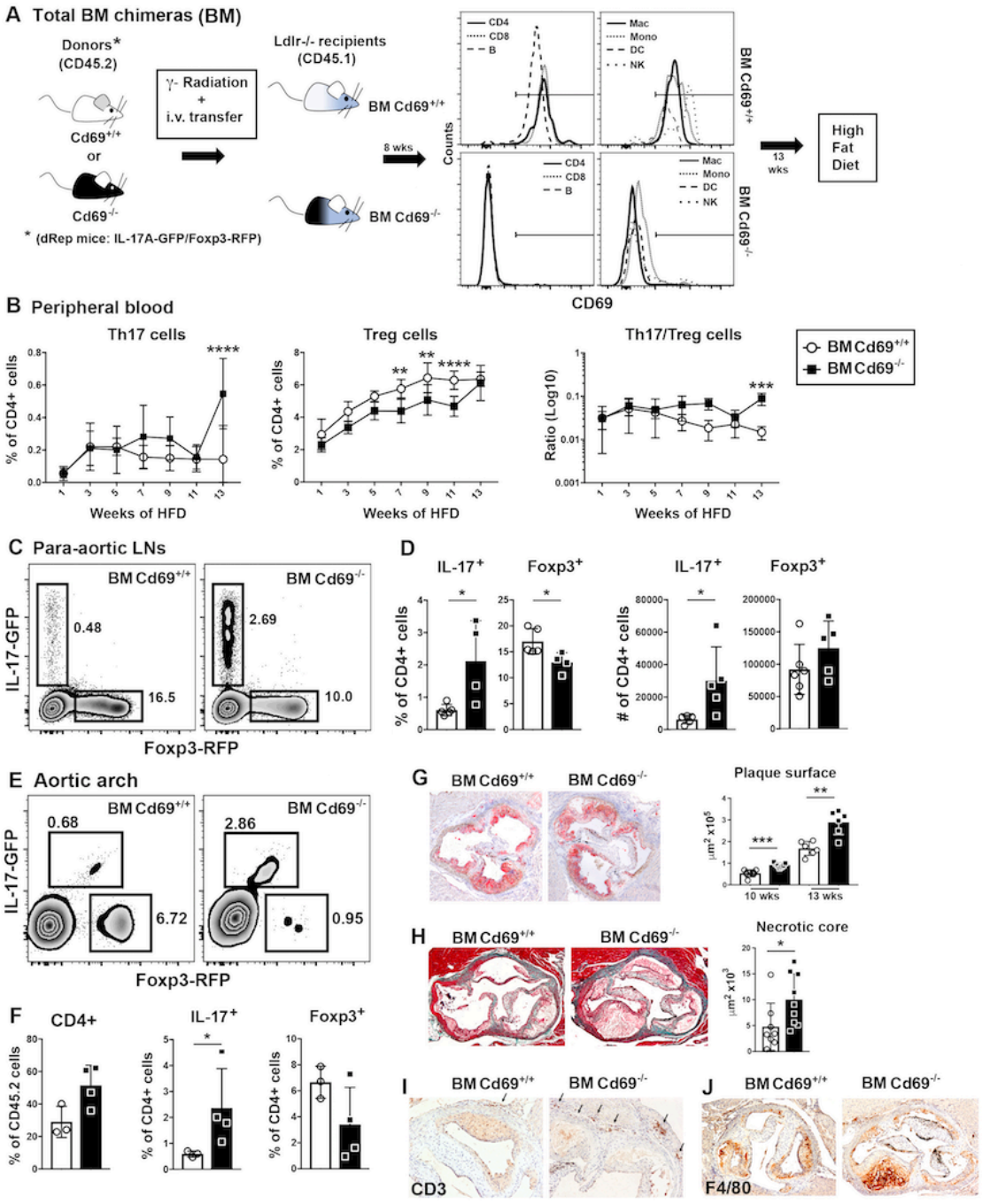

Supplementary Figure 1. CD69 regulates adaptive immune responses in HFD conditions. **A**. Ldlr-/- mice were lethally irradiated and reconstituted with bone marrow from C57BL/6 $Cd69^{+/+}$ or $Cd69^{-/-}$ dRep mice. Eight weeks after reconstitution PBMCs were > 90% $CD45.2^{+}$. Reconstitution of lymphoid and myeloid compartments of $CD45.2^{+}$ cells was assessed by FACS. Histograms show CD69 expression on CD4 and CD8 T cells, B cells (B), macrophages (Mac),

monocytes (Mono), dendritic cells (DC) and natural killer cells (NK). PBMCs were stimulated with anti-CD3/CD28 for lymphoid cells and LPS for myeloid cells, of the indicated groups. **B**. Percentage of Th17 (IL-17-GFP^{+}), Treg (Foxp3-RFP^{+}) CD4^{+} T cells and Th17/Treg ratio in peripheral blood leukocytes of BM Cd69$^{+/+}$ and BM Cd69$^{-/-}$ mice at the indicated time points after HFD initiation. Error bars show SEM, ***P* < 0.01, ****P* < 0.001, **** *P* < 0.0001. *P* values were calculated by 2-way repeated-measures ANOVA (Sidak´s *post hoc* test). **C**. Flow cytometry analysis of Th17 and Treg cells in para-aortic lymph nodes of BM Cd69$^{+/+}$ and BM Cd69$^{-/-}$ mice at 10 weeks after HFD administration, n=12 mice per group. **D**. Percentages and absolute numbers of Th17 and Treg cells from para-aortic lymph nodes of BM Cd69$^{+/+}$ and BM Cd69$^{-/-}$ mice 10 weeks after HFD administration, n=12 mice per group. Error bars show SEM, *p<0.05, as determined by unpaired *t*-test or Mann-Whitney U test.**E**. Flow cytometry analysis of aortic arch 13 weeks after HFD initiation. **F**. Quantification and statistical analysis of data shown in E, n=7 mice per group, **P* < 0.05, as determined by Mann-Whitney U test. **G.** Lack of CD69 on immune cells accelerates atheroma plaque formation. Oil Red O staining in aortic valves from BM Cd69$^{+/+}$ and BM Cd69$^{-/-}$ mice after 13 weeks of HFD (left) and quantification of plaque surface at the indicated time points (right), n=16 mice per group pooled from 3 different experiments. **H**. As before, Masson trichrome staining and quantification of fibrosis and necrotic core after 13 weeks of HFD, n=6 mice/group Error bars show SEM, **P* < 0.05, ***P* < 0.01, ****P* < 0.001, as determined by unpaired *t*-test. **I**. As before, F4/80 staining. **J**. As before, CD3 staining, C and D. representative images of 6 mice/group. Original magnifications: A-C: 4x, D: 10x.

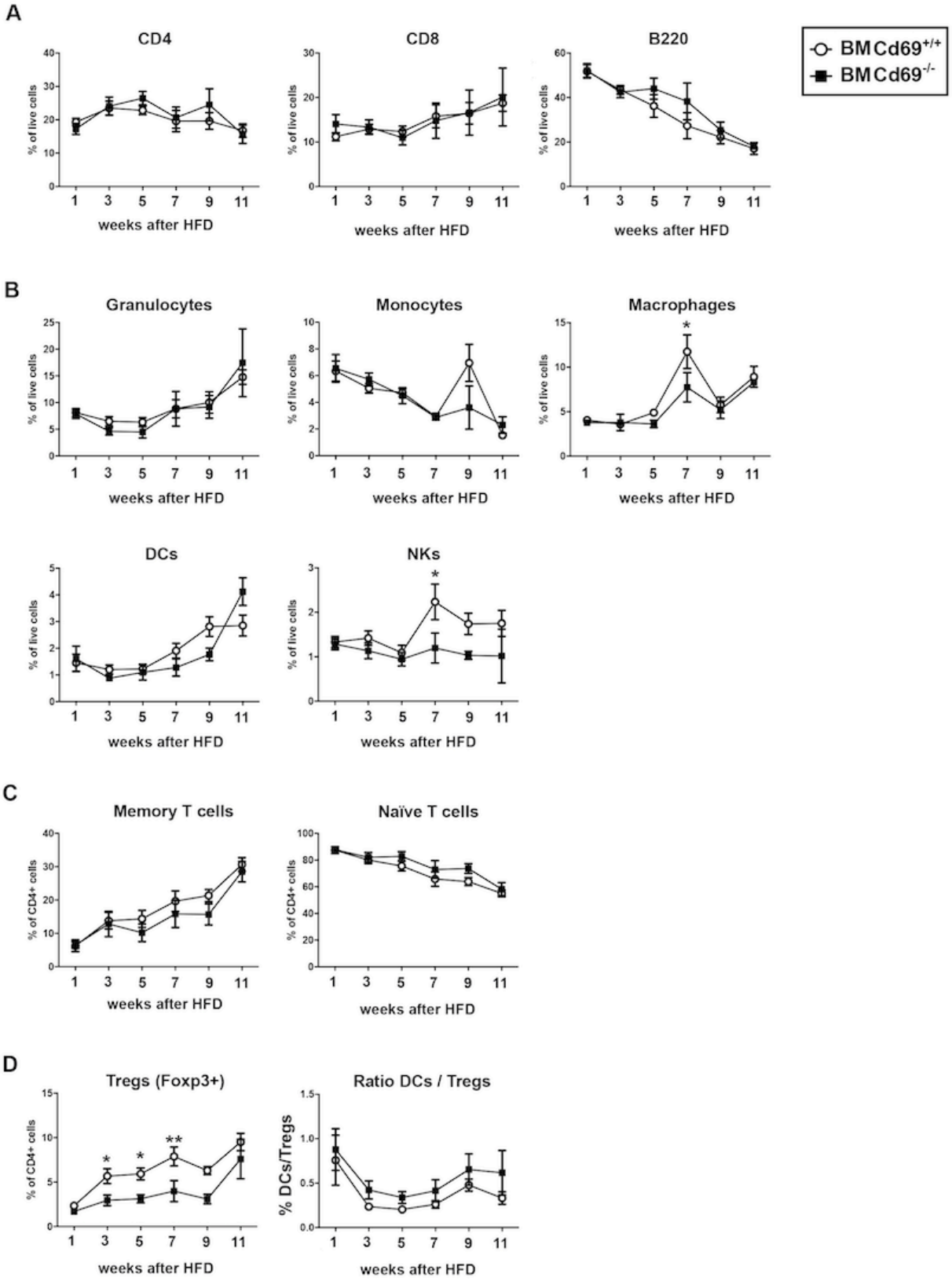

Supplementary figure 2. Analysis of blood leukocyte subsets during high fat diet. The percentages of peripheral blood leukocyte subsets were analyzed during HFD administration. **A**. Analysis of lymphoid CD4+, CD8+ T cells and B

cells (B220) was performed by FACS. **B**. Myeloid cells were analysed after surface staining with anti-CD11b, -CD11c, -Ly6G/C, -F4/80 and NK cells with anti–Nkp46. The percentages of granulocytes, monocytes, macrophages, natural killer cells (NKs) and dendritic cells (DCs) are shown. **C.** Surface staining with anti-CD44/CD62L was performed to distinguish naïve ($CD62L^{hi}$ $CD44^{lo}$) and memory ($CD62L^{lo}$ $CD44^{hi}$) CD4+ T cells. **D**. Percentages of Tregs (Foxp3+) and the ratio between DCs and Tregs is shown. n= 15 BM $Cd69^{+/+}$ and n=13 BM $Cd69^{-/-}$chimeric mice. Error bars show SEM, **P* < 0.05, ***P* < 0.01. *P* values were calculated by 2-way ANOVA (Sidak´s *post hoc* test).

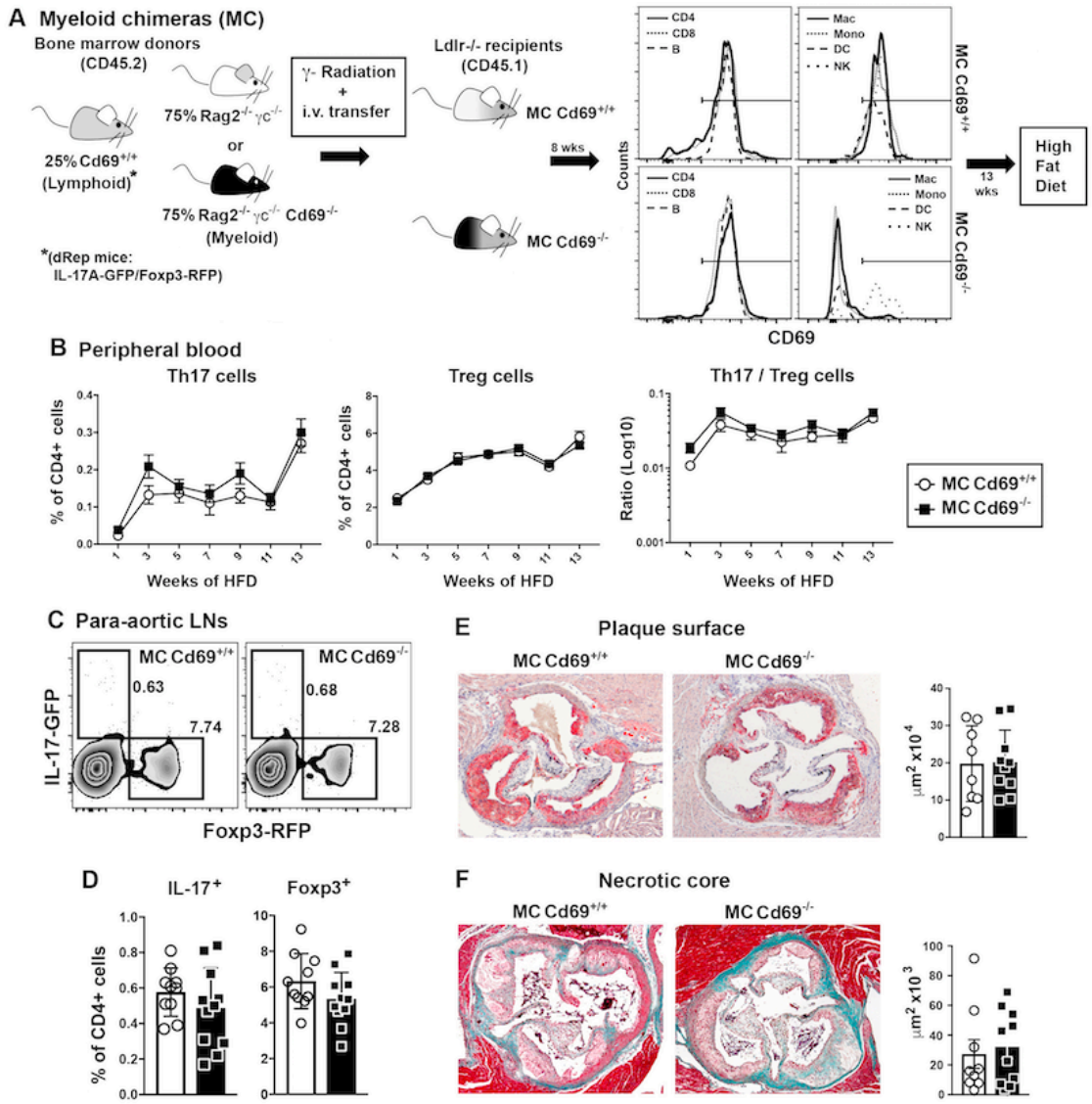

Supplementary figure 3. CD69 deficiency in myeloid cells does not influence atherosclerosis development. A. Scheme illustrating the generation of myeloid chimeras (MC). Ldlr-/- mice were lethally irradiated and reconstituted with mixed bone marrow, from Rag2$^{-/-}$ γ c$^{-/-}$ or Rag2$^{-/-}$ γ c$^{-/-}$Cd69$^{-/-}$ plus bone marrow from C57BL/6-CD69$^{+/+}$ (double-reporter dRep: IL-17-GFP^{+} / Foxp3-RFP^{+}) at a 3:1 ratio, respectively. Eight weeks after reconstitution PBMCs were > 90% CD45.2^{+}. Reconstitution of lymphoid and myeloid compartments of CD45.2^{+} cells was assessed by FACS. Histograms show CD69 expression on CD4 and CD8 T cells, B cells (B), macrophages (Mac), monocytes (Mono),

dendritic cells (DC) and natural killer cells (NK). PBMCs were stimulated with anti-CD3/CD28 for lymphoid cells and LPS for myeloid cells, of the indicated groups. **B**. Kinetics of the adaptive immune response in peripheral blood for Th17 (IL-17-GFP^{+}), Treg (Foxp3-RFP^{+}) CD4^{+} T cells and Th17/Treg ratio in peripheral blood leukocytes after HFD, n=11 mice/group, **C**. Flow cytometry analysis of Foxp3-mRFP+ and IL-17-eGFP+ CD4 T cells in para-aortic LNs of MC *Cd69*$^{+/+}$ and MC *Cd69*$^{-/-}$ mice after 13 weeks of HFD, **D**. Quantification and statistical analysis of data shown in C, n=12 mice per group, **E.** Oil Red O staining and quantification of plaque in aortic valves from MC *Cd69*$^{+/+}$ and MC *Cd69*$^{-/-}$ mice after 13 weeks of HFD, n= 8-10 mice/group, **F**. As in E., Masson trichrome staining and necrotic core quantification, n=8-10 mice/group Original magnifications: 4x. Error bars show SEM. No significant differences were observed between groups as determined by two-way repeated-measures ANOVA (Sidak´s multiple comparisons *post hoc* tests) (B), unpaired *t*-test and Mann-Whitney U test (D-F) as appropriate**.**

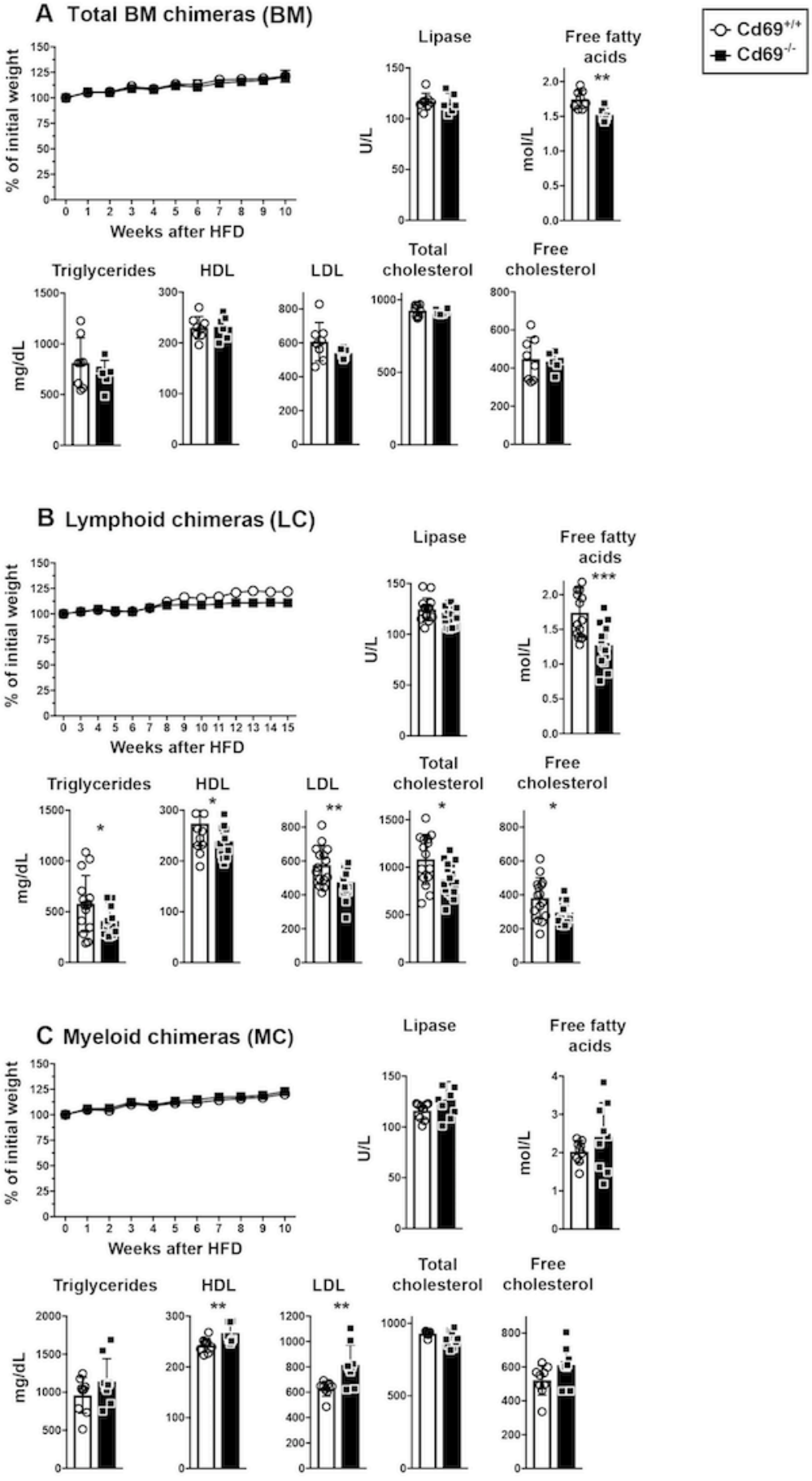
A Total BM chimeras (BM)
Cd69+/+
Cd69-/-
% of initial weight
Weeks after HFD
Lipase
U/L
Free fatty acids
mol/L
**
Triglycerides
HDL
LDL
Total cholesterol
Free cholesterol
mg/dL
B Lymphoid chimeras (LC)
% of initial weight
Weeks after HFD
Lipase
U/L
Free fatty acids
mol/L
***
Triglycerides
HDL
LDL
Total cholesterol
Free cholesterol
mg/dL
*
**
C Myeloid chimeras (MC)
% of initial weight
Weeks after HFD
Lipase
U/L
Free fatty acids
mol/L
Triglycerides
HDL
LDL
Total cholesterol
Free cholesterol
mg/dL
**

Supplementary Figure 4. Analysis of circulating lipids in mice lacking CD69 in total immune, lymphoid or myeloid compartments. Weight gain, lipase activity, free fatty acids, triglyceride and cholesterol levels of the indicated experimental groups were measured. **A**. Weight curve and biochemical profile of chimeric BM *Cd69*$^{+/+}$ and BM *Cd69*$^{-/-}$ mice, n=6-8 mice/group. **B**. as in a, for LC *Cd69*$^{+/+}$ and LC *Cd69*$^{-/-}$ mice, n=15-16 mice/group. **C**. as in A for MC Cd69$^{+/+}$ and MC Cd69$^{-/-}$ mice, n=9 mice/group. No significant differences were observed in weight gain between groups as determined by two-way repeated-measures ANOVA (Sidak´s multiple comparisons *post hoc* tests). Error bars show SEM. **P* < 0.05, ***P* < 0.01, ****P* < 0.001, as determined by unpaired *t*-test and Mann-Whitney U test as appropriate**.**

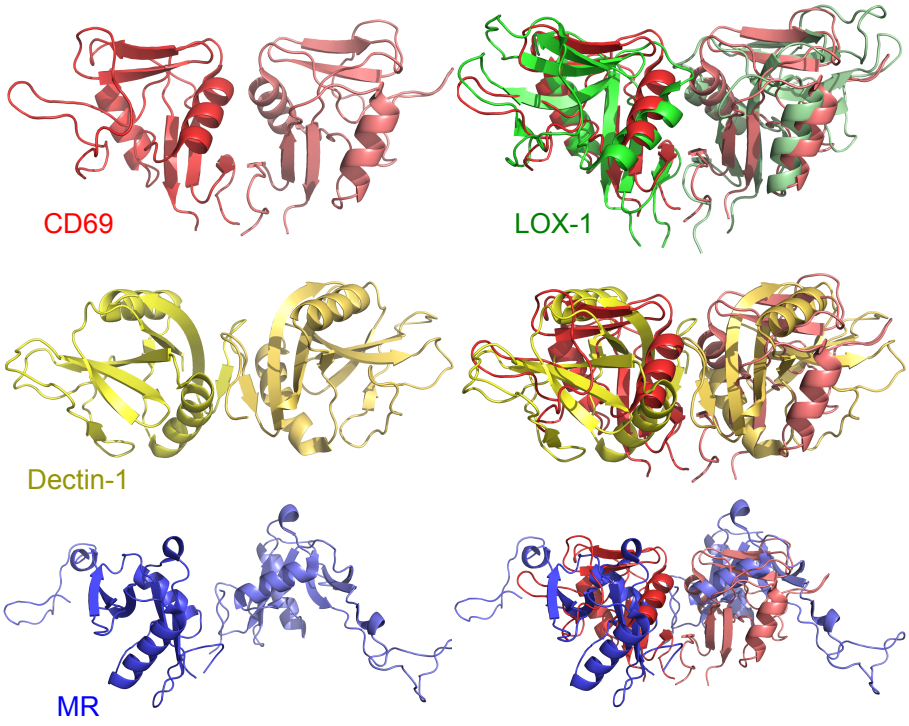

Supplementary Figure 5: The dimeric structures of C-type lectin structures. Ribbon representations of the CD69 (PDB code 1E8I), Dectin-1 (PDB code 2BPD) and the macrophage mannose receptor (MR, PDB code 1EGG) CTLD structures (left panels). Superimposed LOX-1 (PDB code 1YXK), Dectin-1 and MR structures on the CD69 dimer are shown on the right. Prepared with PyMOL.

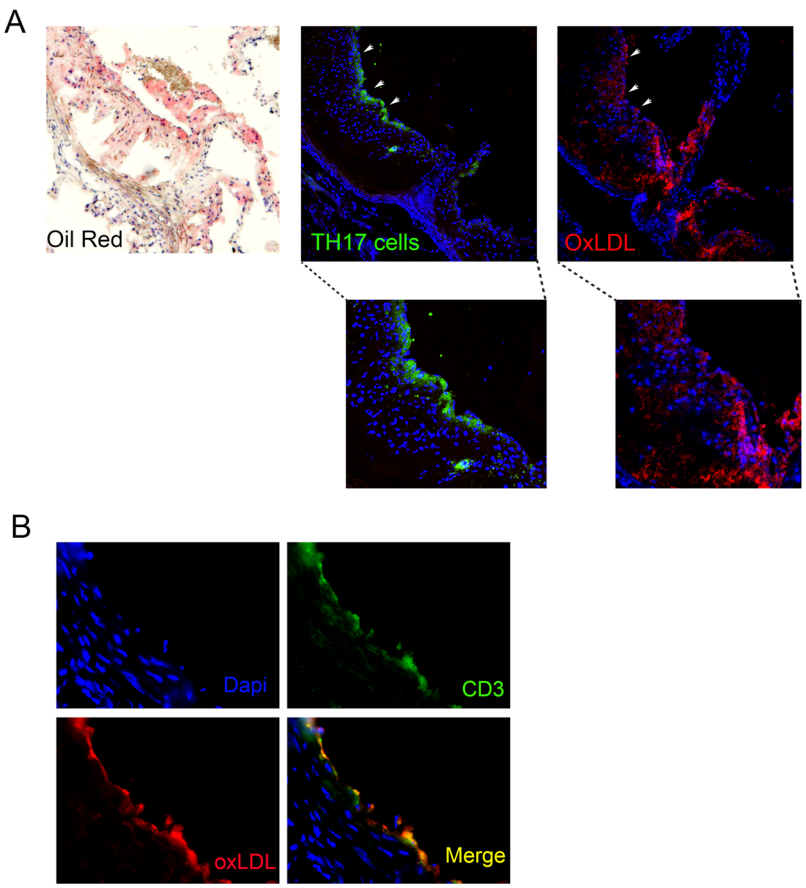

Supplementary Figure 6: Localization of oxLDL and T cells in atheroma plaque. **A**. Lipids, Th17+ T cells and oxLDL in atheroma plaque in aortic valves. Oil Red O staining was used to identify lipids. Endogenous GFP-Th17+ T cells and oxLDL were detected in serial tissue sections of aortic valves from WT *Cd69*$^{+/+}$ mice after 16 weeks of HFD. **B**. Co-localization of CD3+ T cells and oxLDL in atheroma plaque